THE UNIVERSITY *of* EDINBURGH

GPR50, a potential factor involved in psychiatric disorders interacts with Alzheimer's disease-related protein β-secretase (BACE1)

Qian Li

A thesis submitted for the degree of Doctor of Philosophy

The University of Edinburgh

2014

Declaration

I hereby declare that this thesis has been composed by me and that the work presented in this here is my own, unless otherwise stated, and has not been submitted for any other degree or profession qualification.

Qian Li

Acknowledgments

First of all, I would like to sincerely thank my supervisor Dr. Pippa Thomson for her direction and support during my PhD study. It is a great fortune for me to have this opportunity to do research under her supervision. Pippa is my supervisor, and also a friend in life. She taught me how to do science, and also how to be a patient person. Patience is a virtue I will take away together with a degree, and these two precious things are the credit of my lovely supervisor. Thanks a million, Pippa!

I am also very grateful to my second supervisor Dr. Ellen Grünewald for her scientific advice and many insightful discussions. I always say to people that I want to be a PhD with half of the knowledge that Ellen has. I of course must say thanks to my second second supervisor Dr. Helen Newbery for her help and encouragement all the time, especially last year when it was such a difficult time for me that I nearly gave up. I should also say thanks to my thesis committee, Professor David Porteous and Professor Karen Horsburgh for their constructive suggestions and guidance.

I appreciate greatly Dr. Rosie Walker's artful interpretation of the difficult language of statistics. I always got easy answers from her when I was fighting with different sorts of "factors". Also, I owe many thanks to Dr. Elise Malavasi who taught me how to dissect embryonic mouse brain, a skill that makes me proud to have.

I would like to say a big thanks to Nneka, who has been working with me, having dinner with me and laughing with me for the past four years. She is my Nnequeen. I have promised her that, if she ever goes to China, wherever I am, I will rush to her side and make her a cup of flower tea. Thanks to Darragh, my best friend, for helping me all the time, such as teaching me how to swear properly in English, oops…..I also want to say thanks to Shaun, for taking Niamh and Finn to the lab to play with me when I was bored with the experiments during the weekends. Thanks to Evi Evi Evivi, my sweetie, who has witnessed all the happiness and sadness that I have experienced when I was in the lab. Nidhi Sharma, I will never forget her because she is such an adorable girl and I will never forget her name, because of …hmmm…Emmerdale. Also, I want to give a huge thanks to everyone who has been with me through this PhD: Fumiaki, Michelle, Yan, Laura, Kate, Daniel and all the stuff at the MMC.

I want to say many thanks to my parents and my brother who have been encouraging me to complete my PhD, but at the same time have been suffering from missing me at every moment in the past four years. I hope to reunite with them in no time. Also, my husband has assisted me to go through all the difficulties against this PhD. Here I would like to thank him for his support and waiting.

Also, I must say thanks to Brenda Yates. She is my UK mother. She has been looking after me since the first week I came to the UK. We have spent most of the Christmas and Easter holidays with so many unforgettable memories together. I shall take my departure from the UK at Brenda's house. I wish her a happy life and we will be in touch forever.

I want to thank my proof-reader Anna Buxon who kindly offered to read my thesis for free. She is a very kind lady and has taught me so much English I would never learn otherwise as a second language speaker.

Finally, I would like to express my great appreciation to all the people who have helped me during my PhD and my life in the UK.

Table of contents

Declaration II

Acknowledgments III

Table of contents V

List of figures X

List of tables XIII

Abbreviations XV

Units XVIII

Abstract XIX

1 Introduction 1

1.1 G protein-coupled receptor 50 2

1.1.1 The discovery of GPR50 2

1.1.2 GPR50 expression 3

1.1.3 GPR50 interactors 4

1.1.4 GPR50 knockout mice 10

1.2 Beta-site APP cleaving enzyme 1, BACE1 11

1.2.1 The discovery of BACE1 11

1.2.2 BACE1 expression 12

1.2.3 The trafficking of BACE1 12

1.2.4 Main BACE1 substrates 14

1.2.5 BACE1 overexpression transgenic mice 17

1.2.6 BACE1 knockout mice 17

1.3 Mental illnesses 20

1.3.1 Bipolar disorder 20

1.3.2 Schizophrenia 22

1.3.3 Alzheimer's disease 24

1.3.4 A summary of mental illness genetics 28

1.4 The possible links between GPR50 and BACE1 28

1.4.1 The known interactors of GPR50 are associated with BACE1 28

1.4.2 Melatonin: a possible pathway node of regulation 31

1.5 Aim of this thesis 32

2 Characterising the expression and subcellular localisation of GPR50 and BACE1 34

2.1 Introduction 35

2.1.1 The expression of GPR50 35

2.1.2 BACE1 expression 36

2.1.3 Introduction to experiments 40
2.2 Materials and methods 40
2.2.1 Mammalian cell culture 40
2.2.2 Primary neuronal culture 41
2.2.3 Plasmids 41
2.2.4 Lipofectamine 2000 transfection 41
2.2.5 Immunocytochemistry (ICC) 43
2.2.6 Live cell surface labelling technique 45
2.2.7 Western Blotting 45
2.2.8 Real-time quantitative PCR (qPCR) 46
2.2.9 DNA sequencing 47
2.3 Results 48
2.3.1 Antibody characterisation 48
2.3.2 GPR50 is involved in the regulation of BACE1 expression 72
2.4 Discussion 75
2.4.1 The subcellular location of GPR50 and BACE1 75
2.4.2 The possible role of GPR50 in regulating BACE1 expression 76
2.4.3 Further experiments 77
3 The potential of GPR50 to be an interactor of BACE1 78
3.1 Introduction 79
3.1.1 Protein-protein interaction 79
3.1.2 Introduction to experiments 84
3.2 Materials and methods 84
3.2.1 Tissue culture and relative techniques 84
3.2.2 Antibodies 84
3.2.3 Intensity correlation analysis (ICA) 85
3.2.4 Subcellular fractionation-sucrose density gradient fractionation 88
3.2.5 Co-immunoprecipitation (Co-IP) 90
3.3 Results 91
3.3.1 Exogenous GPR50 and BACE1 co-localise in mammalian cell lines and primary neuronal cultures 91
3.3.2 Endogenous GPR50 and BACE1 are co-localised in HEK293 92
3.3.3 Endogenous GPR50 is co-localised with cell-surface BACE1 96
3.3.4 Exogenous GPR50 and BACE1 are located in the same fractions by subcellular fractionation 98

3.3.5 Exogenous BACE1 is co-immunoprecipitated with GPR50 in mammalian cell lines 101
3.3.6 Endogenous BACE1 is co-immunoprecipitated with GPR50 in HEK293 cells 102
3.4 Discussion....104
3.4.1 The interaction between GPR50 and BACE1 105
3.4.2 Further experiments 106
4 The effect of GPR50 over-expression on β-secretase activity in neuronal cells....107
4.1 Introduction....108
4.1.1 The neuronal function of GPR50....108
4.1.2 β-secretase activity in neuronal cells 109
4.1.3 The role of GPR50 in regulating BACE1 activity....111
4.1.4 Introduction to experiments 111
4.2 Materials and methods....112
4.2.1 Primary neuronal culture 112
4.2.2 β-secretase activity assay 113
4.2.3 Knockdown of endogenous Gpr50 in primary cortical neurons....114
4.3 Results....114
4.3.1 Optimisation of transfection efficiency in SH-SY5Y cells and primary cortical neurons 115
4.3.2 Detection of Bace1/BACE1 activity levels in mouse primary cortical neurons and human neuroblastoma cell line SH-SY5Y 116
4.3.3 Optimisation of β-secretase activity assay kit in primary neuronal cultures 117
4.3.4 Is Bace1 activity regulated by GPR50 overexpression?....118
4.3.5 Is Bace1 activity regulated by Gpr50 knockdown? 119
4.4 Discussion....121
4.4.1 Endogenous BACE1 in SH-SY5Y cells 121
4.4.2 The biological significance of β-secretase activity regulation by GPR50/GPR50del....122
4.4.3 Future study: does GPR50/GPR50del affect substrate-specific β-secretase activity? 124
5 Is the trafficking of BACE1 regulated by GPR50 or GPR50del?....125
5.1 Introduction....126
5.1.1 Post translational modification of BACE1 and trafficking 126
5.1.2 Ways to study BACE1 trafficking....131
5.1.3 Introduction to experiments 135

5.2 Materials and methods 135
5.2.1 Antibodies 135
5.2.2 Sucrose density gradient fractionation 136
5.2.3 Fitting of the general linear model with the interaction term 137
5.3 Results 140
5.3.1 The relation between endogenous GPR50 and cell-surface BACE1 140
5.3.2 The effect of exogenous GPR50 on the subcellular localisation of endogenous BACE1 147
5.4 Discussion 161
5.4.1 The GPR50 C-terminal tail might be a key region that mediates the role of GPR50 in β-secretase trafficking 162
5.4.2 Summary 163
5.4.3 Further experiments 164
6 Co-expression of GPR50 and BACE1 in the brain 165
6.1 Introduction 166
6.1.1 GPR50 distribution in the sub-regions of brain tissue 166
6.1.2 BACE1 distribution in the sub-regions of brain tissue 167
6.1.3 Introduction to experiments 168
6.2 Materials and methods 168
6.2.1 Summary of expression data from public database 168
6.2.2 Immunohistochemistry (IHC) 171
6.3 Results 171
6.3.1 The mRNA expression levels of GPR50 and BACE1 in human DLPFC 171
6.3.2 The mRNA levels of Gpr50 and Bace1 in Balb/c mouse 178
6.3.3 The protein levels of endogenous Gpr50 and Bace1 across the brain regions of wild-type C57BL/6 mice 182
6.4 Discussion 190
6.4.1 The co-expression of GPR50 and BACE1 in human PFC 190
6.4.2 The co-expression of Gpr50 and Bace1 in mouse brain 192
6.4.3 Further studies 194
7 The investigation of Gpr50 expression in Alzheimer's disease model TgSwDI mice 196
7.1 Introduction 197
7.1.1 The investigation of AD in mouse models 197
7.1.2 TgSwDI AD mouse model 199
7.1.3 Introduction to experiments 201
7.2 Materials and methods 202

7.2.1 Alzheimer's disease mouse model TgSwDI 202
7.2.2 Immunohistochemistry 203
7.2.3 Imaging and statistical analysis....203
7.2.4 The removal of outlier data 205
7.3 Results....208
7.3.1 Optimisation of Gpr50 staining in TgSwDI mice 208
7.3.2 Aβ and Gpr50 in the entorhinal cortex 210
7.3.3 Aβ and Gpr50 in the hippocampus 217
7.4 Discussion....225
7.4.1 What is the implication of the alteration of GPR50 expression in TgSwDI mice? 226
7.4.2 Is Gpr50 involved in the neurotransmitter signalling system in AD?....227
7.4.3 Suggested future experiments....229
8 Discussion 231
8.1 GPR50 co-localises with BACE1 at functional sites....232
8.1.1 The cell surface 232
8.1.2 The synapse 233
8.2 GPR50 and its illness-related variant have distinct effects on β-secretase activity 234
8.3 What can we conclude from the investigation of GPR50 in the AD TgSwDI mouse model?....236
8.3.1 Why is GPR50 level regulated in AD mouse brain?....236
8.3.2 What do we know about the role of GPR50 in AD?....237
8.3.3 How does the function of GPR50 in the hippocampus/entorhinal cortex link to that in HPA-axis?....239
8.4 Future work....240
Reference 243

List of figures

Figure 1.1 The signalling pathway of G-protein coupled receptor 5
Figure 1.2 Regulation of MT1 signalling by heterodimerisation with GPR50..... 6
Figure 1.3 GPR50 gene structure and position of polymorphisms 22
Figure 1.4 The proteolytic processing of APP 25
Figure 2.1 The alternative splicing of the BACE1 transcript 37
Figure 2.2 Validation of GPR50 antibodies using immunocytochemistry in SH-SY5Y cells 50
Figure 2.3 The localisation of overexpressed GPR50 in SH-SY5Y cells 51
Figure 2.4 Validation of GPR50 antibodies using western blotting in SH-SY5Y cells 52
Figure 2.5 Validation of GPR50 antibodies using immunocytochemistry in HEK293 cells.....53
Figure 2.6 Validation of GPR50 antibodies using immunocytochemistry in primary cortical neurons 54
Figure 2.7 GPR50 antibodies were unable to detect endogenous Gpr50 using immunocytochemistry in primary cortical neurons.....55
Figure 2.8 Endogenous GPR50/Gpr50 was detected in HEK293 cells and mouse brain using western blotting.....56
Figure 2.9 Validation of BACE1 antibodies using immunocytochemistry in SH-SY5Y cells 58
Figure 2.10 The localisation of overexpressed BACE1 in SH-SY5Y cells 59
Figure 2.11 The BACE1 mouse antibody failed to label BACE1 at the surface of SH-SY5Y cells 60
Figure 2.12 Cell surface labelling of BACE1 in SH-SY5Y cells (1) 61
Figure 2.13 Cell surface labelling of BACE1 in SH-SY5Y cells (2) 62
Figure 2.14 Validation of BACE1 antibodies using western blotting in SH-SY5Y cells.....63
Figure 2.15 Validation of BACE1 antibodies using immunocytochemistry in HEK293 cells ...64
Figure 2.16 Endogenous BACE1 was detected in HEK293 cells by immunocytochemistry....65
Figure 2.17 Detection of endogenous BACE1 in HEK293 cells.....66
Figure 2.18 Validation of BACE1 antibodies using immunocytochemistry in primary cortical neurons 67
Figure 2.19 Endogenous Bace1 was detected in mouse primary cortical neurons using immunocytochemistry 68
Figure 2.20 Endogenous Bace1 was detected in mature primary hippocampal neurons using immunocytochemistry 69
Figure 2.21 Endogenous BACE1/Bace1 was detected in HEK293 cells and mouse brain using western blotting.....69
Figure 2.22 Cross-immunoreactivity test in immunocytochemistry double-staining experiments.....71
Figure 2.23 The effect of GPR50 overexpression on endogenous levels of BACE1 protein in HEK293 cells.....72
Figure 2.24 The expression levels of endogenous BACE1 in SH-SY5Y cells 73
Figure 2.25 The effect of GPR50 overexpression on endogenous levels of BACE1 mRNA in SH-SY5Y cells.....74
Figure 2.26 The effect of GPR50 overexpression on endogenous levels of BACE1 protein in SH-SY5Y cells.....75
Figure 3.1 The yeast two-hybrid screening system.....81
Figure 3.2 The schematic diagram of co-immunoprecipitation 82

Figure 3.3 The schematic diagram of fluorescence resonance energy transfer.....83
Figure 3.4 Stimulated models of intensity correlation analysis.....87
Figure 3.5 A diagram of subcellular fractionation from adult mouse brains 90
Figure 3.6 Co-localisation of overexpressed GPR50 and BACE1 in SH-SY5Y cells.....93
Figure 3.7 Co-localisation of overexpressed GPR50 and BACE1 in HEK293 cells 94
Figure 3.8 Co-localisation of overexpressed GPR50 and BACE1 in mouse primary hippocampal neurons 95
Figure 3.9 Co-localisation of endogenous GPR50 and BACE1 in HEK293 cells.....96
Figure 3.10 Endogenous GPR50, cell surface BACE1 and total BACE1 in HEK293 cells 97
Figure 3.11 Co-localisation of GPR50 and cell surface BACE1 in a HEK293 cell endogenously expressed with both.....98
Figure 3.12 Subcellular fractionation of protein lysates from HEK293 cells co-transfected with GPR50 and BACE1 99
Figure 3.13 The distribution of endogenous Gpr50 and Bace1 in adult mouse brain by subcellular fractionation 100
Figure 3.14 Co-immunoprecipitation of overexpressed GPR50 and BACE1 in cultured cell lines.....103
Figure 3.15 Co-immunoprecipitation of endogenous GPR50 and BACE1 in HEK293 cells...104
Figure 4.1 The effects of overexpressed GPR50 or GPR50del on BACE1 activity in HEK293 cells 111
Figure 4.2 The test of endogenous β-secretase activity levels.....117
Figure 4.3 The titration of β-secretase activity detection.....118
Figure 4.4 Effects of GPR50/GPR50del overexpression on Bace1 activity in mouse primary cortical neurons 119
Figure 4.5 The test of endogenous Gpr50 knockdown in mouse primary cortical neurons 120
Figure 4.6 The unsuccessful knockdown of endogenous Gpr50 in mouse primary cortical neurons 121
Figure 5.1 A diagram representing BACE1.....128
Figure 5.2 BACE1 cellular trafficking and representative regulators 129
Figure 5.3 Subcellular fractionation markers used in this chapter 134
Figure 5.4 Intensity correlation analysis of GPR50 with surface BACE1 or total BACE1 in a cluster of cells 142
Figure 5.5 Intensity profiles of GPR50, cell surface BACE1 and total BACE1 in HEK293 cells of a group 144
Figure 5.6 Scatter plots for GPR50 expression level, cell surface BACE1 proportion and cell number.....147
Figure 5.7 Subcellular fractionation of cell lysates transfected with pDEST40, GPR50 or GPR50del 149
Figure 5.8 The distribution proportion of immature BACE1, mature BACE1, VLA-2α, EEA1 and calreticulin in each sucrose fraction in HEK293 cells 150
Figure 5.9 The distribution proportion of immature Bace1, mature Bace1, β-catenin, p115 and calreticulin in each sucrose fraction in mouse primary cortical neurons.....151
Figure 6.1 The mRNA expression profiles of GPR50 and BACE1 in human DLPFC 173
Figure 6.2 The scatterplot of prenatal BACE1 mRNA level and gestational week in human PFC 175
Figure 6.3 The scatterplot of mRNA levels of GPR50 and BACE1 in human DLPFC sampled after birth 176

Figure 6.4 The scatterplot of mRNA levels of GPR50 and BACE1 in human DLPFC sampled after birth in male and female subgroups....177
Figure 6.5 The expression profile and distribution map of Gpr50 mRNA in 51 CNS regions of adult Balb/c mouse....179
Figure 6.6 The expression profile and distribution map of Bace1 mRNA in 51 CNS regions of adult Balb/c mouse....180
Figure 6.7 The scatterplots of mRNA levels of Gpr50 and Bace1 across different CNS regions of adult Balb/c mouse....181
Figure 6.8 Immunostaining of Bace1 in adult mouse brain....183
Figure 6.9 Bace1 co-staining by rabbit2 and goat antibodies....184
Figure 6.10 The expression of Bace1 protein in adult mouse brain....185
Figure 6.11 No primary antibody control for fluorescent IHC in adult mouse brain....187
Figure 6.12 Co-localisation of Gpr50 and Bace1 in C57BL/6 mouse brain....188
Figure 7.1 Preparation work for the quantification in the hippocampus....204
Figure 7.2 Quality checking of photos prior to the analysis....205
Figure 7.3 The method of identifying outliers....207
Figure 7.4 The original photos and post-threshold photos of Gpr50 in the entorhinal cortex layer V of animal 251....207
Figure 7.5 The cortex of 9 months TgSwDI mice stained with GPR50 goat antibody....209
Figure 7.6 The hypothalamus of 9 months TgSwDI mice stained with GPR50 goat antibody....210
Figure 7.7 The immunofluorescence labelling of Aβ and Gpr50 in the entorhinal cortex of 9 months TgSwDI mice....211
Figure 7.8 Representative photos of Aβ and Gpr50 in the entorhinal cortex layer V of the four mouse cohorts....212
Figure 7.9 Comparison of Gpr50 expression in the entorhinal cortex layer V of TgSwDI mice with that of wild-type mice at 3 months or 9 months....216
Figure 7.10 Comparison of Gpr50 expression in the entorhinal cortex layer V of mice between 3 months and 9 months....216
Figure 7.11 Correlation between the expression levels of Aβ and Gpr50 in the layer V of the entorhinal cortex of TgSwDI mice....217
Figure 7.12 The immunofluorescence labelling of Aβ and Gpr50 the in the hippocampus of 9 months TgSwDI mice....219
Figure 7.13 Aβ in the hippocampus of the four mouse cohorts....220
Figure 7.14 Comparison of Gpr50 expression in the hippocampus of TgSwDI mice with that of wild-type mice at 3 months or 9 months....224
Figure 7.15 Comparison of Gpr50 expression in the hippocampus between 3 months and 9 months mice....224
Figure 7.16 Correlation between the expression levels of Gpr50 and Aβ in the hippocamous of TgSwDI mice....225

List of tables

Table 1.1 GPR50 yeast two-hybrid screen hits 7
Table 2.1 Lipofectamine 2000 transfection protocol 42
Table 2.2 Primary antibodies used in this thesis 43
Table 2.3 Fluorescent secondary antibodies used in this thesis 44
Table 2.4 Horseradish peroxidase conjugated secondary antibodies used in this thesis 46
Table 2.5 Setting up real-time quantitative PCR reaction 46
Table 2.6 Primers used for real-time quantitative PCR 47
Table 2.7 Real-time quantitative PCR programme 47
Table 2.8 The competence of antibodies for GPR50 used in this thesis 48
Table 2.9 The competence of antibodies for BACE1 used in this thesis 56
Table 2.10 The relative mRNA expression levels of BACE1 in SH-SY5Y cells transfected with pDEST40 or GPR50 74
Table 3.1 Primary antibodies used in chapter 3 85
Table 3.2 The expression pattern of GPR50 and cell-surface BACE1 in a group of cells 97
Table 4.1 Sample preparation of β-secretase activity assay 114
Table 4.2 Test of different transfection regents in SH-SY5Y cells and primary cortical neurons 115
Table 4.3 Transfection primary cortical neurons with Lipofectamine 2000 116
Table 5.1 Major factors involved in BACE trafficking and associated with Alzheimer's disease 130
Table 5.2 Primary antibodies used in chapter 5 136
Table 5.3 The main SPSS outputs of the general linear model 139
Table 5.4 A summary of the general linear model for the example 140
Table 5.5 ICA parameters for co-localisation analysis of GPR50 with surface BACE1 or total BACE1 142
Table 5.6 Pearson's correlation between GPR50 expression level and cell surface BACE1 proportion 146
Table 5.7 Predication of the general linear model for cell surface BACE1 proportion 147
Table 5.8 A summary of the general linear model for mature BACE1 in HEK293 cells 154
Table 5.9 A summary of the general linear model for immature BACE1 in HEK293 cells 155
Table 5.10 A summary of the predictors of significance or with a trend of significance in the general linear model for mature BACE1 and immature BACE1 in HEK293 cells 156
Table 5.11 A summary of the general linear model for mature Bace1 in primary cortical neurons 158
Table 5.12 A summary of the general linear model for immature Bace1 in primary cortical neurons 159
Table 5.13 A summary of the predictors of significance or with a trend of significance in the general linear model for mature Bace1 and immature Bace1 in primary cortical neurons. 160
Table 6.1 The 51 adult mouse CNS regions investigated in BrainStars database 169
Table 6.2 The general linear model using gestational week and sex to predict prenatal GPR50 and BACE1 mRNA level in human PFC 174
Table 6.3 The Pearson's correlation analysis of prenatal GPR50 and BACE1 mRNA levels during the gestational week 14-20 in human PFC 175

Table 6.4 The general linear model using age and sex to predict GPR50 and BACE1 mRNA level in human DLPFC sampled after birth 176
Table 6.5 The Pearson's correlation analysis of GPR50 and BACE1 mRNA levels in human DLPFC sampled after birth.....176
Table 6.6 The general linear model with the interaction term to predict BACE1 mRNA level in human DLPFC sampled after birth 177
Table 6.7 The Pearson's correlation analysis of adult mouse Gpr50 and Bace1 mRNA levels across 51 CNS regions and across CNS sub-regions of adult Balb/c mouse.....181
Table 6.8 The distribution of endogenous Gpr50 and Bace1 in adult female C57BL/6 mouse brain and the co-localisation between the two proteins.....189
Table 7.1 The two sets of slides for staining Aβ and Gpr50 202
Table 7.2 Brain sections excluded from the analysis 208
Table 7.3 The expression percentage of Aβ and Gpr50 in the entorhinal cortex layer V 213
Table 7.4 A summary of expression percentage of Aβ and Gpr50 in the entorhinal cortex layer V.....214
Table 7.5 The general linear model to predict the expression levels of Aβ and Gpr50 in the layer V of the entorhinal cortex among the four mouse cohorts 215
Table 7.6 The expression percentage of Aβ and Gpr50 in the hippocampus.....221
Table 7.7 A summary of the expression percentage of Aβ and Gpr50 in the hippocampus222
Table 7.8 The general linear model to predict the expression levels of Aβ and Gpr50 in the hippocampus among the four mouse cohorts 223

Abbreviations

Aβ	Amyloid-β
ABCA2	ATP-binding cassette sub-family A member 2
ABCA7	ATP-binding cassette sub-family A member 7
AD	Alzheimer's disease
ADAM	A disintegrin and metalloproteinase
AICD	APP intracellular domain
ANCOVA	Analysis of covariance
ANOVA	Analysis of Variance
APLP1	Amyloid-like protein 1
APLP2	Amyloid-like protein 2
APOE	Apolipoprotein E
APP	Amyloid precursor protein
ARF6	ADP-ribosylation factor 6
ARH	Arcuate nucleus of hypothalamus
BACE1	Beta-site APP cleaving enzyme 1
BD	Bipolar disorder
BLA	Basolateral amygdala
BLAST	Basic Local Alignment Search Tool
BRET	Bioluminescence resonance energy transfer
BSA	Bovine serum albumin
CA1	Cornu Ammonis 1
CA2	Cornu Ammonis 2
CA3	Cornu Ammonis 3
CAA	Cerebral amyloid angiopathy
CAM	Cell adhesion molecule
CDH8	Cadherin molecule 8
CHAPS	3-[(3-cholamidopropyl)dimethylammonio]-1-propanesulfonate
CHL1	Close homolog of L1
CNS	Central nervous system
CSF	Cerebrospinal fluid
CTD	C-terminal domain
CTF	C-terminal fragment
DG	Dentate gyrus
DIV	Day in vitro
DLPFC	Dorsolateral prefrontal cortex
DMH	Dorsomedial nucleus of hypothalamus
EC	Entorhinal cortex
ECL	Enhanced chemiluminescence
EEA1	Early endosome antigen 1
EGF	Epidermal growth factor
ELISA	Enzyme-linked immunosorbent assay
ER	Endoplasmic reticulum
FAD	Familial Alzheimer’s disease
FBS	Foetal bovine serum
FRET	Fluorescence resonance energy transfer

GABA	Gamma-Aminobutyric acid
GAPDH	Glyceraldehyde 3-phosphate dehydrogenase
GC	Glucocorticoid
GFP	Green fluorescent protein
GGA	Golgi-localised γ-ear-containing ADP ribosylation factor-binding protein
GH3	Rat pituitary epithelial-like tumor cell line
GM130	cis-Golgi matrix protein 130 kDa
GPCR	G protein-coupled receptor
GPR50	G protein-coupled receptor 50
GR	Glucocorticoid receptor
GWAS	Genome-wide association study
5-HT	5-hydroxytryptamine, serotonin
HAT	Histone acetyltransferase
HEK293	Human Embryonic Kidney 293
HEPES	2-[4-(2-hydroxyethyl)piperazin-1-y]ethanesulfonic acid
HPA	Hypothalamic–pituitary–adrenal
HRP	Horseradish peroxidase
ICA	Intensity correlation analysis
ICC	Immunocytochemistry
ICQ	Intensity correlation quotient
IHC	Immunohistochemistry
IP	Immunoprecipitation
L1	A family of cell adhesion molecules
LAMP1	Lysosomal-associated membrane protein 1
MT1	Melatonin receptor 1
MT2	Melatonin receptor 2
N1E-115	Mouse neuroblastoma cell line
NMDA	N-Methyl-D-aspartate
NRG	Neuregulin
ORF	Open reading frame
P115	Cis-Golgi marker 115 kDa
PBS	Phosphate buffered saline
PCR	Polymerase chain reaction
PDM	Product of the Differences from the Mean
PFA	Paraformaldehyde
PFC	Prefrontal cortex
PPI	Protein-protein interaction
PS	Presenillin
PSD	Postsynaptic density
PSD95	Postsynaptic density protein 95
PVDF	Polyvinylidene fluoride
RAB7	Ras-related protein
RGS4	Regulator of G protein signaling 4
RHD	Reticulon-homology domain
RIPA	Radioimmunoprecipitation assay buffer
RTN3	Reticulon protein 3
SDS-PAGE	SDS-Polyacrylamide gel electrophoresis
SEZ6	Seizure related 6
SNP	Single-nucleotide polymorphism
SNX12	Sorting nexin 12
SNX5	Sorting nexin 5
SNX6	Sorting nexin 6
SREBP2	Sterol regulatory element-binding protein

SH-SY5Y	Human neuroblastoma cell line
TBP	TATA binding protein
TFRC	Transferrin receptor
TGN	Trans-Golgi network
TIP60	Histone acetyltransferase KAT5
UBC	Ubiquitin C
UTR	Untranslated region
VPS35	Vacuolar protein sorting-associated protein 35
WB	Western blotting
WT	Wild-type
Y2H	Yeast two-hybrid

Units

°C	Degrees centigrade
bp	Base pair
Da	Dalton
g	Gram
hr	Hour
l	Litre
m	Metre
M	Molar
min	Minute
rpm	Revolutions per minute
V	Volt

Abstract

GPR50, an X-linked orphan G protein-coupled receptor (GPCR), is a risk factor for bipolar disorder (BD) in female subjects. It has been shown that GPR50 plays a part in neurite outgrowth, glucocorticoid receptor signalling and leptin signalling by interacting with major factors involved in these events. Yeast two-hybrid screens have identified multiple putative GPR50 interactors involved in neurodevelopment, stress response and apoptosis, lipid and glucose metabolism, as well as regulation of NMDA receptors and GABA transmission. Among these interactors, RTN3, RTN4, SREBP2 and SNX6 are known regulators of β-secretase (BACE1), a key enzyme in Aβ generation, myelination of the central/peripheral nerve, and neurite outgrowth/synapse formation.

Preliminary data indicated that GPR50 expression significantly increased endogenous BACE1 activity in HEK293 cells, so I hypothesised that there is a functional interaction between the two.

In this thesis, I investigated the relationship between GPR50 and BACE1 by identifying the effects of GPR50 on BACE1 expression and function, which may provide an explanation of GPR50's potential association with psychiatric disorders and Alzheimer's disease.

Firstly, studies on expression levels revealed that when GPR50 was over-expressed, BACE1 protein expression was up-regulated in SH-SY5Y cells, but down-regulated in HEK293 cells, suggesting a differentiated regulative system between cell lines. Then I confirmed the physical association between endogenous GPR50 and BACE1 in HEK293 cells by co-localisation and co-immunoprecipitation studies. Their putative interaction sites were located at the plasma membrane and the filopodia/lamellipodia-like structures in HEK293 cells, and at the neurites in mouse primary neuronal cells. Subcellular fractionation of adult mouse brain revealed that endogenous Gpr50 and Bace1 were co-fractionated in the presynaptic vesicles.

Secondly, I showed that, in contrast to HEK293 cells, GPR50 overexpression had no effects on β-secretase activity in mouse primary cortical neurons. However, the BD-associated variant GPR50del significantly decreased β-secretase activity compared to the more common variant GPR50, and showed a trend of diminishing β-secretase activity compared to the control condition. Subcellular fractionation experiments

showed that in HEK293 cells, there was an increased ratio of mature BACE1 against immature BACE1 localised in the plasma membrane fractions, indicating a role in regulation of BACE1 trafficking to one of its putative activity sites; whereas in mouse primary cortical neurons, GPR50del increased co-fractionation of immature Bace1 with endoplasmic reticulum (ER) marker calreticulin, thus potentially retarding the maturation of Bace1. Importantly, the regulative trend of GPR50/GPR50del on β-secretase activity is cell line-specific and is highly correlated to their effects on β-secretase intracellular distribution.

Thirdly, I found that the mRNA levels of human GPR50 and BACE1 were negatively correlated in the dorsolateral prefrontal cortex of female subjects sampled after birth. Mouse Gpr50 and Bace1 mRNA levels were negatively correlated across the telencephalon regions, and had a trend of negative correlation across the hypothalamic regions. Co-localisation of the two proteins was detected in multiple mouse brain regions, with the strongest co-localised signals occurring in CA2 pyramidal neurons, arcuate hypothalamic nucleus and dorsomedial nucleus of the hypothalamus.

Finally, preliminary experiments in Alzheimer's disease model TgSwDI mice, suggested that the expression level of Gpr50 in layer V of the entorhinal cortex was positively correlated with Aβ deposition. Decreased Gpr50 expression was identified in the hippocampus of 9 months transgenic animals compared with age-matched controls. This indicates that Gpr50 expression might be altered in this mouse model co-ordinately with Aβ deposition.

The findings in this thesis provide further evidence of GPR50's correlation to psychiatric illnesses and its interaction with enzyme BACE1 highlights a potential link to neurodegenerative disease.

1 Introduction

Mental illnesses, also known as psychiatric disorders, pose a serious threat to human health, and the number of individuals affected worldwide is increasing each year. The latest facts and figures on mental health showed that approximately 450 million people in the world have a mental health problem, and 1 in 4 families worldwide is likely to have at least one member with a behavioural or mental disorder (Halliwell et al, 2007). Although there has been great progress in the research on mental illnesses, their aetiology has so far not been clarified. The lag in basic research significantly affects the diagnosis and treatment of these diseases, especially the early identification and intervention before the appearance of the main symptoms. The major types of mental illnesses are represented by bipolar disorder and schizophrenia. Another category of mentally related disease that is frequently investigated is dementia, and its most common form is known as Alzheimer's disease (Ballard et al, 2011). The development of the three brain diseases is determined by both genetic and environmental factors.

The goal of this thesis was to investigate the possible functional and physical interaction between two mental illness-associated proteins: G protein-coupled receptor 50 (GPR50), and beta-site APP-cleaving enzyme 1 (BACE1). GPR50 is an orphan G protein-coupled receptor, which has been suggested as a risk factor for mental illnesses through genetic association or with specific protein expression in patients with bipolar disorder, schizophrenia and Alzheimer's disease (Hamouda et al, 2007; Macintyre et al, 2010; Thomson et al, 2005). BACE1 is a key enzyme that initiates the pathological features of Alzheimer's disease and the dysfunction of which results in phenotypes related to schizophrenia and bipolar disorder (Hussain et al, 1999; Marballi et al, 2012; Savonenko et al, 2008). To identify the effects of GPR50 expression on BACE1 function may further inform GPR50's association with psychiatric illnesses and neurocognitive disorders.

This chapter will introduce the discovery and known functions of GPR50 and BACE1, their putative links to each other and the three aforementioned illnesses in which GPR50 and BACE1 are predicted to play a role.

1.1 G protein-coupled receptor 50

1.1.1 The discovery of GPR50

GPR50 belongs to the G protein-coupled receptor (GPCR) superfamily with seven

transmembrane (7TM) spanning domains. GPR50 is a member of the melatonin receptor (MT) subfamily that includes three members melatonin receptor 1A *Mel1a*, melatonin receptor 1b *Mel1b* and melatonin receptor 1c *Mel1c*/GPR50. *Mel1a* and *Mel1b* are expressed in all vertebrates and encode the proteins melatonin receptor 1 (MT1) and melatonin receptor 2 (MT2). *Mel1c* was found only in *Xenopus*, chicken and zebrafish (Ebisawa et al, 1994; Reppert et al, 1995). The ortholog of *Mel1c*, *GPR50* was detected exclusively in mammals and later identified as a member of the MT subfamily due to its sequence identity to the three melatonin receptors (Drew et al, 2001; Drew et al, 1998; Dufourny et al, 2008; Reppert et al, 1996). MT1 and MT2 are native binding receptors for the "hormone of darkness", melatonin, which regulates circadian rhythms and seasonal photoperiodisms (Dubocovich & Markowska, 2005).

The gene of human *GPR50* is localised to Xq28, and mouse *Gpr50* lies in the proximal portion of chromosome X (Gubitz & Reppert, 1999). There are two isoforms of GPR50 protein. The full-length human GPR50 protein consisting of 617 amino acids with a long proline-rich C-terminal tail, shares approximately 45% homology with MT1 and MT2. In the following experimental chapters, if not noted, "GPR50" was referred to as the full-length protein. The other isoform GPR50del differs in the C-terminal, with four amino acids missing (ΔTTGH, amino acid residues 502-505) and one amino acid substitution Thr532Ala (in complete linkage disequilibrium with ΔTTGH). The shorter isoform occurs with an allele frequency of approximately 30% (Grunewald et al, 2009). The role of GPR50 as a melatonin-related receptor is unclear, as it does not bind to melatonin or other known ligands.

Some important functions of GPR50 can be indicated by its expression patterns, by its interacting partners and from its loss-of-function studies.

1.1.2 GPR50 expression

GPR50 is highly expressed in dorsomedial hypothalamus (DMH) neurons, the tanycytes and the pituitary (Levoye et al, 2006). The DMH is a nodal point of neuroendocrine/autonomic circuitries. Almost all major nuclei and areas of the hypothalamus feed information to the DMH, which receives circadian information from the superchiasmatic nucleus, senses leptin and other feeding cues, and sends information to the ventrolateral preoptic area, the locus coeruleus, and the orexin neurons (Mieda et al, 2006). Tanycytes are ependymal cells, with a possible role of

transferring chemical signals from cerebrospinal fluid (CSF) to the central nervous system (CNS) (Rodriguez et al, 2005). The pituitary secretes nine hormones to regulate the homeostasis of the endocrine system, including body processes of growth, blood pressure, breast milk production, sexual function, thyroid gland function, energy metabolism, temperature adjustment, water balance, pigmentation and pain relief (Barron, 2010). Thus, the expression pattern of GPR50 supports its functional role in the hypothalamic-pituitary-adrenal (HPA) axis. In addition, lower levels of GPR50 were detected in the monoaminergic neurons in the brain stem nuclei (Grunewald et al, 2009), and this suggests a wider role of GPR50 in neurotransmitter signalling in the endocrine system and stress response. There are additional GPR50-expressing cites reported by different research groups. Here I focus on the regions that are well-recognised with GPR50 expression and regions that help to establish a link with the function of BACE1. A detailed description of GPR50 expression sites will be introduced in a later chapter.

1.1.3 GPR50 interactors

GPR50 is a member of the G-protein coupled receptor (GPCR) superfamily, which constitutes more than 1000 molecules (Gether, 2000). GPCRs sense extracellular ligands and activate intracellular signal transduction pathways and, ultimately, cellular responses (Figure 1.1). In the inactive state, GPCR is bound to a G-protein complex, a trimer of Gα, Gβ, and Gγ subunits. When activated by the binding of a ligand, GPCR undergoes a conformational change which is transmitted to the Gα subunit. Upon stimulation, Gα exchanges GDP for GTP, and this triggers its dissociation from the Gβγ dimer and from the receptor. Different types of Gα ($G\alpha_s$, $G\alpha_{i/o}$, $G\alpha_{q/11}$, $G\alpha_{12/13}$) and Gβγ subunits interact with corresponding intracellular proteins (such as adenylyl cyclase, phospholipase C). This in turn activates or inhibits downstream second messengers (such as cAMP, diacylglycerol), the alteration of which results in gene expression regulation and diverse biological effects such as proliferation, differentiation, development, cell survival, angiogenesis, hypertrophy and cancer (Marinissen & Gutkind, 2001). The response of GPCR is terminated upon GTP hydrolysis by Gα, which then binds Gβγ and the receptor. This process can be markedly accelerated by the binding of regulators of G protein signalling (RGS), thereby rapidly switching off GPCR signalling pathways.

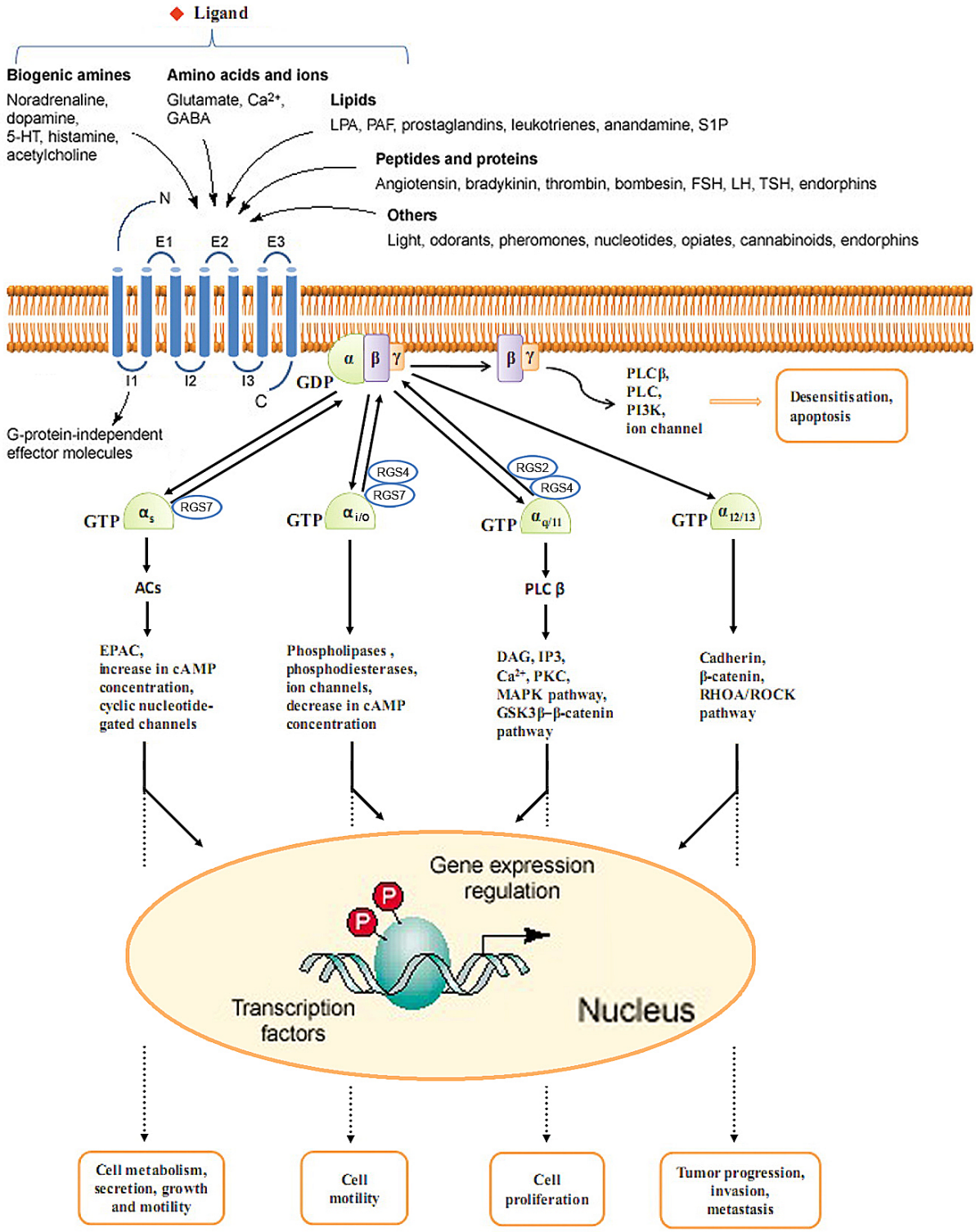

Figure 1.1 The signalling pathway of G-protein coupled receptor. This figure was adapted from (Marinissen & Gutkind, 2001; Wu et al, 2012). GPCRs can be stimulated by binding of diverse ligands, including biogenic amines, amino acids, ions, lipids, peptides and proteins. The activation of GPCR signal transduction cascade ultimately results in the regulation of key biological functions such as cell metabolism and cancer. AC, adenylyl cyclase; PLC, phospholipase C; DAG, diacylglycerol; IP3: Inositol triphosphate; RGS, regulator of G protein signalling; FSH, follicle-stimulating hormone; GEF, guanine nucleotide exchange factor; LH, leuteinizing hormone; LPA, lysophosphatidic acid; PAF, plateletactivating factor; PI3K, phosphoinositide 3-kinase; PKC, protein kinase C; S1P, sphingosine-1-phosphate; TSH, thyroid-stimulating hormone. EPAC: Exchange factor activated by cAMP; MAPK: Mitogen-activated protein kinase; GSK-3β: Glycogen synthase kinase-3β; RHOA: Ras homolog gene family, member A; ROCK: Rho-associated protein kinase.

GPR50 is an orphan GPCR without any known ligand. This has caused difficulty in understanding its function. However, many GPCRs have the ability of forming homodimers or heterodimers to exert functions in signalling and regulation, so looking for interacting partners of orphan GPCRs provides a strategy to investigate their potential roles. GPR50 can form heterodimers with its homologue MT1 to prevent melatonin binding, G-protein coupling and β-arrestin binding (Figure 1.2) (Levoye et al, 2006). Therefore, GPR50 has an inhibitory effect on MT1 signalling. In addition, truncating GPR50 CTD did not affect its heterodimerisation with MT1, but cleared of its antagonist effects on MT1 (Figure 1.2). This indicates that the CTD is required for GPR50 functioning.

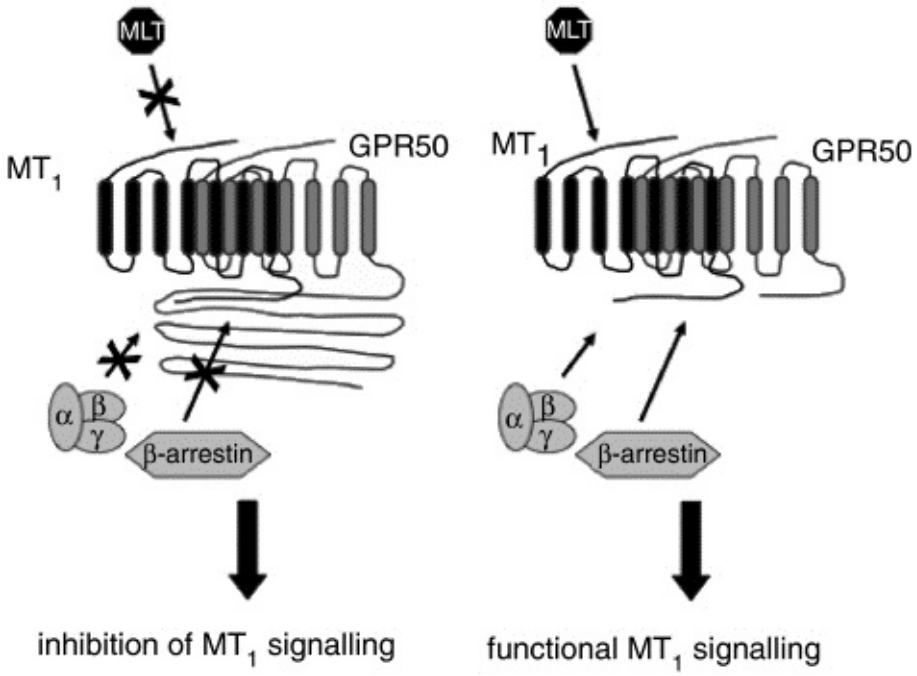

Figure 1.2 Regulation of MT1 signalling by heterodimerisation with GPR50. This picture was adapted from (Jockers et al, 2008). Forming heterodimers with GPR50 prevents high-affinity agonist binding, heterotrimeric G-protein coupling and β-arrestin binding to MT1. Forming heterodimers with C-terminal truncated GPR50 mutant does not affect MT1 functions. MT1, melatonin receotor 1; MLT, melatonin.

Two studies have been published using yeast two-hybrid analysis to identify putative GPR50 interactors (Grunewald et al, 2009; Li et al, 2011). Grunewald et al used two forms of human GPR50 C-terminal tail (GPR50: the insertion form; GPR50del: the deletion form) as baits in a yeast two-hybrid study and screened against a human adult brain cDNA library (Grunewald et al, 2009). 23 putative interaction proteins were identified, including genetic factors that are involved in four areas of interest: neurodevelopment (ABCA2, CDH8, PCDH9, PAX6, RTN3, RTN4, SHOT1), stress

response (SATB1, RTN4, ST13) and lipid metabolism (ABCA2, OSBP2, SREBP2), together with regulation of NMDA receptors and GABA transmission (PICK1, SLC12A5, MADD) (Table 1.1). An independent yeast two-hybrid study using the intracellular CTD of GPR50 as bait screened against a mouse testes cDNA library (Li et al, 2011) identified 11 putative GPR50 C-terminal interactors, which contained two overlapping factors with the first study: SNX5 and SNX6. These two proteins are components of the retromer complex, which is involved in the subcellular trafficking of a number of molecules including the neurotransmitter receptors (Choy et al, 2014). Here, I will introduce several putative interactors: RTN4, ABCA2 and TIP60 that have had follow-up studies, which can provide clues to the function of GPR50 in neuronal development and endocrine homeostasis.

Table 1.1 GPR50 yeast two-hybrid screen hits. The table was adapted from (Grunewald et al, 2009). Shown here are: symbol, full gene name and splice variant number, followed by the number of times each variant was captured by either the insertion (Ins), or the deletion (Del) form of the GPR50 C-terminal tail. PBS, predicted biological score.

Symbol	Gene	Variant	Ins	Del	Global PBS
RTN4	reticulon 4	variant 5	5	2	A
CDH8	cadherin 8	variant 2		2	C
FLJ14752 fis	PNISR			1	C
ABCA2	ATP-binding cassette, sub-family A (ABC1), member 2	variant 2	1	2	D
RTN4	reticulon 4	variant 3	2		D
RTN3	reticulon 3	variant 2		4	D
SHOT1	Shootin-1(KIAA1598)		4	1	D
OSBP2	oxysterol binding protein 2	variant 1		2	D
PCDH9	protocadherin 9	variant 2	1		D
SNX6	sorting nexin 6	variant 2	1		D
MADD	MAP-kinase activating death domain	variant 4		1	D
PSMA1	proteasome (prosome, macropain) subunit, alpha type, 1	variant 1		1	D
SATB1	special AT-rich sequence binding protein 1		1		D
KCC2	potassium-chloride cotransporter		1		D
SLC4A10	solute carrier family 4, sodium bicarbonate transporter-like, member 10		1		D
FLJ34306	LRRC37A3		2		D
PSMA1	proteasome (prosome, macropain) subunit, alpha type, 1	variant 1		1	D
SREBF2	sterol regulatory element binding transcription factor 2		4	10	E
SNX5	sorting nexin 5	variant 2	4	6	E
PICK1	protein interacting with PRKCA 1	variant 1		1	E
SPTAN1	spectrin, alpha, non-erythrocytic 1			2	E
ST13/HIP	suppression of tumorigenicity 13 / HSP70-interacting protein			3	E
CNST	consortin			2	E
PAX6	paired box gene 6 (aniridia, keratitis)	variant 2	2	1	E
DDX24	DEAD (Asp-Glu-Ala-Asp) box polypeptide 24		4	1	E
KIF5C	kinesin family member 5C	variant 15		1	N/A
PTPN5	protein tyrosine phosphatase, non-receptor type 5	variant 2	1		N/A
LOC653086	similar to RAN-binding protein 2-like 1 isoform 2 (RGPD8)	variant 12	1		N/A
GID: 1339887	EPB41L2 ? erythrocyte membrane protein 4.1-like 2				N/A

a) GPR50 and RTN4-A (Nogo-A)

Among the GPR50 interactors identified by yeast two-hybrid studies, reticulon family member, RTN4, also known as Nogo, was ranked as one of the most likely

interactors with the highest predicted biological score (PBS).

The *Nogo* gene generates three major products Nogo-A,-B and -C. All the Nogo isoforms share a reticulon-homology domain (RHD) of 188 amino acids at the C-terminal. Nogo-A is the longest isoform and is an inhibitor of axonal regeneration (GrandPre et al, 2000) and neurite outgrowth (Oertle et al, 2003). Its protein is mainly expressed in oligodendrocytes, but also in subpopulations of neurons. Nogo-A is found at synapses of mature pyramidal neurons in the hippocampus and plays a part in restricting short-term synaptic plasticity (Delekate et al, 2011).

Endogenous Gpr50 co-localised with Nogo-A at the synaptic spines in mouse primary cortical neurons and co-fractionated with Nogo-A in the postsynaptic densities of adult mouse brain (Grunewald et al, 2009; Grunewald et al, 2012). Overexpressed GPR50 and Nogo-A can be co-immunoprecipitated *in vitro*. This physical interaction appeared to cause functional effects, as GPR50 overexpression increased neurite length in neuronal cells, and attenuated the outgrowth inhibiting characteristics of Nogo-A overexpression (Grunewald et al, 2009). Although results from GPR50 knockdown experiments or the *in vivo* binding affinity of GPR50 to Nogo-A are yet to be determined, GPR50 may play an important role in neuronal development, by interfering with the function of Nogo-A.

b) GPR50 and ABCA2

ATP-binding cassette sub-family A member 2 (ABCA2), another putative interactor of GPR50 (Grunewald et al, 2009), is a member of the superfamily of ATP-binding cassette (ABC) transporters, and is predominantly expressed in the brain tissue (Vulevic et al, 2001; Zhao et al, 2000).

ABCA2 is implicated in oligodendrocyte maturation and neural development. Rat Abca2 was detected in late progenitor and immature oligodendrocytes, with an increasing level during the postnatal stage (Zhou et al, 2002). Persistent expression of Abca2 was seen in the grey matter and white matter throughout the spinal cord into adulthood, indicating a role in the onset of myelination in the CNS (Zhou et al, 2002). In mouse brain, Abca2 protein was found in the neurons of the cortex/hippocampus and translocated from neuronal soma to the axis of the neurite during neural differentiation (Broccardo et al, 2006). In addition, the *ABCA2* promoter sequence contains potential binding sites for transcription factors (NF-1,

ETF, EGR2 and WT1) that are involved in the regulation of neural differentiation (Kaminski et al, 2001).

Mouse mRNA levels of Gpr50 and Abca2 are correlated across a time span from E18 to week 5, and are more positively associated at the E18 time point when the activity of neuronal development is the highest (Grunewald et al, 2012). Thus, the role of GPR50 in the neuronal development might also be related to the function of ABCA2.

c) GPR50 and TIP60

A signalling role for GPR50 has been suggested by its connection with HIV-1 tat interactive protein, TIP60. The putative interaction between the two was identified in a yeast two-hybrid screen in mouse and confirmed by co-immunoprecipitation and co-localisation studies (Li et al, 2011).

TIP60 is a transcriptional co-activator with histone acetyltransferase (HAT) activity, which plays essential parts in chromatin remodelling (Hejna et al, 2008), transcription regulation (Nordentoft & Jorgensen, 2003), DNA repair (Hejna et al, 2008) and apoptosis (Ikura et al, 2000), normally by forming complexes with other factors. TIP60 is able to enhance the transcriptional activity of a number of transcription factors including nuclear hormone receptors (NHR), the Myc family of transcription factors, APP intracellular domain (AICD) and nuclear factor kappa light chain enhancer of activated B cells (NF-κB) (Sapountzi et al, 2006). In particular, a complex consisting of TIP60, AICD, the transcriptional protein Fe65 stimulates histone acetylation and regulates the expression of genes which are linked to microtubule dynamics (Muller et al, 2013) and apoptosis-driven neurodegeneration (Lorbeck, 2010). Hence, the role of GPR50 can be further speculated, through its interaction with multi-functional TIP60.

The expression of TIP60 or GPR50 augmented the expression of FK506-binding protein 5, which is a target of TIP60-activated glucocorticoid receptor (GR) signalling (Li et al, 2011). Co-expression of TIP60 and GPR50 enhanced this measure even more. Knockdown of either *TIP60* or *GPR50* attenuated this effect, suggesting a synergetic effect of the two in GR signalling. The target genes controlled by GR signalling include nuclear receptors, cytokines, peptidases, transcription factors, kinases, and enzymes, which are involved in diverse molecular processes of metabolism and biosynthesis (Phuc Le et al, 2005). Additionally, GR

functioning is sensitive to the levels of glucocorticoids, which are released in a circadian manner and in response to stress (Chung et al, 2011). Thus, the function of GPR50 may also be associated with factors required for maintaining endocrine homeostasis and stress response.

1.1.4 GPR50 knockout mice

The function of GPR50 can also be investigated by analysing the consequences of *GPR50* gene deletion or down-regulation. Several studies have revealed the phenotypes of GPR50 knockout (KO) mice. Here, I will summarise the key functions of GPR50 suggested by these studies.

a) Deletion of Gpr50 affects energy metabolism

GPR50 KO mice exhibited resistance to diet-induced obesity, which affects not the food intake but the food consumption efficiency, indicating an altered energy metabolism (Ivanova et al, 2008). Indeed, the attenuated weight gain of these mice resulted from a reduction in body fat. Moreover, GPR50 KO mice lost significantly less body weight during fasting when compared with wild-type mice, suggesting an altered response to negative energy balance. The intensity of wheel-running activity in GPR50 KO mice was enhanced, which means these animals were hyperactive, in line with elevated levels of oxygen consumption and carbon dioxide production. In summary, GPR50 loss-of-function leads to an alteration in the energy metabolic status and hyperactivity in mice.

b) Deletion of Gpr50 affects glucocorticoid receptor signalling

Circulating corticosterone levels were raised in the GPR50 KO mice, although this was not statistically significant (Ivanova et al, 2008). Therefore, these mice showed elevated stress levels, strengthening a possible link between GPR50 and GR signalling. GPR50 KO mice were not responsive to the stimulation of gluconeogenic pathways and were deprived of the inhibitory effect of glucocorticoid on proopiomelanocortin expression in the pituitary (Li et al, 2011). Thus, glucocorticoid-related functions are affected in mice lacking Gpr50, which may indicate that the function of GPR50 is related to GR signalling, probably via the interaction with TIP60.

c) Deletion of Gpr50 affects leptin signalling

Upon food deprivation, GPR50 KO mice consistently entered a state of torpor with dropped oxygen consumption rate and reduced nocturnal body temperature (Bechtold et al, 2012). Leptin is a nutrition responsive hormone primarily secreted by adipocytes (Zhang et al, 2005). As a regulator of food intake and energy expenditure, leptin is able to block torpor (Gavrilova et al, 1999). However, leptin administration failed to attenuate torpor in the GPR50 KO mice as in the wild-type control, suggesting that the leptin signalling system was affected when Gpr50 was lacking. This effect was specific to leptin-induced thermogenesis, but not food intake, which indicated that leptin efficacy in feeding and thermogenic actions were differentiated and that only the latter was modulated by GPR50. Moreover, Gpr50 expression in the DMH was reduced in leptin-deficient mice but restored to wild-type levels by leptin treatment, which was confirmed by *in vitro* promoter-driven luciferase assay (Bechtold et al, 2012). The association with leptin supports the role of GPR50 in the regulation of energy metabolism.

In summary, GPR50 plays an important role in neuronal development, neurotransmitter signalling and endocrine regulation. To further understand the functions of GPR50, in this thesis, I have studied the interaction between GPR50 and BACE1, as they have overlapping roles and both are implicated in mental illnesses. In the following sections I will introduce BACE1, the mental illnesses related to its functions and the existing evidence linking these two proteins.

1.2 Beta-site APP cleaving enzyme 1, BACE1

1.2.1 The discovery of BACE1

Beta-site APP cleaving enzyme 1 (BACE1), also formerly called memapsin 2 and aspartyl protease 2 (Aps2), was identified over a decade ago by five research groups in the search for the secretase responsible for the initiation of Alzheimer's disease (AD) pathology (Gavrilova et al, 1999; Hussain et al, 1999; Lin et al, 2000; Sinha et al, 1999; Vassar et al, 1999; Yan et al, 1999).

The gene for human BACE1 is located on chromosome 11q23.3. BACE1 protein, consisting of 501 amino acids, is a type-I membrane-associated aspartic protease that exhibits all the previously determined characteristics of β-secretase. The accumulation of amyloid-β (Aβ) plaques in the brain is one of the hallmarks of AD.

Research has revealed that BACE1 is the prerequisite for β-cleavage of amyloid precursor protein (APP) *in vivo* and acts as the key rate-limiting enzyme of Aβ deposition (Sinha et al, 1999). Overexpression of BACE1 leads to increased levels of Aβ (Bodendorf et al, 2002), whereas deletion of *BACE1* results in little or no Aβ generation (Luo et al, 2001).

Other non-APP substrates include the APP homolog proteins APLP1 and APLP2 (Li & Sudhof, 2004), neuregulins (NRG) (Hu et al, 2008), neural cell adhesion molecules (Zhou et al, 2012), β-galactoside α2,6-sialyltransferase I (ST6Gal-I) (Sugimoto et al, 2007), P-selectin glycoprotein ligand-1 (PSGL-1) (Lichtenthaler et al, 2003), low-density lipoprotein receptor-related protein (LRP) (von Arnim et al, 2005), the voltage-gated sodium channel (Nav1) β subunits (Navβ2/4) (Gersbacher et al, 2010; Miyazaki et al, 2007), etc. BACE1 mediated cleavage of these proteins may activate certain signal transduction pathways, indicating that BACE1 is an important enzyme with multifunctional interactions. Thus, the regulation of BACE1 expression may be central to diverse physiological events far beyond the pathology of AD.

1.2.2 BACE1 expression

BACE1 mRNA is found with highest expression levels in the pancreas, with moderate levels in the brain, and with low levels in most other peripheral tissues (Vassar et al, 1999; Yan et al, 1999). However, the β-secretase activity is high only in the brain, but almost undetectable in the pancreas (Sinha et al, 1999). This suggests that BACE1 cleavage activity is more related to brain functions.

1.2.3 The trafficking of BACE1

The activity of BACE1 is regulated by its subcellular localisation. BACE1 is initially synthesised as a pro-peptide (proBACE1) in the endoplasmic reticulum (ER), where glycosylation and transient acetylation take place co-translationally, yielding an immature BACE1. ProBACE1 is immediately subjected to addition of complex carbohydrates and removal of the BACE1 pro-domain by furin convertases, producing the mature form. This process mainly occurs in the Golgi compartment. N-glycosylation is known to regulate the enzymatic activity of BACE1 (Charlwood et al, 2001). Therefore, even though proBACE1 can exhibit a minor level of β-secretase activity (Klaver et al, 2010), the catalytic activity of BACE1 is greatly enhanced after maturation (Vassar et al, 2009). The co-localisation of BACE1 with

substrate APP has been reported to occur at the plasma membrane, the endosomal system and the trans-Golgi network (TGN), but there is still controversy regarding the subcellular compartments where BACE1 acts to cleave APP. It is also reported that BACE1 cycles between the cell surface and the endosomal system, and becomes activated during its cellular trafficking (Shimizu et al, 2008). Moreover, as BACE1 activity is optimal in an acidic environment, the activation of substrate cleavage by BACE1 is theoretically most efficient within the TGN and the early endosomes.

Transporters that are able to change the intracellular localisation of BACE1 are thought to regulate β-secretase activity, thus altering the levels of its cleavage products. Regulatory mechanism of BACE1 trafficking can be summarised into three categories. Each mechanism will be elucidated with a corresponding regulator respectively as follows.

a) Regulators retain BACE1 within the ER

Overexpression of reticulon protein RTN3, which can act as an inhibitor of BACE1 activity, significantly increased the retention of BACE1 within the ER, the pH environment of which is neutral, so not optimal for BACE1 activity (He et al, 2004; Shi et al, 2009). *In vivo*, this enhanced ER retention resulted in reduced levels of an intermediate BACE1 cleavage product from APP in the cortical regions of transgenic mice overexpressing RTN3.

b) Regulators sort BACE1 into compartments for optimal cleavage activity

The retromer component sorting nexin 6 (SNX6) is able to modulate BACE1 levels in the TGN (Okada et al, 2010). Reducing SNX6 in cultured cells enhanced the retrograde transport of BACE1 from cell surface to the TGN. This measure increased BACE1-mediated APP cleavage, leading to an increase of Aβ production. On the contrary, SNX6 overexpression decreased the APP cleavage by BACE1, resulting in a reduction in Aβ levels.

c) Regulators transport BACE1 to the lysosomes for degradation

Golgi-localised γ-ear-containing ADP ribosylation factor-binding (GGA) proteins bind directly to the DXXLL motif of BACE1 C-terminal via a VHL domain and regulate the sorting of BACE1 among different subcellular compartments in a BACE1 phosphorylation-dependent manner (Wahle et al, 2005). Depletion or ectopic expression of GGA3 resulted in increased BACE1 levels and activity because of

impaired lysosomal degradation, while the overexpression of GGA3 reduced the levels of BACE1 and Aβ peptides (Kang et al, 2010; Tesco et al, 2007).

The intracellular trafficking system of BACE1 has been widely investigated with a view to further understanding its function in the β-secretase pathway that is responsible for Aβ generation. However, there is a group of functional substrates apart from APP, which may induce BACE1 activity in distinct subcellular sites.

Here, I will introduce several brain disease-associated BACE1 substrates, including APP and homologues, neuregulin 1 and homologues, and neural cell adhesion molecules, which illustrate the potential role of BACE1 in neuronal development, myelination and synaptic functions.

1.2.4 Main BACE1 substrates

a) Amyloid precursor protein (APP) and homologues

In human, the APP gene is located on chromosome 21. Alternative splicing generates at least 11 isoforms of APP, ranging from 365 to 770 amino acids in length. APP protein is membrane-integrated, and expressed in the brain and most peripheral tissues. Certain isoforms are the major Aβ peptide producing proteins: APP695, APP751 and APP770 (Zheng & Koo, 2006). APP695 is primarily expressed in neurons, while APP751 and APP770 are found mostly in non-neuronal glial cells (LeBlanc et al, 1991). Changes in the ratio of neuronal APP isoforms have been suggested to be associated with AD (Johnson et al, 1990; Matsui et al, 2007).

Apart from being the precursor molecule, the proteolysis of which generates Aβ, APP has been implicated in normal biological functions. The other end product of APP generated by BACE1 cleavage, AICD, is capable of nuclear signalling (Konietzko, 2012). APP itself is required for the axon/dendrite outgrowth in neurons (Allinquant et al, 1995; Herard et al, 2006; Perez et al, 1997), but human APP in *Drosophila* resulted in synaptic abnormalities in the larval neuromuscular junction (Mhatre et al, 2014). APP prevents iron accumulation and oxidative stress *in vivo*, while the ferroxidase activity of APP is inhibited by zinc in AD (Duce et al, 2010). Thus, APP may act as a regulator of neuronal development, synapse formation, and iron export.

Amyloid-β precursor-like proteins, APLP1 and APLP2 are the two homolog molecules of APP, and are also cleaved by BACE1. The sites required for β/γ-

secretase cleavage of APP are not conserved in APLP1 and APLP2, thus they lack the capacity to generate Aβ peptides (Li & Sudhof, 2004).

Loss-of-function studies in mice indicate that APP and APLP1/2 have overlapping or synergetic functions that are essential to normal metabolism and neurobehavioural development during the early postnatal stage (Heber et al, 2000; Herms et al, 2004; Phinney et al, 1999; Senechal et al, 2008; von Koch et al, 1997; Weyer et al, 2011). Functional investigation reveals that all three APP family members are up-regulated during induced neuronal differentiation (Adlerz et al, 2003) and are capable of interfering in the function of the regulators of synaptic vesicle exocytosis (Okamoto & Sudhof, 1997; Orcholski et al, 2011; Swistowski et al, 2009), neuronal plasticity (Ashley et al, 2005) and signalling (Biederer et al, 2002). Thus, BACE1 cleavage may control the regular turnover of APP/APLP1/APLP2, thus regulating some important bio-physiological processes, such as neuronal development and synaptic functions.

b) Neuregulin 1 (NRG1) and homologues

NRG1 is one of four proteins in the neuregulin family that act on the receptors of epidermal growth factor (EGF) family. NRG1 contains an EGF-like domain which is released upon cleavage (possibly by BACE1) and signals by stimulating ErbB receptor tyrosine kinases. *NRG1* gene encodes at least 33 isoforms distinguished by six different membrane topologies (types I–VI) (Mei & Xiong, 2008), which allows it to perform various functions, including regulating the normal development of the nervous system (Britsch, 2007) and the maintenance of heart integrity (Liu et al, 2006).

Studies in BACE1 knockout mice revealed that type III NRG1 and type I NRG1 are BACE1 substrates (Hu et al, 2006; Willem et al, 2006). Axonal type III NRG1 in the peripheral nervous system (PNS) mediates the generation of Schwann cell precursors, their subsequent differentiation and migration along the axons of neurons, and also adjusts the thickness and length of myelin sheaths to match the axon calibre, through regulating the membrane growth of Schwann cells (Birchmeier & Nave, 2008; Nave & Salzer, 2006; Perlin et al, 2011). In the CNS, type III NRG1 promotes the myelination of oligodendrocytes without affecting their differentiation (Taveggia et al, 2008). Schwann cell-derived type I NRG1 has been shown to be more efficient than the type III in the activation of the regeneration and

remyelination processes after peripheral nerve injury (Stassart et al, 2013).

NRG1 homologue, NRG3 was also identified as a BACE1 substrate in loss-of-function studies of BACE1 (Hu et al, 2008). NRG3 binds to the extracellular domain of ErbB4, which stimulates the tyrosine phosphorylation of this receptor (Zhang et al, 1997). The primary role of NRG3 has been identified in the development of epidermal organs including the skin, hair, and mammary glands (Panchal et al, 2007). Moreover, recent data showed that the expression level of Nrg3 is associated with the impulsive response in the medial prefrontal cortex of mice (Loos et al, 2014).

In summary, BACE1 may contribute to the development and myelination of CNS and PNS, as a sheddase that can release the functional domain of NRG1 and NRG3.

c) Neural cell adhesion molecules (CAMs)

Ectodomain shedding is the first step for activating the expression and function of specific molecules on the cell surface (Hayashida et al, 2010). This process is normally mediated by certain sheddases including ADAM and BACE1. Recently, BACE1 was identified as a sheddase of a variety of neural CAMs, exemplified by seizure related protein 6 (SEZ6), neuronal cell adhesion molecule L1, close homolog of L1 (CHL1) and contactin-2 (Kuhn et al, 2012). These CAMs are widely expressed in the developing nervous system, especially in the neurons undergoing growth (Hillenbrand et al, 1999; Osaki et al, 2011; Zuellig et al, 1992). The expression and function of neural CAMs are closely related to neuronal functions, including neural cell adhesion/migration, neurite outgrowth, axon projection, dendritic orientation, neuron proliferation/differentiation and synapse formation (Baeriswyl & Stoeckli, 2008; Demyanenko et al, 2004; Dihne et al, 2003; Godenschwege et al, 2006; Gunnersen et al, 2007; Maretzky et al, 2005; Mechtersheimer et al, 2001; Montag-Sallaz et al, 2002; Wolman et al, 2008). These processes are important in the maintenance of normal learning and memory (Savvaki et al, 2008; Stogmann et al, 2013).

The finding that ectodomain shedding of neural CAMs can be mediated by BACE1 points to a central function of this sheddase in the development and correct wiring of the normal brain, far more than its involvement in Aβ deposition in the diseased brain.

The putative functions of BACE1 in neuronal development and myelination have

also been suggested by investigation *in vivo* using mice with overexpression of BACE1 or deletion of Bace1 described below.

1.2.5 BACE1 overexpression transgenic mice

The transgenic mice with overexpressed human BACE1 (BACE1-tg mice) showed a strictly neuronal expression of BACE1 protein mainly in the deep cortical layers, hippocampus and colliculi, as well as Purkinje cells in the cerebellum (Mohajeri et al, 2004). In BACE1-tg mice, intracellular deposition of Aβ but no amyloid plaque was seen at the age of 14 months in BACE1 immunoreactive neurons of the hippocampus, the temporal cortex and the amygdala.

The phenotypes of BACE1-tg mice are dependent on the dose of BACE1 overexpression (Harrison et al, 2003; Rockenstein et al, 2005). Weakness and spasticity of the hind limbs as well as learning deficits have been reported only in robust BACE1 expresser lines (Rockenstein et al, 2005). The BACE1-tg mice with impairments were further revealed as having degeneration of neurons in the neocortex/hippocampus and degradation of myelin sheaths, which might be related to a diminished cAMP/PKA/CREB pathway (Chen et al, 2012b). In addition, the neurotransmitter systems were changed in BACE1-tg mice, represented by an overproduction of serotonin in the cerebellum, the hippocampus, the hypothalamus, the nucleus accumbens and the caudate striatum, as well as a disorganised dopamine turnover with an increase in the hypothalamus, the striatum but a decrease in the hippocampus (Harrison et al, 2003). Thus, BACE1 is implicated in the regulation of neurodegeneration, myelination and neurotransmission, independent of Aβ deposition.

1.2.6 BACE1 knockout mice

BACE1 loss-of-function studies are very useful to discover new BACE1 substrates, such as NRGs. Investigations focusing on different phenotypes of BACE1 knockout (KO) mice may help to clarify the specific functions of certain substrates. The important features of these mice related to my thesis will be introduced as follows.

a) Amyloid clearance

BACE1 KO mice showed abrogated production of Aβ peptides (Luo et al, 2001; Roberds et al, 2001). BACE1 KO/APP-tg mice did not develop amyloid plaques even

in aged animals, suggesting that BACE1 dosage is essential to Aβ deposition. These observations confirmed the key position of BACE1 in the AD pathology.

b) Phenotypes

BACE1 KO mice were initially described as healthy, but later studies revealed that these animals displayed a higher mortality rate during early life, hyperactivity and age-dependent cognitive deficits (Dominguez et al, 2005; Laird et al, 2005). Importantly, BACE1 KO mice shared a number of behavioural traits that resemble those found in $NRG1^{+/-}$ mice (mice with one copy of NRG1 type III gene), such as impaired prepulse inhibition, hyperactivity, supersensitivity to a psychostimulant, a lack of social recognition, and deficits in working and inhibitory avoidance memories, which are referred to as schizophrenia-like phenotypes (Savonenko et al, 2008).

c) Hypomyelination and neural deficits

Another significant abnormality in BACE1 KO mice that has been highlighted is an altered myelination mechanism in the CNS and the PNS. The process of myelination was slightly delayed and myelin thickness of hippocampal/optical/sciatic nerves was markedly reduced in these mice, indicating that BACE1 gene deletion causes hypomyelination (Hu et al, 2008; Hu et al, 2006). Compared to wild-type mice, lower levels of myelin basic protein and proteolipid protein were detected in both developing and adult brains of BACE1 KO mice. This process appeared to stem from decreased levels of proteolytically cleaved NRG1 and consequently reduced activation of down-stream Akt phosphorylation, which regulates the gene expression of myelin proteins (Hu et al, 2013b). Akt signalling in myelination is CNS-specific (Flores et al, 2008; Hu et al, 2006) and increasing Akt activity in oligodendrocytes is sufficient to reverse the hypomyelination phenotype in BACE1 KO mice (Hu et al, 2013b).

The CA1 and CA3 regions of hippocampus in BACE1 KO mice exhibited alterations in mechanisms of presynaptic release, synaptic transmission and synaptic plasticity, indicating that BACE1 is associated with synapse functions (Laird et al, 2005; Wang et al, 2008a). The role of synaptic NRG1/ErbB4 has been implicated in the maturation and maintenance of excitatory spines in the hippocampus (Li et al, 2007). BACE1 KO mice exhibited lower spine density, decreased number of mature spines

and altered spine morphology of CA1 pyramidal neurons, which is in line with a reduced level of ErbB4 in the PSD95-associated pool (Li et al, 2007).

Collectively, the hypomyelination and neural deficient phenotypes observed in BACE1 KO mice correlate with a disturbed NRG1/ErbB4 signalling pathway, which has been suggested in schizophrenia (Nicodemus et al, 2006; Norton et al, 2006). Furthermore, another group of functional substrates, neural CAMs which are required for neurogenesis and synaptogenesis, may also be indicative of the negative effects upon BACE1 abolishment in the nervous system.

d) Altered signalling system

Enhanced glucose tolerance and increased insulin sensitivity were seen in BACE1 KO mice compared with their wild-type littermates (Meakin et al, 2012). On a high-fat diet, these mice retained their ability to dispose glucose and also their insulin sensitivity, unlike the insulin resistance found in wild-type mice. Therefore, inhibition of BACE1 in mice appears to improve glucose homeostasis.

BACE1 KO mice had reduced body weight due to decreased adiposity when compared to the wild-type control, and like GPR50 KO mice, were resistant to high-fat diet-induced obesity, indicated by a decreased level of serum leptin (Meakin et al, 2012). These mice had higher but less efficient energy expenditure, suggested by higher resting metabolic rate/respiratory quotient but unchanged faeces mass. This observation was explained by an elevated thermogenesis of BACE1 KO mice. Further studies revealed that upon BACE1 deletion, the mice had increased leptin sensitivity (Meakin, 2013). This report suggests that BACE1 is involved in the modulation of hypothalamic leptin function in mice. In addition, a significant increased level of serum corticosterone was observed in BACE1 KO mice on a high-fat diet, suggesting a stress response, even though no difference was detected in the locomotor activity.

Interestingly, the metabolic phenotypes observed in BACE1 KO mice are very similar to those in GPR50 KO mice. Therefore, BACE1 and GPR50 might have cooperative functions in body weight maintenance and thermogenesis that are related to leptin signalling.

In summary, BACE1 KO mice studies indicate that complete abolishment of BACE1 activity may have deleterious side effects, thus future research should be alert to the

potential mechanism that may occur with BACE1 inhibitors designed to ameliorate Aβ deposition in AD. Aside from being the key enzyme of Aβ generation, BACE1 is implicated in the neuronal development, myelination, synaptic functions and neurotransmitter signalling.

The functions of GPR50 and BACE1 in neural activities and signalling pathways seem to be overlapping, suggesting a correlation between the two under normal conditions. Their shared roles could be co-regulated in mental illnesses, and the alteration of their correlation will provide clues to the understanding of certain altered physiological processes during disease onset and progression.

1.3 Mental illnesses

Here I will introduce the three aforementioned mentally related illnesses that may link to GPR50 and BACE1.

1.3.1 Bipolar disorder

a) Symptoms of bipolar disorder

Bipolar disorder (BD) has an increasing morbidity and mortality, which makes the disease highly recognised as a serious psychiatric disorder (Martinowich et al, 2009). Symptoms of patients suffering from BD are characterised by two extremes of mood swings between mania and depression, which are accompanied by eating and sleeping disorders. People with BD may have episodes of depression more regularly than mania, or mania more often than depression. Between episodes of depression and mania, periods of "normal" mood are sometimes but not always seen. These conditions may recur after medical treatment, and will probably leave residual effects, such as brain functional impairments. Studies of computerised tomography and magnetic resonance imaging frequently reported that compared with healthy controls, BD patients have enlarged lateral ventricles and third ventricles, more cortical sulcal prominence, and increased white matter hyperintensities (Ahn et al, 2004; Goodwin et al, 2007; Tighe et al, 2012).

b) Heredity of bipolar disorder

The aetiology of BD is poorly investigated, but heritable factors have been proven to be influential. Twin studies reported that the concordance rate for BD was significantly greater among monozygotic twins (78%) than among dizygotic twins

(29%), suggesting a heritability of 63% (Smoller & Finn, 2003). Adoption studies showed that biological relatives of BD patients were significantly more likely to suffer from this disorder than adoptive relatives (Taylor et al, 2002). Furthermore, the recurrence risk for BD in first-degree relatives of BD patients was approximately 9%, nearly 10 times that of the general population (Barnett & Smoller, 2009). However, a concordance rate of less than 100% among monozygotic twins also indicates the involvement of environmental factors.

Despite the abundant evidence of a genetic contribution to BD, there are no specific candidate genes that are the causation factors alone. The pathogenesis of BD is multifactorial, which results from a combination of risk genes or potential proteins, including GPR50 (Xq28), CUX2 (12q23-q24), ANK3 (10q21), CACNA1C (12p13), TRPM2 (21q22.3), and NAPG (18p11) (Ferreira et al, 2008; Glaser et al, 2005; Thomson et al, 2005; Weller et al, 2006; Xu et al, 2009). With an increasing number of genome-wide association study (GWAS) ongoing, there are new genes added to the list of risk loci for BD, such as recently discovered ODZ4 (11q14.1), TRANK1 (3p22.2) and ADCY2 (5p15.31) (Chen et al, 2013; Muhleisen et al, 2014; Psychiatric, 2011). The proteins of these genes have important functions in neuronal development, ion conduction, inflammation, transcription, cell adhesion and signalling cascade.

In particular, multiple polymorphisms of *GPR50* gene were found associated with BD and major depressive disorder (Macintyre et al, 2010; Thomson et al, 2005). The variant within *GPR50* exon 2 that results in the deletion isoform (ΔTTGH) was found associated with an increased risk of BD, especially in female subjects, and was correlated with the age of onset, number of episodes, hypomanic symptoms, and initial thinking time in a highly phenotyped subgroup of women with early-onset major depressive disorder. Apart from one single-nucleotide polymorphism (SNP) Thr532Ala which is in complete linkage disequilibrium with the variant ΔTTGH, another SNP Val606Ile within exon 2 was also identified as a female-specific risk factor for major depressive disorder (Thomson et al, 2005) (Figure 1.3). However, two studies investigating Swedish BD patients and Hungarian children/adolescents with mood disorders failed to replicate the GPR50 insertion/deletion polymorphism findings (Alaerts et al, 2006; Feng et al, 2007). The failure to replicate may be due to the genetic heterogeneity of the populations or the small sample sizes. Additionally, the three psychiatric disorder-associated variants of *GPR50* were also associated with

higher fasting circulating triglyceride levels (Bhattacharyya et al, 2006), which might reflect a predisposition to metabolic syndrome of these diseases.

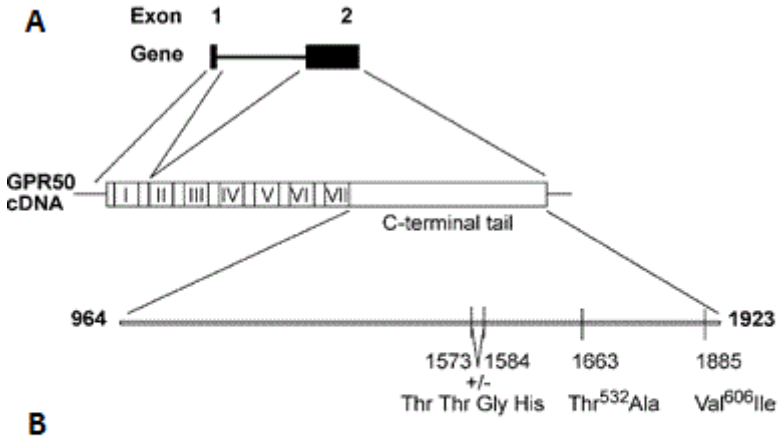

B

Variant Name	Nucleotide change
Δ502-505	Deletion of 1573 → 1584 inclusive (ACC ACT GGC CAC)
Thr^{532}Ala	1663 A → G
Val^{606}Ile	1885 G → A

Figure 1.3 GPR50 gene structure and position of polymorphisms. The figure was adapted from (Thomson et al, 2005). A) The seven transmembrane domains of GPR50 are denoted by Roman numerals I-VII. B) The nucleotide changes of the polymorphisms resulting in alterations of the amino acid sequence.

Elsewhere, NRG1 is a susceptibility gene associated with the mood-incongruent psychotic features of BD (Prata et al, 2009). And this points to BACE1 as a related factor, because NRG1 is a substrate of BACE1. In conclusion, the functions of both GPR50 and BACE1 may be related to the development of this mental disorder.

1.3.2 Schizophrenia

a) Symptoms of schizophrenia

Changes in thinking and behaviour are the most obvious signs of schizophrenia, and different patients can experience symptoms in different ways. The symptoms of schizophrenia are usually classified into two categories:

1) Positive symptoms: such as hallucinations or delusions.
2) Negative symptoms: usually seen with a lack of social function that is expected in a healthy person, for example, lack of emotion, apathetic behaviour, disorganised speech and cognitive deficits.

The first signs of schizophrenia, such as becoming socially withdrawn and unresponsive to communication, can be difficult to identify, as these symptoms often

develop during adolescence and can be mistaken for an adolescent rebellious period. The onset of symptoms can start from young adulthood, with a global prevalence of up to 1% (Zhang et al, 2013).

Schizophrenia patients on average have larger intracranial cerebrospinal fluid (CSF) volumes, including the enlargement of lateral ventricles and cortical sulci, as well as abnormalities in grey matter volumes and white matter volumes (Zipursky et al, 2013). Therefore, like BD, schizophrenia is considered as a disease of brain, but this notion is challenged by some researchers (Williams, 2012).

b) Heredity of schizophrenia

Like BD, there is strong but indirect evidence from family studies and twin studies that schizophrenia is highly heritable. The risk of developing schizophrenia in a random individual, in an individual with one affected first degree relative or two affected first degree relatives is on average 1%, 13% and 46% respectively. The monozygotic twin of a person with schizophrenia has a risk of 48% of developing this disorder, nearly three times that of a dizygotic twin, which is 17% (Cardno & Gottesman, 2000; Gottesman & Moldin, 1997). Schizophrenia endophenotypes result from the additive effects of alteration in multiple genes, combined with environmental factors. Thus, schizophrenia is regarded as a polygenic disorder. This also explains why different schizophrenia patients manifest with different sets of symptoms. The estimated heritability of schizophrenia ranges from 41% to 87% (Cannon et al, 1998), which has directed researchers to identify candidate genes responsible for or related to this psychiatric disorder.

GWAS studies showed that schizophrenia is strongly associated with deletions in chromosomes 1q21.1, 15q13.3, and 22q11.21, duplications in 16p11.2, and SNPs in multiple chromosomes (Levinson et al, 2011; Ripke et al, 2013). The most recent GWAS study reported 128 linkage-disequilibrium-independent SNPs spanning 108 physically distinct genomic loci, 83 of which have not been implicated in schizophrenia previously (Schizophrenia Working Group of the Psychiatric Genomics, 2014). In general, the majority of the risk variants for schizophrenia have small effects on the risk increase (Ripke et al, 2013).

Among the risk genes, an SNP in *NRG1* explained 6.9% of the genetic variation in the spatial processing function of schizophrenia subjects (Greenwood et al, 2011).

The discovery of this gene strengthened the importance of investigating BACE1, because the function of NRG1 can be mediated via its cleavage by this enzyme. Elsewhere, an intronic SNP of *GPR50* rs2072621 was identified in female schizophrenia patients of a Scottish group (Thomson et al, 2005). The sample size of this investigation was very small, and there are no replicate studies. However, it remains interesting to study the involvement of GPR50 in schizophrenia, as a strong candidate gene *RGS4* (regulator of G protein signalling 4) encodes a regulator of GPR50 expression (Vrajova et al, 2011). Besides NRG1 and GPR50, there are a number of other candidate genes for schizophrenia that may also be associated with BD, such as RGS4, G72, DISC1, NCAM1, DAO, GRM3, GRM4, GRIN2B, MLC1, SYNGR1, SLC12A6, CACNA1C as well as recently identified NDST3 and TSNARE1 (Kato, 2007; Lencz et al, 2013; Psychiatric, 2011; Sleiman et al, 2013). A statistical estimation study showed that the genetic correlation calculated as SNP-based coheritability was high between schizophrenia and bipolar disorder ($r_g = 0.68 \pm 0.04$ standard error, s.e.), compared to moderately correlated schizophrenia and major depressive disorder (0.43 ± 0.06 s.e.) or bipolar disorder and major depressive disorder (0.47 ± 0.06 s.e.) (Cross-Disorder Group of the Psychiatric Genomics et al, 2013).

1.3.3 Alzheimer's disease

Alzheimer's disease (AD) is the most common form of dementia and is one of the debilitating illnesses that affect mainly elderly people. It is still controversial whether AD can be viewed as a mental illness, due to its specific post-mortem diagnosis, different treatment approaches, as well as the societal stigma of mental illnesses (Herro, 2011; Sivak, 2010). In the fifth edition of diagnostic and statistical manual of mental disorders (DSM-5) updated in 2013, dementias were renamed as neurocognitive disorders, with various degrees of severity (APA, 2013). Because AD is a memory-associated disease with brain dysfunction, in this thesis, I regard AD as a mentally related illness or brain disease, which has been mentioned in a previous paragraph.

a) Symptoms of Alzheimer's disease

The early signs of AD are characterised by gradually declining memory and functional ability. As the disease advances, symptoms increase ranging from cerebral dysfunction to unpredictable behaviours, including confusion, irritability

and aggression, mood swings, language breakdown, long-term memory loss, declining sense and hallucinations. Gradually, the body loses all of the necessary functions, which eventually leads to death (Bird, 1993).

b) Pathology of Alzheimer's disease

There is at present no cure for AD, but gene-related studies have revealed significant evidence about the pathogenic mechanism of this dementia. The hallmarks of AD brain include overproduction of amyloid plaques, accumulation of neurofibrillary tangles and neuronal degeneration, which results in a reduced brain volume.

The main component of amyloid plaques is Aβ peptide, which is derived from the sequential proteolytic cleavage of APP by β-secretase (BACE1) and γ-secretase, known as the amyloidogenic pathway (Figure 1.4). BACE1 cleaves APP into two fragments: a secreted APP ectodomain (APPsβ) and a membrane-bound carboxyl terminal fragment (CTF), C99. Downstream γ-secretase cleaves C99 into Aβ peptides (Aβ40 or Aβ42) together with an APP intracellular domain (AICD) (Cole & Vassar, 2007). Aβ peptide liberation can be eliminated by the non-amyloidogenic pathway, which cleaves APP within its Aβ peptide domain by α-secretase, generating APPsα and C83 instead. C83 is proteolysed by γ-secretase, releasing non-toxic P3 and the AICD. Thus, BACE1 is a key enzyme in the process of AD development.

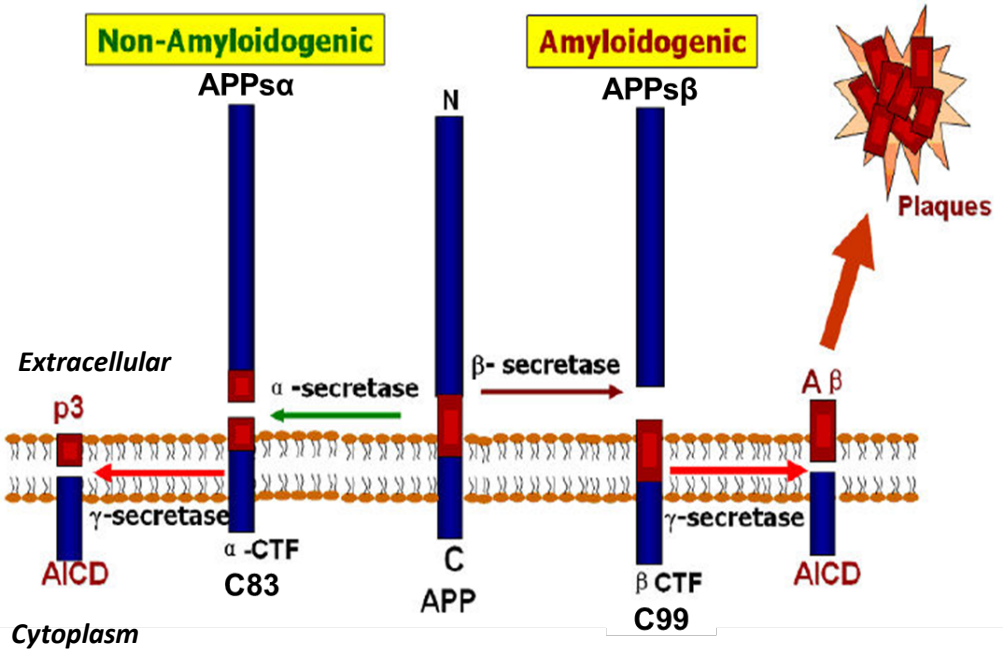

Figure 1.4 The proteolytic processing of APP. This figure was adapted from (Zhang, 2009). AICD, APP intracellular domain; CTF, carboxyl terminal fragment.

Neurofibrillary tangles are formed by hyperphosphorylation of a microtubule-associated protein tau (Goedert et al, 1988). In general, it is believed that tau binds to microtubules and plays a part in their formation and stabilisation. When tau is hyperphosphorylated, it is unable to bind to the microtubules, which become unstable and disintegrate. The unbound tau aggregates in an insoluble form called neurofibrillary tangles. The precise mechanism of tangle formation is not completely understood, and it is still controversial whether tangles are a primary causative factor in AD or play a more peripheral role (Lee et al, 2005).

The neurodegeneration mainly refers to loss of neurons and reduced synaptic density in certain brain areas, which are the contributors to the cortical atrophy of AD brain. The hippocampus formation is the most striking region with neuronal loss in AD subjects (West et al, 1994). The extent of the pyramidal cell loss in the hippocampus progresses with the severity of AD (Rossler et al, 2002). The hippocampus of normal aging individuals and AD patients was observed with an increase of GPR50-immunoreactive cells undergoing degeneration in the dentate gyrus sub-region (Hamouda et al, 2007). Other afflicted brain areas include the entorhinal cortex, several neocortical areas (superior temporal sulcus, prefrontal cortex) and some subcortical brain structures (amygdala, Edinger-Westphal nucleus, substantia nigra) (Zilkova et al, 2006). Many regions of the neocortex and the hippocampus of AD brain demonstrate a decline in synaptic density (Scheff & Price, 2006). A greater loss of synapses than that of neurons was found in the temporal cortex and the frontal cortex, suggesting that synapse loss may precede neuronal loss in AD (Davies et al, 1987). In addition, synapse loss is the major pathological correlate of cognitive dysfunction in AD (Terry et al, 1991).

There are multiple reasons that can lead to the development of AD. Yet in this thesis, regarding to the involvement of BACE1, I sought to focus on the regulation of its cleavage activity and function in AD pathology.

c) Heredity of Alzheimer's disease

AD has a strong genetic background, involving two categories of genes that have been identified as playing a role in affecting whether a person develops AD:

1) Risk genes increase the likelihood of developing AD, but are not causative of this disease.

These genes are normally risk factors for the commonly seen late-onset AD in people over 65 years old. The most influential risk gene for AD is apolipoprotein E-e4 (*APOE-e4*), which is a factor found in 20-25% of AD cases (Sleegers et al, 2010). Other known gene risk factors for AD include PICALM, CLU, CR1, BIN1, MS4A, CD2AP, EPHA1, ABCA7, SORL1 and TREM2 (Guerreiro et al, 2013; Harold et al, 2009; Hollingworth et al, 2011; Jonsson et al, 2013; Naj et al, 2011). A recent GWAS study added 11 new risk factors (HLA-DRB5/HLA0DRB1, PTK2B, SLC24A4-0RING3, DSG2, INPP5D, MEF2C, NME8, ZCWPW1, CELF1, FERMT2 and CASS4) to a growing list of gene variants that are associated with the onset and progression of late-onset AD (Lambert et al, 2014). These genes relate AD to multiple biological pathways, including amyloid and tau pathways, the immune response and inflammation, cell migration, lipid transport and endocytosis, hippocampal synaptic function, the cytoskeleton and axonal transport, as well as myeloid and microglial cell functions.

2) Deterministic genes directly cause AD development, and people who inherit the variations of these genes will develop this disorder.

Deterministic genes lead to "familial Alzheimer's disease (FAD)", because many family members in multiple generations are affected (St George-Hyslop, 1998). Symptoms of FAD develop before age 65 in most cases, and may appear as early as people's 30s or 40s (Harvey et al, 2003). Variations of deterministic AD genes have been found in only a few hundred extended families worldwide, accounting for less than 6% of all AD cases (Hausner et al, 2014).

To date, 12 AD-related mutations have been discovered in the APP gene, 69 mutations in the presenillin-1 (PS-1) gene and 5 mutations in the presenillin-2 (PS-2) gene (Holmes, 2002). Researchers suggest that the different mutations in these three genes lead to a common result, the enhanced deposition of Aβ (Holmes, 2002), which is an event mediated by the protein investigated in this thesis, BACE1. Importantly, even though these mutations only account for around 10% of FAD cases, the prevention of AD heredity is essential.

Twin studies have shown that the heritability for AD was estimated to be 58%-79% (Gatz et al, 2006). Thus, investigations on the function of related genes, such as the key AD mediators (i.e. BACE1) and potential phenotype indicators (i.e. GPR50) are indispensable.

1.3.4 A summary of mental illness genetics

As described earlier, all the three brain diseases have a genetic component. It is important to focus on investigating the functions of putative risk factors, which requires studies of the cell biology, the functional characteristics and the regulation system of those potential proteins involved. Importantly, as the major forms of psychosis seem to have overlapping risk genes, to investigate the functions of these factors may provide early clues about the role of a shared mechanism during the development of several psychiatric conditions, and may help to understand how and why individual patients develop certain symptoms. Such an understanding will eventually lead to the generation of suitable drugs for these conditions.

1.4 The possible links between GPR50 and BACE1

Summarised from earlier introductions, GPR50 and BACE1 are among such factors that are related to the three major brain diseases. GPR50 is a risk gene for BD and schizophrenia, and has region-specific expression related to neurodegeneration in AD patients. BACE1 is a key enzyme of Aβ generation in AD brains and also plays an essential part in the dysfunctional NRG1 signalling system of BD/schizophrenia. Thus, in this thesis, I focused on the functional implications of the two proteins and their interaction. Interestingly, there are potential links of the two factors in terms of their functions. GPR50 and BACE1 share overlapping predicted functions including neurodevelopment, such as neurite outgrowth and synaptogenesis, myelination and endocrine regulation.

Here, I introduce two types of molecules that may link the role of GPR50 and BACE1 under normal or diseased conditions: co-interacting proteins and melatonin.

1.4.1 The known interactors of GPR50 are associated with BACE1

Several putative interactors of GPR50 identified by the yeast two-hybrid screening are co-interactors of BACE1. They play a role in BACE1 function in two ways:

a) Putative co-interactors of GPR50 are directly involved in the regulation of BACE1 properties

These co-interactors include: reticulon proteins RTN3/Nogo (RTN4), sorting nexin family member SNX6 and transcription factor SREBP2 (sterol regulatory element-binding protein) that can alter the trafficking and expression of BACE1 (Deng et al,

2013; Grunewald et al, 2009; Mastrocola et al, 2011; Okada et al, 2010).

RTN3 is known to inhibit β-secretase activity by impeding the trafficking of BACE1 to cleavage-active sites (Deng et al, 2013). Yet, Crossing RTN3 into APP/PS1-tg mice reduced Aβ deposition in the cortex, the CA3 and the dentate gyrus regions of the hippocampus, but it induced dystrophic neurites in the CA1 region (Shi et al, 2009). Therefore, RTN3 is regarded as a neuritic dystrophy inducer, as it is aggregated in the dystrophic neurites in the hippocampus (Hu et al, 2007). RTN3 motivated apoptosis may be also related to the function of BACE1. Inhibition of BACE1 activity by RTN3 might lead to a reduced release of active neural CAMs, which are required for neuronal development and protection.

RTN3 homolog Nogo-B/C also decreased BACE1 activity *in vitro*, but the inhibiting mechanism has not been fully investigated (He et al, 2004; Murayama et al, 2006). Nogo is known to inhibit cell adhesion, axonal regeneration and neurite outgrowth. Deleting *Nogo* restored the expression levels of markers for synapto-dendritic complexity and axonal sprouting, which contributed to the improvement of learning and memory deficits in APP-tg mice (Masliah et al, 2010). Elevated mRNA levels of Nogo and a significantly higher rate of a homozygous CAA insert were identified in the cortex of schizophrenia patients compared with controls (Novak et al, 2002). Further, Nogo-B transcript was found reduced in the frontal cortex of individuals having depression or BD compared with healthy individuals, while Nogo-C was significantly increased in tissues of schizophrenia brain (Novak & Tallerico, 2006). The expression levels of Nogo A/C and the presence of alleles with the schizophrenia-associated CAA insert were positively correlated. The altered expression and mutation of Nogo may dysregulate BACE1 activity, thus contributing to the abnormal neuronal organisation in brain diseases.

GPR50 co-immunoprecipitates with RTN3/Nogo. It has a rescuing effect on the inhibition of neurite outgrowth mediated by Nogo-A (Grunewald et al, 2009). It is intriguing that GPR50 and BACE1 have an overlapping role in neuronal development. These two proteins might cooperate during the process of neurite extension through intermediate molecules RTN3/Nogo.

As mentioned earlier, SNX6 is a negative regulator of BACE1 by promoting its retrograde trafficking away from ideal enzymatic compartments (Okada et al, 2010). Elsewhere, the activation of SREBP2 by exposing cells to high cholesterol induced a

hyper-expression of BACE1 (Mastrocola et al, 2011). These two proteins may also link GPR50 and BACE1 together. However, the functional interaction of GPR50 with SNX6 or SREBP2 has not been established and requires further confirmation.

b) Putative co-interactors of GPR50 participate in BACE1 activity during substrate processing

Co-interactors that fall into this category include TIP60, ABCA2 and cadherin superfamily member CDH8.

TIP60 is capable of rescuing APP-induced apoptosis and axonal transport defects in a *Drosophila* AD Model (Johnson et al, 2014; Pirooznia et al, 2012). Also, gene expression profiles activated by TIP60 can be modified by APP (Pirooznia et al, 2012). Thus, it is suggested that under AD-linked neurodegenerative conditions triggered by excess APP, TIP60 overexpression induces the up-regulation of neuroprotective genes that facilitate cell survival, by forming a transcriptionally active complex with AICD/Fe65 (Johnson et al, 2014). Similarly, TIP60/Fe65 can also form complex with the intracellular domain of LRP (Kinoshita et al, 2003) or APLP1/2 (Li & Sudhof, 2004), which are processed through BACE1 proteolytic cleavage (Hogl et al, 2011; von Arnim et al, 2005; Yanagida et al, 2009). Thus, the activating function of TIP60 is in part related to BACE1 activity. Interestingly, an increased level of BACE1 activity can be mediated by overexpressing GPR50 (Grünewald, 2011). This is consistent with the finding that GPR50 can enhance TIP60-induced transcriptional activity (Li et al, 2011), probably by forming complex with BACE1 cleavage products. Therefore, a putative interaction between GPR50 and BACE1 can be an upstream regulatory unit of TIP60 signalling.

ABCA2 can promote BACE1 cleavage of APP by enhancing APP expression and transporting APP to early endosomes (Chen et al, 2004; Davis et al, 2004b). There is disagreement on whether GPR50 is physically associated with ABCA2 (Anyanwu, 2014; Grunewald et al, 2012). However, co-expression with ABCA2 leads to the internalisation of GPR50 from the cell surface (Anyanwu, 2014). Moreover, the mRNA levels of GPR50 and ABCA2 in developing mouse brain are positively correlated (Grunewald et al, 2012). Thus, APP-induced β-secretase activity might be linked to the function of GPR50 via ABCA2, and this requires further investigation on the association of GPR50 and BACE1.

CDH8 is a calcium-dependent CAM implicated in synaptic adhesion and axonal growth/guidance (Bekirov et al, 2008; Shimoyama et al, 2000). Recently, cadherin molecules including CDH2, CDH6 and CDH8 were identified as members of BACE1/BACE2 putative degradome by shRNA-mediated loss-of-function studies (Stützer, 2012). Meanwhile, GFP-CDH8 was found co-immunoprecipitated with GFP-GPR50, but as both plasmids were GFP-tagged, this physical interaction might result from GFP dimerisation (Grunewald et al, 2012). Mouse Gpr50 and Cdh8 were co-localised in the periventricular hypothalamus and the amygdala, and co-fractionated from postsynaptic densities of mouse brain. Also, the mRNA level of Cdh8 is significantly correlated with GPR50 interactor Nogo-A. Hence, as CDH8, GPR50 and BACE1 are all implicated in neuron growth and related with one another, these three molecules might function as an interacting complex.

1.4.2 Melatonin: a possible pathway node of regulation

Melatonin, an endogenous hormone secreted by the pineal gland is known to regulate the circadian sleep-wake cycle. Significantly lower levels of melatonin were found in patients during euthymic, manic, and depressed episodes compared with healthy controls (Dallaspezia & Benedetti, 2009). Therefore, melatonin is considered as a trait marker and treatment candidate for the disturbance in circadian rhythms related to mental disorders.

Previous studies indicated that the decreased levels of melatonin in AD patients were associated with its important role in reducing Aβ neurotoxicity (Srinivasan et al, 2010). Treatment of APP695-tg mice with melatonin was reported to alleviate the learning and memory deficits of these animals, supported by a neuroprotection role of melatonin related to apoptosis modulation and protection of the cholinergic system (Feng et al, 2004). Another study showed that immunoreactive Aβ deposition was largely reduced in the hippocampus (43%) and entorhinal cortex (37%) of APP/PS1 double transgenic mice by long-term oral administration of melatonin (Olcese et al, 2009). The hippocampal Aβ generation induced by chronic intermittent hypoxia could be abolished by a daily melatonin administration, which reduced the expression level of BACE1 (Ng et al, 2010). Additionally, pro-inflammatory cytokines INF-γ and TNF-α are capable of stimulating APP processing by enhancing BACE1 expression (Yamamoto et al, 2007), and melatonin has an anti-inflammatory potential (Wang & Wang, 2006), thus acting against BACE1 up-regulation during

inflammation. Therefore, melatonin may alleviate the symptoms of AD by mediating the diminishment of BACE1 activity.

As stated earlier, GPR50 does not bind to melatonin directly, but it can prevent the binding of melatonin to MT1 through heterodimerisation. Importantly, it has been found that GPR50 is able to increase BACE1 activity *in vitro* (Grünewald, 2011). This observation indicates that GPR50 may participate in the regulation of BACE1 function through formation of heterodimers with MT1 and abolishing the negative affect of melatonin on BACE1.

1.5 Aim of this thesis

The introduction in this chapter shows that GPR50 has overlapping roles with BACE1 in normal cellular activities, and interacts with BACE1 regulators, particularly in relation to the pathology of mental illnesses. The aim of my PhD project is to further understand the function of GPR50 by investigating its potential interaction with the multifunctional sheddase BACE1. My overarching hypothesis is that GPR50 is involved in the function of BACE1, and by confirming the putative interaction between the two genes/proteins can give clues about their common roles under normal conditions and can further understand their association with mentally related illnesses. In this thesis, I want to answer the following questions:

1) Is GPR50 able to regulate BACE1 expression?
    - In chapter 2, the involvement of GPR50 in BACE1 expression regulation was investigated by real-time quantitative PCR and western blotting.
2) Is there a functional relationship between GPR50 and BACE1?
    - In chapter 3, the physical interaction between GPR50 and BACE1 was investigated by co-localisation and co-immunoprecipitation studies in mammalian cell lines and primary neuronal cultures.
3) Is GPR50 capable of regulating β-secretase activity in neurons?
    - In chapter 4, the potential of GPR50 in the regulation of neuronal β-secretase activity was investigated by the fluorometric activity assay in primary cortical neurons with altered level of GPR50 expression.
4) Is GPR50 involved in the trafficking system of BACE1?
    - In chapter 5, the role of GPR50 in BACE1 trafficking was investigated by cell surface labelling technique and subcellular fractionation studies.
5) Is GPR50 expression co-regulated with BACE1 in the brain and CNS?

- In chapter 6, the co-regulation of GPR50 and BACE1 expression was investigated by statistical correlation analysis in human dorsolateral prefrontal cortex and adult mouse CNS regions, followed by immunohistochemistry studies in adult mouse brain.

6) Is Gpr50 expression altered under AD conditions, and can GPR50 levels be used as a predictor of β-secretase mediated Aβ deposition?
   - In chapter 7, the association of GPR50 with AD pathology was investigated by immunohistochemistry studies in an AD mouse model.

Addressing these questions will provide insights into the investigation of an orphan GPCR. The association of GPR50 with BACE1 will highlight a potential link to psychiatric illnesses.

2 Characterising the expression and subcellular localisation of GPR50 and BACE1

2.1 Introduction

Studies in this thesis focus on the cellular function of psychiatric illness risk factor GPR50 and its potential link to neurodegenerative disorder key enzyme BACE1. The primary step is to characterise the expression features of GPR50 and BACE1 in different cell lines and to validate the findings with others' published data, which will be introduced in the following sections. By doing so, the integrity of the proceeding investigation can be guaranteed. The first aim of this chapter is to validate the antibodies and plasmids, as well as to summarise the expression characteristics of the two proteins. Then, to follow up the finding that overexpressed GPR50 is capable of regulating BACE1 activity in HEK293 cells (Grünewald, 2011), I investigated whether GPR50 overexpression alters the expression levels of BACE1.

2.1.1 The expression of GPR50

GPR50 is endogenously expressed in human cerebral endothelial hCMEC/D3 cells (Levoye et al, 2006), rat pituitary cell line GH3 (Li et al, 2011), mouse primary neuronal cultures (Grunewald et al, 2009) and HEK293T cells (Grunewald et al, 2009). There is no endogenous GPR50/Gpr50 detected in human neuroblastoma cell line SH-SY5Y or mouse neuroblastoma cell line N1E-115 (my unpublished observation). Endogenous and over-expressed GPR50 are localised mainly at the plasma membrane in HEK293 cells, and at synaptic spines and neurites in mouse primary neuronal cultures (Grunewald et al, 2009). A truncated form of GPR50 (tGpr50) lacking the last two transmembrane regions and cytoplasmic domain has been cloned from mouse hypothalamus and pituitary, and localised in the cytoplasm when over-expressed (Li et al, 2011). Yet, there was no report about this GPR50 form in human. Bipolar disorder-associated variant GPR50del is over-expressed at the cell surface, with no obvious alteration of localisation compared with GPR50 (Grünewald, 2011). The deletion and SNP mutations of GPR50 are unique to human DNA sequence. Western blotting confirmed the protein sizes of GPR50, GPR50del and tGpr50 are 67 kDa, 67 kDa and 29 kDa respectively. A dimer of GPR50 was also detected at around 130 kDa (Grunewald et al, 2009; Hamouda et al, 2007; Levoye et al, 2006).

2.1.2 BACE1 expression

2.1.2.1 The expression sites of BACE1

Endogenous BACE1 mRNA has been detected in diverse human neural and non-neural cell lines and tissues, as well as in adult human tissues of the cerebrum, cerebellum, peripheral nerve and skeletal muscle (Satoh & Kuroda, 2000). However, BACE1 mRNA expression is not universal; for instance, it was not detectable in K-562 erythroleukemia cells. There is more than one BACE1 mRNA species identified in human brain and cultured cells, suggesting multiple BACE1 isoforms (Ehehalt et al, 2002; Vassar et al, 1999). In addition, BACE1 mRNA variants are selectively regulated in response to neuronal differentiation and upon exposure to cytokines and growth factors (Satoh & Kuroda, 2000).

The BACE1 protein is a type I membrane protein belonging to the pepsin-like family. In western blotting, overexpression of full-length human BACE1 (variant a) produces two protein bands which are generally believed to be immature BACE1 at around 60 kDa and mature BACE1 at around 70 kDa (Bennett et al, 2000). The immature BACE1 is the initial pro-protein that is synthesised at the endoplasmic reticulum (ER). Then pro-BACE1 undergoes processing in the Golgi to become fully active. Glycosylation and further addition of complex carbohydrates result in a larger mature BACE1 than the immature BACE1 even after the removal of the BACE1 prodomain. The mature form of BACE1 circulates among the early endosomes, the plasma membrane and the trans-Golgi network (TGN) where it may exert enzymatic functions as a protease. Finally, as with most proteins, BACE1 is sorted to lysosomes for degradation. Therefore, BACE1 is likely to be found in various subcellular compartments.

The aforementioned different BACE1 transcripts are a result of differential splicing within the exon 3 and/or exon 4 of BACE1 mRNA (Holsinger et al, 2013). Correspondingly, there are five spliced isoforms of BACE1 protein reported so far (Figure 2.1) (Bodendorf et al, 2001; Ehehalt et al, 2002; Mowrer & Wolfe, 2008; Tanahashi & Tabira, 2001; Tanahashi & Tabira, 2007). These shorter isoforms of BACE1 undergo different post-translational modifications compared to the full length BACE1 and most of them are retained in the ER, resulting in a deficiency or absence of β-secretase activity. The specific physiological function of these spliced

variants is not known. However, the expression of BACE1 spliced transcripts reduced β-secretase activity and Aβ production in HEK293 cells (Mowrer & Wolfe, 2008). Thus, the promotion of BACE1 alternative splicing might be a potential therapeutic strategy for controlling BACE1 activity.

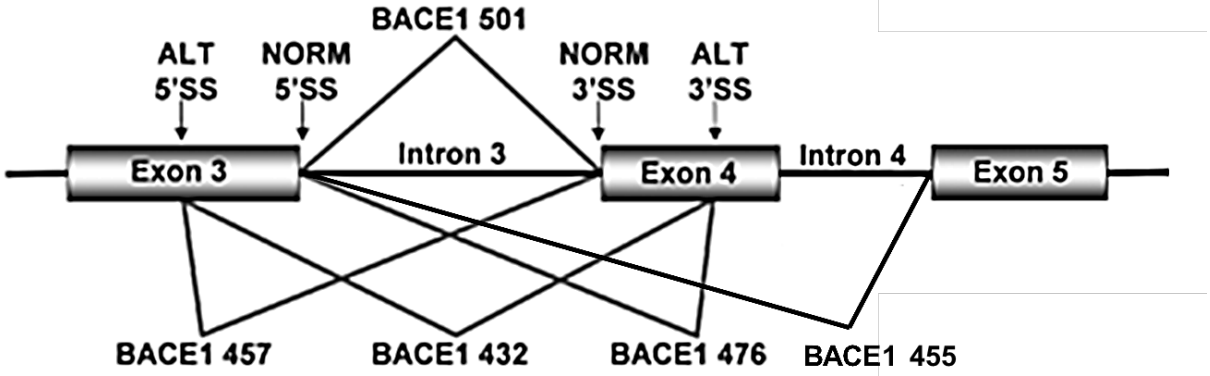

Figure 2.1 The alternative splicing of the BACE1 transcript. The diagram was adapted from (Mowrer & Wolfe, 2008). The numbers followed "BACE1" indicate the peptide lengths of the transcripts. The use of normal splice sites and alternative splice sites of BACE1 generates five RNA transcripts (BACE1 501, BACE1 476, BACE1 457, BACE1 455 and BACE1 432). The alternative 5'-splice site (ALT 5'SS) is in exon 3, and the alternative 3'-splice site (ALT 3'SS) is in exon 4. Use of the normal 5'-splice site (NORM 5'SS) and the normal 3'-splice site (NORM 3'SS) results in the production of the full-length BACE1 501 transcript.

2.1.2.2 Regulation of BACE1 expression

Previous investigations have suggested that both the transcriptional and the translational initiation of BACE1 expression are tightly regulated. The two regulatory mechanisms appear to be independent events for BACE1, for instance, the highest level of BACE1 mRNA is identified in the pancreas (Yan et al, 1999), while BACE1 protein and activity are most abundant in the brain (Sinha et al, 1999).

1) Regulation of BACE1 transcription

The basal promoter element for BACE1 transcription is a 91 bp fragment, which is the core region of neuron preferred promoter (Ge et al, 2004). The regulatory unit of BACE1 gene contains multiple transcription factor binding sites, including GC box, HSF-1, a PU box, AP1, AP2, and the lymphokine response element (Christensen et al, 2004). Transcription factor Sp1 is one of the activators that enhance BACE1 expression, which sequentially induces an elevation of BACE1 protein level and C99/Aβ levels (Christensen et al, 2004). Normally, the activation of BACE1 transcription requires a cascade of signal transduction pathways. The alteration of

signalling components under certain circumstances may contribute to the regulation of BACE1 transcription.

Aβ42 can promote BACE1 promoter activity dependent on NF-κB signal transduction cascade (Buggia-Prevot et al, 2008; Giliberto et al, 2009). NF-κB signalling has been implicated in the process of inflammation, oxidative stress, apoptosis, synaptic plasticity and memory maintenance (Albensi & Mattson, 2000; Freudenthal et al, 1998; Granic et al, 2009; Mattson & Camandola, 2001). NF-κB levels are significantly increased in the brains of AD patients during the neurodegenerative process (Chen et al, 2012a; Lukiw & Bazan, 1998). Functional NF-κB-binding elements have been identified in the BACE1 promoter region. Enhanced NF-κB signalling facilitates BACE1 gene transcription and APP processing (Chen et al, 2012a). NF-κB also mediates the up-regulation of BACE1 promoter activity by GSK3β (glycogen synthase kinase 3β) (Ly et al, 2013).

Elsewhere, aldehydic end product of lipid peroxidation, 4-hydroxynonenal induces up-regulation of BACE1 transcription via the activation of c-Jun N-terminal kinase and p38 mitogen-activated protein kinase signalling pathways which are responsive to stress stimuli (Tamagno et al, 2002; Tamagno et al, 2005).

2) Regulation of BACE1 translation

The 5' transcript leader (TL) located at the upstream of BACE1 mRNA acts as a translation silencer (De Pietri Tonelli et al, 2004). Within TLs, there are three upstream open reading frames (ORFs) that precede the main ORF. Recognition of AUGs in the first two upstream ORFs inhibits the efficiency of the downstream translation and this effect is cell-type differentiated (Rogers et al, 2004). Alternative splicing of BACE1 TL can reduce the number of upstream AUGs and therefore increase the efficiency of correct translation (De Pietri Tonelli et al, 2004). BACE1 undergoes TL alternative splicing in both the exocrine pancreas and neuroblastoma cells, but not in normal human brain. Chronic activation of astrocytes can reduce the inhibiting effect of BACE1 TL on translation initiation independent of alternative splicing, which drives BACE1 translation efficiency up to a level observed in neurons. In addition, it has been proposed that the phosphorylation of translation initiation factor eIF2α (eIF2α-P) is able to enhance BACE1 translation through a variety of different putative mechanisms that overcome the mRNA secondary

structure of the 5' untranslated region (UTR) and inhibitory upstream ORFs or through leaky ribosomal scanning (O'Connor et al, 2008). The regulation of eIF2α-P on BACE1 translation is mediated via protein kinase RNA- like ER kinase (PERK) signalling pathway (O'Connor et al, 2008). Activation of eIF2α was found increased in the frontal cortex of AD patients, and phosphorylated eIF2α levels correlated with elevated BACE1 protein levels (Mouton-Liger et al, 2012).

The 3'-UTR of BACE1 mRNA transcript is also one of the regulatory elements for BACE1 translation. The known regulators following this pattern include AD-related microRNAs. For instance, the levels of microRNA miR-107 are negatively correlated with BACE1 expression in brains of AD cases with different degrades of pathology, probably by targeting the putative microRNA recognition elements (MREs) within the 3'-UTR of BACE1 mRNA (Wang et al, 2008b). MiR-29a/b-1 also down-regulates BACE1 expression and activity (Hebert et al, 2008).

Even though the elevation of BACE1 protein level and activity in the brains of AD patients does not necessarily require an increase in its mRNA level (Zhao et al, 2007), the up-regulation of BACE1 mRNA in AD brains may be region-specific, and may partly contribute to the elevation of BACE1 protein and activity (Coulson et al, 2010). A slight increase of BACE1 protein level may result in a dramatic increase of Aβ peptide production (Li et al, 2006). Importantly, BACE1 expression regulation is normally accompanied by diverse adverse events that occur in brains undergoing damage or that induce the pathogenesis of brain illnesses (such as in AD):

- Traumatic brain injury enhanced levels of BACE1 mRNA, protein and activity in the hippocampus and the cortex of rat (Blasko et al, 2004).
- Transient cerebral ischemia in female rats resulted in elevated levels of BACE1 protein and activity (Wen et al, 2004).
- Under hypoxia conditions, hypoxia-inducible factor 1 was stabilised and bound to the 5'-RCGTG hypoxia-responsive element in the BACE1 gene promoter region, causing a boost in BACE1 mRNA transcription and resulting in an escalation of BACE1 protein level and activity, which was in accordance with Aβ deposition and memory deficit in APP23 transgenic mice subjected to hypoxia (Sun et al, 2006a; Zhang et al, 2007).
- Inflammatory cytokine interferon γ elicited an upturn of BACE1 protein expression in human astrocytoma cells and primary astrocyte culture of AD

model Tg2576 mice through the signal transductor and the activator of transcription 1 (STAT1) (Hong et al, 2003). Interferon γ activated Janus kinase 2 (JAK2) and extracellular-signal-regulated kinases (ERK1/2) signalling pathways, which caused the binding of phosphorylated STAT1 to the STAT1 binding sequences in BACE1 promoter region (Cho et al, 2007).

- Oxidative stress induced by H_2O_2 at a toxic level up-regulated BACE1 expression and activity (Kwak et al, 2011; Tan et al, 2013; Tong et al, 2005).
- Under inflammatory conditions, overproduction of neuronal or inducible nitric oxide (NO) synthase produced NO in excess and causes nitrosative stress (Wink et al, 2000). Low scale of NO overproduction decreased BACE1 mRNA level and sequentially its protein level and activity probably in response to the regulation of the cGMP-PKG signalling system, while high NO concentrations diminished BACE1 activity and Aβ production through post-translational N-nitrosylation without any effect on BACE1 protein level (Kwak et al, 2011).

In summary, the regulation of BACE1 transcription and translation is involved with various regulation factors and signalling systems and this ultimately affects BACE1 activity. As GPR50 is involved in the regulation of BACE1 activity, it might be a potential factor in BACE1 expression regulation.

2.1.3 Introduction to experiments

In this chapter, the antibodies used for GPR50 and BACE1 in this thesis are validated. To do this, the expression features of endogenous/exogenous GPR50 and BACE1 were investigated in human neuroblastoma cell line SH-SY5Y, human embryonic kidney cell HEK293 and mouse primary cortical neurons by immunocytochemistry and western blotting. Then, the effects of GPR50 overexpression on BACE1 expression levels were investigated in SH-SY5Y and HEK293 cells by real time quantitative PCR and western blotting.

2.2 Materials and methods

2.2.1 Mammalian cell culture

SH-SY5Y and HEK293 cells were grown in 75 cm^3 culture flasks in Dulbecco's Modified Eagle Medium (DMEM) containing 10% foetal bovine serum (FBS). Cells were cultured at 37^oC with 5% CO_2 and were split when cells were over 70%

confluent. For immunocytochemistry, cells were prepared on glass coverslips in 12-well plates, with 1×10^5 cells per well. Transfection was performed using Lipofectamine 2000 and transfection media after overnight culture (see 2.2.4). For protein lysates preparation, cells were grown on 10 cm plates until a confluency of 80-90%, which normally took 2 days with a starting cell number of 2×10^6 per plate.

2.2.2 Primary neuronal culture

Primary neuronal cultures were prepared from embryonic day 18 (E18) C57BL/6J mice. Mice were purchased from Biomedical Research Resources Unit, Western General Hospital, Edinburgh. The plugging date was marked as E0. The cortex was dissected and isolated from E18 pups in dissection buffer (HBSS + HEPES + GlutaMAX^{TM}, Invitrogen) at a cool temperature. Dissected tissue was further dispersed in 0.1% TryExpress at 37°C for 45 min. Neurons were isolated and seeded on poly-D-lysine (Sigma-Aldrich, St. Louis, USA) coated coverslips in 12-well plates and cultured in 2 ml neurobasal medium supplemented with 2% B-27 and 1% GlutaMAX^{TM} for 3, 9 or 28 days-in-vitro (DIV3, DIV9, DIV28). Cultures were maintained in a humidified environment at 37°C with 5% CO_2. Half of the media (1 ml) was replaced every three days.

2.2.3 Plasmids

All materials were purchased from Invitrogen (Life technologies) unless stated otherwise. BACE1 gene has five isoforms (a-e), and the shorter isoforms are the result of the alternative splicing of parts of exon 3 and/or exon 4 (Figure 2.1). TrueClone plasmid (Origene) containing untagged full-length of BACE1 (variant a, the longest isoform) and untagged plasmid GPR50-pDEST40 were used in all the experiments. All the vectors were isolated from transformed *E. coli* DH10B, selected on agar plates with ampicillin and extracted using the Qiagen miniprep or maxiprep kits following the manufacturer's instructions. All constructs were sequenced and checked for correct expression using their corresponding antibodies by western blotting.

2.2.4 Lipofectamine 2000 transfection

The optimised amounts of plasmid, Lipofectamine 2000 and transfection media used per transfection are summarised in Table 2.1. When different amounts of plasmid

were required between wells in an experiment, the empty vector pDEST40 was used to keep the DNA amount per well identical.

Table 2.1 Lipofectamine 2000 transfection protocol

		12 wells	6 wells	10 cm
DNA	GPR50	1 µg	2.5 µg	12 µg
	BACE1	2 µg	5 µg	12 µg
	GPR50+BACE1	1 µg+2 µg	2.5 µg+5 µg	12 µg+12 µg
Lipofectamine 2000		4 µl	10 µl	40 µl
Transfection media		50 µl+50 µl	125 µl+125 µl	500 µl+500 µl
Dilute after incubation		200 µl	500 µl	2 ml
Total volume/well		300 µl	750 µl	3 ml

For SH-SY5Y cells and HEK293 cells, transfection media OptiMEM (Invitrogen) was used. The plasmids and Lipofectamine 2000 were separately diluted in OptiMEM and incubated at room temperature for 5 min. The two solutions were mixed and incubated at room temperature for a further 20 min. After the incubation, the mixture was diluted with 2×volume of OptiMEM. Before adding the diluted transfection mix, the plated cells were briefly washed with pre-warmed OptiMEM. The transfection mix was added to the cells, which were left to transfect for 6 hr at 37^{o}C with 5% CO_2. Afterwards, the medium was replaced with pre-warmed DMEM/10% FBS and left overnight.

For primary neuronal cells, Neurobasal medium plus B-27 was used as the transfection media. The plasmids/Lipofectamine 2000 mixture was incubated for 1 hr at 37^{o}C before adding to the neurons. At the same time, the media in each well were collected in a clean tube and kept at 37^{o}C. The media was reused because it contains the growth factors produced by neurons. The neurons were briefly washed and incubated in the transfection media for 1 hr. Then the transfection mixture was added to the transfection media on top of the neurons and left for 4 hr. After transfection, the mixture was replaced with the old media, which contained Neurobasal medium, B27, GlutaMAX^{TM} and growth factors released by the neurons. Cells were left overnight at 37^{o}C with 5% CO_2.

2.2.5 Immunocytochemistry (ICC)

Transfected cells growing overnight were fixed with 500 µl ice cold methanol (pure) for 10 min and were then washed three times with PBS plus 0.2% Bovine Serum Albumin (BSA, Sigma-Aldrich). Fixed cells were blocked in PBS/0.2% BSA with 10% donkey serum (corresponding to the host of secondary antibody) for 30 min. After blocking, cells were incubated with primary antibodies diluted in PBS/0.2% BSA for 1 hr at room temperature, followed by washing with PBS/0.02% BSA for 3×5 min. Secondary antibodies were diluted in PBS/0.2% BSA with 10% serum, and cells were incubated with the solution at room temperature for 1 hr. After another 3 washes by PBS/0.2% BSA, all the coverslips were mounted with Mowiol/DAPI and kept in the dark for at least 24 hr. Antibodies used in this thesis and dilutions are summarised in Table 2.2. Secondary antibodies Alexa Fluor® dyes from Invitrogen (Life technologies), were normally used at a dilution of 1:500 for wavelength 488 nm, or 1:1000 for 594 nm and 647 nm (Table 2.3). Fluorescent photos were taken on a Nikon A1R confocal microscope with the z-stack programme.

Table 2.2 Primary antibodies used in this thesis

Antibody	Host	Immunogen	Application	Supplier
GPR50 goat	Goat polyclonal	Within residues 400-450 of human GPR50	ICC (1:2000/1:500)* IHC (1:50/1: 10)* WB (1:5000/1:500) * IP (2.4 µg/1mL)	Santa Cruz Biotechnology, sc-50590
GPR50 63	Rabbit polyclonal	Residues 516-530 of human GPR50	ICC (1:200) WB (1:1000)	In-house
GPR50 rabbit	Rabbit polyclonal	Residues 294-317 of human GPR50	ICC (1:2000) WB (1:1000)	Proteintech, 21514-1-AP
BACE1 rabbit1	Rabbit polyclonal	Residues 485-501 of human BACE1	ICC (1:500) WB (1:1000)	Abcam, ab2077
BACE1 rabbit2	Rabbit polyclonal	Residues 485-501 of human BACE1	ICC (1:5000) IHC (1:300) WB (1:10,000)	Covance, B-690
BACE1 mouse	Mouse monoclonal	Residues 22-460 of human BACE1	ICC (1:500) WB (1:1000)	Santa Cruz Biotechnology, sc-73729
BACE1 goat	Goat polyclonal	Residues 22-460 of human BACE1	ICC (1:200) IHC (1:50)	R&D systems, AF931
Pan Cadherin	Mouse monoclonal	C-terminus of human cadherins	ICC (1: 200) WB (1: 500)	Abcam, ab22744
VLA-2α	Mouse monoclonal	Residues 42-245 of human VLA-2α	ICC (1:500) WB (1: 1000)	BD Transduction Laboratories, 611016
β-catenin	Rabbit polyclonal	Residues surrounding Pro714 of human β-catenin	ICC (1:800) WB (1:5000)	Cell signalling technology, 8480

EEA1 mouse1	Mouse monoclonal	Within residues 50-150 of human EEA1	ICC (1:50)	Abcam, ab70521
EEA1 mouse2	Mouse monoclonal	Residues 3-281 of human EEA1	ICC (1:500) WB (1: 5000)	BD Transduction Laboratories, 610457
Calreticulin mouse	Mouse monoclonal	Calreticulin-maltose binding fusion protein	ICC (1:5000) WB (1:10,000)	Abcam, ab22683
Calreticulin rabbit	Rabbit polyclonal	Full length human calreticulin	ICC (1:5000) WB (1:10,000)	Abcam, ab2907
58K Golgi	Mouse monoclonal	Purified full length native from rat liver	ICC (1: 500) WB (1: 500)	Abcam, ab27043
P230 trans Glogi	Mouse monoclonal	Residues 2063-2179 of human p230 trans Golgi	WB (1: 500)	BD Transduction Laboratories, 611280
P115	Mouse monoclonal	Residues 843-955 of rat p115	WB (1: 500)	BD Transduction Laboratories, 612260
LAMP2b	Rabbit polyclonal	Within residues 350 to the C-terminus of human LAMP2b	ICC (1: 500) WB (1: 500)	Abcam, ab18529
RAB7	Mouse monoclonal	Residues 163-177 of human RAB7	ICC (1: 200)	Abcam, ab50533
GAPDH	Mouse monoclonal	Recombinant GAPDH	WB (1: 40,000)	Thermo scientific, MA5-15738
RTN3	Rabbit polyclonal	Residues 1-90 of human RTN3	WB (1:2000)	Santa Cruz Biotechnology, sc-33599
PSD-95	Mouse monoclonal	Purified recombinant rat PSD-95	WB (1: 5000)	Thermo scientific, 7E3-1B8
Synaptophysin	Mouse monoclonal	Rat retina synaptosome	WB (1: 50,000)	Sigma, S5768
Aβ 6E10	Mouse monoclonal	Residues 1-16 of human Aβ.	WB (1:500)	Sigma, SIG-39320

*** There were two batches of GPR50 goat antibody with inconsistent performances, so different concentrations were used.**

ICC: immunocytochemistry; IHC: immunohistochemistry; WB: western blotting; IP: immunoprecipitation.

Table 2.3 Fluorescent secondary antibodies used in this thesis

Antibody	Host	Reactivity	Working dilution	Supplier
Alexa Fluor 488	Donkey	Goat	1: 500	Life technologies
Alexa Fluor 594	Donkey	Goat	1:1000	Life technologies
Alexa Fluor 488	Donkey	Rabbit	1: 500	Life technologies
Alexa Fluor 594	Donkey	Rabbit	1:1000	Life technologies
Alexa Fluor 647	Donkey	Rabbit	1:1000	Life technologies
Alexa Fluor 488	Donkey	Mouse	1: 500	Life technologies
Alexa Fluor 594	Donkey	Mouse	1:1000	Life technologies

2.2.6 Live cell surface labelling technique

Cells were plated onto coverslips in a 12-well plate and incubated at 37°C overnight. To label BACE1 on the cell surface, the goat antibody raised against the ectodomain of human BACE1 were diluted in OptiMEM (1:200) and added to cells after a brief wash. The BACE1 mouse antibody was also tested for this technique, but with no success. The cells with the antibody were agitated at 4°C for 1 hr, followed by two washes with ice-cold PBS+1% BSA. Then 500 ml 4% PFA were added to each well for 10 min to fix the cells, which were incubated by secondary antibody donkey-anti-goat 488 at room temperature for 1 hr. After incubation, cells were permeabilised with 0.2% Triton X-100 for 10 min, followed by a 20 min blocking step with PBS+1% BSA+10% donkey serum. Afterwards, total BACE1 were double stained by BACE1 rabbit2 antibody with the plasma membrane marker VLA-2α mouse antibody or by BACE1 mouse antibody with GPR50 rabbit antibody. The primary antibodies were diluted in PBS+1% BSA. Then cells were washed and incubated with appropriate secondary antibodies diluted in PBS+1% BSA+10% donkey serum for 1 hr at room temperature.

2.2.7 Western Blotting

Protein lysates were extracted by RIPA buffer (50 mM Tris pH 7.4, 150 mM NaCl, 1% NP-40, 0.1% SDS, 0.5% sodium deoxycholate, protease inhibitors added). Then proteins were separated on 7% NuPage Tris-Acetate gels (Invitrogen) and transferred onto PVDF membranes (Invitrogen), for 1.5 hr at a constant voltage of 30 V. Membranes were stained with Ponceau S for 1 min to check whether the transfer of proteins from the gels was successful. Ponceau S was washed off with dH_2O, and the membranes were blocked overnight at 4°C in washing buffer (1×PBS/0.2% Tween 20) containing 5% skimmed milk powder (Marvel). On the following day, membranes were washed briefly and incubated with diluted primary antibodies for 1-1.5 hr at room temperature. A brief wash, one wash for 15 min and three washes for 5 min each with the washing buffer were applied. Membranes were then incubated with horseradish peroxidase (HRP) conjugated secondary antibodies diluted in the washing buffer for 30 min at room temperature. The membranes were washed again as mentioned above and then detected using chemiluminescence (ECL-Plus, Amersham Biosciences, GE healthcare) and exposed to films. All the primary antibodies were diluted in the washing buffer during the staining and the dilutions

were shown in Table 2.2. All the secondary antibodies were purchased from Dako (Table 2.4).

Table 2.4 Horseradish peroxidase conjugated secondary antibodies used in this thesis

Host	Reactivity	Working dilution	Supplier
Swine	Rabbit	1:3000	Dako
Rabbit	Goat	1:5000	Dako
Goat	Mouse	1:10,000	Dako

2.2.8 Real-time quantitative PCR (qPCR)

Total RNA was extracted from SH-SY5Y cells transfected with the same amounts of pDEST40 (empty vector control) and GPR50-pDEST40 (abbreviated as GPR50) by using RNase easy kit (Qiagen). The first strand cDNA was synthesised from 200 ng of DNase I-treated RNA as the template using oligo(dT) primers (Maxima H Minus Reverse Transcriptase, Thermo) for extension according to the instruction of the supplier. Prior to qPCR, all cDNAs and no-transcriptase controls were used as templates of reverse transcription PCR. Gel electrophoresis was performed to check the quality of cDNAs and the specificity of products. cDNAs were diluted 10-fold with DNAse/RNAse -free dH_2O (Life technologies) before being used for qPCR.

Real-time qPCR using SYBR Green Supermix ($MgCl_2$; dATP, dCTP, dGTP, dUTP; AccuStart Taq DNA polymerase; SYBR Green I dye; 20nM fluorescein; Uracil-N-glycosylase; stabilisers; from Quanta, 95067-100) in a 20 µl PCR system (Table 2.5) was performed on the Bio-Rad iCycler with the iQ software. Primers (Table 2.6) for GPR50, BACE1, as well as housekeeping genes transferrin receptor (TFRC), TATA binding protein (TBP) and ubiquitin C (UBC) were optimised over a gradient of annealing temperatures and 60.1^{o}C was selected. PCR efficiencies for each pair of primers were achieved from standard curves produced by PCR of three sequential 10-fold dilutions of corresponding cDNAs as templates.

Table 2.5 Setting up real-time quantitative PCR reaction

Component	20 µl reaction	Final Concentration
2X SYBR Green Supermix	10 µl	1X
2 µM Forward Primer	2 µl	200 nM
2 µM Reverse Primer	2 µl	200 nM
cDNA or no-transcriptase control	2 µl (diluted)	-
DNAse/RNAse -free water	4 µl	-

Table 2.6 Primers used for real-time quantitative PCR

Primer name	Forward sequence	Reverse Sequence	Size/Genomic
GPR50 1-2[a]	CATGGTCATTTTGGCTGTGA	ACCCGACCATCTGGCACT	176/3038 bp
BACE1 1-2[a]	TTTGTGGAGATGGTGGACAA	TGGTAGTAGCGATGCAGGAA	164/18737 bp
TFRC human	CGCTGGTCAGTTCGTGATTA	GCATTCCCGAAATCTGTTGT	210/1731 bp
TBP human	TGCCCGAAACGCCGAATATA	TTTCTTGCTGCCAGTCTGGA	150/5037 bp
UBC human	GATTTGGGTCGCAGTTCTTG	TCCAGCAAAGATCAGCCTCT	191/1003 bp

a. primers also work in mouse.

Targeted samples, standard curves and negative controls were run on the same plates. In case of splitting different genes into separate plates, at least two calibrators were included. All reactions were run in triplicate. Amplification was carried out according to a programme summarised in Table 2.7. After completion of the amplification reaction, a melting curve was generated by increasing the temperature in small increments (+0.5^{o}C) and monitoring the fluorescent signal at each step.

Table 2.7 Real-time quantitative PCR programme

Initial denaturation	95^{o}C	3 min	1 cycle
Denaturation	95^{o}C	15 s	40 cycles
Annealing	60.1^{o}C	45 s	
Extension	72^{o}C	30 s	
Melting	95^{o}C	1 min	1 cycle
	55^{o}C	1 min	
	+0.5^{o}C	10 s	80 repeats

2.2.9 DNA sequencing

Plasmids were subjected to DNA sequencing when a new single clone of transformed *E.Coli* DH10B was picked for plasmid proliferation. For each reaction of 10 µl, 100 ng of plasmid was used for cycle sequencing reactions according to the manufacturer's instructions (Big Dye Terminator v3.1 Cycle Sequencing Kit). The programme was described as follows: 96^{o}C for 1 min; 25 cycles, 96^{o}C for 10 s, 50^{o}C for 5 s, 60^{o}C for 4 min; 10^{o}C for holding. The clean-up step of the extension products followed the protocol of ethanol/sodium acetate precipitation. Briefly, the 96-well reaction plate was removed from the thermal cycler and spun for a few seconds. Then 2 µl of 3 M sodium acetate (pH 4.6) and 50 µl of 95% ethanol were added to each well. The plate was sealed with aluminium tape and inverted several times. The mixture in the plate was incubated at room temperature for 15 min and then centrifuged at 1400-2000×g for 45 min. The plate was inverted on a piece of tissue and spun at 700×g for 1 min. Then 150 µl of 70% ethanol was added to each well. The plate was sealed, inverted several times and then centrifuged at maximum speed

for 10 min. After the spin, the plate was inverted on a piece of tissue and spun at 700×g for 1 min. The samples were frozen if sequencing was not to be done on the same day. Sequencing was performed by the staff in Human Genetics Unit, University of Edinburgh. The sequencing results were checked and compared to expected sequences by BLAST against the reference genome in the UCSC database.

2.3 Results

2.3.1 Antibody characterisation

Antibodies used in this thesis are all commercially available (see Table 2.2). These antibodies were tested on overexpressed proteins from untagged vectors for detection in SH-SY5Y cells by immunocytochemistry and western blotting. Endogenous protein expression was tested in HEK293 cells and mouse primary neuronal cultures.

2.3.1.1 GPR50 antibodies

Two commercial antibodies for GPR50 were used in this thesis. The performances of these two antibodies are summarised briefly in Table 2.8.

Table 2.8 The competence of antibodies for GPR50 used in this thesis

	Exogenous GPR50	Endogenous GPR50				Note
		SH-SY5Y	HEK293	Mouse neurons	Mouse brain	
GPR50 goat	√		√		√	Detects endogenous GPR50 in HEK293 cells by western blotting and Gpr50 in mouse brain by immunohistochemistry
GPR50 rabbit	√		√		√	Not suitable for detecting Gpr50 in mouse brain by immunohistochemistry

GPR50 goat and rabbit antibodies detected exogenous GPR50 at the cell surface of SH-SY5Y cells (Figure 2.2). Then I examined the sites of overexpressed GPR50 by double-staining with known subcellular compartment markers (Figure 2.3). It was shown that overexpressed GPR50 was strongly co-localised with the plasma membrane marker VLA-2α (Figure 2.3), confirming that GPR50 is mainly located at the cell surface. The co-localisation between GPR50 and the early endosome marker EEA1, the ER marker calreticulin, the Golgi marker 58K Golgi or the late endosome marker RAB7 was not convincing, because even though there was a seemingly

orange colour that could be merged from green (GPR50) and red channels (markers), GPR50 signal did not have the punctate structure of the endosomes or other internal compartments. In addition, the majority of GPR50 was not expected to localise in the ER, as most of GPCRs experience ER exit after synthesis and are exported along the secretory pathway to the plasma membrane so as to function as sensors of the extracellular information and then to activate inside signal transduction pathways (Magalhaes et al, 2012). Therefore, the merged signal might be an overlapping pattern of the cell surface GPR50 with the internal markers. However, the internal location of GPR50 cannot be ruled out, because it can be expressed internally in certain circumstances, such as in HEK293 cells (Grünewald, 2011). The subcellular localisation of overexpressed GPR50 appeared identical to endogenous GPR50 in HEK293 cells (Figure 2.5, also see Figure 3.9-3.10).

In GPR50-transfected SH-SY5Y cells, the rabbit antibody of GPR50 detected a band at 67 kDa by western blotting (Figure 2.4). This is the expected size of GPR50, which is in line with previous reports (Grunewald et al, 2009) and is supported by the same observation using an in-house rabbit antibody GPR50 63. The GPR50 goat antibody detected a doublet band at 67 kDa. It is not clear whether the smaller band is an alternative splicing product of GPR50 transcript, and it does not correspond to the truncated isoform of mouse Gpr50 (29 kDa) reported by Li and colleagues (Li et al, 2011). No bands were detected in untransfected samples, indicating GPR50 is not endogenously expressed in SH-SY5Y cells. This was in line with the finding that no immunoreactivity of GPR50 was found in untransfected SH-SY5Y (Figure 2.2). The following real-time PCR results also support these observations (see 2.3.2.3, Figure 2.25.A).

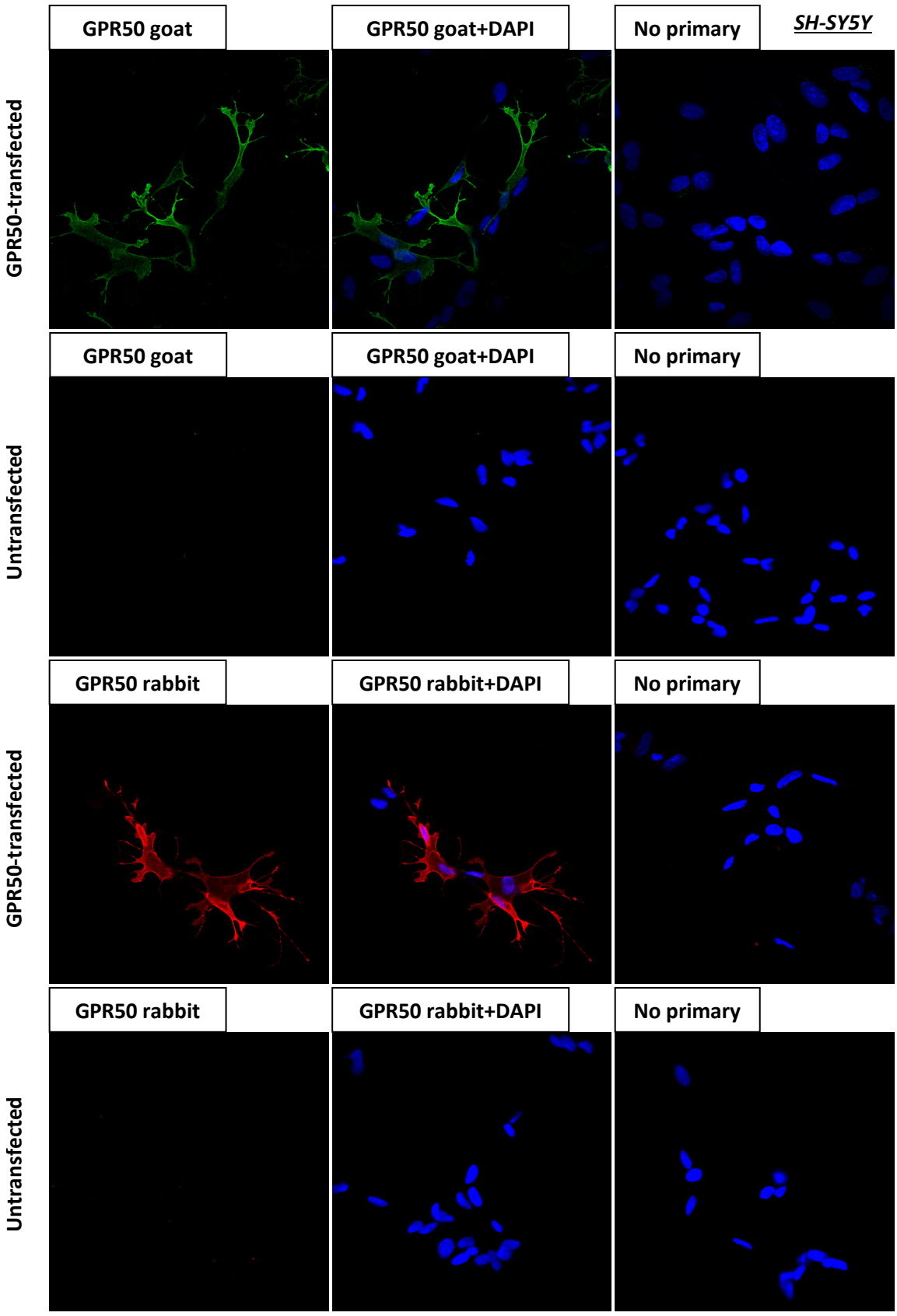

Figure 2.2 Validation of GPR50 antibodies using immunocytochemistry in SH-SY5Y cells. Untagged GPR50 plasmid was transfected. GPR50-transfected cells and untransfected cells were singly immunostained with GPR50 goat or rabbit antibodies. Negative controls were only stained with secondary antibodies donkey-anti-goat 488 (green) or donkey-anti-rabbit 594 (red) while the primary antibodies were skipped. The two antibodies showed similar patterns of overexpressed GPR50. No endogenous GPR50 was detected in SH-SY5Y cells.

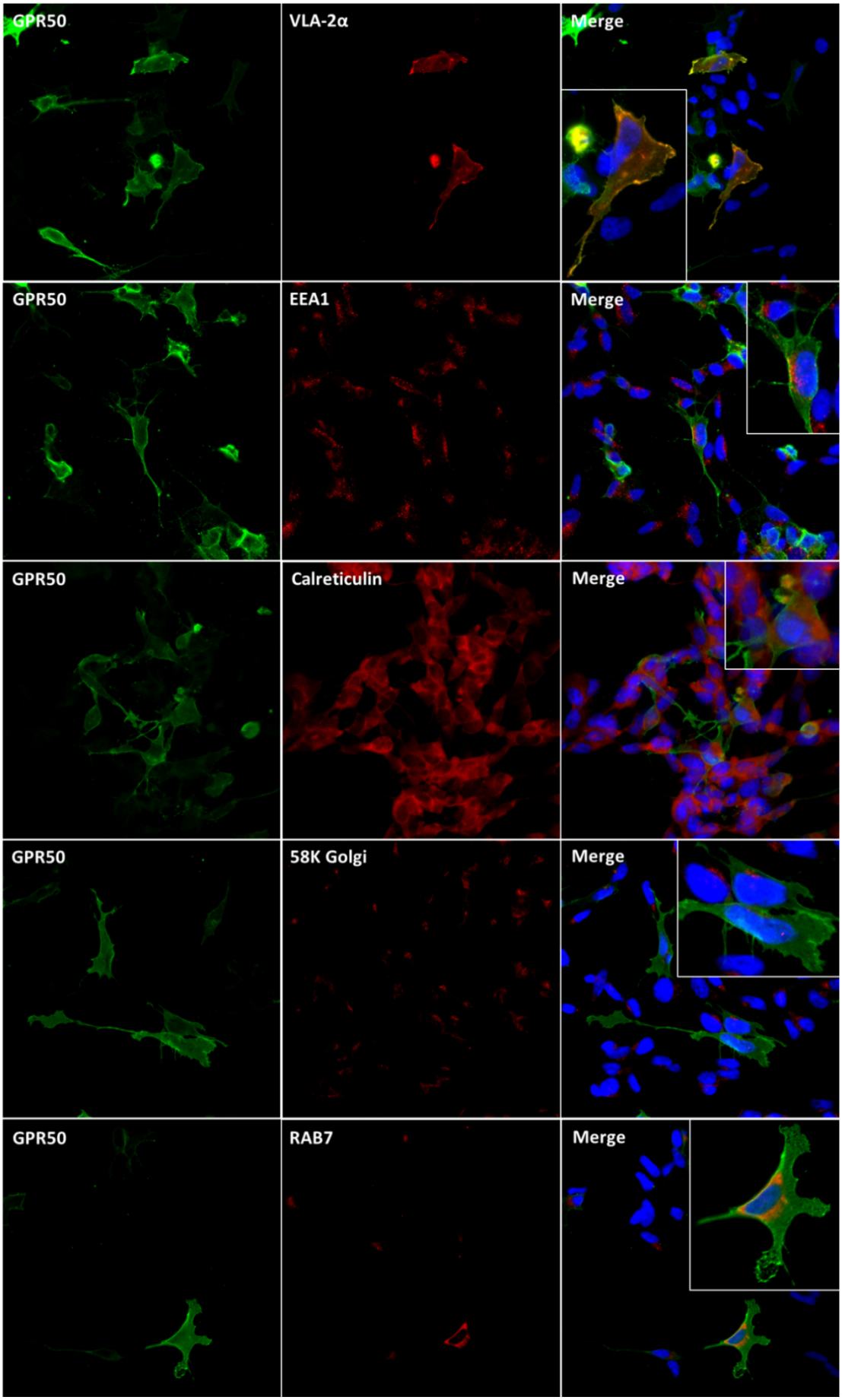

Figure 2.3 The localisation of overexpressed GPR50 in SH-SY5Y cells. GPR50 goat antibody (green) was used in this experiment.

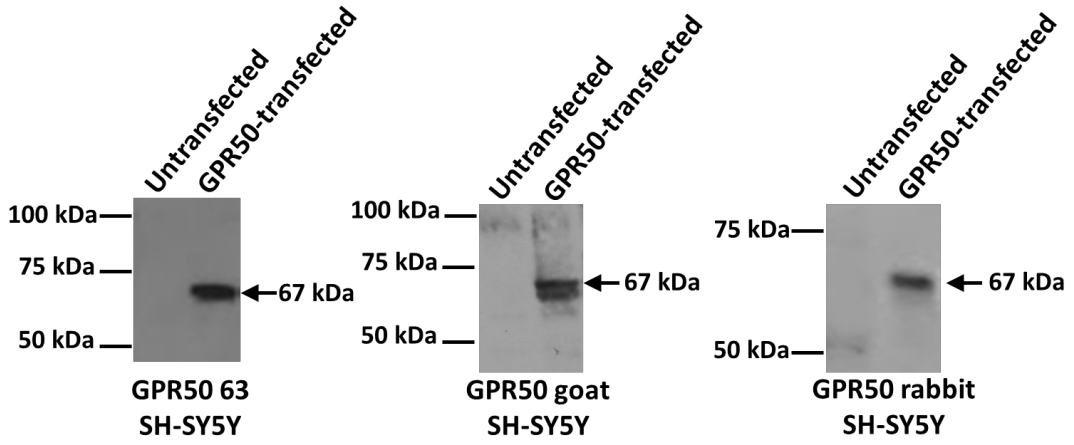

Figure 2.4 Validation of GPR50 antibodies using western blotting in SH-SY5Y cells. Untagged GPR50 plasmid was transfected. Protein lysates were extracted by RIPA buffer. In each lane, 10 µg proteins were loaded and separated in 7% tris-acetate gels. GPR50 63 and rabbit antibodies recognised a single band at 67 kDa, the expected size of GPR50. GPR50 goat antibody detected a doublet band. No bands were detected in untransfected cells, indicating that GPR50 is not endogenously expressed in SH-SY5Y.

Endogenous GPR50 is expressed in HEK293 cells with a percentage of 1-10% depending on the age of the cells (Grünewald, 2011). GPR50 goat antibody showed a punctate staining pattern in the internal compartments of untransfected HEK293 cells, which is uncommon for GPR50 (Figure 2.5). These signals were found in all the cells, suggesting that the labelling of GPR50 goat antibody was unspecific in detecting endogenous GPR50. GPR50 rabbit antibody appeared to stain specific cells with an acceptable percentage of endogenous GPR50 in HEK293 cells (two cells were stained in a 21-cell group). However, both GPR50 goat and rabbit antibodies detected endogenous human GPR50 in HEK293 cells with an expected size of 67 kDa in western blotting (Figure 2.8). In mouse primary cortical neurons, the two antibodies co-localised well in picking up overexpressed GPR50 (Figure 2.6). The GPR50 goat antibody showed additional staining which was originally thought to be endogenous mouse Gpr50. However, the blocking peptide failed to erase the signals detected by GPR50 goat antibody in untransfected neurons (Figure 2.7). GPR50 rabbit antibody was also unable to recognise endogenous Gpr50 in primary cortical neurons by immunocytochemistry, even though by western blotting it detected a 63 kDa band from brains of embryonic mice (E18) and new born pubs (P0) (Figure 2.8). According to the predicted sizes of Gpr50 (Uniprot: 67 kDa for human GPR50, 65 kDa for mouse Gpr50), this band should be the endogenous Gpr50, as mouse Gpr50 protein consists of 591 amino acids, shorter than its human homologue which contains 617 amino acids.

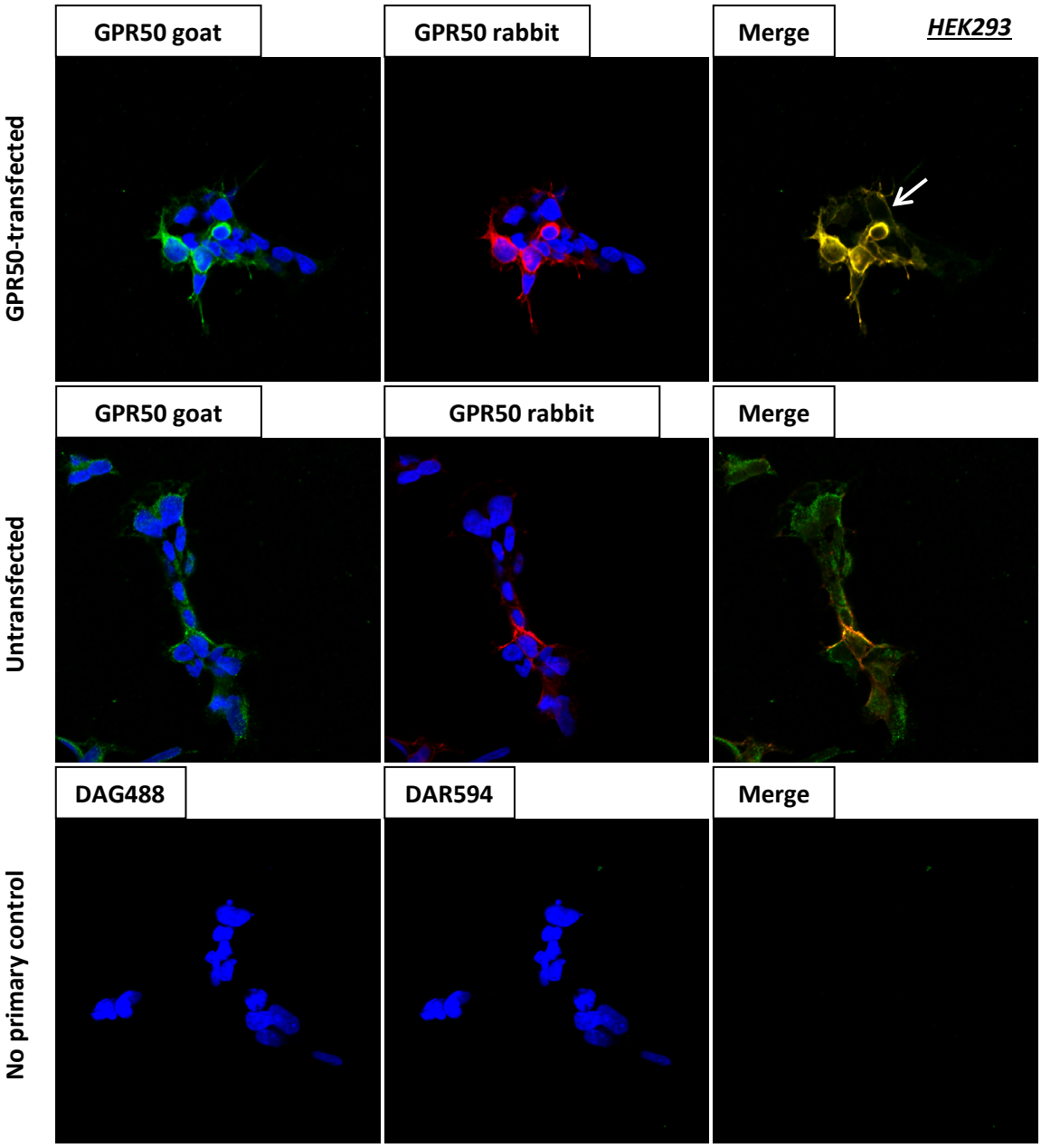

Figure 2.5 Validation of GPR50 antibodies using immunocytochemistry in HEK293 cells. Cells were transfected with untagged GPR50 plasmid or untransfected. Immunocytochemistry was carried out by double-staining cells with GPR50 goat antibody and rabbit antibody. Negative controls were only stained with secondary antibodies donkey-anti-goat (DAG) 488 and donkey-anti-rabbit (DAR) 594 while the primary antibodies were skipped. GPR50 goat and rabbit antibodies co-localised perfectly in cells transfected with GPR50. Some weaker signals indicated by a white arrow might represent endogenous GPR50 in HEK293 cells. GPR50 goat antibody stained all the untransfected cells with an unspecific pattern, as most of the signals were internal speckles, uncommon for the majority of GPR50. Whereas, GPR50 rabbit antibody appeared to stain specific cells with a percentage common to the proportion of endogenous GPR50 in HEK293 cells.

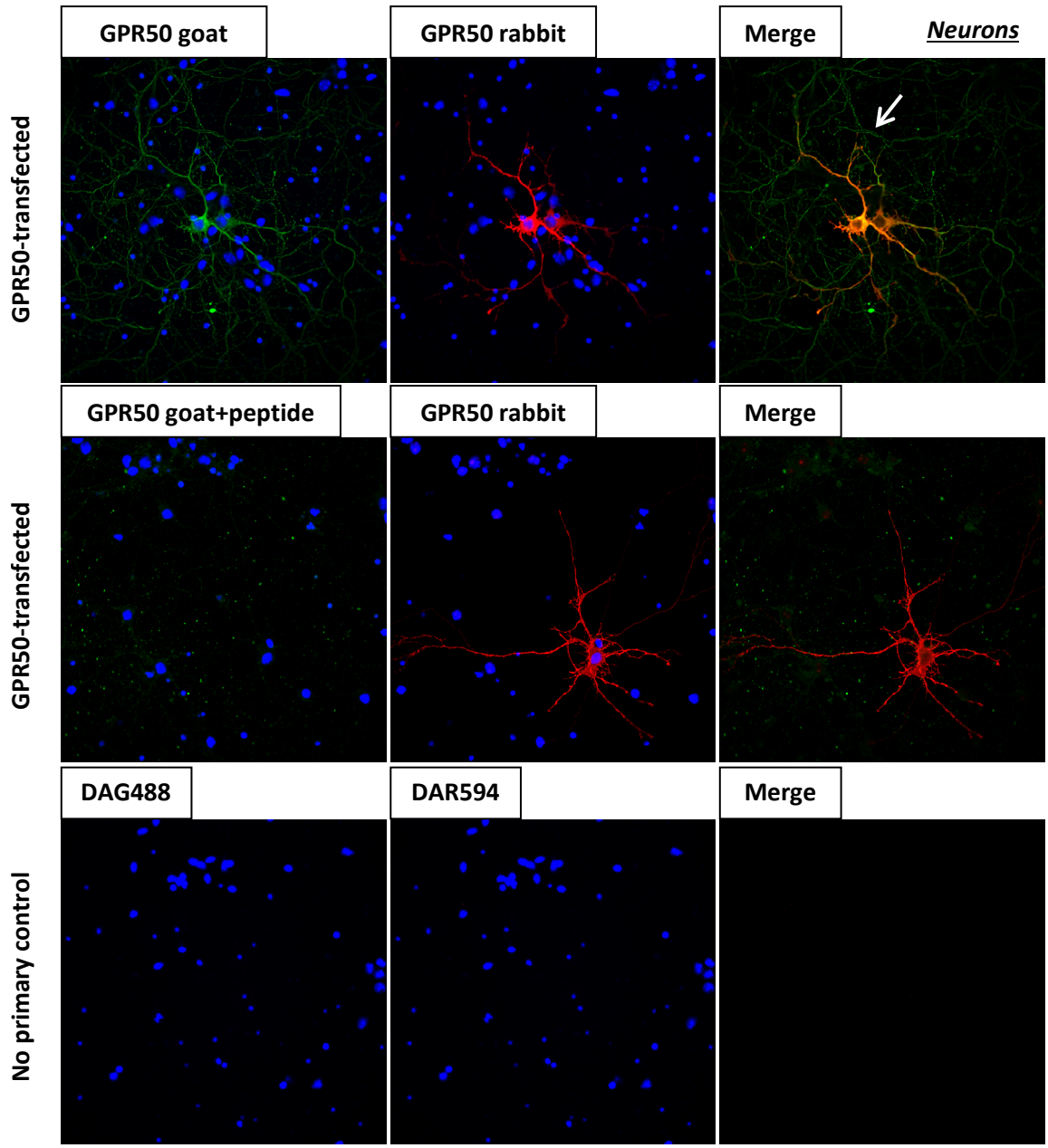

Figure 2.6 Validation of GPR50 antibodies using immunocytochemistry in primary cortical neurons. Untagged GPR50 plasmid was transfected. DIV15 post-transfection neurons were double-immunostained with GPR50 rabbit antibody together with goat antibody or goat with the pre-absorption of blocking peptide. Negative controls were only stained with secondary antibodies donkey-anti-goat (DAG) 488 and donkey-anti-rabbit (DAR) 594 while the primary antibodies were skipped. GPR50 goat and rabbit antibodies co-localised well in cells obviously labelled with GPR50 rabbit. GPR50 goat detected additional signals indicated by a white arrow.

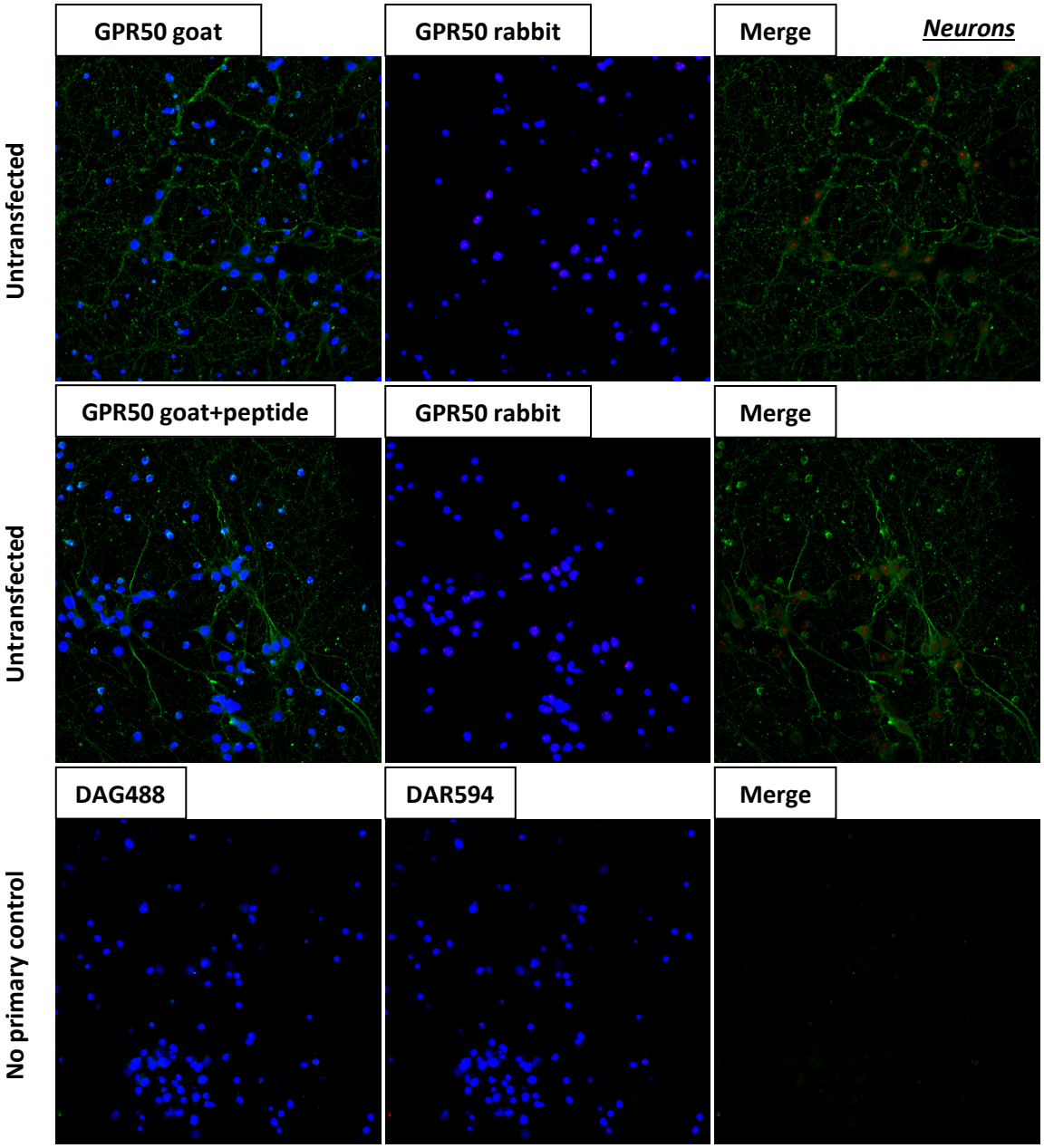

Figure 2.7 GPR50 antibodies were unable to detect endogenous Gpr50 using immunocytochemistry in primary cortical neurons. Untransfected DIV15 neurons were double-immunostained with GPR50 rabbit antibody together with goat antibody or goat with the pre-absorption of blocking peptide. Negative controls were only stained with secondary antibodies donkey-anti-goat (DAG) 488 and donkey-anti-rabbit (DAR) 594 while the primary antibodies were skipped. Both the antibodies failed to show a credible signal for endogenous Gpr50 in primary cortical neurons.

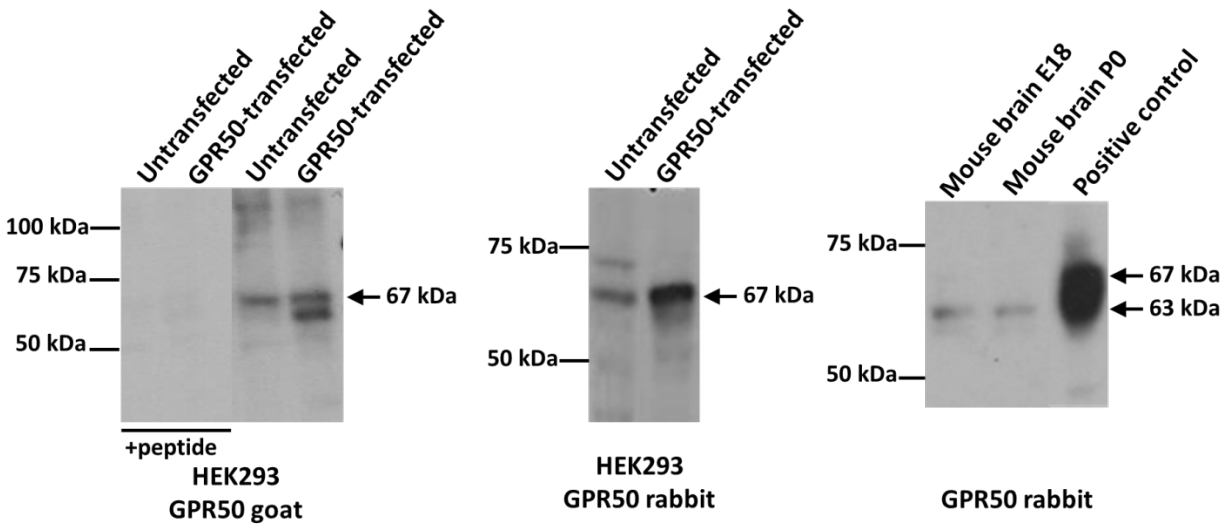

Figure 2.8 Endogenous GPR50/Gpr50 was detected in HEK293 cells and mouse brain using western blotting. E18: embryonic day 18; P0: postnatal day 0, new after birth; positive control: HEK293 cells overexpressed with GPR50.

2.3.1.2 BACE1 antibodies

In this thesis, four commercial antibodies for BACE1 were used in different experiments according to their performance in the detection of human/mouse BACE1, endogenous/exogenous BACE1 and immature/mature BACE1 (see Table 2.9 for a brief summary). Antibodies used for each experiment were specified at the beginning of each chapter.

Table 2.9 The competence of antibodies for BACE1 used in this thesis

	Exogenous BACE1	Endogenous BACE1				Note
		SH-SY5Y	HEK293	Mouse neurons	Mouse brain	
BACE1 rabbit1	√					Rabbit1 and 2 antibodies have the same epitope at the C-terminal
BACE1 rabbit2	√	√	√	√	√	Needs a higher concentration for endogenous BACE1
BACE1 mouse	√		√			Mouse and goat antibodies have the same epitope at the N-terminal
BACE1 goat	√		√	√	√	Detects endogenous BACE1 better in immunocytochemistry

According to the intracellular trafficking system of BACE1, it will be expressed in multiple subcellular organelles {(Cole & Vassar, 2007); also detailed in chapter 5}. As is shown in Figure 2.9, BACE1 antibodies detected overexpressed BACE1 in

various intracellular locations in SH-SY5Y cells. The BACE1 mouse antibody and two rabbit antibodies labelled almost identical signals for BACE1. Previous immunocytochemistry studies showed that BACE1 can be found in the plasma membrane, the early endosomes, the ER, the Golgi and the late endosomes/lysosomes (Griffiths et al, 2011; Guglielmotto et al, 2012; Kang et al, 2010). My results showed that BACE1 was co-localised with the plasma membrane marker pan cadherin (Figure 2.10), confirming that a proportion of BACE1 is cycled to the cell surface. The majority of BACE1 is expressed internally, as supported by its co-localisation with the early endosome marker EEA1, the Goigi marker 58K Golgi and the late endosome marker RAB7 (Figure 2.10). This agrees with previous studies. However, there is no obvious co-localisation between BACE1 and the ER marker calreticulin, contradictory to a former report (Griffiths et al, 2011).

Next, the expression of exogenous BACE1 at the plasma membrane was verified by the cell surface labelling technique. The BACE1 mouse and goat antibodies are raised against the N-terminal extracellular domain of human BACE1, so they are more likely to detect plasma membrane-bound BACE1 on the cell surface, before cells are permeabilised. A previous report showed that it is difficult to label cell surface BACE1 by its own antibody, and it could only be surface-labelled with an antibody against V5 when the BACE1 sequence was tagged with the V5 epitope (Kinoshita et al, 2003). Here, the BACE1 mouse antibody failed to produce valid fluorescent signal during the cell surface labelling process (Figure 2.11), even though it worked well in fixed permeabilised cells (Figure 2.9). However, the BACE1 goat antibody successfully identified BACE1 on the cell surface (Figure 2.12, 2.13). In SH-SY5Y cells, an external signal was detected by the goat BACE1 antibody, which was unlikely to enter the cells because the staining was performed in chilled live cells, prior to permeabilisation. The signal was found co-localised with the plasma membrane marker VLA-2α and total BACE1 which were stained after permeabilisation, confirming that it was a part of BACE1 expressed at the plasma membrane (Figure 2.12). In addition, this BACE1 pool was also co-localised with β-catenin (Figure 2.13), which is mostly tethered with E-cadherin as a component of a protein complex that forms the adherens junctions (Du et al, 2009). The labelling of cell surface BACE1 in SH-SY5Y was a punctate staining pattern.

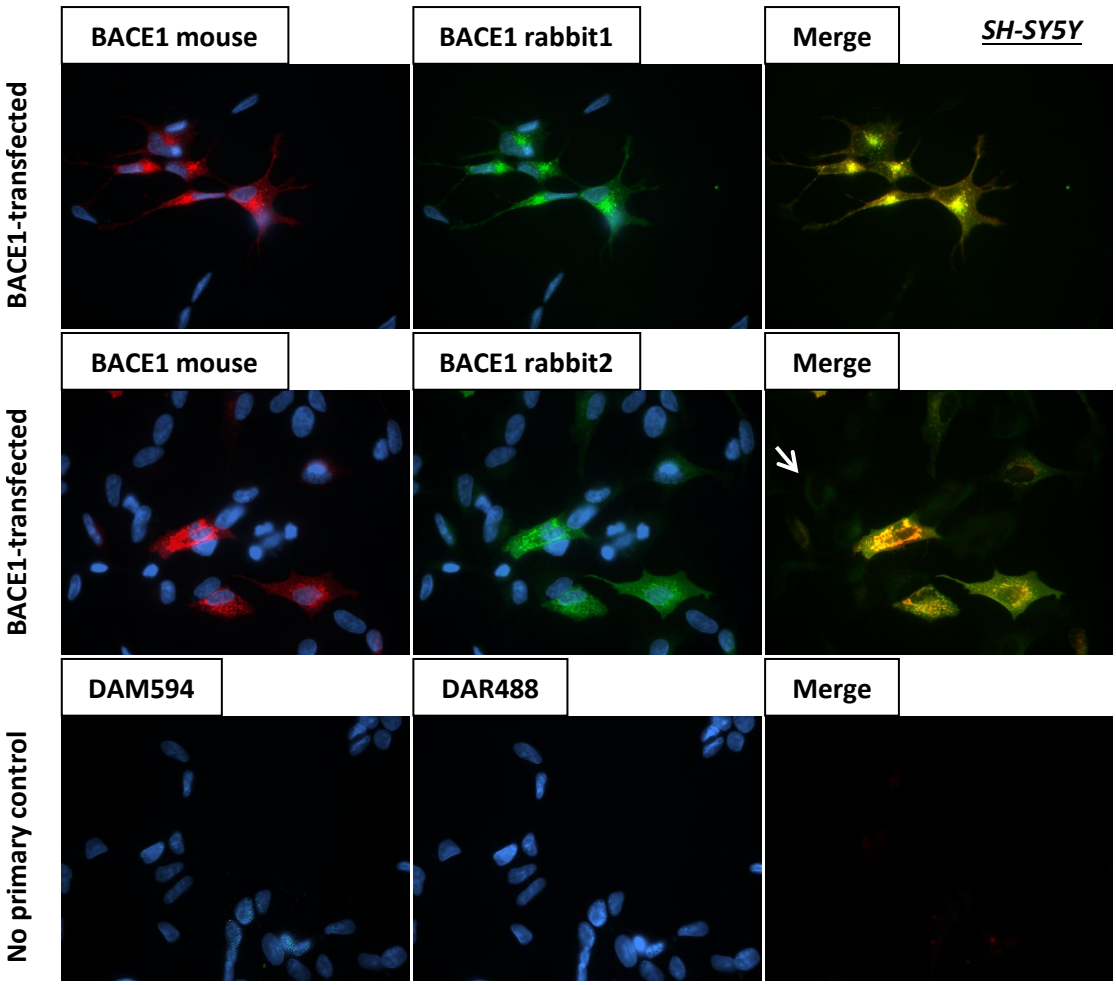

Figure 2.9 Validation of BACE1 antibodies using immunocytochemistry in SH-SY5Y cells. Untagged BACE1 plasmid was transfected. Cells were double-immunostained with BACE1 mouse and rabbit1/2 antibodies. Negative controls were only stained with secondary antibodies donkey-anti-mouse (DAM) 594 and donkey-anti-rabbit (DAR) 488 while the primary antibodies were skipped. BACE1 mouse and rabbit1 antibodies co-localised perfectly at multiple sites. BACE1 rabbit2 detected additional signals which were not recognised by the mouse antibody. These weaker signals (indicated by a white arrow) may represent endogenous BACE1 in SH-SY5Y cells.

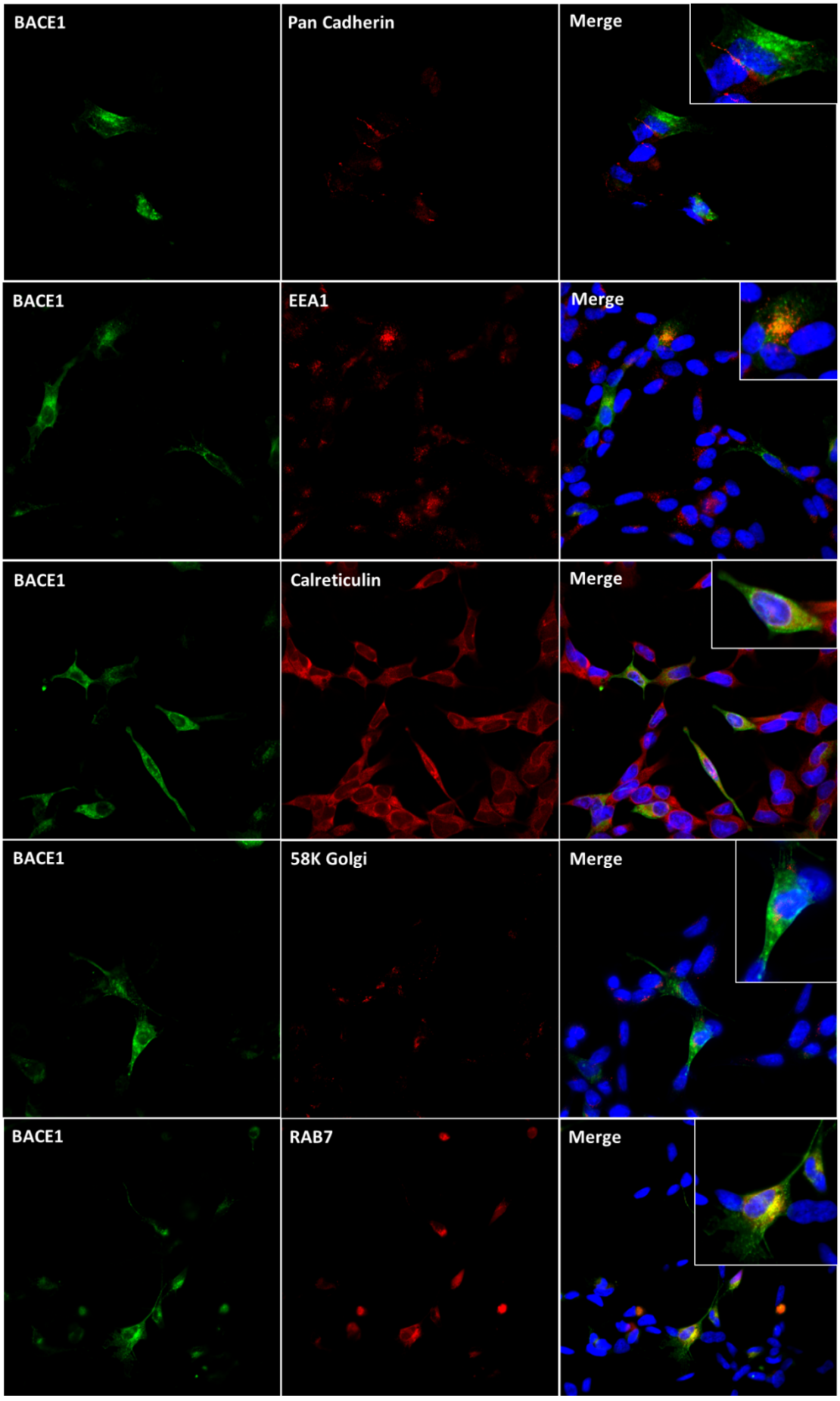

Figure 2.10 The localisation of overexpressed BACE1 in SH-SY5Y cells. BACE1 rabbit2 antibody (green) was used in this experiment.

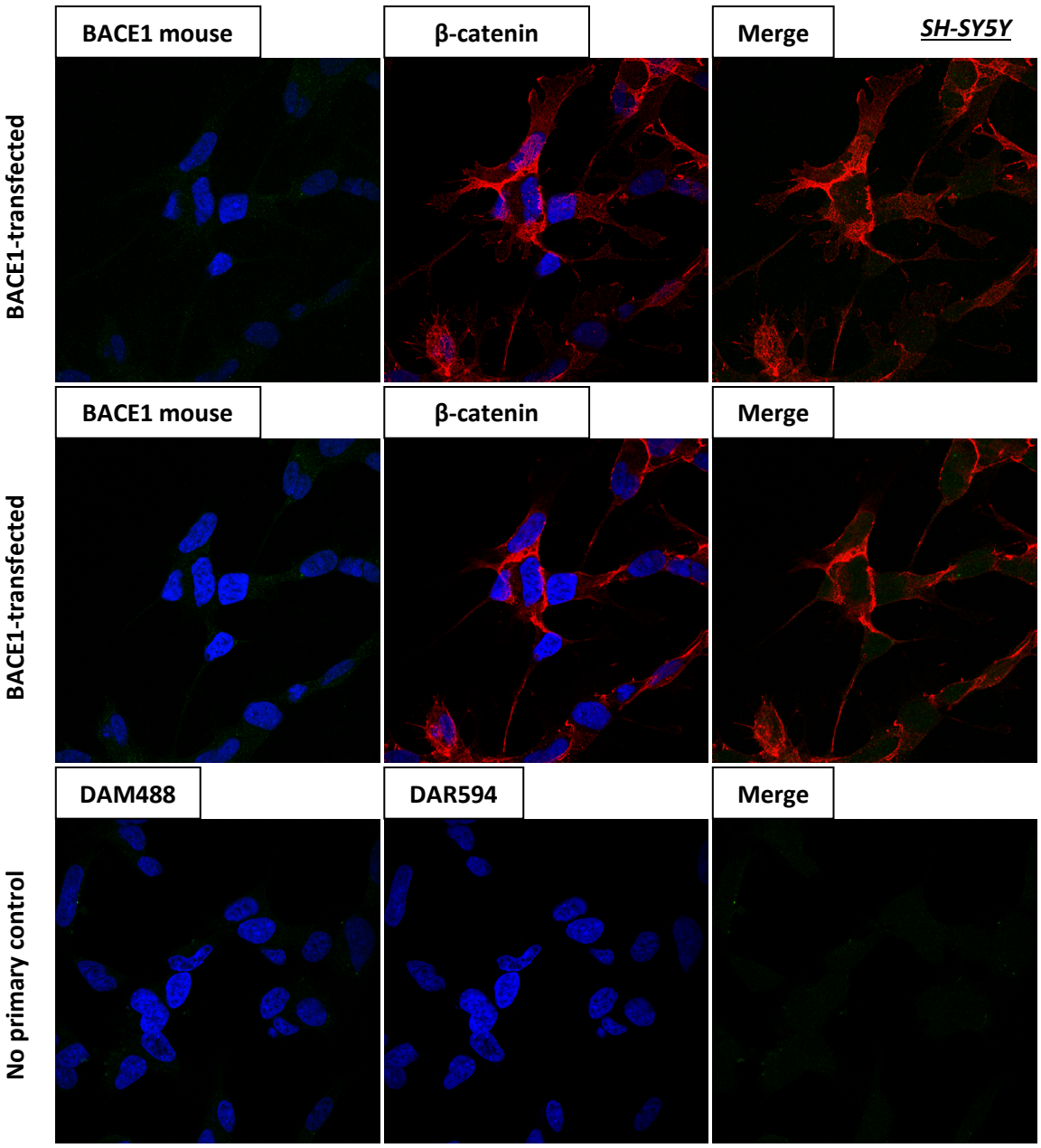

Figure 2.11 The BACE1 mouse antibody failed to label BACE1 at the surface of SH-SY5Y cells. Top panel, a top slice from a z-stack; middle panel, a middle slice from a z-stack; bottom panel, no primary antibody control, was only stained with secondary antibodies donkey-anti-mouse (DAM) 488 and donkey-anti-rabbit (DAR) 594 while the primary antibodies were skipped.

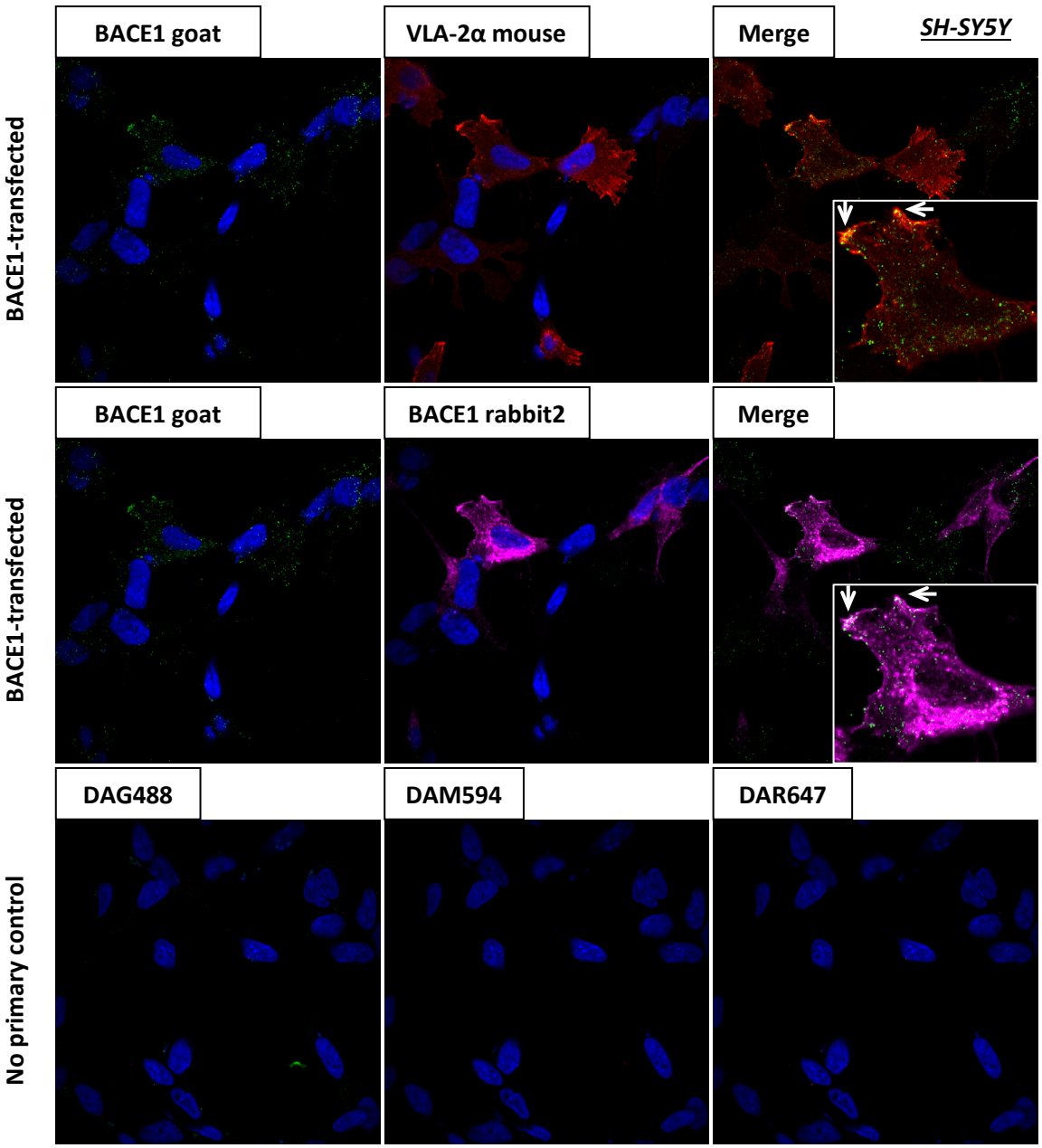

Figure 2.12 Cell surface labelling of BACE1 in SH-SY5Y cells (1). Cells were stained by the goat antibody, co-stained with VLA-2α mouse antibody or BACE1 rabbit2 antibody. No primary antibody controls were only stained with secondary antibodies donkey-anti-goat (DAG) 488, donkey-anti-mouse (DAM) 594 and donkey-anti-rabbit (DAR) 647 while the primary antibodies were skipped. The localisation of surface-labelled BACE1 was indicated by the white arrows.

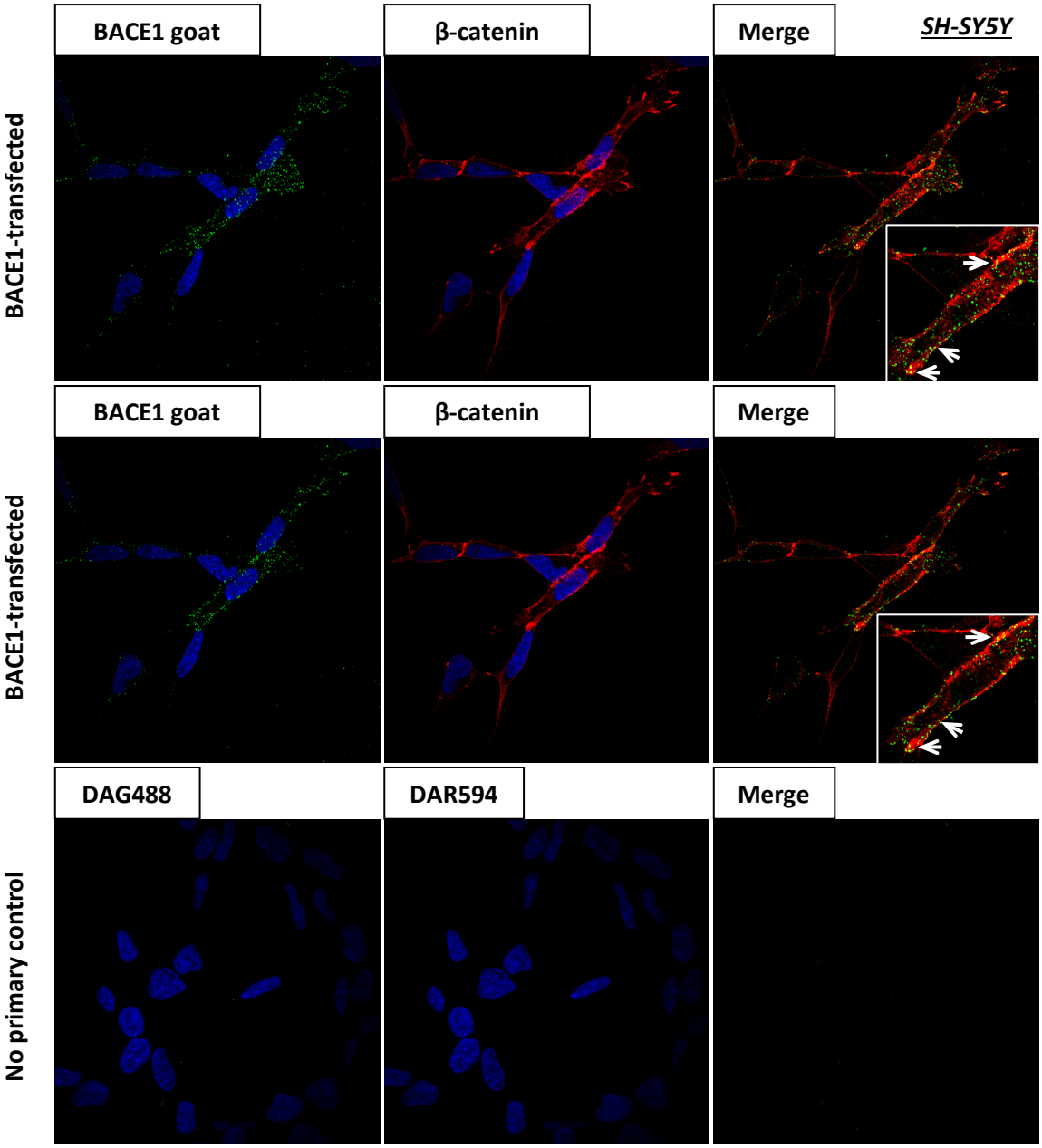

Figure 2.13 Cell surface labelling of BACE1 in SH-SY5Y cells (2). Cells were stained by the goat antibody co-stained with β-catenin rabbit antibody. Top panel, a top slice from a z-stack; middle panel, a middle slice from a z-stack; bottom panel, no primary antibody control, was only stained with secondary antibodies donkey-anti-goat (DAG) 488 and donkey-anti-rabbit (DAR) 594 while the primary antibodies were skipped. The localisation of surface-labelled BACE1 was indicated by the white arrows.

In western blotting, two bands at around 55 kDa and 65 kDa were detected by both N-terminal antibody (mouse) and C-terminal antibodies (rabbit1&2) (Figure 2.14), corresponding to immature BACE1 and mature BACE1. The molecular weights observed for BACE1 were slightly smaller than the generally reported sizes of 60 kDa for immature BACE1 and 70 kDa for mature BACE1. This discrepancy is not uncommon as prestained protein ladders may have different migration abilities in

various SDS-PAGE buffer and gel systems due to the coupling of chromophores which affect the prediction of the molecular weight. Other researchers have also showed the 65 kDa mature BACE1 using the rabbit1 antibody (Xie et al, 2007; Xu et al, 2014).

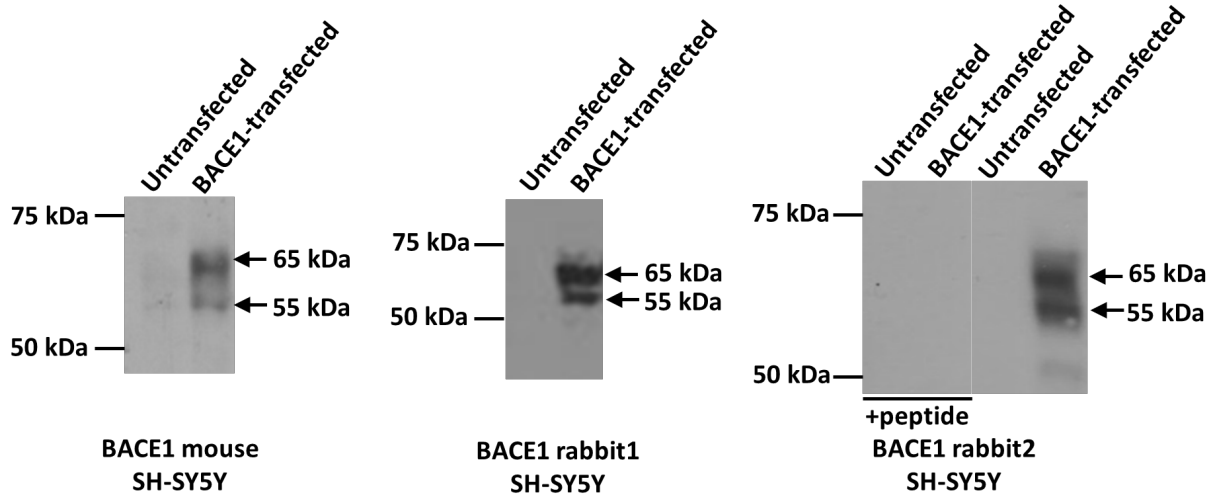

Figure 2.14 Validation of BACE1 antibodies using western blotting in SH-SY5Y cells. Untagged BACE1 plasmid was transfected. Protein lysates were extracted by RIPA buffer. In each lane, 10 µg proteins were loaded and separated in 7% tris-acetate gels. BACE1 mouse and rabbit1/2 antibodies recognised two bands at 55 kDa and 65 kDa indicated by black arrows, corresponding to immature and mature BACE1. The blocking peptide for BACE1 rabbit2 antibody completely eliminated the signals. Note that no signal was detected in untransfected cells, but this did not mean that BACE1 was not endogenously expressed in SH-SY5Y cells (see 2.3.2.2).

The BACE1 goat antibody co-localised well with BACE1 rabbit2 antibody in picking up exogenous BACE1 in both HEK293 cells and primary cortical neurons (Figure 2.15, 2.18). However, the BACE1 goat antibody was more competent in recognising endogenous BACE1/Bace1, which could be labelled by BACE1 rabbit2 antibody with a concentration double of that used for overexpressed BACE1 (Figure 2.16, 2.19). All the signals indicated by BACE1 rabbit2 antibody could be eliminated by its blocking peptide. The endogenous expression of BACE1/Bace1 was also detected by BACE1 mouse antibody (Figure 2.17, 2.20).

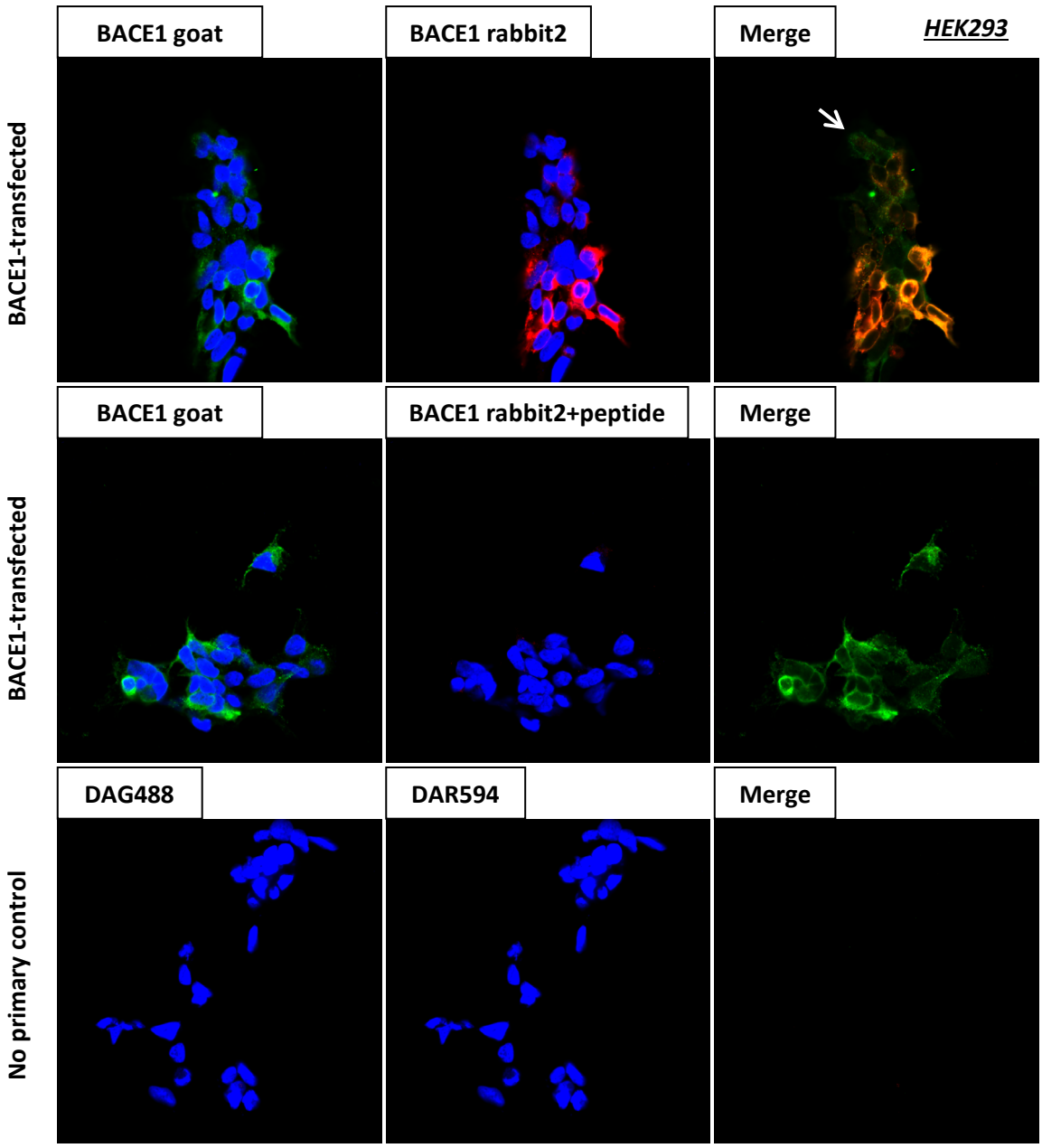

Figure 2.15 Validation of BACE1 antibodies using immunocytochemistry in HEK293 cells. Untagged BACE1 plasmid was transfected. Cells were double-immunostained by BACE1 goat antibody together with BACE1 rabbit2 antibody or rabbit2 with the pre-absorption of blocking peptide. Negative controls were only stained with secondary antibodies donkey-anti-goat (DAG) 488 and donkey-anti-rabbit (DAR) 594 while the primary antibodies were skipped. BACE1 goat and rabbit2 antibodies co-localised well in cells obviously labelled with rabbit2. BACE1 goat detected additional signals (indicated by a white arrow) which may represent endogenous BACE1 in HEK293 cells. The signals indicated by BACE1 rabbit2 were eliminated by its blocking peptide.

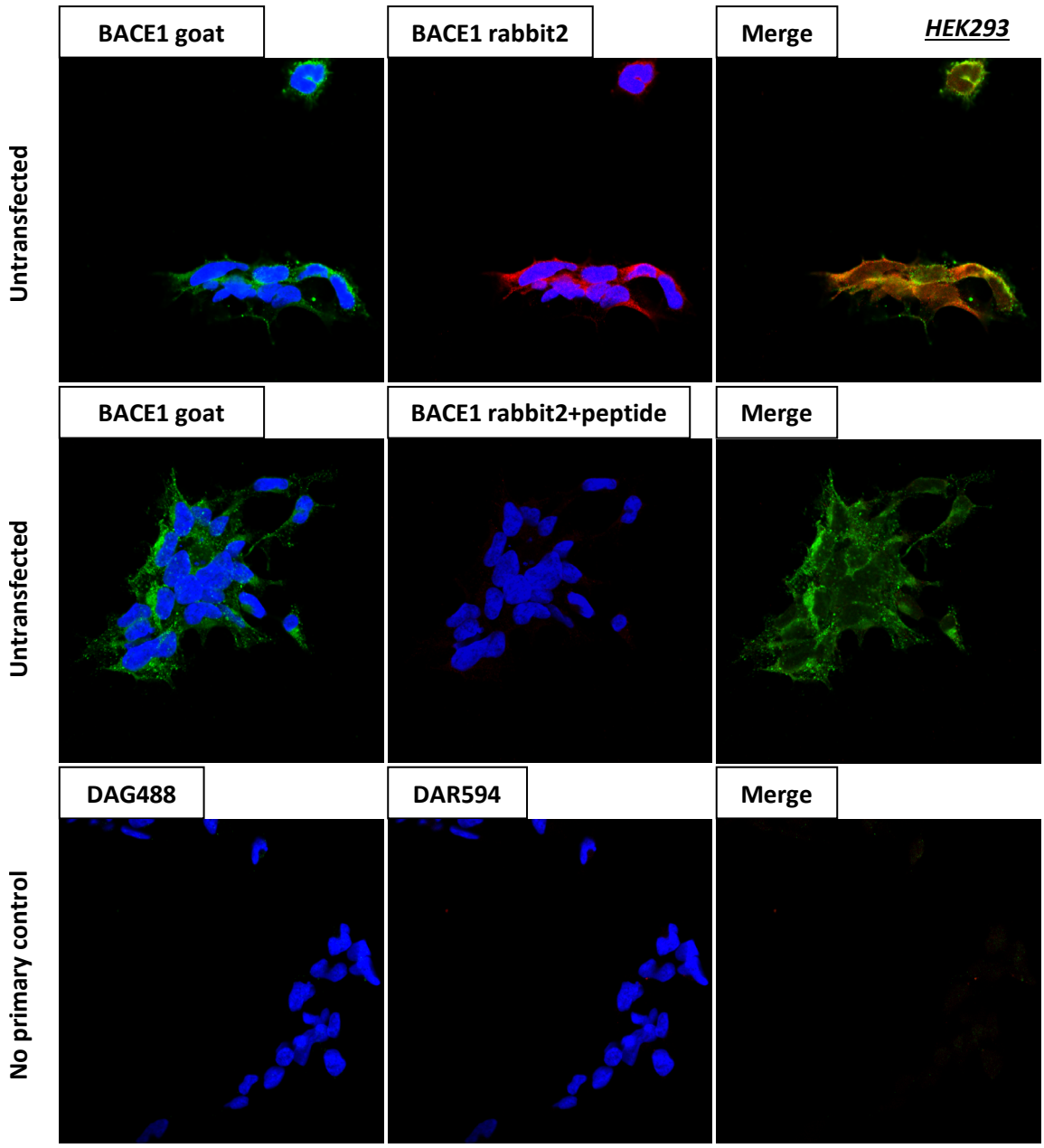

Figure 2.16 Endogenous BACE1 was detected in HEK293 cells by immunocytochemistry. Untransfected cells were double-immunostained by BACE1 goat antibody together with BACE1 rabbit2 antibody or rabbit2 with the pre-absorption of blocking peptide. Negative controls were only stained with secondary antibodies donkey-anti-goat (DAG) 488 and donkey-anti-rabbit (DAR) 594 while the primary antibodies were skipped. BACE1 goat and rabbit2 antibodies co-localised in nearly every cell. The signals indicated by BACE1 rabbit2 were eliminated by its blocking peptide.

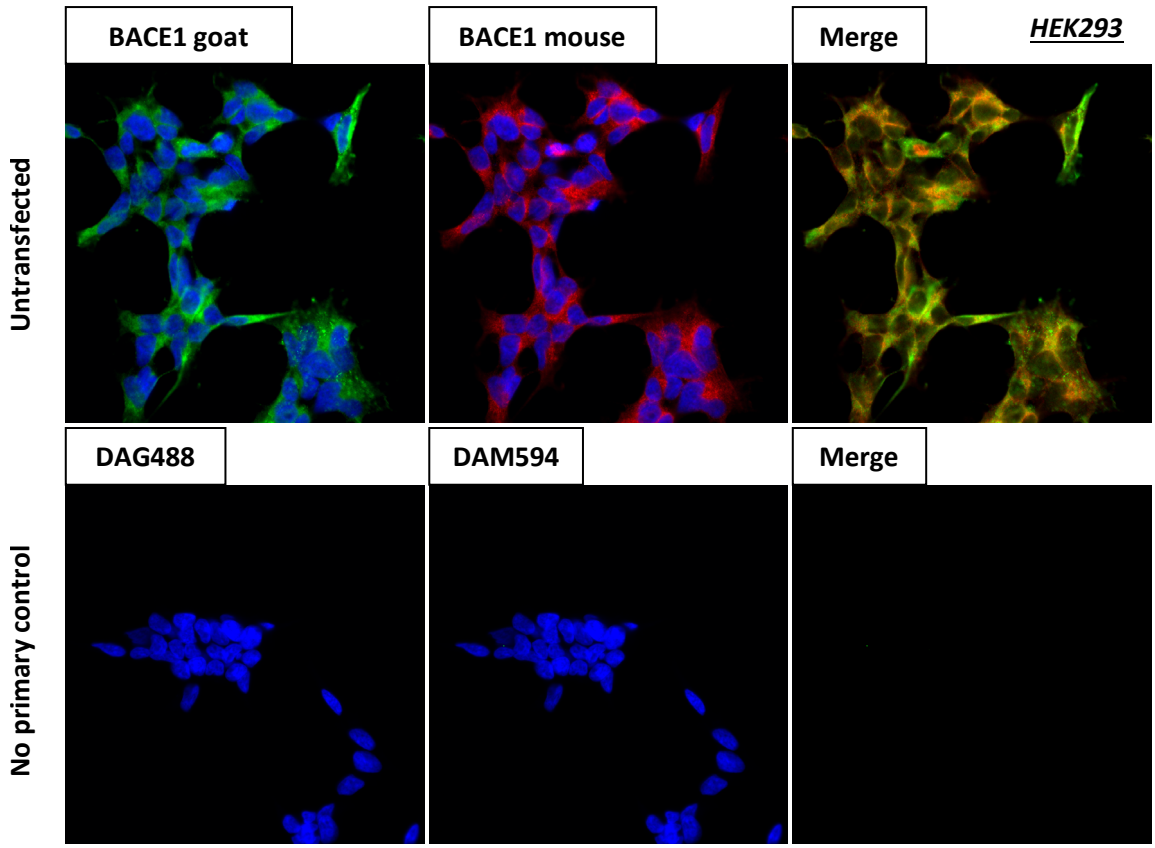

Figure 2.17 Detection of endogenous BACE1 in HEK293 cells. This was further supported by a third antibody using immunocytochemistry. Untransfected cells were double-immunostained with BACE1 goat and mouse antibodies. Negative controls were only stained with secondary antibodies donkey-anti-goat (DAG) 488 and donkey-anti-mouse (DAM) 594 while the primary antibodies were skipped. The two antibodies co-localised in nearly every cell.

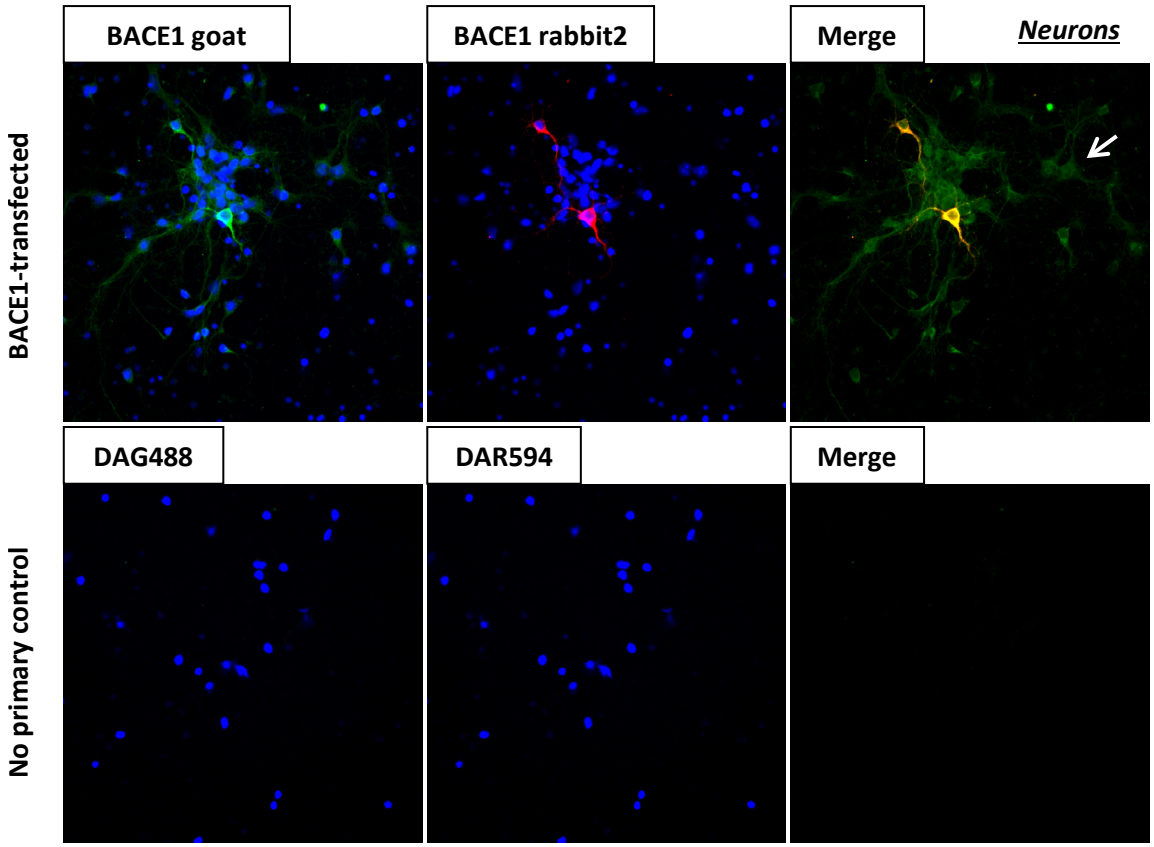

Figure 2.18 Validation of BACE1 antibodies using immunocytochemistry in primary cortical neurons. Untagged BACE1 plasmid was transfected. DIV4 post-transfection neurons were double-immunostained with BACE1 goat and rabbit2 antibodies. Negative controls were only stained with secondary antibodies donkey-anti-goat (DAG) 488 and donkey-anti-rabbit (DAR) 594 while the primary antibodies were skipped. BACE1 goat and rabbit2 antibodies co-localised well in cells obviously labelled with rabbit2. BACE1 goat detected additional signals (indicated by a white arrow) which may represent endogenous Bace1 in neurons.

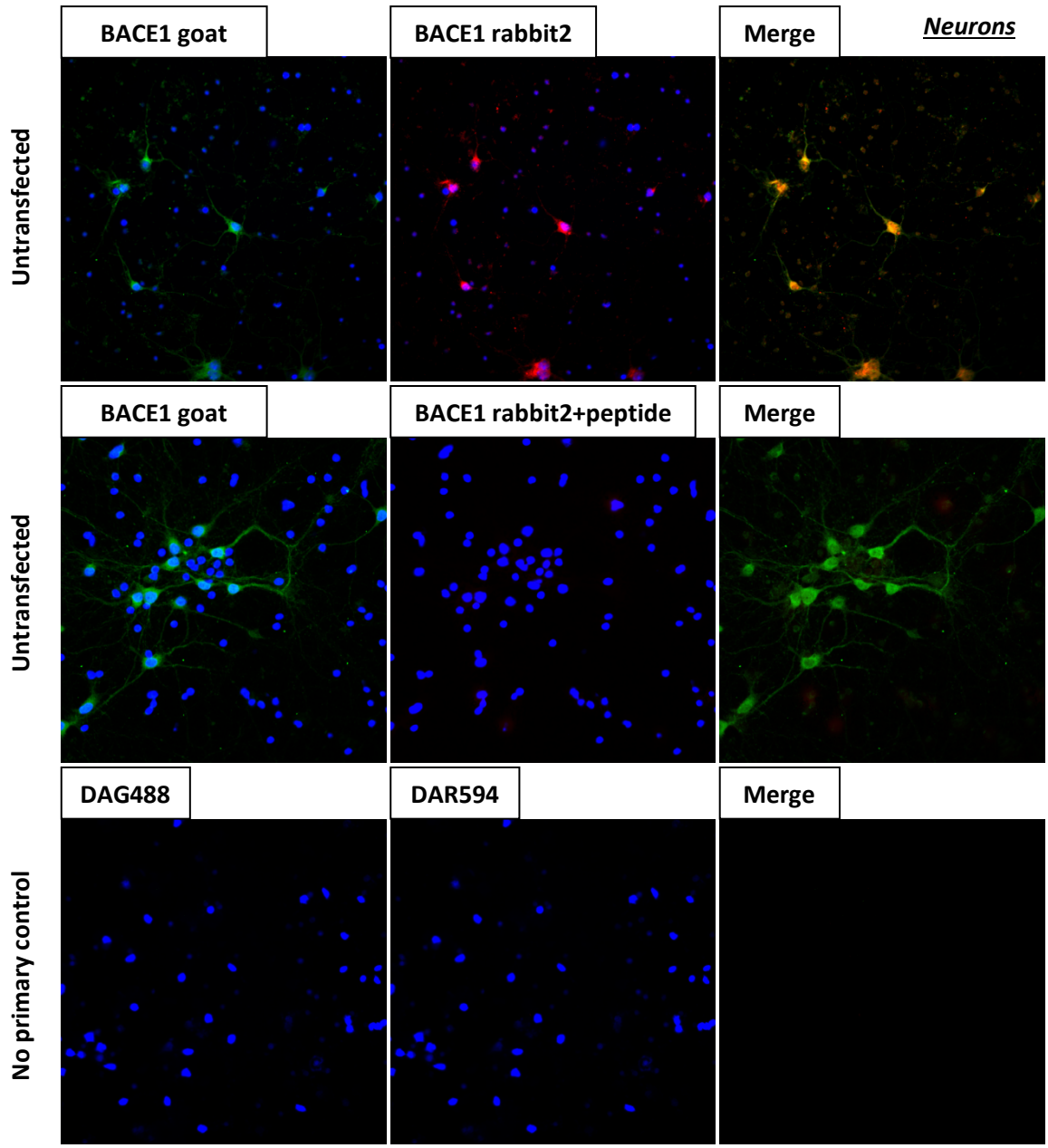

Figure 2.19 Endogenous Bace1 was detected in mouse primary cortical neurons using immunocytochemistry. Untransfected DIV4 neurons were double-immunostained by BACE1 goat antibody together with BACE1 rabbit2 antibody or rabbit2 with the pre-absorption of blocking peptide. Negative controls were only stained with secondary antibodies donkey-anti-goat (DAG) 488 and donkey-anti-rabbit (DAR) 594 while the primary antibodies were skipped. BACE1 goat and rabbit2 antibodies co-localised in neurons. The signals indicated by BACE1 rabbit2 were eliminated by its blocking peptide.

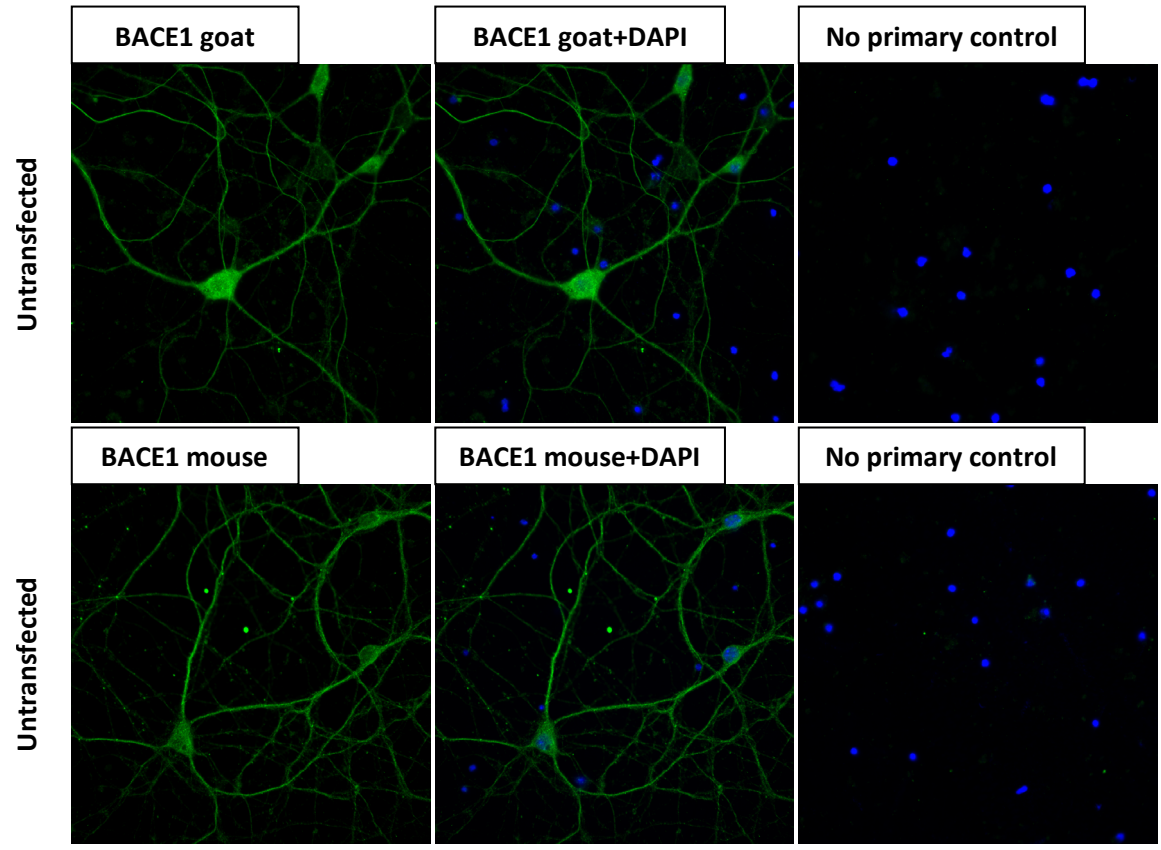

Figure 2.20 Endogenous Bace1 was detected in mature primary hippocampal neurons using immunocytochemistry. Untransfected DIV28 neurons were separately immunostained by BACE1 goat and mouse antibodies. Negative controls were only stained with secondary antibodies donkey-anti-goat 488 or donkey-anti-rabbit 488 while the primary antibodies were skipped. Both the two antibodies detected endogenous Bace1 in mature neurons.

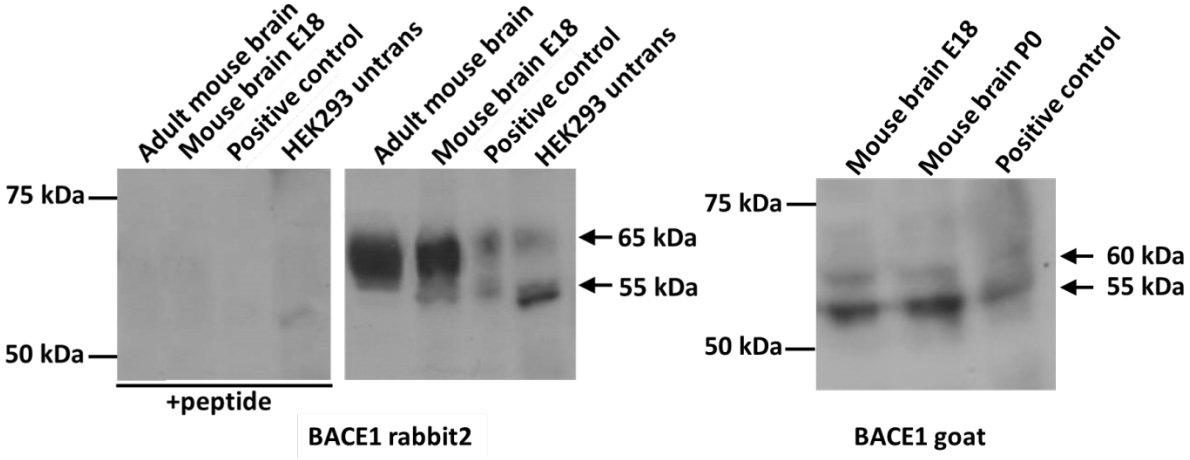

Figure 2.21 Endogenous BACE1/Bace1 was detected in HEK293 cells and mouse brain using western blotting. E18: embryonic day 18; P0: postnatal day 0, new after birth; positive control: SH-SY5Y cells overexpressed with BACE1.

By western blotting, BACE1 rabbit2 detected both immature and mature endogenous BACE1/Bace1 in protein lysates prepared from untransfected HEK293 cells, adult mouse brain and embryonic mouse brain (Figure 2.21). The blocking peptide validated the detection of this antibody. The diffuse band at around 65 kDa indicated a highly glycosylated Bace1. It predominated in the mouse brain samples, suggesting a high β-secretase activity in the brain because glycosylation appears important for the enzymatic activity of BACE1 (Charlwood et al, 2001). BACE1 goat antibody also recognised two bands, but the top band was not as dominating as the one probed by rabbit2. This band was slightly smaller, which might represent a partly glycosylated BACE1. The immunogen sequence of BACE1 goat antibody covers the four glycosylation sites at the N-terminal. Therefore, this observation might also indicate that glycosylation affects antibody binding.

2.3.1.3 Primary antibody omitting experiments

In immunofluorescence double-staining experiments, it is essential to make sure that there is no cross-immunoreactivity between primary antibodies and secondary antibodies. In other words, the secondary antibody for one primary antibody must not react to the other primary antibody. In previous sections, most of the primary antibodies (for instance, the subcellular markers) used for double staining have been tested by the staff in our lab. I, myself, tested the primary antibodies for GPR50 and BACE1 used in this thesis, exampled by GPR50 goat and BACE1 rabbit2 antibodies. As is shown in Figure 2.22, the donkey-anti-goat 594 secondary antibody was able to expose GPR50 signal only when GPR50 goat antibody was used. The donkey-anti-rabbit 488 secondary antibody exposed BACE1 signal only when BACE1 rabbit2 antibody was used. Therefore, there was no cross-immunoreactivity in this experiment. Other antibodies showed a good performance similarly (not shown). Thus, all the antibodies listed in this thesis were suitable for use in immunofluorescence double staining.

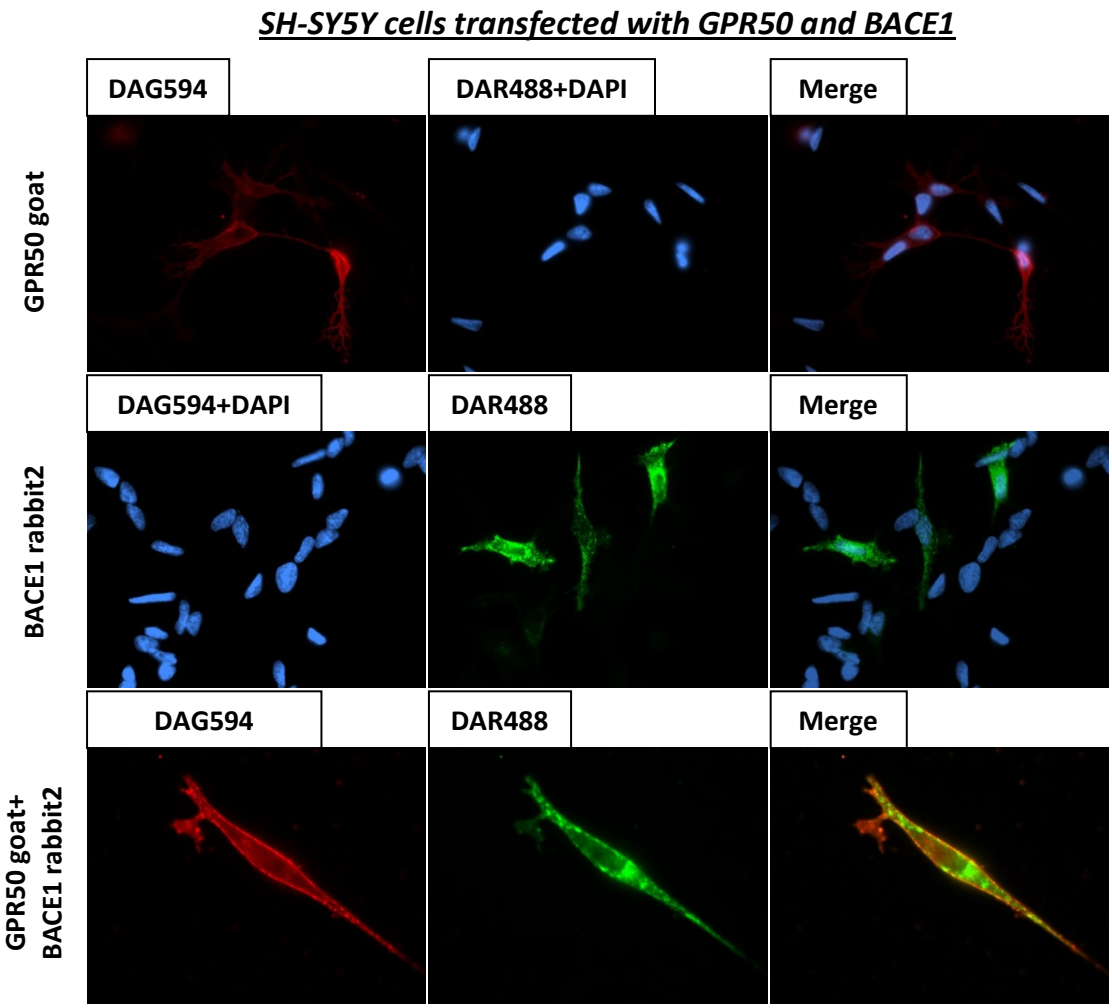

Figure 2.22 Cross-immunoreactivity test in immunocytochemistry double-staining experiments. SH-SY5Y cells were double-transfected with untagged GPR50 and BACE1 plasmids. Top panel: cells were incubated only with GPR50 goat primary antibody, followed by staining with both secondary antibodies, donkey-anti-goat (DAG) 594 and donkey-anti-rabbit (DAR) 488; middle panel: cells were incubated only with BACE1 rabbit2 primary antibody, followed by staining with both secondary antibodies, DAG594 and DAR488; bottom panel: cells were incubated with both GPR50 goat and BACE1 rabbit2 primary antibodies, followed by staining with both secondary antibodies, DAG594 and DAR488.

2.3.1.4 Conclusion

Preliminary testes validated the integrity of antibodies for GPR50 and BACE1 used in this thesis. Immunocytochemistry performed with major antibodies showed viable staining patterns of subcellular distribution that have been described in earlier research. Uncertain staining pattern of GPR50 goat antibody has been pointed out and will be cautiously attended to in subsequent experiments. Western blotting analysis with each antibody detected proteins of the expected sizes. Thus, the antibodies can be confidently used in this thesis according to their effectiveness in different experiments.

2.3.2 GPR50 is involved in the regulation of BACE1 expression

The overexpression of GPR50 is capable of elevating endogenous β-secretase activity of human BACE1 (Grünewald, 2011). To investigate whether this regulation result is attributed to the alteration of BACE1 expression upon GPR50 overexpression in HEK293 cells, I compared the mRNA and protein levels of endogenous BACE1 with or without exogenous GPR50 in HEK293 and SH-SY5Y cells.

2.3.2.1 The protein level of mature BACE1 is decreased by GPR50 overexpression in HEK293 cells

The relative densities of BACE1 bands detected by BACE1 rabbit2 antibody were calculated in ImageJ and normalised against those of GAPDH. In HEK293 cells, GPR50 overexpression decreased the protein level of mature BACE1 by around 60%, but had no significant effect on immature BACE1, compared with the control condition (Figure 2.23). The β-secretase activity is mainly contributed by mature BACE1, as immature BACE1 exhibited trivial enzymatic activity (Zhong et al, 2007). GPR50 is known to increase BACE1 activity significantly in this cell line, which cannot be explained by the regulative effect of GPR50 on BACE1 protein expression. Another mechanism (trafficking of BACE1) that may affect BACE1 activity via GPR50 was investigated in chapter 5.

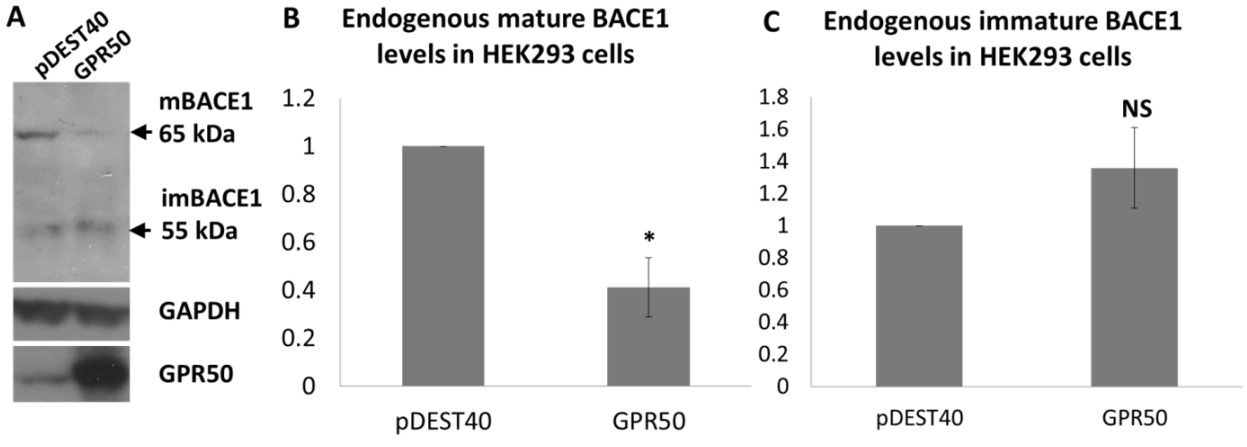

Figure 2.23 The effect of GPR50 overexpression on endogenous levels of BACE1 protein in HEK293 cells. A) Mature BACE1 (65 kDa) and immature BACE1 (55 kDa) in cells transfected with empty vector pDEST40 or GPR50. B) Normalised endogenous mature BACE1 protein levels, N=3, *p=0.0035<0.05 by paired Student's t-test. C) Normalised endogenous immature BACE1 protein levels, N=3, NS: p=0.29>0.05 by paired Student's t-test.

2.3.2.2 The analysis of endogenous BACE1 in neuroblastoma cell line SH-SY5Y

PCR products of cDNA synthesised from untransfected and BACE1-transfected SH-SY5Y cells were sequenced and verified as BACE1 fragments. As is shown in Figure 2.24.A, a moderate level of endogenous BACE1 mRNA was detected in SH-SY5Y cells. Yu and colleagues identified a higher level of BACE1 mRNA in SH-SY5Y than in HEK293 cells, which was attributed to the differences in promoter strength that regulate the transcriptional activation (Li et al, 2006). It was also suggested that BACE1 promoter activity is greater in neuronal cells than in non-neuronal cells (Sun et al, 2005). However, the protein level of BACE1 in SH-SY5Y cells can be very low (Qing et al, 2004), concomitant with a minor Aβ level (Xue et al, 2006). The western blotting results revealed a single band at around 60 kDa, which was lacking when BACE1 rabbit2 antibody was pre-absorbed by the blocking peptide. The molecular weight of the detected protein is neither the expected size of 65kD mature BACE1 nor 55 kDa immature BACE1, unlike in HEK293 cells and mouse brain in which both of the isoforms exist (Figure 2.21). It is likely that this BACE1 is an intermediate isoform prior to complete maturation, which has been reported by others (Costantini et al, 2007; Ko & Puglielli, 2009).

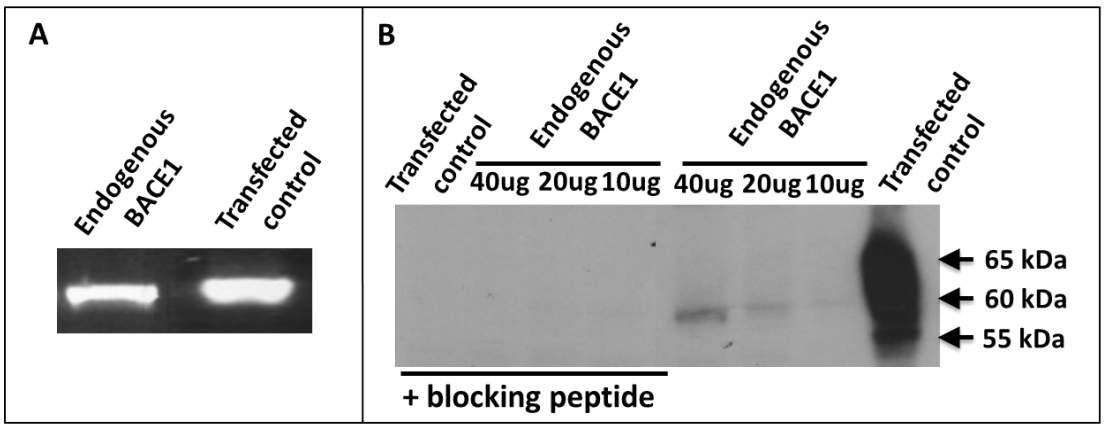

Figure 2.24 The expression levels of endogenous BACE1 in SH-SY5Y cells. A) Endogenous BACE1 mRNA. B) Endogenous BACE1 protein. Transfected control: SH-SY5Y cells transfected with untagged BACE1 plasmid. BACE1 rabbit2 antibody was used in this experiment.

2.3.2.3 The mRNA level of endogenous BACE1 is decreased by GPR50 overexpression in SH-SY5Y cells

Six biological replicates were performed for the real-time PCR experiment. Expression levels of endogenous BACE1 and overexpressed GPR50 were normalised against three housekeeping genes: TFRC, TBP and UBC. One replicate

was identified as a potential outlier based on the normal range of BACE1 mRNA level among the six replicates, according to the interquartile range rule (see 7.2.4 for detail). Upon overexpression of GPR50, there was a significant decrease of BACE1 mRNA level compared with the control condition, after the removal of the outlier replicate (Table 2.10, Figure 2.25).

Table 2.10 The relative mRNA expression levels of BACE1 in SH-SY5Y cells transfected with pDEST40 or GPR50

		pDEST40	GPR50
Replicate A		1	0.984647
Replicate B		1	0.811340
Replicate C		1	0.769962
Replicate D		1	0.447656
Replicate E		1	3.041578
Replicate F		1	0.476823
With E	Average	1	1.088668
	Standard deviation	0	0.893347
	Standard error	0	0.364707
Without E	Average	1	0.698086
	Standard deviation	0	0.230099
	Standard error	0	0.042645

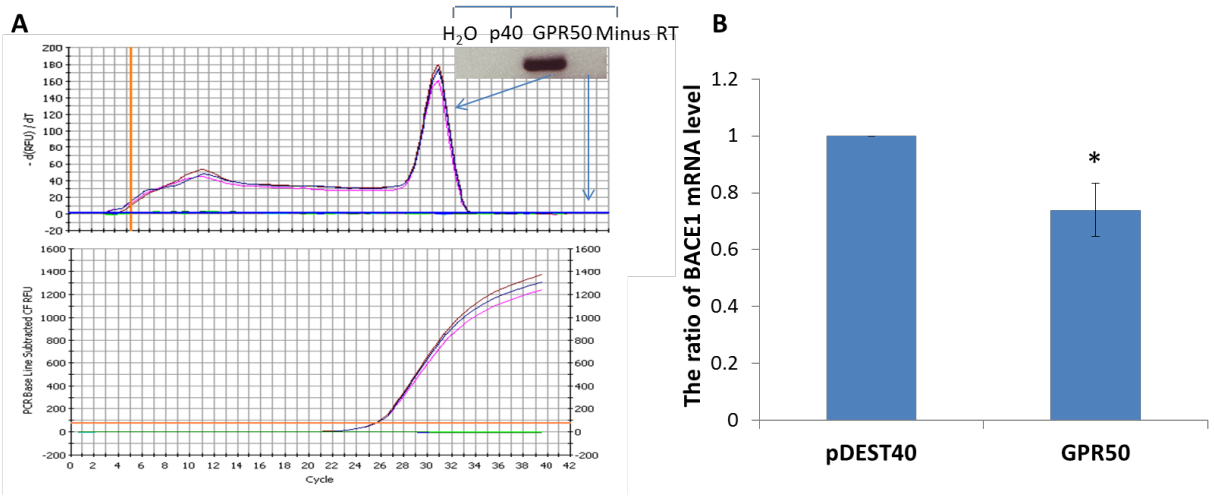

Figure 2.25 The effect of GPR50 overexpression on endogenous levels of BACE1 mRNA in SH-SY5Y cells. A) Validation of GPR50 transfection. The peaks indicated three experimental replicates for a successful amplification of GPR50 from cDNA of GPR50-transfected cells. The pDEST40-transfected cells did not express GPR50 endogenously, so there was no GPR50 amplification, indicated by a flat line. A flat line for the dH_2O control suggested that there was no contamination during the qPCR process. A flat line for the no-transcriptase control (Minus RT) suggested that there was no contamination during the processes of RNA extraction and cDNA synthesis. B) Normalised endogenous BACE1 mRNA levels. The same amounts of empty vector pDEST40 were transfected as the control of the untagged GPR50 plasmid, N=6, *P=0.039<0.05 by paired Student's t-test.

2.3.2.4 The protein level of BACE1 is increased by GPR50 overexpression in SH-SY5Y cells

Next, I determined whether GPR50 overexpression has an effect on BACE1 protein level in SH-SY5Y cells by western blotting. It was found that exogenous GPR50 induced a 47% increase of endogenous BACE1 protein level in SH-SY5Y cells versus the empty vector control (Figure 2.26). It is interesting that the regulative impact of GPR50 expression on BACE1 protein level was opposite to that on BACE1 mRNA level. This indicates that GPR50 is a multi-functional factor, which may be involved in the different stages of BACE1 regulation system. Another possibility is that GPR50 participates in the inhibitory feedback loop of BACE1 protein level on its gene transcription (mRNA level).

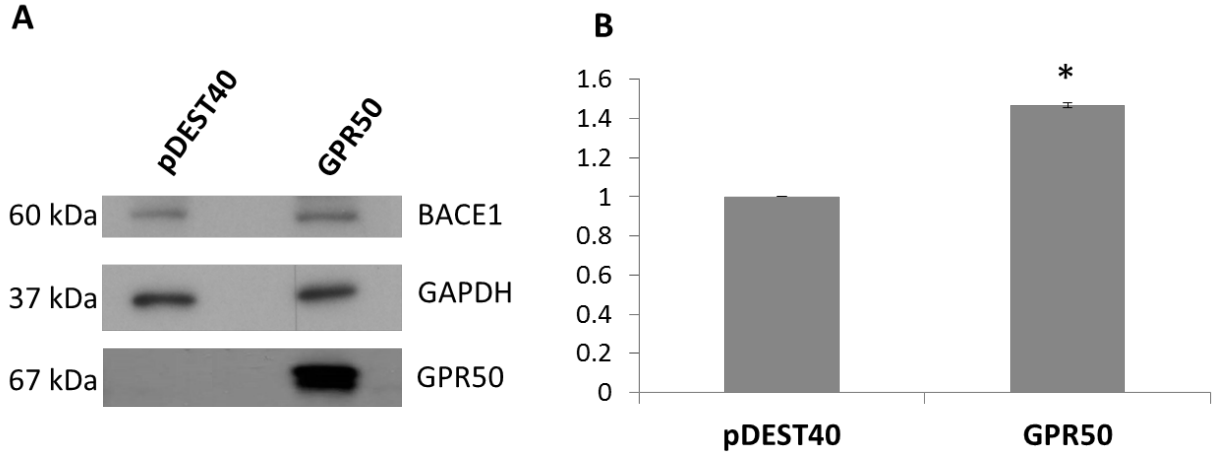

Figure 2.26 The effect of GPR50 overexpression on endogenous levels of BACE1 protein in SH-SY5Y cells. A) BACE1 in cells transfected with empty vector pDEST40 or GPR50; B) Normalised endogenous BACE1 protein levels, N=3, *p=0.0035<0.05 by paired Student's t-test. Antibodies: BACE1 rabbit2, GPR50 goat, GAPDH mouse.

2.4 Discussion

In this chapter, antibodies used in this thesis were validated. The subcellular localisation of exogenous GPR50 and BACE1 were confirmed in SH-SY5Y and HEK293 cells, and the results are in agreement with the published data. Further, diversified regulative effects of exogenous GPR50 on BACE1 expression levels were identified in these two cell lines.

2.4.1 The subcellular location of GPR50 and BACE1

The subcellular localisation of GPR50 was mainly at the cell surface. Although the internally expressed GPR50 was detectable, the location of this pool was not clear, as

the co-localisation of GPR50 with other subcellular markers was not convincing. This observation was not a result of overexpression, as the endogenous GPR50 detected in HEK293 cells was also predominantly located at the plasma membrane, but occasionally at internal-like sites (Grünewald, 2011). It requires further investigation why a small percentage of this GPCR was not targeted to the cell surface.

Earlier studies showed that overexpressed BACE1 was found in post-ER sites including the plasma membrane, the early endosomes, the Golgi and the lysosomes. This result was validated by immunocytochemistry in this chapter. The co-staining pattern of BACE1 and the ER marker calreticulin showed no clear evidence for co-localisation. A previous study showed part co-localisation between BACE1 and calreticulin in SH-SY5Y cells (Griffiths et al, 2011). However, it seems that the majority of BACE1 was located outside the ER, with a punctate staining style that might match similar patterns in other compartments, normally the TGN and the endosomes as observed by myself and others (Kang et al, 2012; Prabhu et al, 2012). Time-lapse recording showed that BACE1 fluorescent particles moved rapidly through the ER and accumulated predominantly in Golgi-like complexes (Sun et al, 2006b). My observation also agrees with the fact that the maturation process of BACE1 is transient. In addition, a small amount of BACE1 was successfully labelled on the cell surface of SH-SY5Y cells, especially in the filopodia/lamellipodia structures, the formation of which can be induced by GPR50 overexpression (Grünewald, 2011). This pool of BACE1 may directly mediate cell surface proteolysis of cell adhesion molecules (Kuhn et al, 2012) or undergo internationalisation to the early endosomes for more robust β-secretase activity (Sannerud et al, 2011).

2.4.2 The possible role of GPR50 in regulating BACE1 expression

GPR50 overexpression resulted in a negative effect on BACE1 protein level in HEK293 cells. This adds more complexity in understanding GPR50's regulative role in BACE1 function, as the result was not supporting the previous finding of the positive modulation of BACE1 activity by GPR50 overexpression in the same cell line (Grünewald, 2011). Other mechanisms related to BACE1 activity regulation need to be further investigated, such as the trafficking network of BACE1 (see chapter 5).

Real-time qPCR and western blotting were performed in SH-SY5Y cells to investigate the regulative potential of GPR50 on BACE1 mRNA and protein levels respectively. Surprisingly, the decreased BACE1 mRNA level upon transfection of exogenous GPR50 did not lead to a declined protein level in SH-SY5Y cells. In contrast, a significant increase of BACE1 protein level was observed with GPR50 overexpression, compared with the pDEST40 control in SH-SY5Y cells.

There are several questions raised that might contribute to the contradiction of the regulation results of mRNA and protein in the same cell line:

1) The samples used for qPCR and western blotting were not from the same cells, but prepared separately.
2) The qPCR experiment made use of three housekeeping genes (TFRC, TBP and UBC) to normalise BACE1 mRNA levels, while a different housekeeping gene (GAPDH) was singly utilised in the western blotting to normalise BACE1 protein levels.
3) Is the effect of GPR50 overexpression on BACE1 levels dose-dependent?
4) Is it reasonable to remove outliers according to the dataset with a small sample size?
5) Does the overexpression of empty vector pDEST40 have an impact on BACE1 levels?
6) Are the housekeeping genes equally stable?
7) Is it more reasonable to use single or multiple housekeeping genes?

In summary, my results suggested that a differentiated regulative system of BACE1 might exist between cell lines, such as between non-neural cells and neuronal cells.

2.4.3 Further experiments

Results in this chapter showed that GPR50 is involved in the regulation system of BACE1 transcription and translation. The next step is to study whether there is a direct interaction between the two proteins. Therefore, in chapter 3, I tested this hypothesis using techniques for investigating the protein-protein interaction.

3 The potential of GPR50 to be an interactor of BACE1

The multiple potential interactors of GPR50 identified by the yeast two-hybrid analysis are associated with BACE1 expression (SNX6, SREBP2), trafficking (RTN3, SNX6) or activity (RTN4, ABCA2, CDH8) (Davis, 2011; Deng et al, 2013; Mastrocola et al, 2011; Murayama et al, 2006; Okada et al, 2010; Stützer, 2012). Preliminary findings showed that in HEK293 cells, overexpression of GPR50 resulted in an increase of BACE1 activity and appeared with the opposite effect of known BACE1 co-interactors RTN3 and RTN4 (Nogo) (Grünewald, 2011). In chapter 2, I showed that overexpressed GPR50 affected the expression levels of BACE1, but this did not provide sufficient evidence on the regulation of BACE1 activity. I proposed that GPR50 is involved in the physiological function of BACE1 directly or through cooperating with co-interactors. Thus, in this chapter, I investigated whether GPR50 is an interactor of BACE1.

3.1 Introduction

3.1.1 Protein-protein interaction

Diverse biological processes involve with a group of active proteins. These functional factors rarely act alone, but by forming a physical complex as a result of biochemical events and/or electrostatic forces, which is referred to as protein-protein interaction (PPI). Signal transduction, molecule trafficking and cell metabolism are all examples of PPI. These interactions are essential to the maintenance of the regular function in cells and organisms. Thus, aberrant PPIs can be indicative or causative of multiple diseases, such as neurodegenerative disorders and cancers (Kuzmanov & Emili, 2013).

3.1.1.1 Types of protein-protein interaction

PPI can be further characterised as stable or transient interactions. Stable interactions are commonly seen in multi-subunit protein complex. The subunits can be identical or different, known as homo-oligomers or hetero-oligomers. A variety of GPCRs interact to form homo-dimers/oligomers, which is important for G protein binding and activation (Palczewski, 2010). Co-expressed GPCRs may also form hetero-dimers/oligomers to alter the performances of the components; for instance, GPR50 is able to form a heterodimer with MT1, inhibiting the binding of G-protein and melatonin response (Levoye et al, 2006).

Transient interactions are temporary, but can be strong or weak, fast or slow, and always in a reversible manner. These interactions typically occur in certain cellular contexts, such as phosphorylation, conformational changes or trafficking to a particular cellular site. Transiently interacting proteins are involved in the majority of cellular processes, including protein modification, transport, folding, signalling, and cell cycling. For instance, newly synthesised BACE1 can only reach the Golgi apparatus after acetylation, by interacting with acetyltransferases, ATase1 and ATase2 in the ER/ER Golgi intermediate compartment; otherwise, the non-acetylated nascent protein is degraded by PCSK9/NARC-1 (Coulson et al, 2010; Ko & Puglielli, 2009).

3.1.1.2 Techniques to investigate protein-protein interaction

There are numerous ways to detect PPI. Each of the methods has its own advantages and disadvantages, especially with the consideration of the sensitivity and specificity of the approach. The most commonly used techniques are briefly introduced as follows.

- **Yeast two-hybrid screening** takes advantage of the integrity of the gene transcription system. Yeast cells are transfected with two plasmids separately containing the bait (cDNA of protein of interest or a certain fragment of the protein, fused with the DNA-binding domain of a yeast transcription factor, for example Gal4), and the prey (a library of cDNA fragments linked to the activation domain of the transcription factor proximal to a reporter gene) (Figure 3.1). Transcription of the reporter gene only occurs when the bait and prey interact with each other so as to form a functional transcription factor. Thus, the interaction between proteins can be indicated by the presence of the expression product from the reporter gene. The advantage of yeast two-hybrid screening is the provision of high-throughput analysis, as this method allows the access to almost the entire cellular proteome (Bruckner et al, 2009). However, the yeast two-hybrid takes place in the nucleus. If two interacting proteins are not localised to the nucleus, they may be found to be non-interacting. Also, the outcome may include false positive binding partners, because the conformation of the bait or prey is easily affected (i.e. the extensive use of fusion proteins), which may alter the original binding property (Sobhanifar, 2003). Thus, a confidence score is normally calculated for each of the prey interactors (Global Predicted Biological

Score, Global PBS), inferring the likelihood of a true interaction. Other techniques are needed to verify the putative interactions, normally starting from those with the highest PBS score. For instance, in the yeast two-hybrid study of GPR50 interactors, Nogo was identified as a candidate with the highest score (PBS=A) (Grunewald et al, 2009). Following studies successfully validated the physical interaction between GPR50 and Nogo-A (Grünewald, 2011; Grunewald et al, 2009).

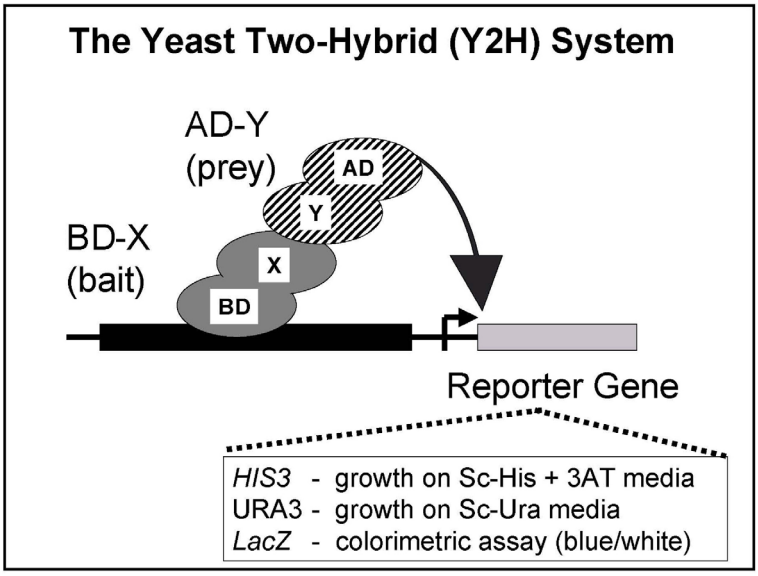

Figure 3.1 The yeast two-hybrid screening system. This figure was adapted from (Walhout, 2006). X, the bait protein; BD, the binding domain of a transcription factor; Y, the prey protein; AD, the activation domain of a transcription factor.

- **Co-localisation** refers to the observation of a spatial overlap between two (or more) fluorescent labels with different emission wavelength in fluorescence microscopy. This technique provides preliminary evidence to whether the different fluorophore-labelled proteins are located in the same site within the cell. The information obtained from co-localisation can be interpreted in two ways: 1) co-occurrence, which reflects the presence of two fluorophores in the same pixel (the two proteins are not necessarily related, for instance, BACE1 is located in EEA1-marked early endosomes, but BACE1 and EEA1 may not correlate, see Figure 2.10); 2) correlation, a statistically significant relationship between the two fluorophores, indicating a biological interaction between the two proteins. The statistical method to evaluate co-localisation indicated interaction is detailed in 3.2.3. A good example of perfect co-localisation is to detect the same protein with two different antibodies, as is shown in chapter 2 (Figure 2.5, 2.9). The strength of co-localisation is that it is easy to operate and can be useful to predict the interaction location of two proteins by applying subcellular compartments

markers. Yet, it is hard to explain the "non-perfect" interaction situations, which are affected by the presence of non-colocalising signals. Also, the technique relies on highly specific antibodies and clear fluorescent background. Co-localisation is widely utilised as the first step to test the possibility of a true interaction between two proteins.

- **Co-immunoprecipitation** (co-IP) is a popular technique for confirming the physical interaction between proteins (Figure 3.2). The "bait" protein is immunoprecipitated by its specific antibody, and a binding partner/protein complex, the so-called "prey", will be co-precipitated from the protein lysate. The antibody-binding protein complex is then immobilised on protein A or protein G sepharose beads and any proteins not precipitated on the beads will be eliminated by washing. This concept of pulling a protein complex out of the cell lysates is sometimes called a "pull-down". The protein complex is eluted from the beads and dissociated by SDS sample buffer. Proteins are then separated in SDS-PAGE gels, followed by western blotting with specific antibodies to identify the bait or prey. Co-IP is considered highly specific and compatible with most methods of downstream analysis (SDS-PAGE, immunoblotting, mass spectrometry). The main disadvantage is that there are occasionally difficulties in obtaining antibodies with high specificity and avidity (Miernyk & Thelen, 2008). Co-IP is often used for confirming the yeast two-hybrid screening results.

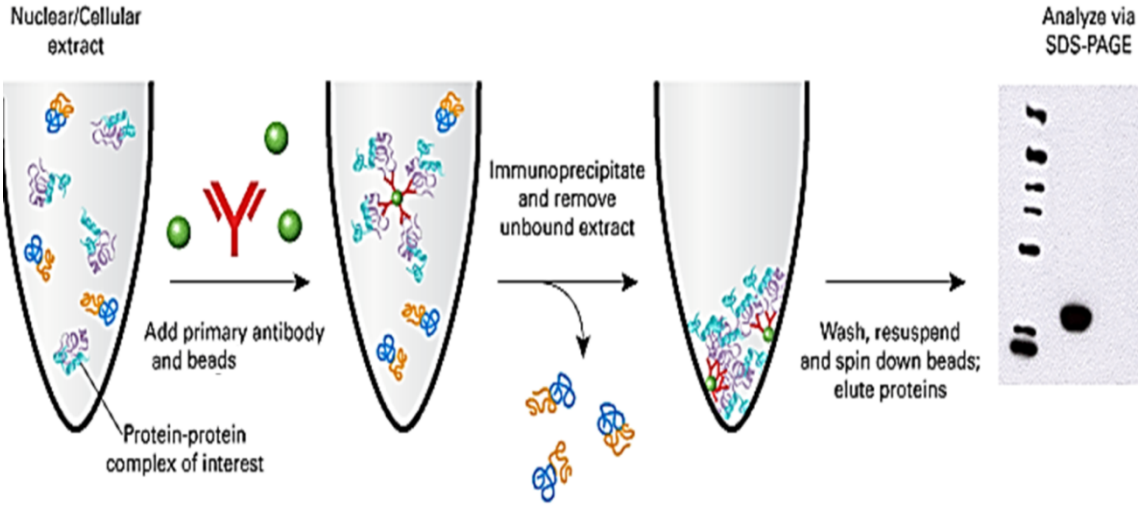

Figure 3.2 The schematic diagram of co-immunoprecipitation

- **Fluorescence resonance energy transfer** (FRET) is the mechanism of an excited donor transferring energy to an acceptor through a non-radiative process (defined as "resonance"). A donor molecule is excited by a photon within its excitation spectrum and then relaxes to the lowest excited singlet state, S1

(Figure 3.3). The relaxation of the electron energy results in the emission of a photon (fluorescence) by the donor fluorophore, concomitant with an energy drop. If there is an acceptor molecule within a short distance (<10 nm), energy transfer occurs from the donor to the acceptor, engendering acceptor fluorescence. In other words, the energy released when the donor electron returns to the ground state (S0) may simultaneously excite the acceptor molecule. Then the excited acceptor emits a photon and returns to its ground state. Thus, by attaching proper fluorophores to proteins that might interact with each other, the proximity of these putative interactors can be measured by determining if fluorescence resonance energy is transferred from the donor to the acceptor (Xu, 2001). A limitation of FRET is the requirement for external illumination to excite the donor fluorophore, which can lead to photobleaching, autofluorescence or direct excitation of the acceptor fluorophore. To avoid these disadvantages, bioluminescence resonance energy transfer (BRET) has been developed, in which the donor fluorophore is replaced by a luciferase that emits bioluminescence in the presence of a substrate and consequently excites the acceptor fluorophore. BRET has a great potential in assessing PPIs in living cells and in real time (Xu, 2001). For instance, Levoye et al identified GPR50 homodimer and GPR50/$MT_{1/2}$ heterodimers in living HEK293 cells by using BRET (Levoye et al, 2006).

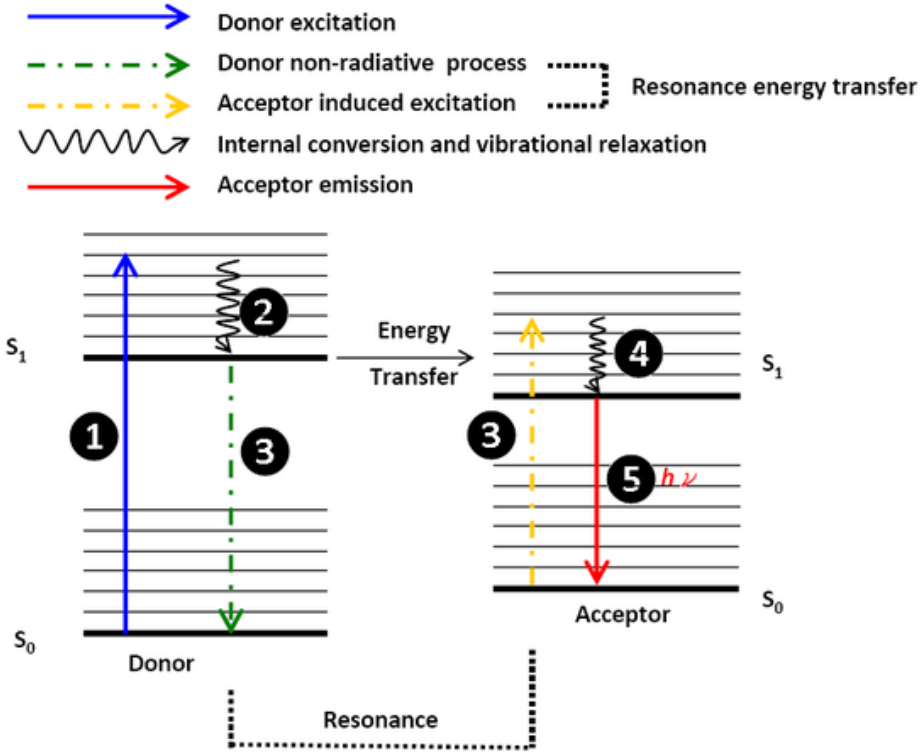

Figure 3.3 The schematic diagram of fluorescence resonance energy transfer. This diagram was adapted from (Selvin, 2003). S1, singlet state; S0, ground state.

3.1.2 Introduction to experiments

To confirm the possible interaction between GPR50 and BACE1, I performed preliminary biological tests in mammalian cells, described as follows.

1) To examine if there is a possibility of GPR50 and BACE1 proximity, co-localisation by immunocytochemistry was carried out in cells over-expressing human GPR50 and BACE1 and in cells expressing the two proteins endogenously.
2) To verify the results observed in the co-localisation experiments, subcellular fractionation was performed to check whether GPR50 and BACE1 co-fractionate in fractions containing specific organelles.
3) To further validate if GPR50 and BACE1 are physically associated, co-immunoprecipitation experiments were performed at both exogenous and endogenous levels.

3.2 Materials and methods

3.2.1 Tissue culture and relative techniques

HEK293, SH-SY5Y and murine neuroblastoma cell line N1E-115 were grown in 12-well plates and 10 cm plates (see 2.2.1). Primary neuronal cultures used for immunocytochemistry were prepared from the hippocampi of E18 CD1 mice (purchased from Biomedical Research Resources Unit, Western General Hospital, Edinburgh). Plasmids used in this chapter were described in 2.2.3. The transfection protocol was summarised in 2.2.4. For the methods of immunocytochemistry, cell surface labelling and western blotting, see 2.2.5, 2.2.6 and 2.2.7 respectively. All the fluorescence images were taken on a Nikon A1R confocal microscope with a size of 1024×1024 in the z-stack programme.

3.2.2 Antibodies

The primary antibodies used in this chapter and their application conditions are summarised in Table 3.1. The full information for these antibodies can be found in 2.2.5 (Table 2.2). The fluorescent secondary antibodies and horseradish peroxidase conjugated secondary antibodies used in this chapter are shown in Table 2.3 and Table 2.4.

Table 3.1 Primary antibodies used in chapter 3

Antibody	Host	Immunogen	Application in this chapter
GPR50 goat	Goat polyclonal	Within residues 400-450 of human GPR50	ICC (1:2000/1:500)* WB (1:5000/1:500) * IP (2.4 µg/1mL)
GPR50 63	Rabbit polyclonal	Residues 516-530 of human GPR50	WB (1:1000)
GPR50 rabbit	Rabbit polyclonal	Residues 294-317 of human GPR50	ICC (1:200) WB (1:1000)
BACE1 rabbit1	Rabbit polyclonal	Residues 485-501 of human BACE1	ICC (1:500) WB (1:1000)
BACE1 rabbit2	Rabbit polyclonal	Residues 485-501 of human BACE1	ICC (1:5000) WB (1:10,000)
BACE1 mouse	Mouse monoclonal	Residues 22-460 of human BACE1	ICC (1:500) WB (1:1000)
BACE1 goat	Goat polyclonal	Residues 22-460 of human BACE1	ICC (1:200)
VLA-2α	Mouse monoclonal	Residues 42-245 of human VLA-2α	ICC (1:500) WB (1: 1000)
β-catenin	Rabbit polyclonal	Residues surrounding Pro714 of human β-catenin	ICC (1:800)
EEA1 mouse2	Mouse monoclonal	Residues 3-281 of human EEA1	WB (1: 5000)
Calreticulin mouse	Mouse monoclonal	Calreticulin-maltose binding fusion protein	WB (1:10,000)
58K Golgi	Mouse monoclonal	Purified full length native from rat liver	WB (1: 500)
LAMP2b	Rabbit polyclonal	Within residues 350 to the C-terminus of human LAMP2b	WB (1: 500)
RTN3	Rabbit polyclonal	Residues 1-90 of human RTN3	WB (1:2000)
PSD-95	Mouse monoclonal	Purified recombinant rat PSD-95	WB (1: 5000)
Synaptophysin	Mouse monoclonal	Rat retina synaptosome	WB (1: 50,000)

*** There were two batches of GPR50 goat antibody with inconsistent performances, so different concentrations were used.**

3.2.3 Intensity correlation analysis (ICA)

Qualitative analysis of co-localisation was achieved by using the ICA plugin in ImageJ. This plugin generates intensity correlation analysis (Li et al, 2004), Pearson's correlation coefficients and Mander's overlap coefficients (Manders, 1993). The process can be run using the whole image or region of interest (ROI). The images were background subtracted and auto-thresholded during analysis.

3.2.3.1 Intensity correlation quotient (ICQ)

The key features of ICA method include coloured scatter plot, ICA plots and intensity correlation quotient (ICQ). Paired pixel staining intensity values for dye A

and B from selected ROIs are recorded and normalised to a 0-1 range according to the formula:

$$X_{i(normalised)} = \frac{x_i - x_{min}}{x_{max} - x_{min}}$$

X_i= the i^{th} value of variable X,
X_{min} = the minimum value for variable X,
X_{max} = the maximum value for variable X.
A scatterplot of the normalised A versus B staining intensities is generated, which shows different patterns representative of different staining relationships (Figure 3.4, left column). The means of normalised A and B are determined ($\overline{A}$ and $\overline{B}$) and the Product of the Differences from the Mean (PDM) is calculated for each paired pixel: $PDM = (A_i - \overline{A}) \times (B_i - \overline{B})$. ICA plots are generated by A_i (or B_i) versus PDM. The simulated staining patterns of ICA plots are summarised in Figure 3.4, middle and right columns.

For each image, the number of pixels that generate positive or negative PDM values is counted. A ratio of the number of positive values to the total number of pixel pairs reflects the degree of dependency between A and B. The ICQ is generated by subtracting 0.5 from this value, which is used to identify whether the staining intensities are associated in a random (ICQ~=0), dependent ($0 < ICQ \leq 0.5$) or segregated ($0 > ICQ \geq -0.5$) manner. Non parametric sign test is carried out to judge whether the median of differences between two sets of intensity values equals 0 (ICQ=0).

3.2.3.2 Pearson's correlation coefficient (Rr)

Pearson's correlation coefficient Rr is generated by correlating paired intensity values of A and B ($R_r = \frac{\sum(A_i - \bar{A}) \times (B_i - \bar{B})}{\sqrt{\sum(A_i - \bar{A})^2 \times \sum(B_i - \bar{B})^2}}$). Conventionally, the values for Rr range from 1 to -1. A value of 1 indicates perfect correlation, -1 means perfect exclusion and zero represents a random relationship. However, this is not totally the case for images. While reliable co-localisation always gets a value close to 1, exclusion does not give a value of -1. Negative values and those close to zero only mean that there is no perfect co-localisation and can be resulted from mixed patterns.

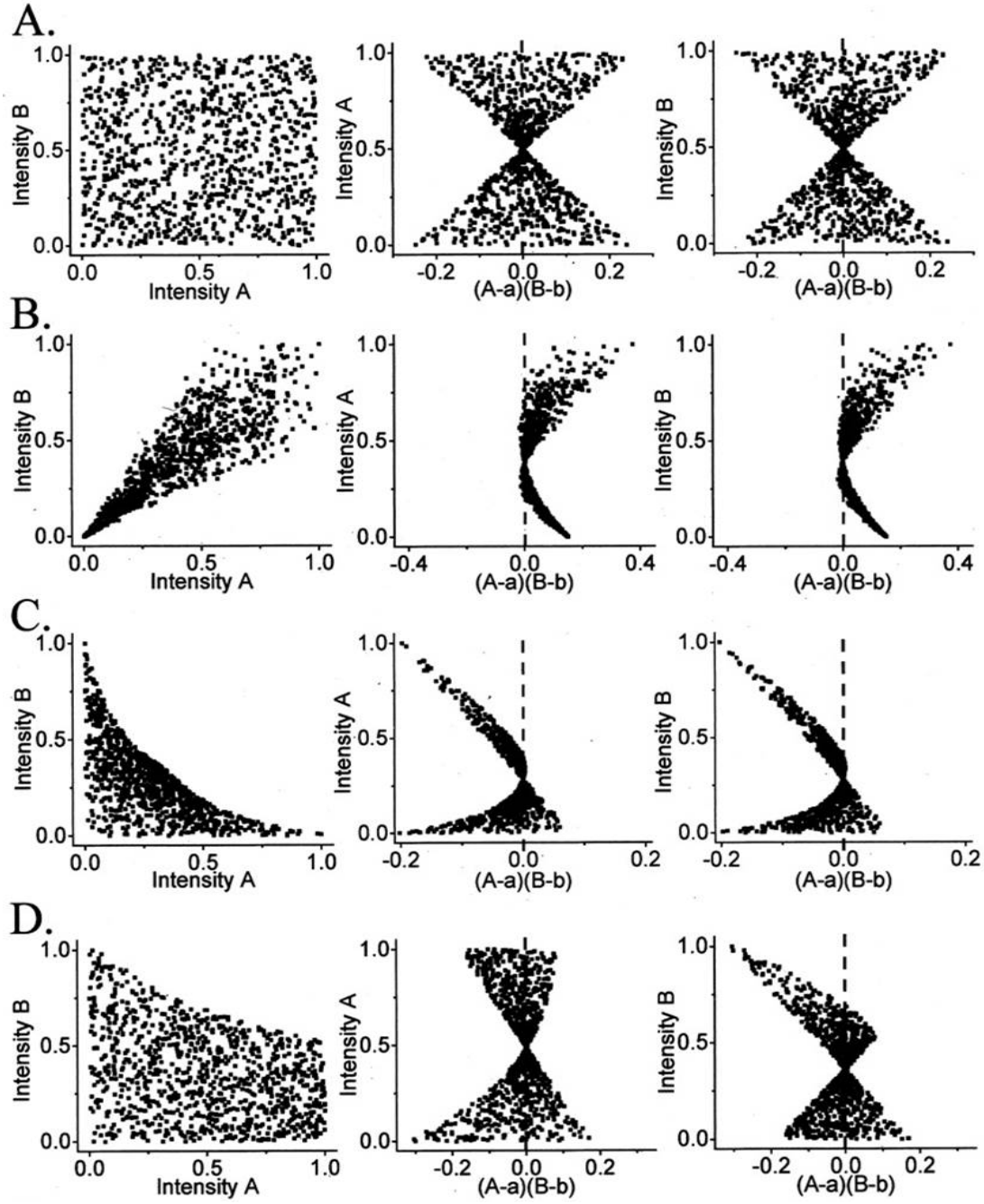

Figure 3.4 Stimulated models of intensity correlation analysis. This figure was adapted from (Li et al, 2004). The left columns of A-D represent a scatterplot of 1000 paired normalised values of Ai versus Bi intensities. The middle and right columns show plots of individual Ai and Bi against their respective PDM values. A) Intensity plot of random staining, ICQ=0.023, p>0.05; B) intensity plot of dependent staining, ICQ=0.39, p<0.001; C) intensity plot of segregated staining, ICQ=-0.269, p<0.001; D) intensity plot model simulating random A staining distribution but with segregated B staining, ICQ=-0.12, p<0.001.

3.2.3.3 Mander's overlap coefficient (R)

Mander's overlap coefficient ($R = \frac{\sum(A_i)\times(B_i)}{\sqrt{\sum(A_i)^2\times\sum(B_i)^2}}$) does not take into account the average intensity values, meaning that it generates values that are distributed from 0 to 1. Zero corresponds to non-overlapping images and the value of 1 reflecting 100%

co-localisation between both images. The coefficient R is strongly affected by the ratio of red to green pixels and should only be used when there are roughly equal numbers of pixels from the two channels (Nred/Ngreen pixels~1). The split coefficients of Mander's co-localisation (M1= $\frac{\sum A_{i,colocal}}{\sum A_i}$ and M2= $\frac{\sum B_{i,colocal}}{\sum B_i}$) are normalised against total pixel intensity, therefore avoiding issues relating to absolute intensities of the signal. There is one coefficient per channel calculating the proportion of pixels in this channel that coincide with pixels in the other channel, so the split coefficients mainly represent how well one channel overlaps the other. However, as these coefficients are sensitive to local variations of intensity, this interpretation of the Mander's coefficients as percentage of intersection only holds when the intensities are homogeneous. A more general interpretation is described as the amount of pixels in one channel whose intensities match with some pixels in the other channel.

3.2.4 Subcellular fractionation-sucrose density gradient fractionation

3.2.4.1 Subcellular fractionation from HEK293 cells

HEK293 cells were grown for 36 hr in 10 cm dishes and transfected when cells reached a confluency of nearly 90%. The cultured cells were left overnight post-transfection before being collected on ice using a cell scraper and suspended into sucrose buffer {0.25 M sucrose, 10 mM Tris-HCl buffer (pH 7.4), 1 mM $Mg(Ac)_2$, protease inhibitor}. The lysates were passed through a 23 gauge needle 20 times, followed by incubation on ice for 20 min. The homogenates were loaded onto the top of a discontinuous gradient comprised of 1.5 ml of 2 M sucrose, 2.5 ml of 1.3 M sucrose, 2.5 ml of 1.16 M sucrose, 2 ml of 0.8 M sucrose, 2 ml of 0.5 M sucrose, and 1 ml of 0.25 M sucrose prepared in 10 mM Tris-HCl buffer (pH 7.4) and 1 mM $Mg(Ac)_2$. The gradients were then centrifuged at 10,000×g (22,000 rpm, SW41 Ti Beckman) for 18 hr at 4^{o}C. Twelve 1 ml fractions were collected from the top, followed by methanol-chloroform precipitation. Proteins were detected by western blotting after electrophoresis on a 4-12% Bis-tris Nupage gel.

3.2.4.2 Subcellular fractionation from adult mouse brains

Brains were removed from ten 8-10 week old adult C57BL/6 mice and homogenised in solution A (320 mM sucrose, 1 mM HEPES, pH7.5, 1 mM $NaHCO_3$, 1 mM $MgCl_2$, protease inhibitor) on ice by a borosilicate glass homogeniser (Dounce, 7ml,

tight; 2 brains/10 ml, 10 strokes). From this point on, all the materials and buffers were kept at 4°C throughout the preparation. The homogenates were centrifuged at 1000×g for 10 min (Beckman, JA25.5). The supernatant (S1) was collected. The pellet (P1) was re-suspended in 10 ml of solution A and 3 strokes were applied with the homogeniser. The homogenates were centrifuged again and the supernatant was added to S1. The pellet, which contains nuclei and large cellular debris, was discarded. S1 was centrifuged at 13,800×g for 10 min (Beckman, JA25.5). Both the supernatant (S2) and the pellet (P2, crude synaptosome) were collected. S2 was centrifuged at 165,000×g for 2 hr (Beckman, TLA-100.3). The supernatant (S3, cytosol) was discarded and the pellet (P3, light membranes) was washed twice with solution B (40 mM sucrose). P2 was re-suspended in 18 ml of solution B and applied 3 strokes in the homogeniser. The P2 suspension was added to the sucrose density gradient (3 ml 1.2 M, 3 ml 1.0 M, 3 ml 0.85 M) and centrifuged at 82,000×g for 2 hr (Sorvall, TH-641). After spinning, four layers were formed isolated by three enriched stripes, which were the synaptosome, the ER-Golgi and the myelin, from the top to the bottom. The pellet was the mitochondria. The fractions were carefully collected using a plastic pastette.

For presynaptic fractions, half of the synaptosomal fraction was diluted with 5 volumes of solution B and centrifuged at 32,800×g for 20 min (Beckman, TLA-100.3). The supernatant was removed. The pellet was re-suspended in 3 ml of solution C (1 M HEPES-NaOH buffer, pH 7.4, used for osmotic shock) and applied 3 strokes with the homogeniser. The homogenates were incubated for 45 min at 4ºC and centrifuged at 32,800×g for 20 min (Beckman, TLA-100.3). Both the supernatant (LS1) and pellet (LP1, synaptosomal membranes) were collected. LS1 were centrifuged at 165,000×g for 2 hr. The supernatant (LS2, synaptosomal cytosol) and the pellet (LP2, synaptic vesicles enriched fraction) were collected separately.

For postsynaptic densities (PSD), the other half of the synaptosomal fraction was diluted with equal volume of solution D (1% Triton X-100) and incubated for 15 min at 4ºC. The homogenates were divided into 3 tubes: “1/6”, “1/6” and “4/6” fraction and centrifuged at 39,000 rpm for 30 min (Beckman, TLA-100.3). The pellet of the first “1/6” fraction was washed once with 1 ml of solution B and stored as “one-triton” fraction. The pellet of the second “1/6” fraction was washed once with solution B and re-extracted with 1 ml of solution E (0.5% Triton X-100) for 15 min at 4ºC (“two-triton” fraction). The pellet of the “4/6” fraction was washed once with

solution B and re-extracted with 1 ml of solution F (3% N-lauroylsarcosinate) for 15 min at 4ºC ("one-triton+Sarcosyl" fraction). After the incubation, the three fractions were centrifuged at 61000 rpm for 1 hr (Beckman, TLA-100.3). All the pellets were washed once with 1 ml of solution B and re-suspended separately in solution H (40mM Tris-HCl, pH8.0; 0.3% SDS + protease and phosphatase inhibitor cocktail) and sonicated on ice until dissolved. Protein concentrations were measured using the Bradford assay (Bio-Rad DC protein assay kit).

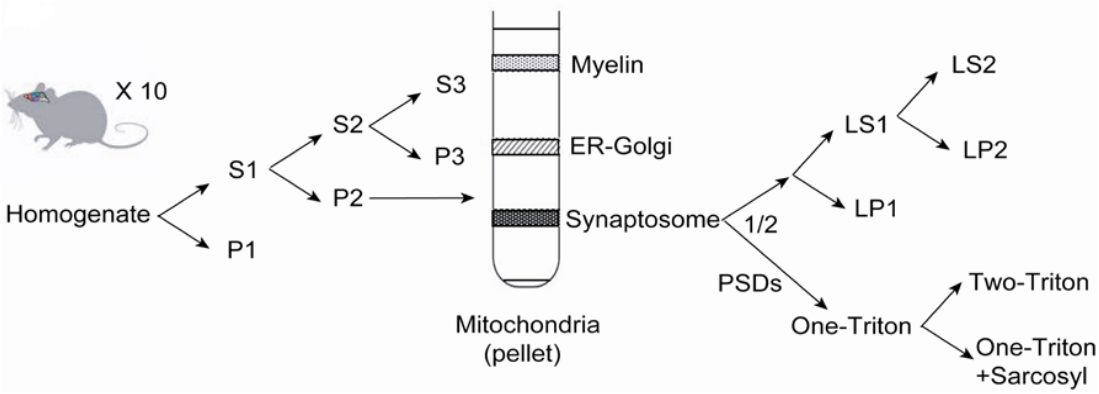

Figure 3.5 A diagram of subcellular fractionation from adult mouse brains. This photo was cited from (Grünewald, 2011).

3.2.5 Co-immunoprecipitation (Co-IP)

After transfection and overnight culture, cells grown on 10 cm plates were firstly washed using 5 ml ice cold PBS with protease inhibitor cocktail (1 tablet/50 ml, Roche), followed by adding 750 µl of RIPA buffer. Cells were collected using a cell scraper and incubated at 4^{o}C on a wheel at a speed of 20 rpm for 30 min, and subsequently centrifuged at 13,000 rpm for 10 min. The supernatant was collected into a new tube. If the cell lysates were too viscous, due to the release of genomic DNA, lysates were sonicated for 10 s on ice. 50 µl of supernatant was taken out as a positive lysates control and preserved in an equal amount of Laemmli sample buffer (4% SDS, 20% glycerol, 100 mM Tris pH 6.8, and 0.2% bromophenol blue). The concentrations of protein lysates were determined by the Bradford assay, using Bio-Rad DC protein assay kit, which were adjusted to 2 mg/ml with RIPA buffer. 1 ml protein lysates were incubated at 4^{o}C with 2.4 µg of antibody used for immunoprecipitation for 2 hr to overnight. To capture the antigen/antibody, 20 µl of IgG-sepharose beads (100 µl beads in 300 µl PBS) was added to the lysates, and incubated for 1.5 hr on a roller. Then, beads were spun down by centrifugation at 4^{o}C, 13,000 rpm for 3 min and washed 5 times with RIPA buffer. The complex of

antigen/antibody was released from beads by adding 40 µl Laemmli sample buffer and incubated at 40^{o}C for 10 min. This step causes the IgG heavy chain to move from 50 kDa to 140 kDa in an SDS-PAGE gel as compared to boiling the lysates. The supernatants were collected by centrifugation at 10,000 rpm for 3 min.

3.3 Results

3.3.1 Exogenous GPR50 and BACE1 co-localise in mammalian cell lines and primary neuronal cultures

The subcellular localisation results in SH-SY5Y cells shown in chapter 2 indicate that GPR50 and BACE1 do not seem to have much overlap in expression. Briefly, GPR50 is mostly located in the external plasma membrane, whereas, BACE1 is mainly localised in diverse intracellular organelles, with a small proportion on the cell surface. From this observation, it is suggested that if the two proteins interact, the most likely area of co-localisation will be the plasma membrane. I investigated if GPR50 and BACE1 co-localise in SH-SY5Y cells, HEK293 cells and mouse primary hippocampal neurons.

In double-transfected SH-SY5Y cells, GPR50 and BACE1 appeared to co-localise at the external compartments, the plasma membrane and the neurite extensions (Figure 3.6). The ICA plots were skewed towards positive values for both red and green intensity pixels, indicating a dependent staining pattern of the two colours in the ROI. The scatter plot of red pixels versus green pixels showed with a positive correlation (Rr=0.425). The pseudocoloured PDM images exposed the exact sites where GPR50 and BACE1 co-localised, as is shown by the yellow colour that the strongest co-localisation occurs at the plasma membrane and the extended neurites. Mander's overlap coefficient (R=1.046) reflected a strong overlapping between the localisation of the two proteins. Specifically, in this ROI, 99.7% of GPR50 shared its location with BACE1, and 98.6% of BACE1 shared its location with GPR50. These two co-localisation figures were independent of the absolute intensity values of GPR50 and BACE1. Finally, the ICQ value (ICQ=0.202) confirmed that the staining of the two colours was a significant dependent pattern ($p<0.05$). The co-localisation was moderate, as it is clearly seen that the region selected contained intracellular organelles with overexpressed BACE1, but lack of GPR50. Similar dependent pattern of red and green intensity pixels was observed in HEK293 cells with a strong

co-localisation of exogenous GPR50 and BACE1 at the plasma membrane (Figure 3.7).

Neuronal Gpr50 was reported to be expressed at the post-synaptic densities (Grunewald et al, 2009), and Bace1 was located at the synapse where APP cleavage takes place (Cao et al, 2012; Kandalepas et al, 2013). The co-localisation of exogenous GPR50 and BACE1 at neurites was more obviously seen in mouse primary hippocampal neurons (Figure 3.8), which was supported by a significant ICQ value (ICQ=0.222, $p<0.05$). The strongest co-localisation appeared at the neurite tips and dendritic spines (Figure 3.8, F1-3), similar to the co-localisation pattern of GPR50 and the neurite outgrowth inhibitor Nogo-A (Grunewald et al, 2009).

3.3.2 Endogenous GPR50 and BACE1 are co-localised in HEK293

I further investigated whether endogenous GPR50 and BACE1 follow the co-localisation pattern of their exogenous proteins. As SH-SY5Y cells do not express GPR50 endogenously and our GPR50 antibodies worked poorly in the detection of endogenous Gpr50 in mouse primary neuronal cultures, I performed this experiment in HEK293 cells.

Of HEK293 cells, 1-10% expresses endogenous GPR50 at the cell surface, depending on the age of the cells (Grünewald, 2011). A moderate level of endogenous BACE1 was detected in the HEK293 cell line used, and its distribution pattern is similar to exogenous BACE1, with most of the protein located in the internal compartments and a small percentage at the plasma membrane. Co-localisation of endogenous GPR50 and BACE1 was found at the plasma membrane (Figure 3.9, A-C) and the filopodia/lamellipodia-like structures (Figure 3.9, D-F) of HEK293 cells.

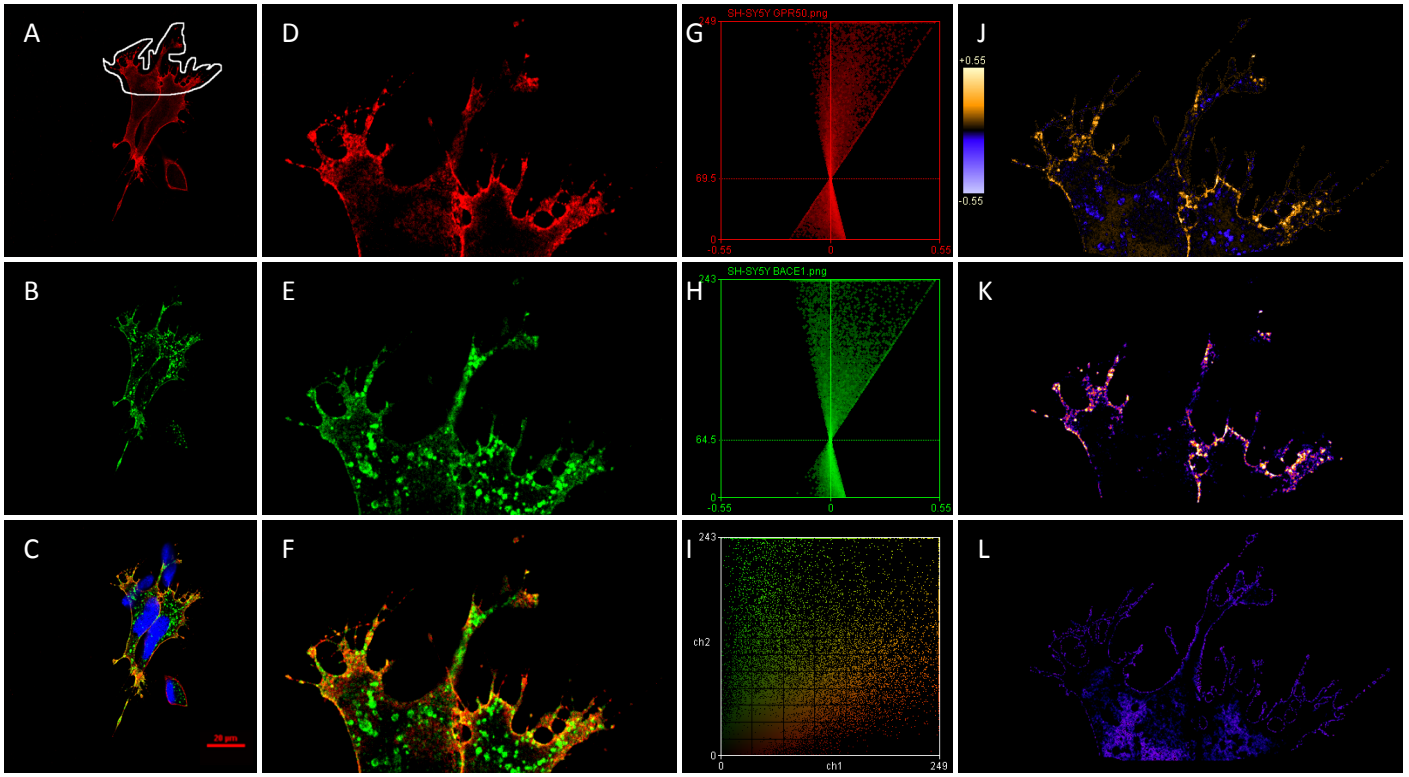

M

Rr	R
0.425	0.781
M1	**M2**
0.986	0.997
ch1:ch2	**ICQ**
1.046	0.234 (p<0.05)

Figure 3.6 Co-localisation of overexpressed GPR50 and BACE1 in SH-SY5Y cells. A) GPR50 (red), the white shut line indicated region of interest (ROI) that was analysed; B) BACE1 (green); C) merged photo of GPR50, BACE1 and DAPI; D) GPR50 ROI; E) BACE1 ROI; F) merged ROI; G) ICA plot of GPR50; H) ICA plot of BACE1; I) pixel scatter-plot of red intensities (GPR50) v.s. green intensities (BACE1); J) pseudocoloured PDM image with PDM scale bar: the hot yellow colour indicates a positive PDM value, representing the synchronisation between the two colours; K) positive PDM values resulting from both pixels above the mean; L) positive PDM values that have pixels in each channel which are both below the mean; M) ICA parameters. The PDM value is the product of the differences from the mean. For each pixel, PDM = (red intensity- mean red intensity)×(green intensity – mean green intensity). Rr: Pearson's correlation coefficient; R: Mander's overlap coefficient; ch1: channel 1 (GPR50); ch2: channel 2 (BACE1); ch1: ch2, the red: green pixel ratio; M1 and M2: Mander's co-localisation coefficients for channel 1 and channel 2; ICQ: intensity correlation quotient; non-parametric sign test was used to test if ICQ was significantly different from 0 (random staining). Scale bar: 20 µm. Antibodies: GPR50 goat, BACE1 rabbit2. In total, six different ROIs from six cells were analysed to determine the co-localisation result, ICQ=0.237±0.028.

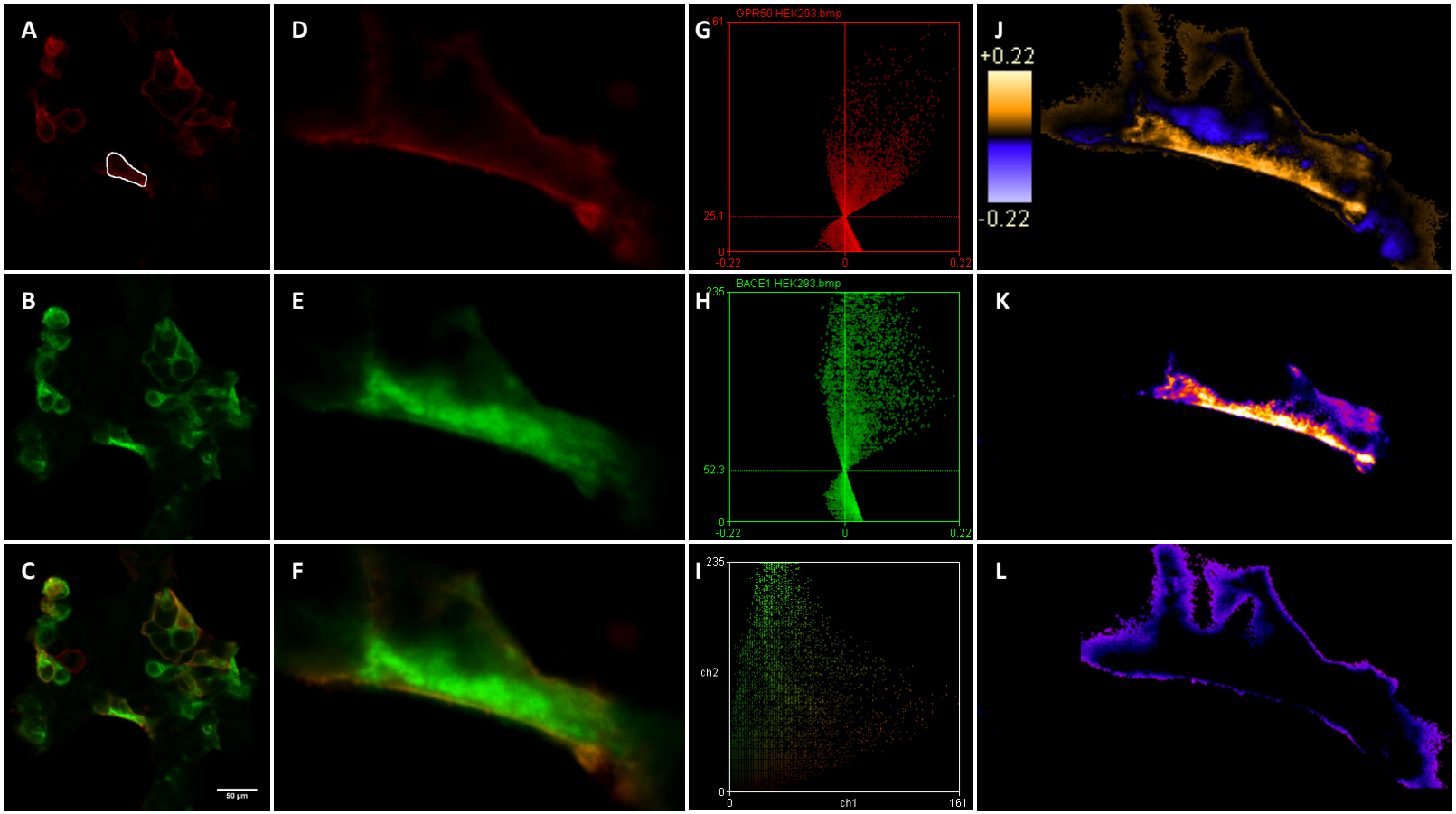

M

Rr	R
0.392	0.737
M1	**M2**
0.976	0.945
ch1:ch2	**ICQ**
0.79	0.24 (p<0.05)

Figure 3.7 Co-localisation of overexpressed GPR50 and BACE1 in HEK293 cells. A) GPR50 (red), the shut line indicated the ROI; B) BACE1 (green); C) merged photo of GPR50 and BACE1; D) GPR50 ROI; E) BACE1 ROI; F) merged ROI; G) ICA plot of GPR50; H) ICA plot of BACE1; I) scatter-plot of red intensities v.s. green intensities; J) pseudocoloured PDM image with PDM scale bar; K) positive PDM values resulting from both pixels above the mean; L) positive PDM values resulting from both pixels below the mean; M) ICA parameters. Scale bar: 50 µm. Antibodies: GPR50 goat, BACE1 rabbit2. In total, five different ROIs from five cells were analysed to determine the co-localisation result, ICQ=0.206±0.044.

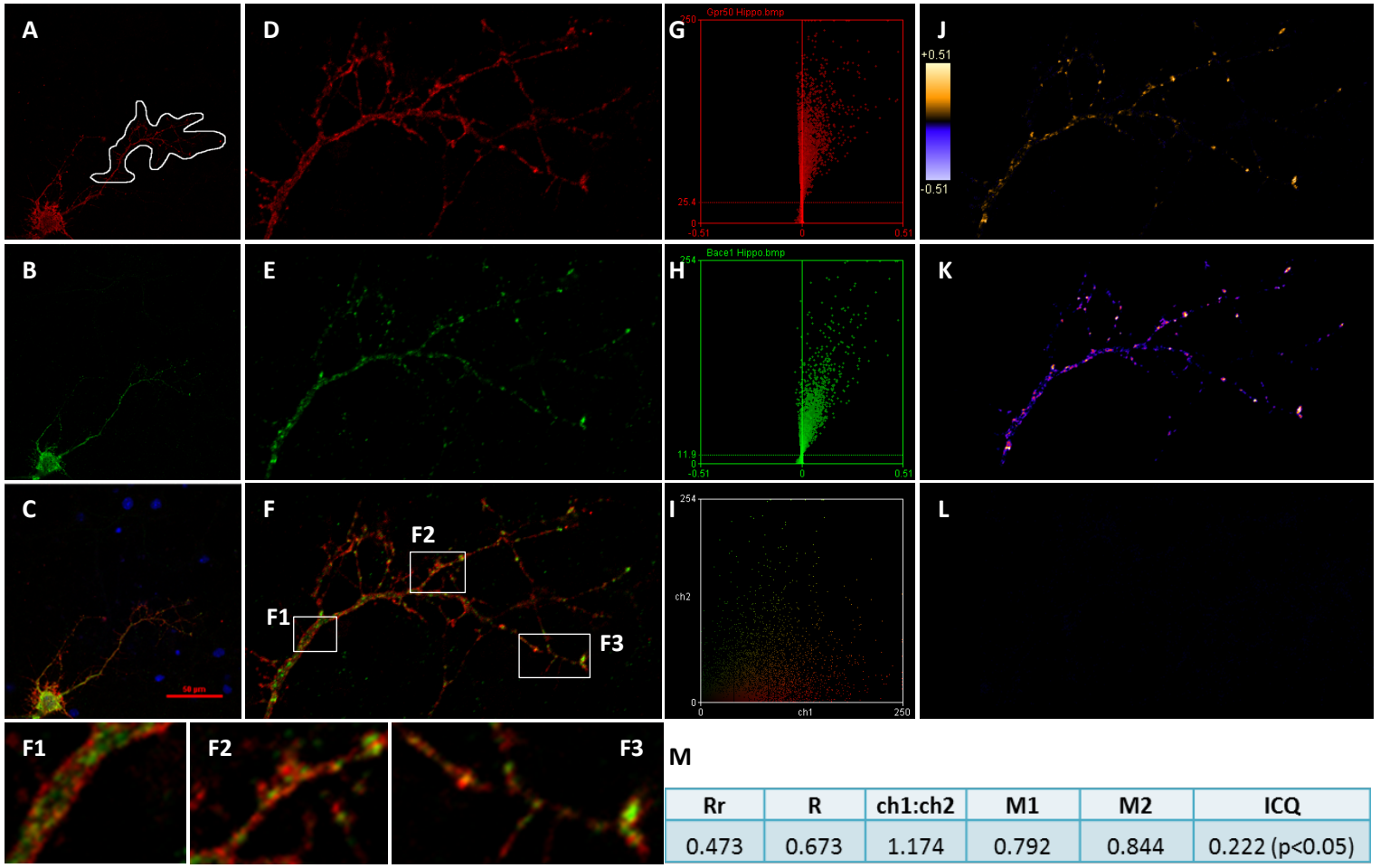

Rr	R	ch1:ch2	M1	M2	ICQ
0.473	0.673	1.174	0.792	0.844	0.222 (p<0.05)

Figure 3.8 Co-localisation of overexpressed GPR50 and BACE1 in mouse primary hippocampal neurons. A) GPR50 (red), the shut line indicated ROI; B) BACE1 (green); C) merged photo of GPR50, BACE1 and DAPI; D) GPR50 ROI; E) BACE1 ROI; F) merged ROI, F1-3: enlarged areas; G) ICA plot of GPR50; H) ICA plot of BACE1; I) scatter-plot of red intensities v.s. green intensities; J) pseudocoloured PDM image with PDM scale bar; K) positive PDM values resulting from both pixels above the mean; L) positive PDM values resulting from both pixels below the mean; M) ICA parameters. Scale bar: 50 µm. Antibodies: GPR50 goat, BACE1 rabbit2. In total, six different ROIs from six cells were analysed to determine the co-localisation result, ICQ=0.283±0.035.

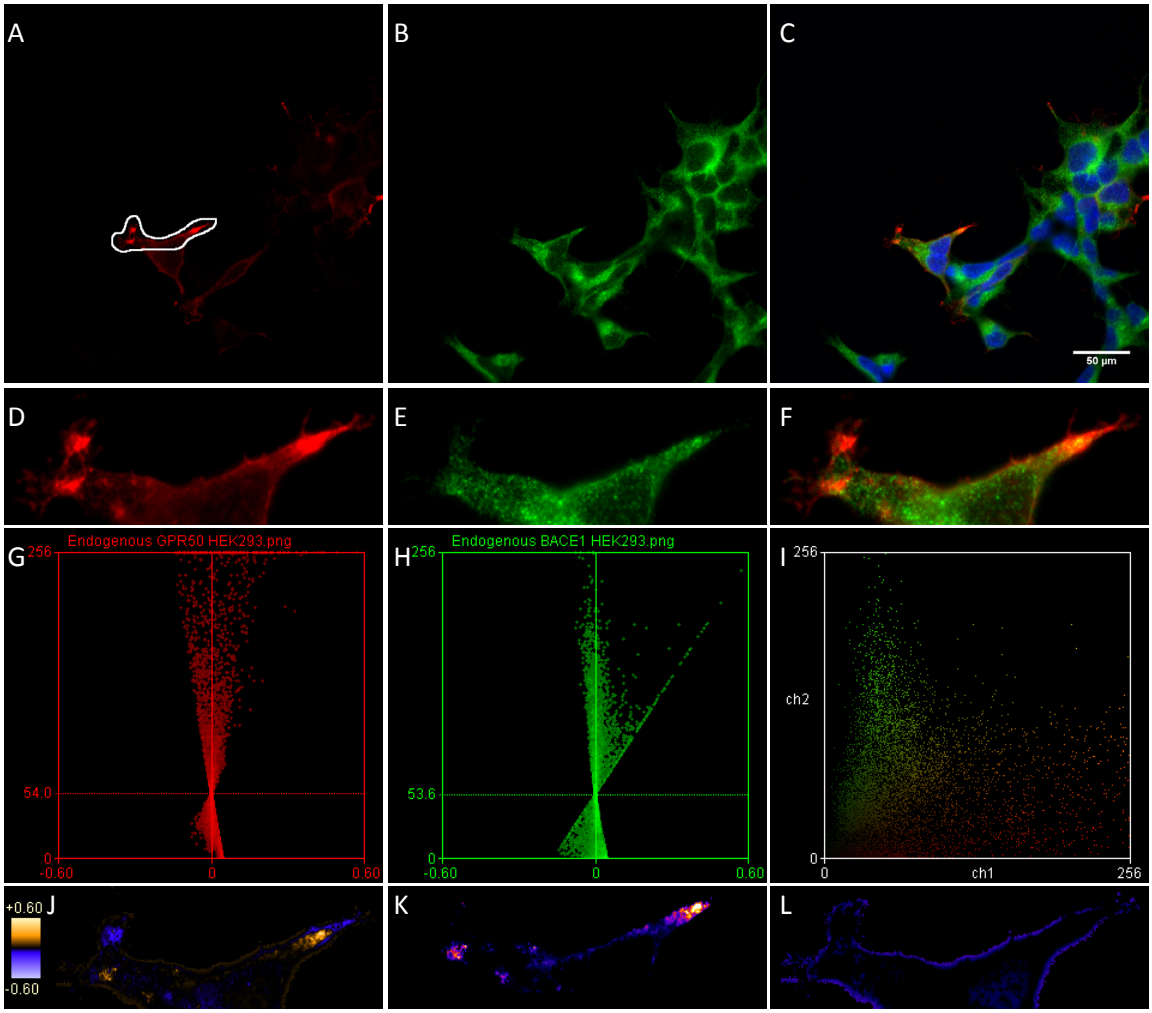

M

Rr	R	ch1:ch2	M1	M2	ICQ
0.216	0.677	1.131	0.954	0.998	0.14 (p<0.05)

Figure 3.9 Co-localisation of endogenous GPR50 and BACE1 in HEK293 cells. A) GPR50 (red), the shut line indicated ROI; B) BACE1 (green); C) merged photo of GPR50, BACE1 and DAPI; D) GPR50 ROI; E) BACE1 ROI; F) merged ROI; G) ICA plot of GPR50; H) ICA plot of BACE1; I) scatter-plot of red intensities v.s. green intensities; J) pseudocoloured PDM image with PDM scale bar; K) positive PDM values resulting from both pixels above the mean; L) positive PDM values resulting from both pixels below the mean; M) ICA parameters. Antibodies: GPR50 rabbit, BACE1 mouse. Scale bar: 50 µm. In total, six different ROIs from six cells were analysed to determine the co-localisation result, ICQ=0.199±0.038.

3.3.3 Endogenous GPR50 is co-localised with cell-surface BACE1

To confirm the co-localisation of GPR50 and BACE1 at the plasma membrane, I used a live cell staining technique to label BACE1 at the cell surface prior to permeabilisation of cells. GPR50 was detected in a second step after permeabilisation. An abundant pool of external BACE1 was detected in HEK293 cells, which clearly lined along the cell surface (Figure 3.10), and much stronger than the punctate pattern in SH-SY5Y cells (Figure 2.12, 2.13). This also indicated that the endogenous active BACE1 protein in HEK293 cells was more than that in SH-

SY5Y cells. It seems that in HEK293 cells, there were more cells singly labelled with GPR50 or surface BACE1 than cells that expressed both (Table 3.2), but there was strong co-localisation between the two in cells with both of them (Figure 3.11).

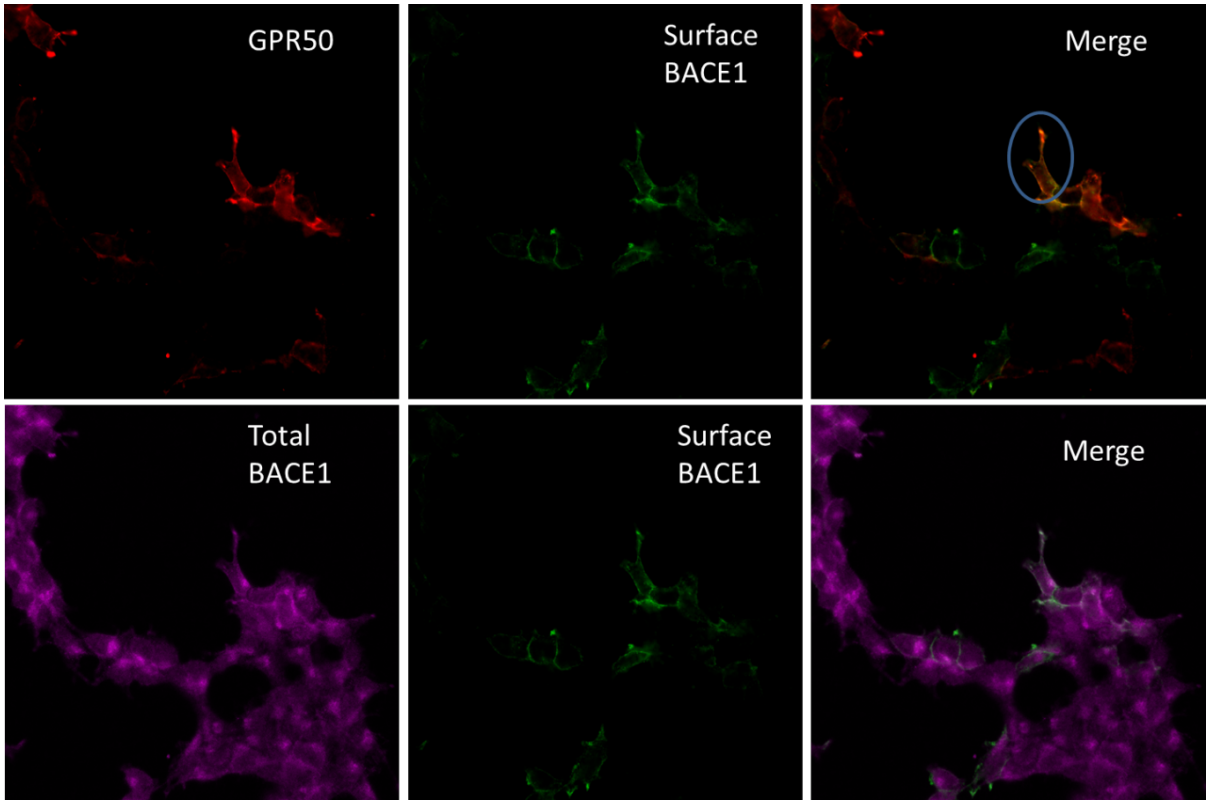

Figure 3.10 Endogenous GPR50, cell surface BACE1 and total BACE1 in HEK293 cells. The circled area represented a cell labelled with both GPR50 and surface BACE1 (see Figure 3.11). Antibodies: GPR50 rabbit (red), BACE1 goat (green) for surface BACE1, BACE1 mouse (purple) for total BACE1.

Table 3.2 The expression pattern of GPR50 and cell-surface BACE1 in a group of cells

		GPR50	surface BACE1
Relicate A	Total number	100	100
	Expressed in the same cells	40	28
	Expressed in different cells	60	72
Relicate B*	Total number	57	79
	Expressed in the same cells	27/47.4%	27/34.2%
	Expressed in different cells	30/52.6%	52/65.8%
Relicate C	Total number	100	100
	Expressed in the same cells	31	24
	Expressed in different cells	69	76

* There were less than 100 cells expressed with surface BACE1 or GPR50 in total in this replicate

In a single cell containing both GPR50 and surface BACE1 (Figure 3.11), the ICA plots for the two were both positively skewed, which meant that the staining of GPR50 and surface BACE1 were dependent on each other. The near to 1 Mander's

overlap coefficients indicated that the location of GPR50 and surface BACE1 in this cell was almost identical. Moreover, a significant positive ICQ of 0.32 confirmed the correlation of the two staining patterns. Importantly, the ICQ value of GPR50 and surface BACE1 was significantly larger than that of GPR50 and total BACE1 (see Figure 3.9, ICQ_{total}=0.199±0.038, $ICQ_{surface}$=0.306±0.019, N=6, p<0.00039 by t-test). This may indicate that GPR50 is more correlated to the BACE1 pool in the plasma membrane.

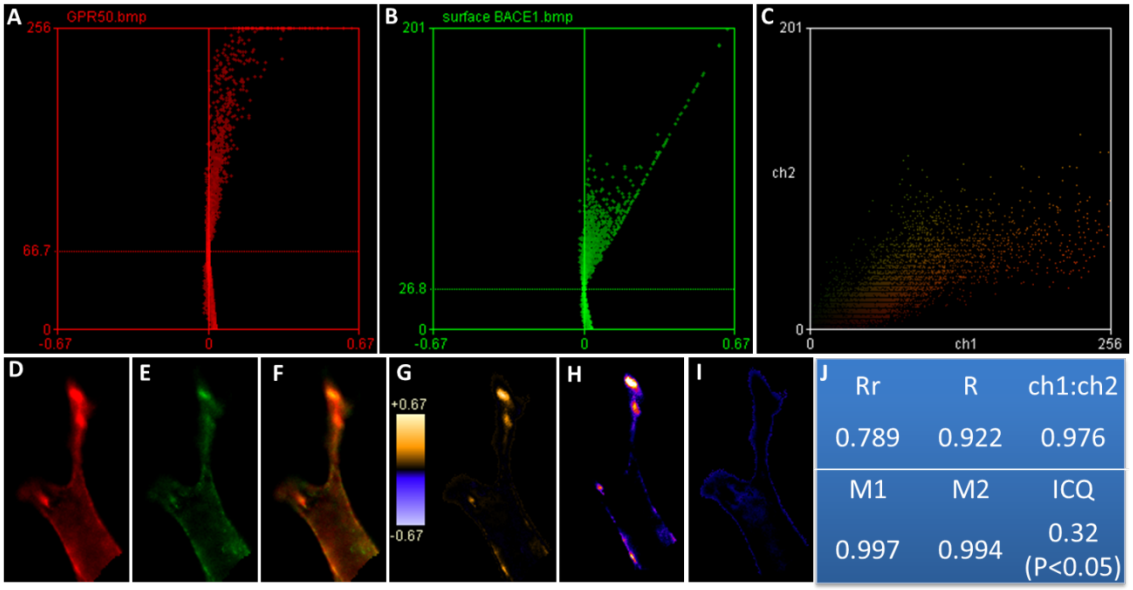

Figure 3.11 Co-localisation of GPR50 and cell surface BACE1 in a HEK293 cell endogenously expressed with both. A) ICA plot of GPR50 (red); B) ICA plot of cell surface BACE1 (green); C) scatter-plot of red intensities (GPR50) v.s. green intensities (cell surface BACE1); D) GPR50; E) cell surface BACE1; F) merged photo; G) pseudocoloured PDM image with PDM scale bar; H) positive PDM values resulting from both pixels above the mean; I) positive PDM values resulting from both pixels below the mean; J) ICA parameters. Antibodies: GPR50 rabbit, BACE1 goat. In total, six different ROIs from six cells were analysed to determine the co-localisation result, ICQ=0.306±0.019.

3.3.4 Exogenous GPR50 and BACE1 are located in the same fractions by subcellular fractionation

Following the ICC experiments, sucrose subcellular fractionation was performed to locate over-expressed GPR50 and BACE1 from double-transfected HEK293 cells, or endogenous Gpr50 and Bace1 from adult mouse brain. As GPR50 and BACE1co-localised in certain compartments of cells, it was expected that the two proteins would co-fractionate from fractions containing the subcellular organelles where co-localisation of the two was detected.

3.3.4.1 Overexpressed GPR50 and BACE1 from HEK293 cells are located in the same fractions

Exogenous GPR50 and BACE1 appeared to co-fractionate in the same fractions (Figure 3.12) including the plasma membrane (marked by VLA-2α), where by immunocytochemistry their co-localisation was found. Meanwhile, one must be cautious that some of the plasma membrane fractions also contained early endosomes (fraction 5-6, marked by EEA1), lysosomes (fraction 5-12, marked by lamp2b) and broken ER (fraction 10-12, marked by calreticulin). It has been reported that a proportion of overexpressed BACE1 was distributed in the early endosomes, which was diminished with the existence of RTN3 (Shi et al, 2009). In my results, BACE1 was not predominantly present in the early endosomes when co-transfected with GPR50, but only in fractions 5 and 6 that contained both the early endosomes and the plasma membrane. The endogenous 23 kDa RTN3 which is known to be a BACE1 activity inhibitor (Murayama et al, 2006), was also found in the same fractions in which both GPR50 and BACE1 were co-localised.

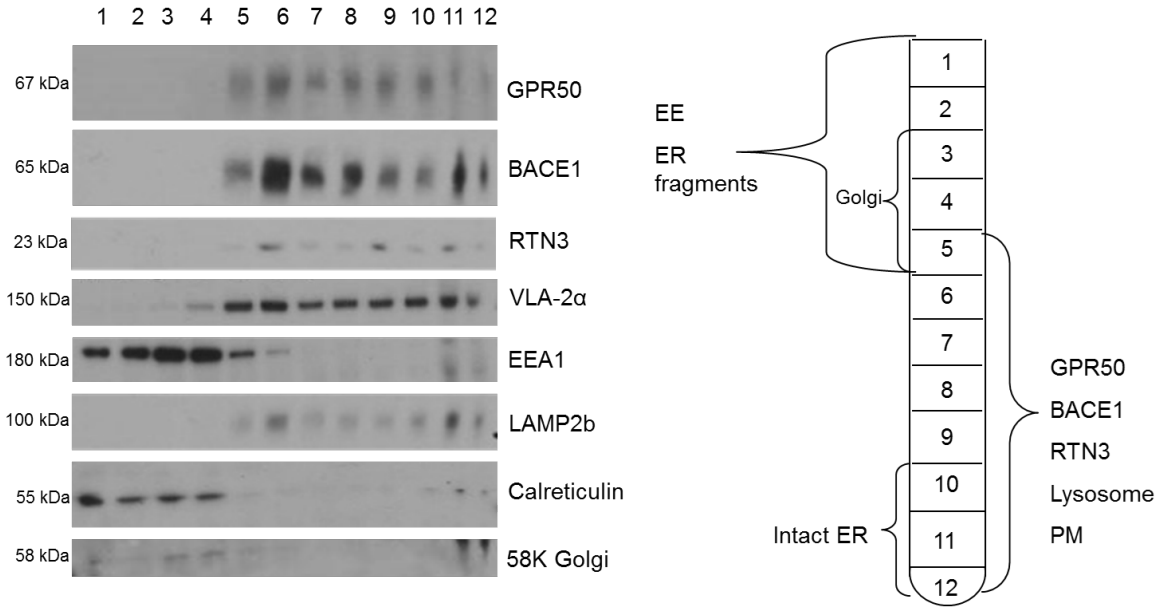

Figure 3.12 Subcellular fractionation of protein lysates from HEK293 cells co-transfected with GPR50 and BACE1. VLA-2α, EEA1, LAMP2b, calreticulin and 58K Golgi are subcellular compartment markers for the plasma membrane (PM), the early endosomes (EE), the lysosomes, the ER, and the Golgi respectively. Antibodies GPR50 goat and BACE1 rabbit2 were used. This experiment was successfully repeated once.

3.3.4.2 Endogenous Gpr50 and Bace1 from adult mouse brain are located in the presynaptic fractions

Next, I performed subcellular fractionation of wild-type adult mouse brain to further confirm the co-localisation of endogenous Gpr50 and Bace1 (Figure 3.13). Fractions

of the presynaptic terminals and postsynaptic densities (PSDs) were separated from synaptosomes, as indicated by markers synaptophysin and PSD-95 respectively. Presynaptic terminals are specialised structures that release neurotransmitters and form synapses with other cells, while the PSDs are in close proximity to the presynaptic active zone and organise the neurotransmitter receptors.

The subcellular localisation of Gpr50 is reportedly enriched in PSDs of the mouse brain (Grunewald et al, 2012). I failed to replicate the result by the GPR50 goat antibody, probably due to the suboptimal quality of the second batch of this antibody. However, the GPR50 rabbit antibody detected several bands in the less insoluble PSDs (PSD1 and PSD2), but not in the fraction closer to the PSD core (PSD3). The positive control from E18 embryonic brain revealed that the 63 kDa band is likely to be the mouse Gpr50. The band was also present in the fraction of synaptic vesicles (LP2).

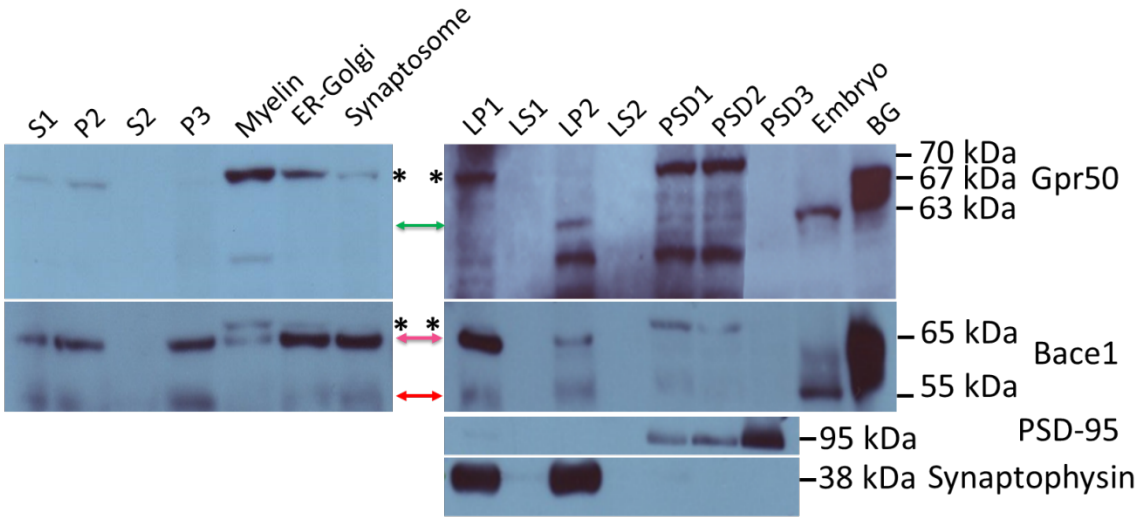

Figure 3.13 The distribution of endogenous Gpr50 and Bace1 in adult mouse brain by subcellular fractionation. S1: homogenates after first spin (nuclei and large cellular debris were removed). S2: homogenates after second spin (most of nuclei and large cellular debris were pelleted). P2: crude synaptosome. P3: light membranes. LP1: synaptosomal membrane. LP1: LS2+LP2. LS2: synaptosomal cytosol. LP2: synaptic vesicles. PSD: post synaptic densities (PSD1: One-Triton, PSD2: Two-Triton, PSD3: One-Triton+Sarcosyl). PSD95: post synaptic marker. Synaptophysin: pre-synaptic marker. Embryo: homogenates of E18 embryotic brain extracted with 1% CHAPS (positive control). BG: the positive control, representing over-expressed GPR50 and BACE1 that were double-transfected in HEK293 cells. Gpr50, mature Bace1 and immature Bace1 are indicated by green, pink and red arrows respectively. The asterisks indicate non-specific bands from the secondary antibody. Antibodies GPR50 rabbit and BACE1 rabbit2 were used. This experiment was successfully replicated once.

Both mature Bace1 (65 kDa) and immature Bace1 (55 kDa), were present in multiple fractions, including the light membranes and ER-Golgi fractions, the normal sites

where BACE1 is expressed in mammalian cell lines, and synaptosomes, the location where BACE1 cleavage of APP, CHL1 and L1 (neural cell adhesion molecules) takes place (Zhou et al, 2012). There was a small portion of mature Bace1 located in the myelin layer, the formation of which is highly regulated by Bace1 substrate Neuregulin1 type III (Fleck et al, 2013; Taveggia et al, 2008) and which is also a potential novel site for Aβ peptide generation in the central nervous system (Skaper et al, 2009). Interestingly, Bace1 was enriched in the synaptosomal membrane (LP1) and synaptic vesicles (LP2), but very little Bace1 was detected in PSDs, which is in agreement with a previous study (Kandalepas et al, 2013). In addition, Bace1 was co-fractionated with Gpr50 in the fraction of synaptic vesicles.

This observation corresponds to the result that overexpressed GPR50 and BACE1 co-localise at the axonal tips of primary neuronal cells. Similar results were observed in a second replicate of this experiment.

3.3.5 Exogenous BACE1 is co-immunoprecipitated with GPR50 in mammalian cell lines

To further confirm if the co-localisation of GPR50 and BACE1 indicates physical interaction between the two, co-immunoprecipitation experiments were performed. The antibodies used in this section are summarised in Table 3.1. Briefly, the size of human GPR50 protein is around 67 kDa. Two bands at 55 kDa and 65 kDa corresponding to immature BACE1 and mature BACE1 were detected by western blotting.

In HEK293 cells, GPR50 was successfully immunoprecipitated by the GPR50 goat antibody from protein lysates with overexpressed GPR50. The immunoprecipitation of endogenous GPR50 was not detected possibly because the cell line used in this experiment was HEK293 of a young passage number (only 1% expressing endogenous GPR50). No obvious endogenous BACE1 was detected either. BACE1 was co-immunoprecipitated with GPR50 only in protein lysates prepared from double-transfected cells (Figure 3.14.A). No signal of BACE1 was detected in control samples of untransfected cells, or cells singly transfected with GPR50 or BACE1 after co-immunoprecipitation.

Overexpressed BACE1 was also co-immunoprecipitated with GPR50 in SH-SY5Y cells (Figure 3.14.B). This might indicate that overexpressed GPR50 is involved in

the function of BACE1 related to brain activities. However, this result was obtained from one test and was not repeated due to the poor quality of the second batch of GPR50 goat antibody and lack of time.

In mouse neuroblastoma cell line N1E-115 cells, an increasing amount of BACE1 was co-immunoprecipitated with the same amount of overexpressed GPR50 when the input of BACE1 was elevating (Figure 3.14.C). This experiment was replicated once and the same result was observed. These results indicate that the physical interaction between GPR50 and BACE1 is relatively stable.

To further confirm the physical interaction between GPR50 and BACE1, the immunoprecipitation of BACE1 was also attempted in order to test if GPR50 was co-immunoprecipitated. However, no BACE1 antibody pulled down BACE1 successfully (date not shown), so this experiment was terminated.

3.3.6 Endogenous BACE1 is co-immunoprecipitated with GPR50 in HEK293 cells

Next I tested whether endogenous GPR50 and BACE1 are physically associated by co-immunoprecipitation. HEK293 cells of high passage numbers were used to guarantee a detectable level of endogenous GPR50 (~10%), which was successfully pulled down by GPR50 goat antibody (Figure 3.15).

The BACE1 mouse antibody detected two bands in protein lysates prepared from untransfected HEK293 cells: one at around 55 kDa for immature BACE1 and the other at 65 kDa for mature BACE1. The size of BACE1 that was co-immunoprecipitated with GPR50 is 68 kDa, slightly larger than the mature BACE1 detected in the lysates. I realised that this was a discrepancy between the sizes of proteins detected in the lysates and in the co-immunoprecipitated protein complex. Therefore the same membrane was stripped and re-probed with the BACE1 rabbit2 antibody. There were extra bands exposed together with the two bands detected by the BACE1 mouse antibody, and one of them was at 68 kDa.

It is known that BACE1 is highly glycosylated and can measure up to 75 kDa depending on the glycosylation system in specific cell lines (Tamagno et al, 2012). The 68 kDa band might be a more glycosylated mature BACE1, which is supposed to have higher β-secretase activity than the simply glycosylated BACE1 (Charlwood

et al, 2001). I also detected multiple bands of mature BACE1 in HEK293 cells after subcellular fractionation (see Chapter 5). This experiment was repeated and the same results were observed. Thus, my results reveal that at the endogenous level, GPR50 is physically interacting with BACE1, and importantly with a more active form of this protease in HEK293 cells.

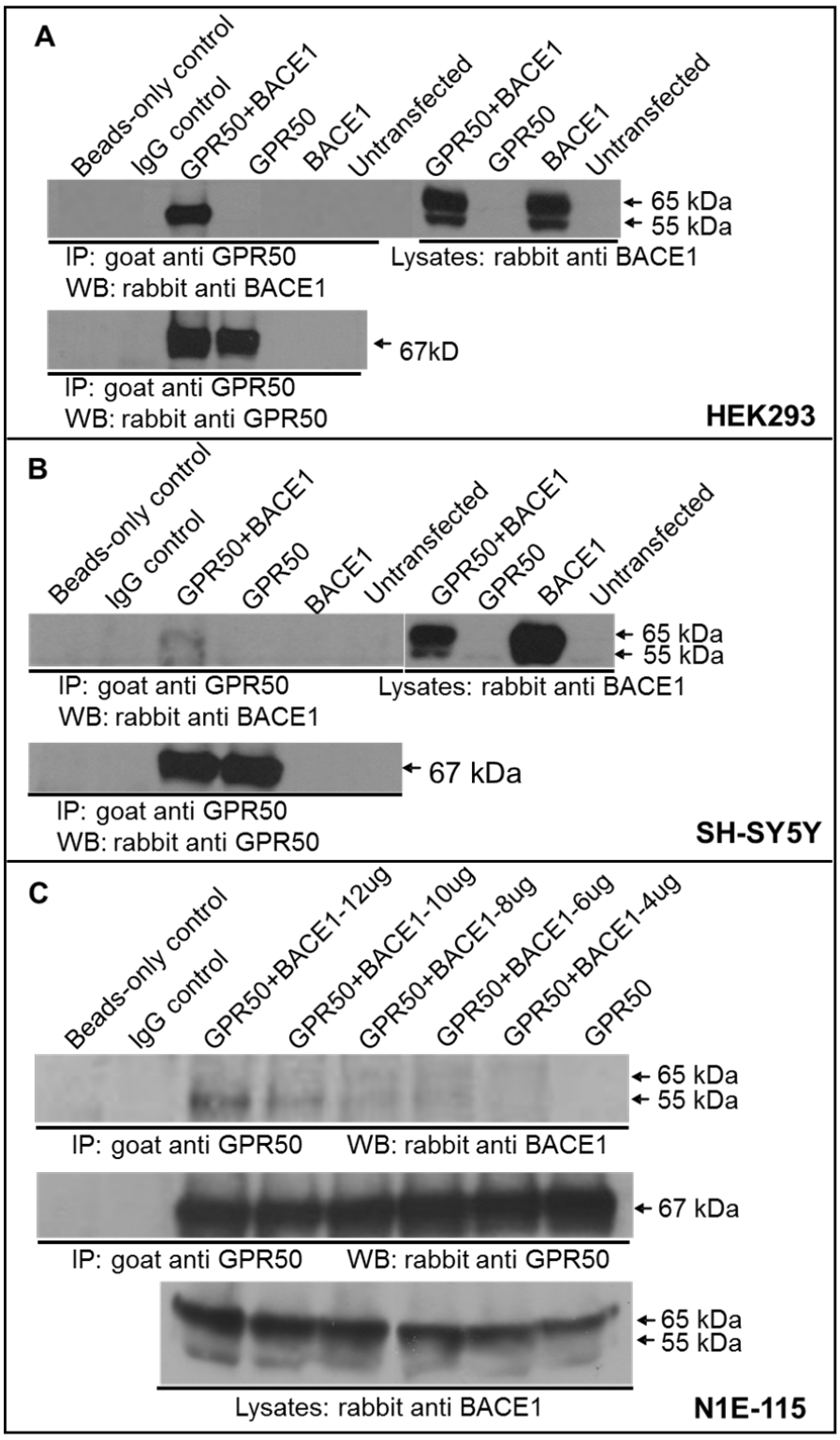

Figure 3.14 Co-immunoprecipitation of overexpressed GPR50 and BACE1 in cultured cell lines. A) HEK293 cells, B) SH-SY5Y cells, C) N1E-115 cells. WB: western blotting; IP: immunoprecipitation.

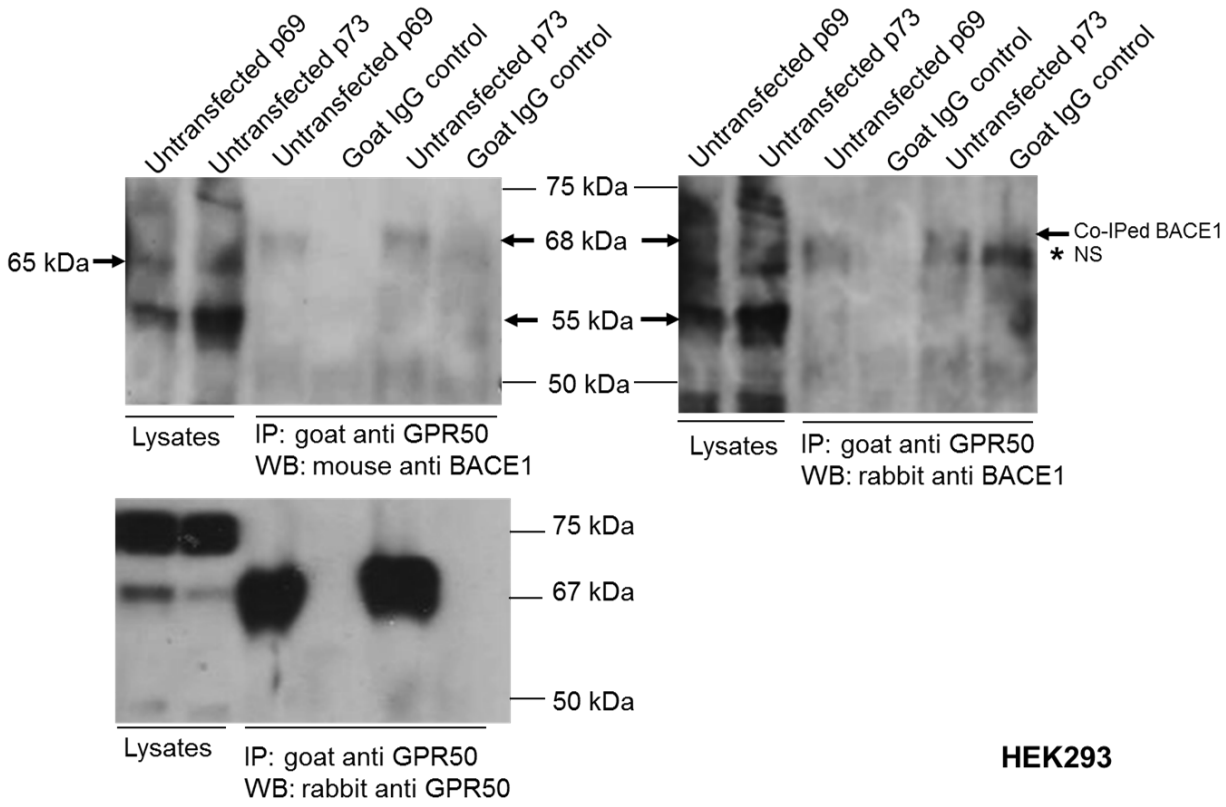

Figure 3.15 Co-immunoprecipitation of endogenous GPR50 and BACE1 in HEK293 cells. NS: unspecific band. WB: western blotting; IP: immunoprecipitation. P69 and p73 are passage numbers of HEK293 cells, here representing two independent replicates (run on the same gel) of this experiment.

3.4 Discussion

In this chapter, I have shown that GPR50 and BACE1 were co-localised and co-fractionated in cells at both exogenous level and endogenous level. A sub-pool of endogenous BACE1 was present at the plasma membrane of HEK293 cells, and it co-localised with endogenous GPR50 in cells that expressed both. The neuronal GPR50 and BACE1 were co-localised at the neurites in SH-SY5Y cells and primary hippocampal neurons. Co-immunoprecipitation studies further confirmed the physical interaction between the two proteins. At the endogenous level, GPR50 was associated with a more mature form of BACE1, strengthening the hypothesis that GPR50 is involved in the regulation of BACE1 activity. However, it must be noted that some of the experiments need more replicates to draw a robust conclusion (i.e. the co-immunoprecipitation of GPR50 and BACE1 in SH-SY5Y cells). A reverse co-immunoprecipation (pull down BACE1 instead) should also be performed when a BACE1 antibody that works in this technique is available.

3.4.1 The interaction between GPR50 and BACE1

The co-localisation of GPR50 and BACE1 occurred at cell external compartments, including the plasma membrane, the neurites and the filopodia-like structures in different cell lines.

GPR50 was able to increase filopodia and lamellipodia-like structures in Neuroscreen-1 cells and primary cultured neurons, indicating that GPR50 might be involved in the activation of actin dynamics by GTPases Rho/Rac/Cdc42 (Grünewald, 2011). GPR50 was also shown to attenuate the effect of neurite outgrowth inhibitor Nogo-A, supporting a role of GPR50 in neuronal development (Grunewald et al, 2009). GTPases RhoA and Rac1 are molecules affecting Nogo signalling and mediating the growth inhibiting characteristics of Nogo-A (Gross et al, 2007; Niederost et al, 2002). Therefore, GPR50 may play a part in the GTPase signalling pathway. Recent studies revealed that BACE1 is the major sheddase of molecules involved in neurite outgrowth (SEZ6, L1, LRRN1, neurotrimin, CHL1, brain EGF-repeat containing transmembrane protein, voltage-gated sodium channels β2 subunit) and synapse formation (neurexin-1a and neuroligins) (Kim et al, 2007; Kuhn et al, 2012). Interestingly, inhibition of RhoA downstream effector ROCK2 negatively regulated BACE1 cleavage of APP by promoting the transportation of BACE1 from the early endosomes to the lysosomes (Herskowitz et al, 2013). Another GTPase Rab11 positively mediated the axonal sorting of BACE1 to presynaptic terminals in hippocampal neurons (Buggia-Prevot et al, 2014). The co-localisation sites of GPR50 and BACE1 seem to locate at the areas where BACE1 cleavage is likely to take place. In addition, GPR50 overexpression up-regulated BACE1 activity in HEK293 cells (Grünewald, 2011), which indicates that the interaction of GPR50 and BACE1 may be closely related to the functional cleavage by BACE1 signalled by GTPase system. It is worth mentioning that the intervention of GPR50 in BACE1 activity is not necessarily restricted to APP cleavage. My co-localisation results suggest that GPR50 may play a signalling role in the diverse function of BACE1 as a protease, such as the above mentioned performance in shedding of neurite outgrowth factors.

Co-immunoprecipitation experiments further confirmed that GPR50 was physically associated with BACE1. In previous studies, both mature and immature BACE1 were found co-immunoprecipiated with another factor. Interacting with mature

BACE1 may affect the trafficking system of this enzyme, and ultimately regulate its activity levels, for example sortilin (Finan et al, 2011; Murayama et al, 2006). Whereas, interaction with immature BACE1 might imply a role of the interactor in the maturation process of BACE1, such as previously reported presenilin-1 and prion protein (Griffiths et al, 2011; Hebert et al, 2003). The mature form of endogenous BACE1 could be pulled down together with endogenous GPR50 in HEK293 cells. This result indicates that GPR50 is likely to play a direct part in BACE1 function after maturation. Indeed, GPR50 overexpression significantly regulated endogenous BACE1 activity in HEK293 cells (Grünewald, 2011).

Importantly, the physical interaction between GPR50 and BACE1 can be direct or indirect, as the pulled down protein complex by GPR50 antibody might consist of a group of molecules that link GPR50 to BACE1. The regulation of BACE1 is known to be involved with a complicated network of multiple factors, and the yeast two-hybrid studies revealed several co-interactors of GPR50 and BACE1, for example, the reticulon proteins. Whether GPR50 is directly affecting BACE1 function or through sending regulative signals to their co-interactors is very interesting and needs further investigation. Experiments such as FRET/BRET may help to answer this question. It is also worthwhile to study the effect of GPR50 knockdown or variation/mutation on the localisation and enzymatic activity level of BACE1.

3.4.2 Further experiments

Results in this chapter preliminarily confirm that there is physical interaction between GPR50 and BACE1. The co-localisation sites of the two include the location where BACE1 cleaves its substrates (such as neurites), and this may suggest that GPR50 is involved in the cleavage process of BACE1. It is already known that GPR50 regulates endogenous BACE1 levels in HEK293 cells (see chapter 2). The next step is to study if this outcome can also be verified in neuronal cells, in which intense co-localisation of GPR50 and BACE1 is found at the neurites. The neurons are also the cell origins where native β-secretase cleavage takes place in brain. Chapter 4 will look into this proposal in detail.

4 The effect of GPR50 over-expression on β-secretase activity in neuronal cells

4.1 Introduction

In previous chapters, it was suggested that GPR50 has a functional connection with BACE1, as it is involved in the modulation of BACE1 expression (see chapter 2). Further, a physical association between GPR50 and BACE1 was identified (see chapter 3). These preliminary findings have strengthened the link of GPR50 to BACE1 and brain illnesses in which BACE1 acts as a key enzyme.

Importantly, neurodegeneration is commonly seen in the brains with mental illnesses. Therefore, to investigate the pathology of these disorders, considerable studies have been carried out on the function of risk factors in neuronal cells. The neuronal functions of GPR50 have been suggested in several studies, including neuronal development and neurotransmitter signalling (Grunewald et al, 2009; Grunewald et al, 2012). As to BACE1, its function is also closely related to its neuronal activity, due to the diversity of β-secretase substrates in neurons. In chapter 3, it was revealed that exogenous GPR50 and BACE1 co-localised extensively at the neurites of SH-SY5Y cells and primary hippocampal neurons, indicating a functional interaction at an important site for BACE1 activity. Additionally, GPR50 and BACE1 have overlapping roles in neuronal functioning, such as in promoting neurite extension (Grunewald et al, 2009; Miyazaki et al, 2007). Hence, in this chapter, I sought to further investigate the potential of GPR50 in the regulation of neuronal β-secretase activity.

4.1.1 The neuronal function of GPR50

As introduced earlier, the neuronal function of GPR50 was initially proposed by a yeast two-hybrid study, which identified multiple interactors of GPR50 with a neuron-related role. Among these were ABCA2, CDH8, PCDH9, PAX6 and shootin1, proteins known to be important for neurogenesis (Asahina et al, 2012; Broccardo et al, 2006; Carbe et al, 2013; Garel et al, 2000; Toriyama et al, 2010); and RTN3, RTN4 (Nogo), proteins that are relevant to neuronal damage (Karnezis et al, 2004; Shi et al, 2013). In particular, GPR50 was able to attenuate the inhibitory actions on neurite outgrowth by Nogo-A (Grunewald et al, 2009). Further, the overexpression of GPR50 alone was sufficient to induce an increase in the neurite length (Grunewald et al, 2009). Hence, GPR50 appears to be a positive regulator during the elongation process of neurons.

The expression profile of GPR50 in the developing mouse brain also indicates a role during the neuronal development. Gpr50 mRNA was detected from E13, reached a peak at E18 and increased again at adolescent week 5 (Grunewald et al, 2012). As E18 is a developmental stage important for axon growth/guidance and synapse formation, the up-regulation of Gpr50 expression at this time point agrees with a role in neurogenesis. This speculation was supported by the finding that the mRNA levels of Gpr50 and Cdh8 were correlated at E18, as embryonic Cdh8 expression has been suggested in the neuromeric organisation of the early embryonic CNS and in the brain morphogenesis (Korematsu & Redies, 1997a; Korematsu & Redies, 1997b). An increase of Gpr50 mRNA level at week 5 is indicative of its potential during the later developmental stage, possibly in the neuron maturation and maintenance. Furthermore, GPR50 is predominantly expressed in NeuN-positive postmitotic neurons, but not in GFAP-positive astrocytes or O4-positive oligodendrocytes (Grunewald et al, 2012). Thus, further research on GPR50 expression in neurons is essential to clarify its function, as well as to understand its interaction with the key molecules implicated in the neuronal development.

4.1.2 β-secretase activity in neuronal cells

Primary neuronal cultures and neuronal cell lines derived from human and rodents represent a useful tool to study neuronal factors and their effects on the basic physiological properties of neurons. As introduced in chapter 2, BACE1 is widely expressed in multiple tissues, but β-secretase activity is mostly concentrated in the brain. Neurons are the major source of endogenous BACE1 expression, even though there are low levels of BACE1 detected in microglia and astrocytes, normally under activated conditions, such as inflammation (Bourne et al, 2007; Zhao et al, 2011).

In addition to APP, there are over 60 putative substrates of BACE1 identified through the technique of quantitative proteomics/mass spectrometry (Hemming et al, 2009). The majority of these molecules are type I transmembrane proteins. Yet the shedding of GPI-linked proteins (i.e. ephrin-A5) and type II membrane proteins (i.e. Golgi integral membrane protein 4) by BACE1 were also validated. Members of these putative substrates were divided into several functional categories, with half of them involved in contact-dependent intercellular communication. Substrates of this category include proteins implicated in neurodevelopment and migration, immune function, and cell fate determination. Other putative substrates have been described

to function as peptide and lipoprotein receptors, cellular adhesion molecules, proteases, and in intracellular protein trafficking. The discovery of diverse BACE1 substrates has broadened the role of β-secretase activity in many biological processes.

In particular, among the characterised molecules as BACE1 shedding target, some of them claim significant neuronal functions with high expression levels in neurons. For example, cleavage of Neuregulin 1 type III precursor protein by endogenous Bace1 in primary neurons releases the EGF-like domain β-sEGF, which mediates the activation of ErbB receptors and triggers PI3 kinase downstream signalling (Fleck et al, 2013). BACE1 activity in neurons also regulates the release of neural adhesion molecules L1, CHL1 and contactin-2 from cell surface, which regulates axon guidance through interaction with other molecules and contributes to myelination (Gautam et al, 2014; Kuhn et al, 2012). Elsewhere, BACE1 shedding of neuronal signalling molecule Jagged1 controls the balance between astrogenesis and neurogenesis via Notch signalling during the early developmental stages of mouse hippocampus (Hu et al, 2013a). Moreover, BACE1, by cleaving β2 subunit of voltage-gated sodium channel (Na_v1), modulates Na_v1 α-subunit levels and controls the membrane excitability of hippocampal neurons (Kim et al, 2007).

Thus, apart from the initiation of Aβ amyloid deposition, β-secretase activity in neurons induces pleiotropic neuronal effects, including myelination, cell adhesion, neurite outgrowth, axon guidance, cell signalling, and cognitive functions (Chen et al, 2012a; Corbett et al, 2013; Willem et al, 2006; Zhou et al, 2012). As the biological function of BACE1 is far beyond its role in Aβ generation, one must be careful to predict the adverse events upon regulation of BACE1 activity in brain, which is likely to be achieved through understanding the function of specific substrates and regulators. In addition, the findings of BACE1 shedding of those cell surface proteins may clarify the dispute on the cellular location where BACE1 cleavage takes place. While mounting evidence showed that BACE1 processes APP in the early endosomes (Das et al, 2013; Sannerud et al, 2011), the localisation of other BACE1 substrates at the cell surface, especially in the presynaptic sites (Alberi et al, 2013; Leshchyns'ka et al, 2006; Zhong et al, 2008), may support the BACE1 shedding in the plasma membrane and synapse.

4.1.3 The role of GPR50 in regulating BACE1 activity

GPR50 is implicated in the function of BACE1, as it has a potential in the regulation of BACE1 activity (Grünewald, 2011). It has been shown that in HEK293 cells, overexpression of GPR50 significantly increased BACE1 activity compared with the empty vector control (Figure 4.1), whereas the mental disorder related GPR50del showed no significant effect. The reticulon proteins RTN3, Nogo-A and Nogo-C are physical interactors of GPR50 (Grünewald, 2011). While RTN3 and Nogo-C reduced BACE1 activity in HEK293 cells, Nogo-A overexpression had no effects (Grünewald, 2011). Further, no difference in BACE1 activity has been found when HEK293 cells were co-transfected with GPR50 or GPR50del and RTN3 or Nogo-C compared to the control. GPR50 thus appears to partially counteract the inhibiting effects of RTN3 and Nogo-C on BACE1 activity (Grünewald, 2011).

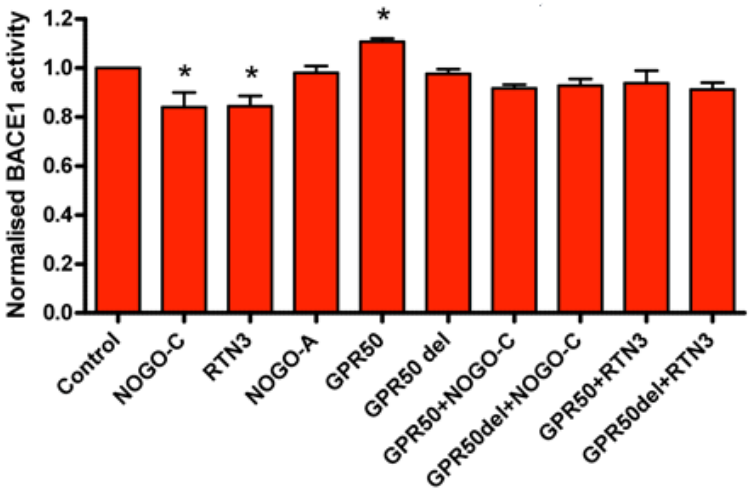

Figure 4.1 The effects of overexpressed GPR50 or GPR50del on BACE1 activity in HEK293 cells. The figure was adapted from (Grünewald, 2011).

4.1.4 Introduction to experiments

GPR50 immunoreactivity has been detected in the neurodegenerative cells of post-mortem AD brain (Hamouda et al, 2007). Meanwhile, the yeast two-hybrid study by Grünewald and colleagues have revealed that GPR50 interacts with BACE1 activity regulators (RTN3, Nogo, SNX6, ABCA2, and CDH8) (Grunewald et al, 2009). With my previous findings confirming that GPR50 and BACE1 can physically associate (chapter 3), I hypothesised that GPR50 is an effector of BACE1 activity through protein-protein interaction, thus an alteration of their interaction induced by certain factors, such as an abrupt increase of GPR50 expression, may indicate a state of disease, including brain diseases.

Specifically, I wanted to further investigate if the regulatory effects of GPR50/GPR50del on BACE1 activity in HEK293 cells also take place in neuronal cells, which are more relevant to the function of BACE1 in mental illnesses. Interestingly, GPR50 co-localised with BACE1 at the cell surface and neurites, as was shown in chapter 3. Also, endogenous Gpr50 and Bace1 were co-fractionated in the presynaptic vesicles (LP2 fraction of mouse brain). GPR50 may have an important role in the regulation of neuronal β-secretase activity, and the aim of this chapter is to investigate this hypothesis. Briefly, I measured the endogenous β-secretase activity in the mouse primary cortical neurons upon the transfection of GPR50 or GPR50del, the risk variant in the GPR50 C-terminal domain associated with bipolar disorder and schizophrenia. At the same time, the knockdown of endogenous Gpr50 in neurons was attempted as a loss-of-function technique, in order to better understand its effect on Bace1 activity.

4.2 Materials and methods

The main methods have been introduced in chapter 2 and 3. The following paragraphs describe additional techniques that were mainly used for experiments in this chapter.

4.2.1 Primary neuronal culture

Primary neuronal cultures were prepared from embryonic day 18 (E18) C57BL/6 mice (purchased from Biomedical Research Resources Unit, Western General Hospital, Edinburgh). See 2.2.2 for detailed protocol of dissection and neuron preparation. Neurons were isolated from the cortex and 5×10^6 cells/well were seeded on poly-D-lysine (Sigma-Aldrich, St. Louis, USA) coated 6-well plates and cultured in 4 ml neurobasal medium supplemented with 2% B-27 and 1% GlutaMax^{TM} for 3 days-in-vitro (DIV3). Cultures were maintained in a humidified environment at 37°C with 5% CO_2. On DIV3, neurons were transfected by Lipofectamine 2000 and left for 24 hr post-transfection (see 2.2.4). On the next day, cells were washed with PBS and collected in fresh warm neurobasal medium. For each condition, 2×10^6 cells were used for β-secretase activity assay and the rest of the cells were subjected to total RNA extraction. Real-time qPCR was performed to confirm the successful transfection of GPR50/GPR50del.

4.2.2 β-secretase activity assay

The β-secretase activity assay kit was provided by Abcam (ab65357). The assay makes use of a β-secretase-specific peptide conjugated to two reporter molecules EDANS and DABCYL. In the uncleaved form, the fluorescent emissions from EDANS are quenched by the DABCYL moiety because of their physical proximity. Cleavage of the peptide by β-secretase separates EDANS and DABCYL leading to the release of a fluorescent signal. The level of β-secretase activity in samples is proportional to the level of fluorescence intensity detected.

On DIV3, neurons were transfected with equal amounts of pDEST40 (p40)/GPR50-pDEST40 (GPR50)/GPR50del-pDEST40 (GPR50del) by Lipofectamine 2000 for 4 hr, and then cultured at 37°C overnight for 24 hr. The neurons were washed with ice cold PBS, and scraped in fresh pre-warmed neurobasal media. Equal number of cells was counted using a cell counter, collected and re-suspended in 170 µl chilled extraction buffer (included in the kit). Cell lysates were placed on ice for 10 min and then centrifuged at 10,000×g for 5 min. The supernatant was collected in a new Eppendorf tube. For each condition, 50 µl lysate, 50 µl reaction buffer and 2 µl β-secretase substrate were added to a 96-well Costar black plate in duplicate (Table 4.1). The controls were prepared for each biological replicate, including: 1) background control, which used extraction buffer instead of cell lysates; no substrate control for each condition, the sample of which only contained cell lysates; 2) positive control, containing active recombinant BACE1 enzyme plus extraction buffer; 3) negative control, which added BACE1 inhibitor to positive controls (Table 4.1). The mixture was then incubated in dark at 37ºC for 2 hr. Absorbance readings were performed in the EnVision multilabel plate reader (PerkinElmer) with excitation wavelength 340 nm and emission wavelength 495 nm. The absolute BACE1 activity levels were sample readings subtracted from their respective "no substrate" controls. The relative BACE1 activity levels were normalised against those in p40 (empty vector) transfected cells. The mean differences in relative BACE1 activity were calculated using two-tailed paired Student's t-test from 5 independent replicates.

Table 4.1 Sample preparation of β-secretase activity assay

<table>
<tr><td colspan="2">Background control</td><td>50 µl extraction buffer</td><td rowspan="5">+50 µl reaction buffer
+2 µl substrate</td></tr>
<tr><td colspan="2">Negative control:
β-secretase+inhibitor</td><td>50 µl extraction buffer+ 1.5 µl β-secretase+1.5 µl inhibitor</td></tr>
<tr><td colspan="2">Negative control:
untransfected sample cells+inhibitor</td><td>50 µl lysates +1.5 µl inhibitor</td></tr>
<tr><td colspan="2">Positive control:
β-secretase</td><td>50 µl extraction buffer+ 1.5 µl β-secretase</td></tr>
<tr><td colspan="2">Positive control:
untransfected sample cells</td><td>50 µl lysates</td></tr>
<tr><td rowspan="3">Samples</td><td>p40</td><td rowspan="3">50 µl lysates, duplicate</td><td rowspan="3">+50 µl reaction buffer
+2 µl substrate</td></tr>
<tr><td>GPR50</td></tr>
<tr><td>GPR50del</td></tr>
<tr><td colspan="2">No substrate control</td><td>50 µl lysates</td><td>+50 µl reaction buffer</td></tr>
</table>

4.2.3 Knockdown of endogenous Gpr50 in primary cortical neurons

Three different 29-mer shRNA constructs targeting human/mouse GPR50 coding sequence in an untagged pRS vector were purchased from Origene (TR312642). The shRNA sequences are: sh61 (5'-CTCGCACCTACACCTGCATCTTCAACTAT-3'), sh62 (5'-TTTCTAACCATGTTTGTGATCTTCCTCCT-3'), and sh63 (5'-ATCAACCGTTACTGCTACATCTGCCACAG-3'). A 29-mer scrambled shRNA cassette in the pRS vector was used as the control. The plasmids were isolated from *E. coli* DH10B and extracted with Qiagen Endofree maxiprep kits according to the manufacturer's instructions. For each transfection in 6-well plates, 30 µg shRNA vectors (6 µl) were used. Other steps of transfection were carried out according to 2.2.4. Real-time quantitative PCR (qPCR, see 2.2.8) was performed to confirm the successful knockdown by Gpr50 shRNAs.

4.3 Results

Overexpressed GPR50 has been found to up-regulate BACE1 activity in HEK293 cells (Grünewald, 2011), and my previous results showed a promising interaction between GPR50 and BACE1 at the endogenous level (see chapter 2). Considering that the regulation of BACE1 activity is most closely related to the brain function, I wanted to further investigate whether GPR50/GPR50del/deficient Gpr50 has effects on the activity levels of β-secretase in neurons. Mouse primary cortical neurons were used for this experiment, in which endogenous β-secretase activity has been detected for Aβ generation (Kao et al, 2004) and ectodomain shedding of neural cell adhesion molecules (Gautam et al, 2014).

4.3.1 Optimisation of transfection efficiency in SH-SY5Y cells and primary cortical neurons

High transfection efficiency in cells is crucial to study the possible effect of overexpressed GPR50 on β-secretase activity. Different transfection regents were tested including Lipofectamine 2000 (Invitrogen), HappyFect (Tecrea), Nucleofector solution V (Lonza), Ingenio electroporation kit (Mirus) and TransIT-Neural® transfection reagent (Mirus). Cells were plated onto coverslips in 12-well plates, and transfected with GPR50-p40 (untagged). Cell viability was assessed by comparison with untransfected controls. Immunocytochemistry was carried out to calculate transfection efficiency by labelling cells with the GPR50 goat antibody. Transfection results using different regents in SH-SY5Y cells and primary cortical neurons are summarised in Table 4.2. It is shown that Lipofectamine 2000 was the most efficient transfection regent and retained the highest cell viability among all tested methods in both cell lines. Transfection efficiency was further optimised in primary cortical neurons by adjusting the amount and proportion of plasmid and Lipofectamine 2000 (Table 4.3). The number of neurons that were plated into culture wells was also optimised to guarantee neuron viability after transfection. The optimal input was 2 μg plasmid/4 μl Lipofectamine 2000 (1:2) for 2×10^6 neurons in a well surface area of 4 cm^2 (12-well plate). In later experiments, 5×10^6 neurons were plated in 6-well plates (surface area 10 cm^2), and a combination of 5 μg plasmid/10 μl Lipofectamine 2000 was used for transfection to retain the optimised proportion of culture area: cell number: DNA amount: transfection reagent amount.

Table 4.2 Test of different transfection regents in SH-SY5Y cells and primary cortical neurons

	SH-SY5Y (1×10^5)		**Primary cortical neurons (2×10^6)**	
Reagent	***Cell viability***	***Transfection efficiency***	***Cell viability***	***Transfection efficiency***
Lipofectamine 2000	+++	20-30%	++	4.9%-9.3%
HappyFect	+++	5-15%	-	NA
Nucleofector solution V	++	6.2%	NA	NA
Ingenio electroporation	++	15.6%	+	0%
TransIT-Neural®	NA	NA	+++	0%

+++: no obvious cell death, ++: small percentage of cell death, +: half cells died, -: all cells died, NA: not tested.

Table 4.3 Transfection primary cortical neurons with Lipofectamine 2000

Plasmid/µg	*Lipofectamine/µl*	*Cell viability*	*Transfection efficiency*
1	2	++	0%
2	2	++	<1%
4	2	++	4.90%
1	4	++	0%
2	4	++	8.42%
4	4	++	7.26%
1	8	++	0%
2	8	+	3.37%
4	8	+	9.29%

++: small percentage of cell death, +: half cells died.
2×10^6 neurons were used in each test.

4.3.2 Detection of Bace1/BACE1 activity levels in mouse primary cortical neurons and human neuroblastoma cell line SH-SY5Y

The kit for β-secretase activity assay (Fluorometric) is commercially available (Abcam, ab65357) and has been described in use for β-secretase activity in human HEK293 cells (Grünewald, 2011), rat primary hippocampal neurons (Cui et al, 2011) and mouse cortex/hippocampus tissues (Barbero-Camps et al, 2013; Hook et al, 2011; Wen et al, 2011). Here, I sought to validate the application of this kit in mouse primary cortical neurons and human neuroblastoma SH-SY5Y cells.

The absolute β-secretase activity levels of 1.5 µl recombinant BACE1 enzyme, 5×10^5 primary cortical neurons and 5×10^5 SH-SY5Y cells were within a range of 210000-260000 fluorescent units (Figure 4.2). These readings were equivalent to those measured for around 1×10^6 HEK293 cells (Grünewald, 2011). Adding 1.5 µl inhibitor to the three aforementioned enzyme sources of β-secretase resulted in a reduction of 45.0%, 14.3% and 2.0% in the florescence levels respectively. After consulting the manufacturers of the β-secretase activity kit, these numbers were deemed to be a sufficient indication that the kit was working. This meant that the Bace1 activity in primary cortical neurons could be diminished by the inhibitor provided, which indicated that there was a certain level of active β-secretase present in neurons. This scale of inhibition in neurons was comparable to that in HEK293 cells (Grünewald, 2011). However, the inhibitor almost failed to suppress the florescence levels in SH-SY5Y cells, implying that even though there was endogenous BACE1 mRNA detected in this cell line (see chapter 2), its protein form

was not fully active. A partial explanation of this may be that the major form of endogenous BACE1 protein in SH-SY5Y cells is an intermediate product of the full-length BACE1 before maturation, which has been reported previously (Costantini et al, 2007; Ko & Puglielli, 2009). Therefore, in the following experiments, only primary cortical neurons were used to assess the effect of GPR50/GPR50del overexpression and Gpr50 knockdown on β-secretase activity levels.

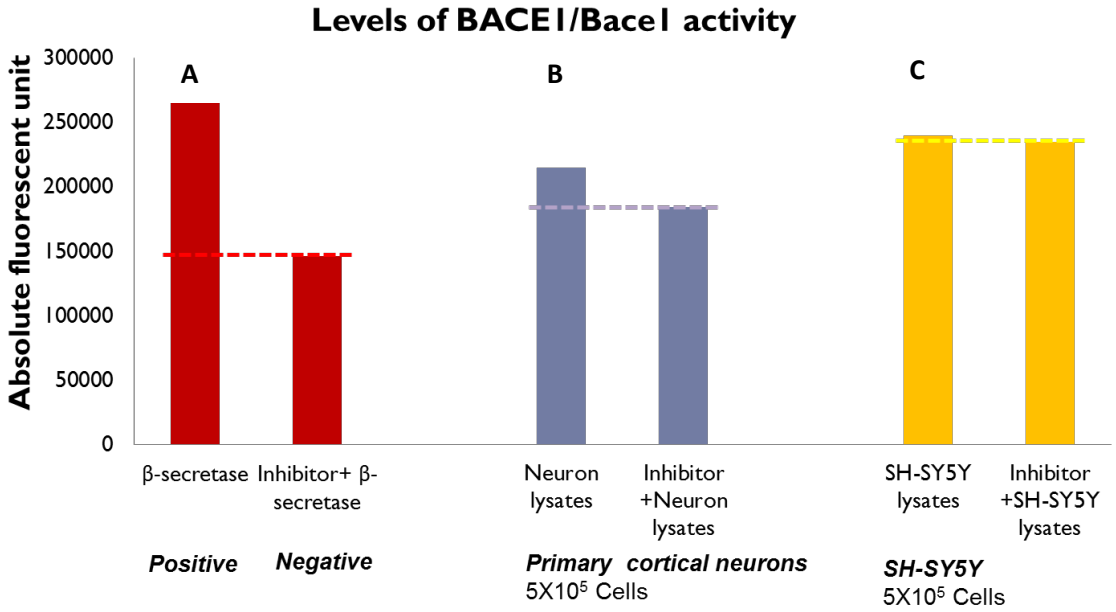

Figure 4.2 The test of endogenous β-secretase activity levels in B) primary cortical neurons and C) SH-SY5Y cells, compared with A) the positive control of recombinant β-secretase. This experiment was performed twice. The absolute fluorescent unit here represents an empirical expression of fluorescence activity, commonly given in terms of arbitrary units proportional to detector response (WHO, 2006).

4.3.3 Optimisation of β-secretase activity assay kit in primary neuronal cultures

In order to identify the effective detection range of β-secretase activity levels, the BACE1 positive control was titrated (Figure 4.3.A). It was found that the absolute fluorescent units fell into the exponential phase of detection by using 0.1-2.5µl recombinant BACE1 enzyme. Higher input was not tested because of the limited amount of enzyme provided. As the background reading is high (around 100000) due to the natural properties of such fluorescence quenching assay, I sought to set the valid range of fluorescent readings to 150000-300000. Then I tested the minimum cell input for primary cortical neurons that could yield a reading between the range (Figure 4.3.B), within the exponential phase of detection. This set a minimum cell number of 1.5×10^5 for primary neurons. As the "no-substrate" control also generated a value of 60000-80000, the cell number needed to be increased to a level that

obviously exceeded that value. Finally, a number of 5×10^5 that generated a value of 200000-300000 was used in the following experiments.

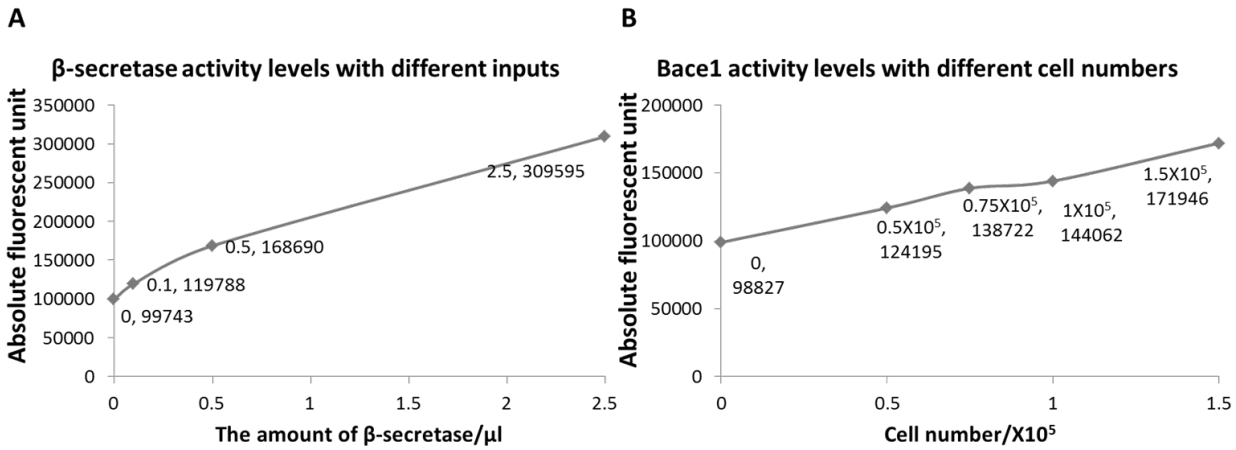

Figure 4.3 The titration of β-secretase activity detection. A) The experiment to ensure the reading of β-secretase activity was located within an interval of sensitivity for detection. B) The examination of cell input for primary cortical neurons in β-secretase activity assay.

4.3.4 Is Bace1 activity regulated by GPR50 overexpression?

For protein overexpression, an equal amount of GPR50 and GPR50del was transfected in DIV3 primary cortical neurons, and pDEST40 was used as control. The total RNA was extracted from neurons that grew in the same pool as the neurons that were used for activity assay and qPCR was carried out to confirm the relative mRNA expression levels of GPR50/GPR50del/Gpr50 against the controls. As is shown in Figure 4.4, there was a low level of endogenous Gpr50 expressed in mouse primary cortical neurons, which is in line with previous findings (Grunewald et al, 2009; Grunewald et al, 2012). It has been reported that endogenous Gpr50 mRNA in mouse brain was robustly expressed at E18 (half a day before birth), but its level decreased after birth (Grunewald et al, 2012). The GPR50 rabbit antibody did detect endogenous Gpr50 protein from mouse brains of E18 and P0 (the day of birth) (see chapter 2, Figure 2.8).

Five independent replicates were performed for this experiment. GPR50 and GPR50del were successfully transfected in all replicates. The absolute Bace1 activity readings were normalised against p40 and evaluated by two-tailed paired t-test. No significant difference was identified with GPR50 overexpression ($p=0.98 >0.05$), but there was a trend of decrease in the Bace1 activity level observed with GPR50del-transfected neurons (7.9% decrease, $p=0.079<0.1$), compared with the control. Interestingly, there was a significant loss of Bace1 activity in GPR50del-

overexpressed neurons compared with GPR50-overexpressed neurons (8.1% decrease, $p=0.021<0.05$).

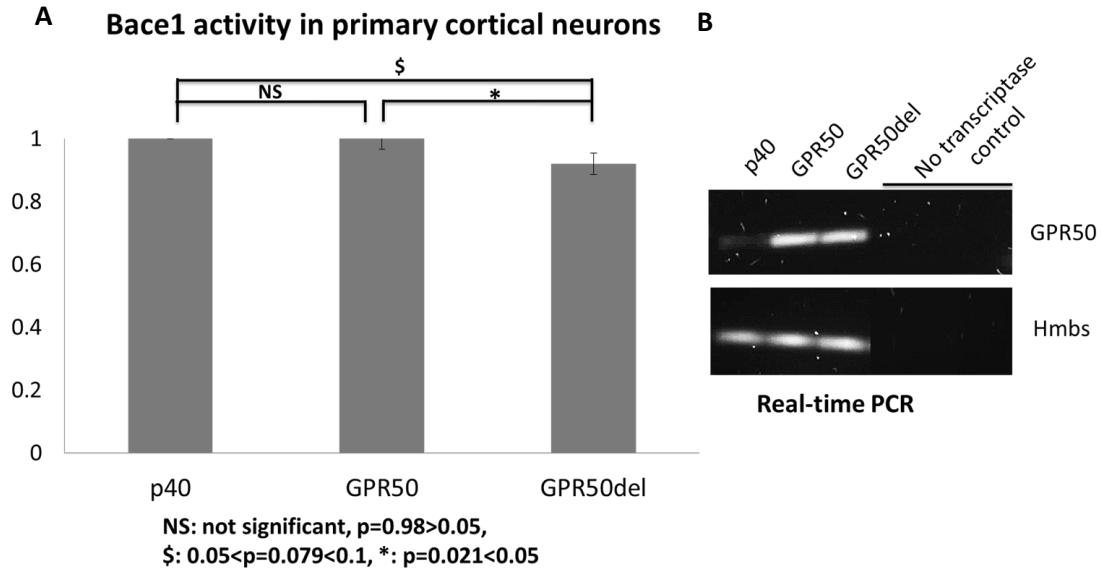

Figure 4.4 Effects of GPR50/GPR50del overexpression on Bace1 activity in mouse primary cortical neurons. A) Normalised Bace1 activity in primary neurons transfected with pDEST40 (p40), GPR50 and GPR50del. N=5, the statistical analysis of significance was examined by paired Student's t-test. B) Endogenous Gpr50 mRNA levels in neurons transfected with p40, GPR50 and GPR50del. These neurons were grown in the same pool as those used for activity assay. Hydroxymethylbilane synthase (Hmbs) was used as the housekeeping gene for equal loading control. The clean negative control (No transcriptase control) indicated that there was no contamination during the processes of total RNA extraction and cDNA synthesis.

4.3.5 Is Bace1 activity regulated by Gpr50 knockdown?

In order to assess β-secretase activity in a Gpr50 loss-of-function system, three 29-mer shRNAs (shRNA61, 62, 63) targeting Gpr50 mRNA were transfected singly or jointly to reduce the endogenous expression level of Gpr50 in mouse primary cortical neurons (see 3.2.2). qPCR was performed for the detection of Gpr50 knockdown. As is shown in Figure 4.5.B, all the three shRNA constructs successfully diminished the mRNA levels of endogenous Gpr50 in 5×10^6 primary cortical neurons. ShRNA61, 62 and 63 decreased Gpr50 level by 89.0%, 98.4% and 84.9% respectively. Thus, in later experiments, 30 μg shRNA62 or a mixture of the three shRNAs (10 μg shRNA61+10 μg shRNA62+10 μg shRNA63, 1/3 for each construct) were applied to obtain optimal knockdown result. The expression of human GPR50 plasmid in primary neurons was the positive control, which also indicated a successful transfection of these plasmids (Figure 4.5.A).

Five independent replicates for the determination of β-secretase activity in Gpr50 deficient neurons were performed. Unfortunately, the detection of endogenous Gpr50 knockdown ended up unsuccessful in these replicates (Figure 4.6). The cell number of neurons in each culture well (5×10^6) and the transfection mixture proportion (30 µg shRNA construct/10 µl Lipofectamine 2000) were identical throughout the experiment. However, while all the neurons (5×10^6) in the initial knockdown test (Figure 4.5) were used for measuring Gpr50 mRNA levels by qPCR, the neurons used for the following five replicates were split into two portions, 2×10^6 for the activity assay and around 3×10^6 for the qPCR experiment. It is possible that the Gpr50 mRNA expression can only be detected when sufficient neurons were harvested, 5×10^6 in this case. Indeed, from Figure 4.6, it is shown that the endogenous Gpr50 level was hardly detected in most replicates. Hence, a possible reason for the failure of Gpr50 knockdown is that the cell number used for mRNA detection was inadequate. In fact, it is not known whether the knockdown was actually not achieved or the detection of a successful knockdown failed. As it could not be guaranteed that the primary neurons had Gpr50 deficiency, the Bace1 activity assay was not analysed in cells that were transfected with scramble, shRNA62 or shRNA61+62+63. Further optimisation was not performed due to lack of time.

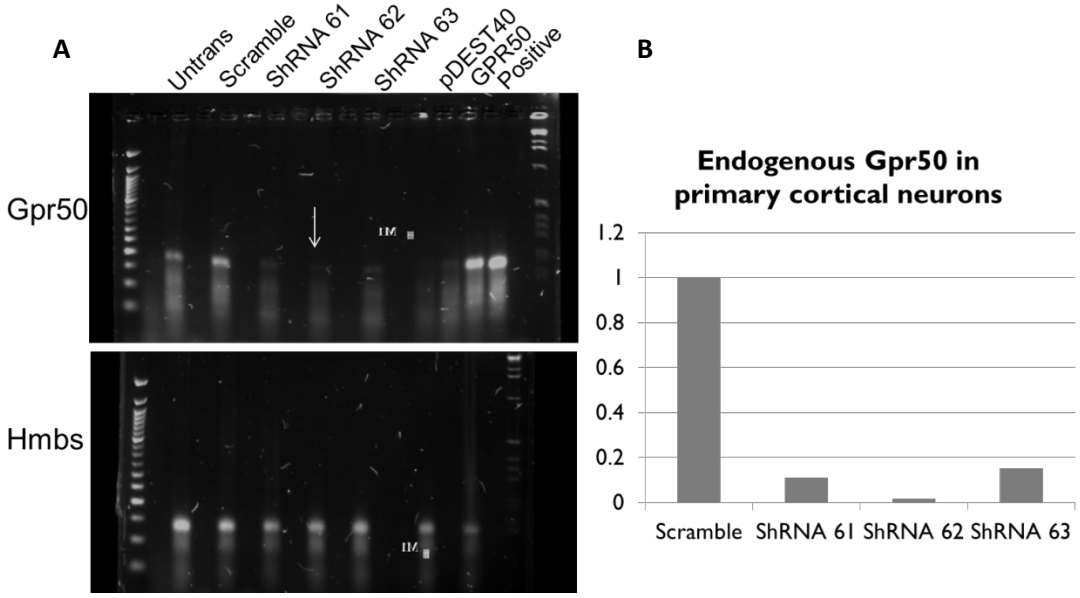

Figure 4.5 The test of endogenous Gpr50 knockdown in mouse primary cortical neurons. A) ShRNA61, 62 or 63 targeting Gpr50 were transfected singly in mouse primary cortical neurons. Real-time qPCR was performed for the detection of Gpr50 mRNA. Hmbs was used as the housekeeping gene for the loading control. The adjacent lane, on the left of each lane with a positive band, was its no-transcriptase negative control. The GRP50 plasmid was transfected for the detection of successful transfection. The protein lysates of E18 mouse brain was used as the positive control for the detection of endogenous mouse Gpr50. B) Quantification of Gpr50 knockdown by the three shRNAs.

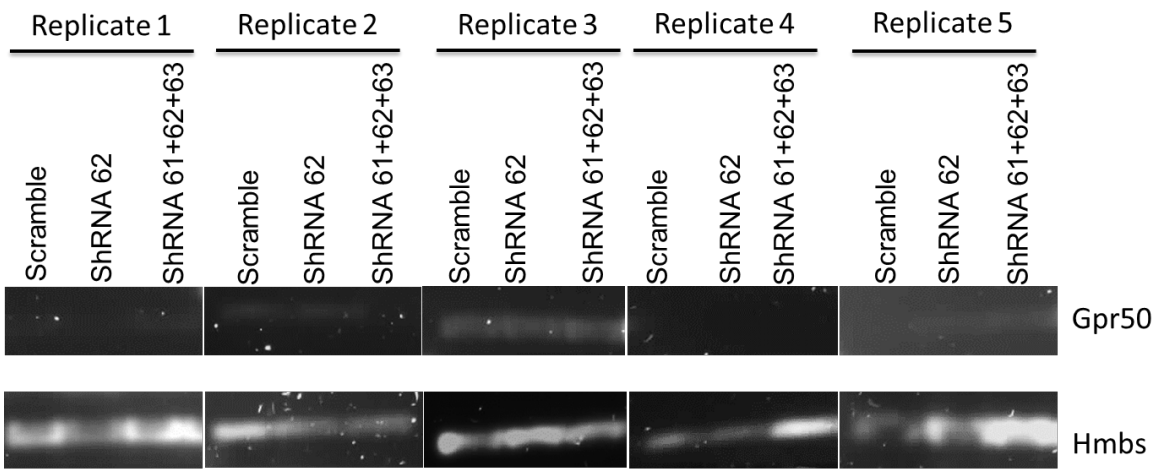

Figure 4.6 The unsuccessful knockdown of endogenous Gpr50 in mouse primary cortical neurons. Scramble, shRNA62, shRNA61+62+63 were transfected in mouse primary cortical neurons. Real-time qPCR was performed for the detection of Gpr50 mRNA. Hmbs was used as the housekeeping gene for the loading control.

4.4 Discussion

In this chapter, the potential of Gpr50 in regulating endogenous β-secretase activity in neuronal cells was investigated. The β-secretase activity assay in neuroblastoma cell line SH-SY5Y was terminated because endogenous BACE1 activity was not detected. In mouse primary cortical neurons, no significant alteration of Bace1 activity level was found upon GPR50 overexpression. However, GPR50del overexpression resulted in a trend of decline in Bace1 activity level compared with the empty vector control ($p=0.079$). Importantly, Bace1 activity level in primary neurons transfected with GPR50del was significantly lower (8.1%) than those transfected with GPR50 ($p=0.021$). Therefore, contrary to the up-regulation effect by GPR50, mental disorder-related GPR50del in neuronal cells appears to have an inhibitory effect on BACE1 functions, and this might indicate a disruption of the normal function exhibited by GPR50. Further functional studies (i.e. analysing specific BACE1 substrates) need to be carried out to confirm the consequence of GPR50 deletion/SNP on its general function, as well as the impact on β-secretase activity regulation.

4.4.1 Endogenous BACE1 in SH-SY5Y cells

Even though there is a moderate expression level of endogenous BACE1 mRNA in SH-SY5Y cells (see chapter 2), the protein level can be very low (Li et al, 2006; Sarajarvi et al, 2009). It has been reported that a biosynthetic intermediate form of BACE1 is endogenously expressed in SH-SY5Y cells (Costantini et al, 2007; Ko &

Puglielli, 2009). This intermediate product is less glycosylated than the fully mature BACE1 (Costantini et al, 2007), thus it has a lower molecular weight (see chapter 2). N-glycosylation is essential to BACE1 activity. A BACE1 mutant that contains only two out of the four N-glycosylation sites showed decreased BACE1 activity (Charlwood et al, 2001). The level of BACE1 activity was also reduced when treated with Tunicamycin, which inhibits N-glycosylation (Murayama et al, 2006). Therefore, it is expected that partly glycosylated BACE1 has lower or little activity. Additionally, BACE1 enzymatic activity correlates with mature BACE1 level instead of total BACE1 level (Zhong et al, 2007).

There is another possibility that the translation system of endogenous BACE1 in SH-SY5Y cells is similar to that in the pancreas, which possesses low levels of normal BACE1 protein and activity despite robust mRNA expression (Bodendorf et al, 2001). Elsewhere, alternative splicing of the BACE1 transcript leader occurred in both the exocrine pancreas and neuroblastoma cells, but not in normal human brain (De Pietri Tonelli et al, 2004). Some shorter isoforms, such as BACE1 476 and BACE1 455, were abundantly expressed in the pancreas, but low in the brain (Mowrer & Wolfe, 2008). These BACE1 variants undergo different post-translational modifications compared to the full length BACE1 501 and were demonstrated to be deficient in β-secretase activity (Ehehalt et al, 2002; Mowrer & Wolfe, 2008). Thus, it is likely that the endogenous BACE1 protein with a lower molecular weight is a product of alternative splicing in SH-SY5Y cells, but this needs further validation.

In summary, I argue that the actual proportion of functional BACE1 protein is very low in SH-SY5Y cells, so there is nearly undetectable BACE1 activity. Hence, in chapter 5 where the trafficking system of endogenous BACE1 was investigated, I used HEK293 cells and mouse primary neuronal cultures instead of SH-SY5Y cells.

4.4.2 The biological significance of β-secretase activity regulation by GPR50/GPR50del

In HEK293 cells, GPR50 overexpression appears to up-regulate BACE1 activity by around 9% compared with the control condition, while GPR50del has no significant effects (Grünewald, 2011). Therefore, cells overexpressed with GPR50del may generally have lower β-secretase activity than cells overexpressed with GPR50. This is consistent with my findings in mouse primary cortical neurons, in which

GPR50del overexpression resulted in a significant 8.1% decrease of Bace1 activity compared to GPR50 overexpression. An interesting difference between the results found in the two cell lines is that GPR50 has significant effects on non-neuronal β-secretase activity, whereas GPR50del exhibits a potential in regulating neuronal β-secretase activity. Thus, the involvement of GPR50 protein in the regulation of BACE1 function might be cell type differentiated. The variation of deletion/SNP in *GPR50* sequence is likely to switch the function of the protein from non-neurons to neurons, and this is in line with previous reports that GPR50del is associated with psychiatric disorders, in which neuronal β-secretase activity may be dysregulated (Ly et al, 2013; Savonenko et al, 2008; Vassar et al, 2009). In addition, it is worth mentioning that the transfection efficiency in HEK293 cells (>50%) is far higher than in primary neuronal cultures. According to Table 4.3, less than 10% neurons overexpressed GPR50 or GPR50del, which generated an 8% alteration of activity. Thus, GPR50del seems to be more effective in regulating neuronal β-secretase activity than GPR50 in non-neuronal β-secretase activity. It needs additional analysis of the generation of Bace1 cleavage products to answer the question if Bace1 activity inhibition of such a magnitude (8.1%) is of biological significance.

RTN3 is a well characterised inhibitor of BACE1 activity. In HEK293 cells, transfection of exogenous RTN3 could diminish the relative level of endogenous BACE1 activity by 18-22% (Grünewald, 2011; He et al, 2004), which may consequently result in a reduction of up to 60% in the secretion of both Aβ40 and Aβ42 (He et al, 2004; Murayama et al, 2006). Considering the difference in transfection efficiency between the HEK293 cells and primary cortical neurons, and the inhibitory effect of RTN3 in HEK293 cells, one can argue that the regulation of Bace1 activity engendered by GPR50/GPR50del transfection in primary cortical neurons is likely to be biologically significant.

Another type of BACE1 inhibitor, the components of the retromer complex SNX6 and SNX12, have similar patterns of interaction with BACE1, as both of them negatively regulate BACE1 endocytosis and Aβ generation (Okada et al, 2010; Zhao et al, 2012). Interestingly, SNX12 inhibited APP processing without affecting β-secretase activity (Zhao et al, 2012). This suggests a regulation mechanism, by which BACE1 interactors can still play a part in the functional cleavage, even though they do not have a significant effect on BACE1 activity. Nonetheless, it is important to note that, with the overall activity level of BACE1 unchanged, the enzyme in

different subcellular compartments (the plasma membrane, the endosomes, the Golgi, etc) may be redistributed for specific substrate cleavage, resulting in a local regulation of BACE1 activity. The effect of GPR50/GPR50del overexpression on BACE1 subcellular localisation was investigated in chapter 5.

4.4.3 Future study: does GPR50/GPR50del affect substrate-specific β-secretase activity?

As introduced previously, BACE1 plays multiple roles in neuronal activity by cleaving diverse molecules. The activity levels detected in neurons may come from a joint effect of cleaving multiple substrates by β-secretase activity, reflecting diverse aspects of cell physiology. To better understand the function of β-secretase cleavage and its interacton with GPR50/GPR50del, it is essential to examine which molecules are involved in the regulation of β-secretase activity by GPR50/GPR50del. By using cells transfected with p40/GPR50/GPR50del, one can perform ELISA immunoassay and western blotting to measure and compare the levels of end products from β-secretase cleavage, such as Aβ40/42, AICD, EGF; and intermediate products, such as C99, sβAPP, NRG1-βNTD, NRG1-βCTD. These products can be intracellular, membrane-bound or secreted. Therefore, it is also helpful to fractionate cells and to collect relevant culture media for separating different products and investigating the ratio of different cleavage activities. Additionally, quantitative proteomics/mass spectrometry (that is widely used for the detection of novel BACE1 substrates) (Hemming et al, 2009) can be carried out to identify the cleaved peptide(s) from the medium cultured with GPR50/GPR50del overexpressed neurons.

In conclusion, results in this chapter revealed that GPR50 has a potential to regulate neuronal β-secretase activity. The deletion/SNP variation of GPR50 encoding sequence appears to be functionally effective, because GPR50del showed distinct function from the full-length isoform. This finding expands the association of GPR50 polymorphism with mentally related illnesses, possibly by changing the normal interaction between GPR50 and neuronal BACE1.

5 Is the trafficking of BACE1 regulated by GPR50 or GPR50del?

5.1 Introduction

In previous chapters, I have shown that GPR50 is physically associated with BACE1 by co-immunoprecipitation experiments and is directly involved in the regulation of neuronal BACE1 activity. Transcriptional regulation of BACE1 is tightly related to the altered levels of its activity, as was detailed in chapter 2. However, the activity modulation is not necessarily dependent on the turnover of this enzyme (Tan et al, 2013). There are distinct subcellular compartments in cells with different composition and pH values, so the proteolytic properties of BACE1 also depend on how this protein is spatially located (Cole & Vassar, 2007). This suggests that the trafficking system of BACE1 is equally if not more important in determining its activity than the regulation of gene expression.

5.1.1 Post translational modification of BACE1 and trafficking

It is well recognised that the amyloidogenic processing of amyloid precursor protein (APP) by BACE1 gives rise to the accumulation of Aβ peptides, the main hallmark in the AD brain. Other substrates have also been identified that decide the multifunctional importance of BACE1, for instance APLP1/2 (Eggert et al, 2004; Li & Sudhof, 2004), neuregulin-1/3 (Hu et al, 2008; Hu et al, 2006), $Na_v\beta_2/\beta_4$ (Kim et al, 2007; Miyazaki et al, 2007), CHL1 (Kuhn et al, 2012) , etc. As APP is the most commonly studied substrate of BACE1, here I will focus on introducing the regulation of BACE1 trafficking that is related to Aβ peptide production. The consensus has not been reached on the subcellular compartments where APP cleavage occurs. There are two putative sites of action: the early endosomes and the plasma membrane (Chia & Gleeson, 2011). Some researchers argue that the acidic environment (pH 4.0-5.5) of the early endosomes is optimal for BACE1 to operate (Siegenthaler & Rajendran, 2012). Deficiency in retromer components (i.e. sorting nexin family members SNX6, SNX12) is likely to block BACE1 in the endosomes, which promotes its cleavage activity in the amyloidogenic APP processing (Sullivan et al, 2011; Wang et al, 2012). However, there is also experimental data demonstrating that cholesterol and sphingolipids-rich lipid rafts in the plasma membrane are the sites of Aβ production (Rushworth & Hooper, 2010). Indeed, targeting BACE1 to the lipid rafts via an anchor glycosylphosphatidylinositol (GPI) up-regulates β-site processing of APP (Cordy et al, 2003) . Also, Marquer and colleagues observed that in live neuronal cells APP and Bace1 are in proximity at the

plasma membrane, and increasing the cholesterol level in the plasma membrane brings APP into the lipid rafts that already contain Bace1 (Marquer et al, 2011). Interestingly, there are two pathways for BACE1 to reach the early endosomes, either by being transported directly via Trans-Golgi network (TGN) after maturation, or through recycling from the plasma membrane through internalisation (Tan & Evin, 2012). Thus, targeting BACE1 to the plasma membrane can also promote BACE1 activity, as this pool of BACE1 may undergo endocytosis towards the endosomes for theoretically more efficient APP cleavage.

The cycling of BACE1 is closely associated with a series of post translational modifications. Synthesised as a zymogen, immature BACE1 consists of a signal peptide (1-21), a pro-domain (22-45), a protease domain (46-460), a transmembrane domain (461-477) and a cytosolic tail (478-501) (Figure 5.1). There are two modifications that take place in the ER: the first step of glycosylation within the protease domain (Asparagine residues 153, 172, 223, 354), which is co-translational (Charlwood et al, 2001); and transient acetylation of seven lysine residues at N-terminal (Lys126, 275, 279, 285, 299, 300, 307) that stabilises pro-BACE1 (Tan & Evin, 2012) and facilitates its trafficking through the secretory pathway. The pro-domain assists in the proper folding of BACE1, and is removed in the Golgi. However, the presence of the pro-peptide does not inhibit BACE1 activity, as evidence suggests that this pro-sequence fails to block APP entering the active cleft of BACE1 (Shi et al, 2001). Also in the Golgi, further complex glycosylation is achieved, which increases the molecular weight of BACE1 by 30% and fundamentally controls BACE1 activity (Tan & Evin, 2012). Immature BACE1 is thought to have much less β-secretase activity due to lack of glycosylation (Zhong et al, 2007). Sulfation can be introduced on the N-glycosylation sites as a part of BACE1 maturation, and inhibition of endogenous heparan sulfate synthesis or sulfation induces elevated levels of BACE1 activity (Scholefield et al, 2003).

The trafficking regulators are normally co-localised with BACE1 and are generally found linked to at least one of its modification processes (Figure 5.2). Most of the modification sites for trafficking are located in the cytosolic domain (Figure 5.1). Phosphorylation at serine 498 occurs exclusively on the fully maturated BACE1 after the removal of pro-peptide and complex glycosylation. This action facilitates the binding to GGA1 in the Golgi, permitting the cycling to the plasma membrane (von Arnim et al, 2004). Phosphorylation may also modulate the adjacent dileucine motif

(Leucine 499, 500) (Pastorino et al, 2002), which is essential to the internalisation sorted by GTPase ADP-ribosylation factor 6 (ARF6) (Sannerud et al, 2011). BACE1 undergoes S-palmitoylation at four Cys residues (Cysteine 474, 478, 482, 485) at the junction of transmembrane and cytosolic domains (Vetrivel et al, 2009), and these modifications fulfil a role in locating BACE1 in the lipid rafts (Bhattacharyya et al, 2013). Ubiquitination at lysine 501 is the recognition signal of GGA3 for targeting BACE1, which is transported to the lysosomes for degradation and consequently its turnover is regulated (Kang et al, 2010). In addition, down-regulation of retromers accelerates the endocytosis of BACE1 from the cell surface (SNX12) (Zhao et al, 2012) or retrograde trafficking of internalised BACE1 from the early endosomes to perinuclear structures (SNX6) (Okada et al, 2010).

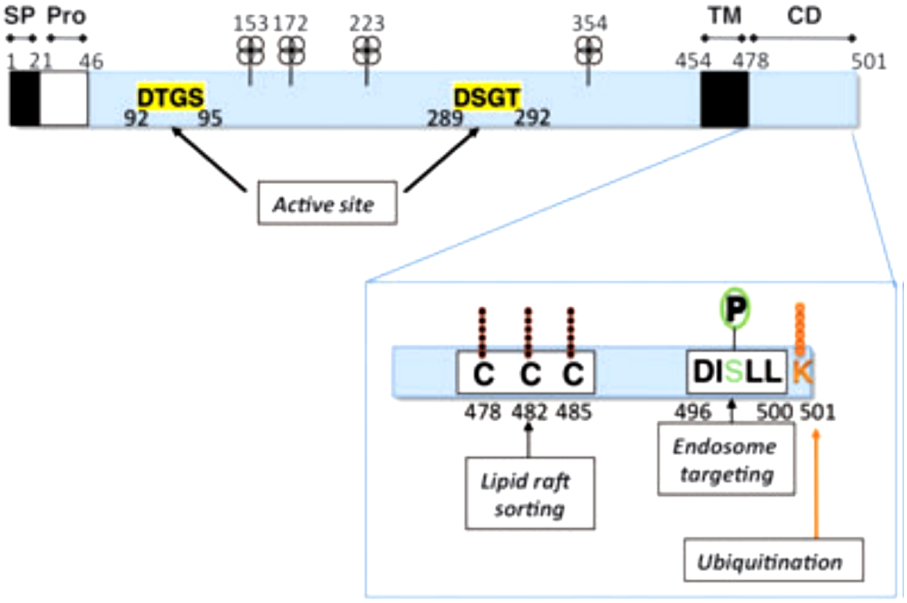

Figure 5.1 A diagram representing BACE1. This diagram was adapted from (Tan & Evin, 2012). Precursor BACE1 contains a signal peptide (SP), a pro-sequence (Pro) and a transmembrane domain (TM), followed by a cytosolic domain (CD). It undergoes glycosylation at four sites (represented with four-node symbols). The two motifs DTGS/DSGT form the enzymatic active site. Enlarged cytosolic domain shows the post-translational modifications that affect BACE1 cellular trafficking: palmitoylation at three cysteine residues (C), phosphorylation at serine 498 (S) within the DXXLL sorting motif, and ubiquitination at lysine 501 (K). The fourth palmitoylation site (C474) was not shown as it is located out of the cytosolic domain.

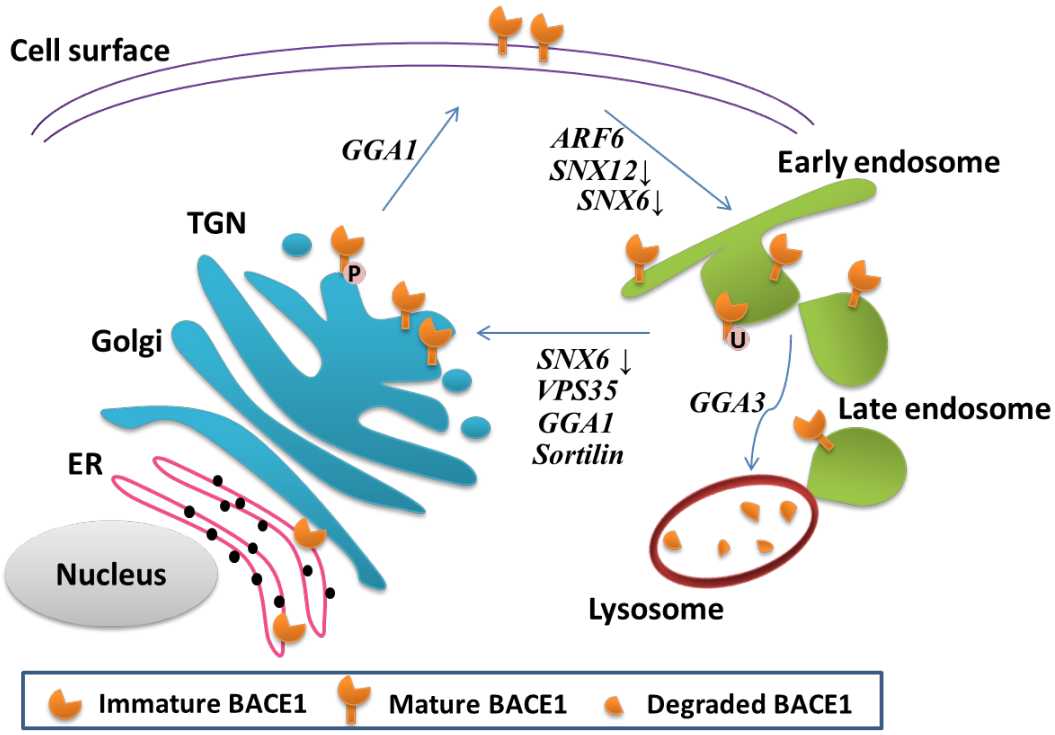

Figure 5.2 BACE1 cellular trafficking and representative regulators. ER: endoplasmic reticulum; TGN: trans-Golgi network; P: phosphorylation; U: ubiquitination. The black down arrows indicate down-regulation of the regulators. ARF6: ADP-ribosylation factor 6, a member of the ADP ribosylation factor family of GTP-binding proteins, is required for the internalisation of BACE1 from cell surface to endosomal compartments (Sannerud et al, 2011). GGA1: a member of Golgi-localised, gamma adaptin ear-containing ARF-binding (GGA) protein family, regulates the retrograde trafficking of internalised BACE1 from endosomal compartments to TGN and the recycling of phosphorylated BACE1 to the cell surface (von Arnim et al, 2004; Wahle et al, 2005). GGA3: a member of GGA protein family mediates the transport of BACE1 to lysosomes for degradation (Kang et al, 2010). SNX6: a member of the sorting nexin (SNX) family that is a component of the retromer complex, the down-regulation of which facilitates the retrograde transport of cell surface-derived BACE1 from the endosomes to the perinuclear structure, including TGN (Okada et al, 2010). SNX12, a member of the SNX family, the down-regulation of which facilitates the endocytosis of BACE1 (Zhao et al, 2012). VPS35: vacuolar protein sorting-associated protein 35, the largest subunit of retromer, promotes the retrieval of BACE1 from the endosomes to the Golgi (Wen et al, 2011). Sortilin: a Vps10p domain-sorting receptor, is a positive modulator of BACE1 retrograde trafficking from the endosomes to TGN (Finan et al, 2011).

Table 5.1 Major factors involved in BACE trafficking and associated with Alzheimer's disease

Protein	General function	Interaction with BACE1	Effect on BACE1 trafficking	Investigation in Alzheimer's disease	References
GGA1	Adaptor sorting protein	(496–500) DXXLL motif Phosphorylated Ser_{498}	Recycle BACE1 from endosomes to plasma membrane via the Golgi	Decreased in AD frontal cortex	*(Santosa et al, 2011; von Arnim et al, 2004; Wahle et al, 2005; Wahle et al, 2006)*
GGA3	Adaptor sorting protein	(496–500) DXXLL motif Ubiquitinated Lys_{501}	Sort BACE1 from endosomes to lysosomes for degradation	Marked decrease in AD frontal cortex	*(Kang et al, 2010; Santosa et al, 2011; Tesco et al, 2007)*
RTN3*	Neuronal function	Transmembrane region	Retain BACE1 in ER	Enriched in RTN3 immunoreactive dystrophic neurites (RIDNs) in AD brains	*(Deng et al, 2013; Murayama et al, 2006; Shi et al, 2009)*
Seladin-1	Cholesterol biosynthesis	Indirect	Control cholesterol level in rafts; prevent casp-3 cleavage of GGA3	Down-regulated in affected neurons in AD	*(Crameri et al, 2006; Greeve et al, 2000; Sarajarvi et al, 2009)*
ARF6	Protein endocytosis	(499–500) LL motif	Sort BACE1 from plasma membrane to early endosomes	Decreased level in AD brain	*(Sannerud et al, 2011)*
SORLA	Neuronal apolipoprotein E receptor	Co-immunoprecipitation with BACE1 and APP	Prevent APP/BACE1 interaction in the Golgi	Suspect gene for AD; decreased levels in AD brain.	*(Scherzer et al, 2004; Spoelgen et al, 2006; Willnow et al, 2010)*
SNX6*	Retromer subunit	Co-immunoprecipitation	Its down-regulation facilitates recycling BACE1 from cell surface through the endosomes to perinuclear structure, including TGN	Impaired retromer complex in AD	*(Okada et al, 2010; Small et al, 2005)*
SNX12	Retromer subunit	Co-immunoprecipitation	Its down-regulation accelerates BACE1 endocytosis	Dramatically decreased in AD brain	*(Zhao et al, 2012)*
VPS35	Largest subunit of retromer	Co-immunoprecipitation	Retrograde trafficking of BACE1 from endosomes to Golgi	Hemizygous deletion of Vps35 in Tg2576 mouse model leads to earlier-onset AD-like phenotypes	*(Wang et al, 2012; Wen et al, 2011)*
Sortilin	Retromer-mediated retrograde transport	Through cytoplasmic tail of sortilin; Co-immunoprecipitation	Retrograde trafficking of BACE1 from endosomes to TGN	With Increased levels in AD brain.	*(Finan et al, 2011; Gina, 2010)*

Interactors of GPR50 identified by the yeast two-hybrid study (Grunewald et al, 2009)

It is worthwhile mentioning that the disorder of BACE1 trafficking is commonly associated with adverse cellular conditions, such as apoptosis and stress. In the brains of AD patients that may undergo neuronal apoptosis, the levels of GGA3 are significantly decreased, resulting in an accumulation of BACE1 in the early endosomes, and impairing its trafficking to the lysosomes where it is degraded (Tesco et al, 2007; Walker et al, 2012). Oxidative stress may diminish VPS35 levels in the brain, which may in turn damage the retrograde sorting of BACE1 from the endosomes (Wang et al, 2012; Wen et al, 2011). It is summarised in Table 5.1 the BACE1 regulators that play a part in BACE1 trafficking and have a link to AD. Interestingly, two of the major factors, RTN3 and SNX6, have been reported as GPR50 putative interactors, identified by the yeast two-hybrid study (Grunewald et al, 2009). Interaction between GPR50 and RTN3 has been identified by co-localisation and co-immunoprecipitation experiments (Grünewald, 2011). This suggests that GPR50 may acts as a synergistic factor that regulates BACE1 localisation in cells. Further, the mental disorder associated deletion/SNP variant GPR50 del appears to alter the normal function of GPR50, such as in the neurite extension and in the interaction with RTN3 (Grunewald et al, 2009; Grunewald et al, 2012). Thus, in this chapter, the effect of both GPR50 isoforms was investigated on BACE1 trafficking.

5.1.2 Ways to study BACE1 trafficking

The critical role played by the trafficking machinery in regulating BACE1 activity, hence the production of Aβ in AD, has led to an increased interest in different approaches for studying the mechanisms of BACE1 trafficking. Three main techniques have been applied for studies of BACE1 transport across the subcellular compartments and during the internalisation.

5.1.2.1 Immunocytochemistry identifying the pathways of BACE1 cycling by co-staining with diverse subcellular markers

Immunofluorescence labelling is a powerful technique involving a variety of antibodies. Cells can be fixed and permeabilised, followed by multi-staining of antibodies against BACE1 and subcellular markers. In chapter 2, I showed that overexpressed BACE1 was localised in the plasma membrane (marked by pan cadherin, VLA-2α and β-catenin), the endosomes (marked by EEA1), the Golgi

(marked by 58K Golgi) and the late endosomes (marked by RAB7). To investigate how a putative interactor affects BACE1 trafficking, this method can be applied to observe the redistribution of BACE1 among different compartments of cells overexpressed with or deficient of the interactor. For instance, Wen and colleagues investigated the potential role of VPS35 in BACE1 circulation, by making use of the co-immunostaining analysis of exogenous BACE1 with endogenous Vps35, cis-Golgi marker GM130, and lysosome marker LAMP1 in NLT cells transfected with control or shRNA-Vps35 (Wen et al, 2011). It was revealed that in VPS35-deficient cells, BACE1 was no longer confined to the Golgi, but relocated to the endosomes/lysosomes, suggesting that VSP35 is crucial for BACE1 to be retained in the Golgi.

Alternatively, antibodies that recognise specific extracellular epitopes can be introduced to trace BACE1 on the cell surface in live cells. Under non-permeabilised conditions, only proteins on the plasma membrane will be labelled. The antibody is generally assumed to stay bound to the protein throughout the endosomal pathway and become dissociated in lysosomes where both the targeted protein and the antibody are degraded (Arancibia-Carcamo et al, 2006). The antibody binding step is normally performed at 4°C, which blocks the membrane trafficking so as to inhibit the endocytosis of molecules. The media used to dilute the antibody is regularly buffered with HEPES and salts. In chapters 2 and 3, I showed that BACE1 was successfully labelled on the cell surface by the BACE1 goat antibody. For quantitative studies of the endocytosis and the internalisation, cells are returned to incubation at 37^{o}C for desired period of time, and then fixed (by 4% paraformaldehyde). Kinoshita et al studied the localisation of APP and BACE1 on the cell surface and in the endocytic pathway, by labelling the two with antibodies against their extracellular regions at 4°C and allowing cells to undergo endocytosis at 37°C for varying intervals (Kinoshita et al, 2003). Their results showed that at 0 minute, APP and BACE1 were found co-localised in nearly identical clusters on the cell surface. At 15-30 minutes, complete co-localisation of the two signals was detected in the endosomes. By the time 60 minutes, distinct localisation of BACE1 and APP was identified, with most of APP having moved to the lysosomes.

5.1.2.2 An immunoblotting approach to detect BACE1 in a given sample of tissue homogenate or cell extract subjected to subcellular fractionation and compare with different subcellular compartment markers

Subcellular fractionation is one of the most commonly used methods for localisation assessment or protein enrichment. This technique provides a flexible tool to detect the abundance and the dynamic movements of proteins from tissues or cells at the organelle level.

Mild homogenisation of tissues or cells is carried out as the first step to disrupt the capture of organelles and release them. The cytoplasmic structure and cytoskeletal organisation vary enormously between different cell lines and tissues, indicating that to keep compartments separate but intact, homogenisation conditions need to be optimised for samples of different origins. To keep the organelles as intact as possible, cold temperature (normally 4°C) is essential, and homogenising buffer is also a key factor, which basically contains: sucrose, for high osmolarity, specific ions ($CaCl_2$, $MgAc_2$) for stabilisation and mixture of protease inhibitors to protect protein constitutes from degradation.

As soon as the homogenates are ready, they immediately undergo high resolution separation of multiple subcellular organelles by ultra-centrifugation through a density gradient. Distinctively charged particles move towards their equal densities of medium, which is known as the isopycnic point. Commonly used fractionation media include sucrose, Ficoll 400, Percoll, metrizamide, Nycodenz and iodixanol. The centrifugation is carried out in swinging bucket rotors with least disturbance. And post-fractionated gradients will be collected sequentially and used to identify certain targeted proteins by co-immunoblotting with known organelle makers. Subcellular compartment markers used in this chapter are summarised in Figure 5.3.

Using subcellular fractionation to confirm the localisation of BACE1 is widely applied. In chapter 3, using sucrose gradient subcellular fractionation, I showed that in GPR50 and BACE1 co-transfected HEK293 cells, most of BACE1 was distributed in fractions containing the plasma membrane and the lysosomes; while in adult mouse brain, endogenous Bace1 was mostly present in fractions containing ER-Golgi, synaptosomes, and presynaptic fractions. Shi and colleagues observed altered localisation of BACE1 in subcellular compartments upon overexpression of RTN3,

by performing sucrose gradient centrifugation to HEK293 cells. In control cells, most of BACE1 was localised in the Golgi and a smaller portion in the early endosomes; whilst in RTN3 stably-expressed cells, the majority of BACE1 was detected in the ER fractions with only a low amount of BACE1 in the Golgi fractions (Shi et al, 2009). It is believed that retaining BACE1 in the ER is the mechanism that accounts for the inhibition of BACE1 activity by RTN3 and reduced deposition of Aβ was observed in the brain of Tg-APPsw/PSEN1DE9 mice when crossed with Tg-RTN3 mice.

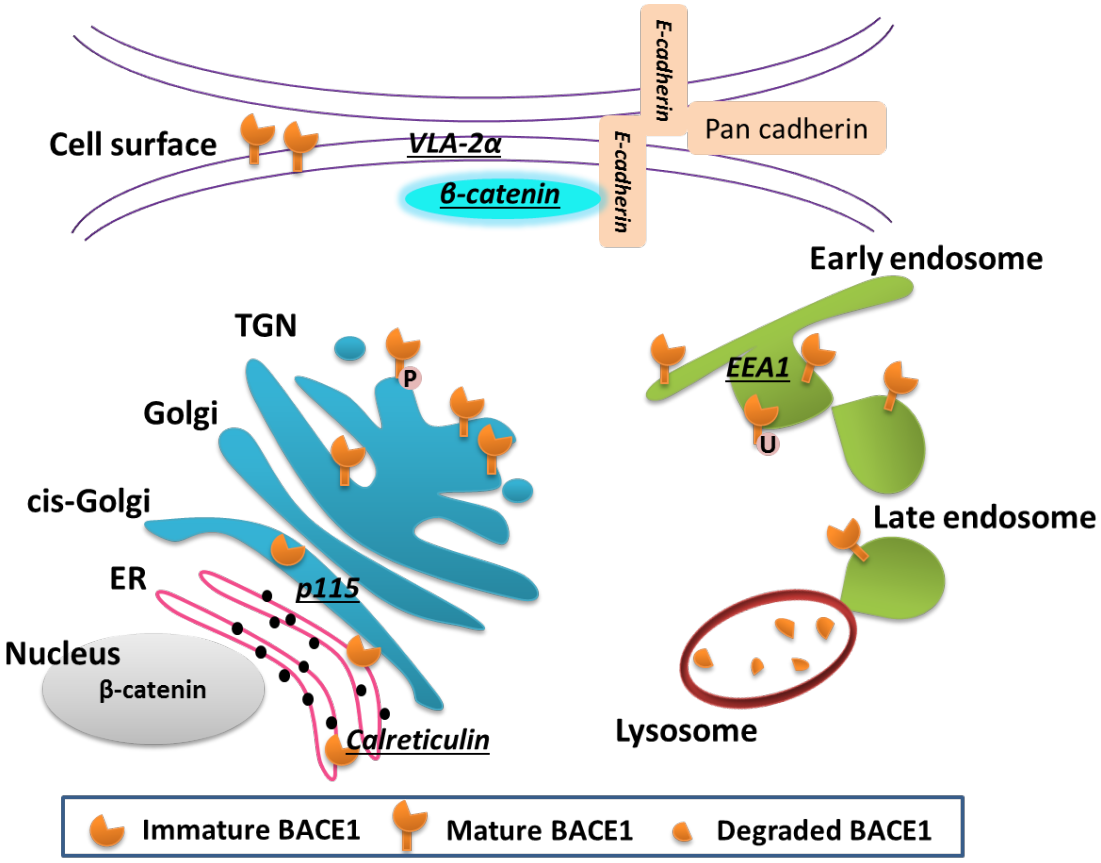

Figure 5.3 Subcellular fractionation markers used in this chapter. The markers are shown in italics and underlined.

5.1.2.3 A biochemical approach based on the covalent bonding of cell surface proteins with biotin, taking advantage of the strong interaction between biotin and streptavidin for the purification of biotinylated proteins

In most cases, the membrane proteins are biotinylated on amino acid residues located in extracellular domains and subsequently enriched using magnetic streptavidin beads. Then the captured proteins are released from the beads and detected by specific antibodies for targeted members. This method is applied by some researchers for investigating BACE1 trafficking and internalisation, exploiting the

long ectodomain of this protein. For example, the cell surface protein biotinylation assay employed by Zhao et al showed that the endocytosis of BACE1 under normal conditions occurred at about 15 min after chasing began, whereas in cells with SNX12 down-regulation, an observable endocytosis of BACE1 was detected early at 5 min after chasing, suggesting that reduced amount of SNX12 can accelerate the endocytosis of BACE1 (Zhao et al, 2012).

5.1.3 Introduction to experiments

In chapter 2, it was shown that the GPR50 is capable of decreasing mature BACE1 protein level in HEK293 cells. However, this observation cannot explain why overexpressed GPR50 up-regulates BACE1 activity (Grünewald, 2011). In order to find out more about the mechanism of BACE1 activity regulation by GPR50, further investigations were carried out with a focus on the effect on BACE1 trafficking in this chapter. By use of immunocytochemistry and cell surface labelling techniques, the proportion of BACE1 located on the cell surface was analysed, and the impact of GPR50 expression was assessed. Next, subcellular fractionation was performed in HEK293 cells and primary cortical neurons in which the regulation of β-secretase activity by GPR50/GPR50del has been observed {(Grünewald, 2011); my chapter 4}. The localisation of both immature and mature BACE1 was tested for correlation with subcellular compartment markers, and any quantifiable shift was assessed.

5.2 Materials and methods

For tissue culture, transfection, immunocytochemistry, western blotting, cell surface labelling and real-time quantitative PCR, see 2.2.1-2.2.8 for detail. The following paragraphs describe additional techniques that were used for experiments in this chapter.

5.2.1 Antibodies

The primary antibodies used in this chapter and their application conditions are summarised in Table 5.2. The full information for these antibodies can be found in 2.2.5. The working conditions of secondary antibodies used in immunocytochemistry and western blotting have been introduced in Table 2.3 and Table 2.4.

Table 5.2 Primary antibodies used in chapter 5

Antibody	Host	Immunogen	Application in this chapter
GPR50 rabbit	Rabbit polyclonal	Residues 294-317 of human GPR50	ICC (1:200) WB (1:1000)
BACE1 rabbit2	Rabbit polyclonal	Residues 485-501 of human BACE1	ICC (1:5000) WB (1:10,000)
BACE1 goat	Goat polyclonal	Residues 22-460 of human BACE1	ICC (cell surface labelling, 1:200)
VLA-2α	Mouse monoclonal	Residues 42-245 of human VLA-2α	WB (1: 1000)
β-catenin	Rabbit polyclonal	Residues surrounding Pro714 of human β-catenin	WB (1:5000)
EEA1 mouse2	Mouse monoclonal	Residues 3-281 of human EEA1	WB (1: 5000)
P115	Mouse monoclonal	Residues 843-955 of rat p115	WB (1: 500)
Calreticulin rabbit	Rabbit polyclonal	Full length human calreticulin	WB (1:10,000)
GAPDH	Mouse monoclonal	Recombinant GAPDH	WB (1: 40,000)

5.2.2 Sucrose density gradient fractionation

The technique of sucrose density gradient fractionation used in HEK293 cells was described in 3.2.4.1. The usage of this method in primary neuronal cultures was introduced as follows.

Primary cortical neurons from E18 embryos of C57BL/6 mice were cultured for 3 days (DIV3) in a 6-well plate coated with poly-D-lysine. As neuronal cells do not divide after being plated, it is essential to count the cell number correctly and place enough cells to the plates. For one well of a 6-well plate, 5×10^6 cells were counted by a cell counter and plated to guarantee an optimal cell viability for transfection. For cultured neurons, the transient transfection of the three plasmids (pDEST40, GPR50 and GPR50del) using Lipofectamine 2000 (see 2.2.4) was verified by qPCR, due to relatively low transfection efficiency; while for HEK293 cells there was a much higher cell input and high transfection efficiency, western blotting was performed to confirm successful transfection. The cultured cells were left overnight post-transfection before being scraped into sucrose buffer. The lysates were homogenised with a 23 gauge needle, followed by incubation on ice for 20 min. The homogenates were loaded onto the top of a discontinuous sucrose gradient and then centrifuged at 10,000×g (22,000 rpm, SW41 Ti Beckman) for 18 hr at 4^{o}C (see 3.2.4.1 for detail). Twelve fractions were collected from the top, followed by methanol-chloroform precipitation.

Both HEK293 cells and primary cortical neurons express quantifiable mature and immature BACE1/Bace1. EEA1, VLA-2α and calreticulin were ready to use as subcellular markers for the early endosomes, the plasma membrane and the ER in HEK293, as was shown in chapter 3 (Figure 3.12). However, EEA1 and VLA-2α failed to work in primary cortical neurons. To replace these two markers for compartments known to hold mature BACE1, β-catenin was used for external compartments and p115 as cis-Golgi marker (Dejgaard et al, 2007; Park et al, 2008). Strictly speaking, β-catenin is not a "marker", because there is also a "free pool" located in the nucleus (normally in the heaviest fractions), where it acts as a transcription co-activator (Orsulic et al, 1999). However, this is only a small proportion of β-catenin, with the majority pool bundled to E-cadherin in the plasma membrane (Du et al, 2009). There are also reports about β-catenin being located in caveolae by interacting with caveolin-1 (Galbiati et al, 2000). Hence, for primary neuronal cells in this experiment, β-catenin was employed as an alternative to VLA-2α in HEK293 cells as the external compartment marker.

In order to measure the distribution of BACE1/Bace1 and the subcellular markers, the amount of immunostained protein in each fraction was quantified by densitometry with ImageJ. The percentage of the proteins in each fraction from 1 to 12 was calculated to reflect their distribution.

5.2.3 Fitting of the general linear model with the interaction term

Data from three biological replicates of the subcellular fractionation was pooled for each of the three independent groups: pDEST40-transfected cells (empty vector control, abbreviated as p40 in the following passages), GPR50-transfected cells and GPR50del-transfected cells. Thus, there are 36 data points (3×12 fractions) for each of the three groups. Distribution (percentage in one fraction out of all fractions) of BACE1/Bace1 was predicted by correlating with that of the markers under the 3 conditions using the general linear model, and the fitness of the prediction was compared.

Asking if a predictor has different regression weights for different groups is equivalent to asking if there is an interaction between this predictor (i.e. β-catenin) and group membership (i.e. p40 group V.S. GPR50 group). Specifically, by incorporating a dummy variable for group membership and an interaction term for group membership with an independent variable, one can better identify what effects,

if any, differ across groups. This can be achieved through the general linear model with an interaction term included in SPSS. The general equation is:

Candidate = a+ b_1 group + b_2 predictor + b_3 (group×predictor)

If b_3 is significant, then there is a difference between the predictor regression weights of the two groups. However, in terms of multiple predictors, this approach may get over complicated. With three predictors, each interaction term is designed to tell us if a particular predictor has a regression slope difference across the groups. The equation evolves into:

Candidate = a+ b_1 G + b_2 P_1+ b_3 (G×P_1) + b_4 P_2 + b_5 (G×P_2) + b_6 P_3 + b_7 (G×P_3)
G=group, P=predictor.

Because the collinearity among the predictors, the collinearity among interaction terms, as well as the collinearity between a predictor's term and other predictors' interaction terms all influence the weight of a single interaction term, there has been dissatisfaction with how efficiently this method works for multiple predictors. Thus, in the following analysis, single general linear models will be applied.

An example will be illustrated by using β-catenin to predict mature Bace1 (mBace1) in groups p40 and GPR50.

mBace1= a+ b_1 condition + b_2 β-catenin + b_3 condition×β-catenin

The "condition" here is a categorical variable that represents different groups, such as the two-category variable (p40, GPR50). A dummy variable can sort data into mutually exclusive categories by taking the value 0 or 1, such as (p40=1, GPR50=0). By including the interaction term of a dummy variable with an independent variable (such as β-catenin), it is able to indicate whether the absence or presence of one category (such as group GPR50) will shift the outcome of the predicted model; in other words, this tests whether there is a difference between categories in the model prediction of a dependent variable (such as mBace1) by an independent variable (such as β-catenin).

SPSS refers the group that is coded as 1 to the dummy, whose values are set to 0. And the rest of the group(s) will be coded as 0, whose values are kept. In the example introduced here, a dummy variable labelled with "p40ref_GPR50com" is coded as p40=1 (reference group, p40ref_GPR50com=0), GPR50=0 (comparison

group, p40ref_GPR50com=1). To better understand the coefficients, the main SPSS outputs of this model are listed in Table 5.3. The summary of this model is shown in Table 5.4. In the result section, only the summary tables will be presented.

Table 5.3 The main SPSS outputs of the general linear model:

mBace1= a+ b_1 p40ref_GPR50com + b_2 β-catenin + b_3 p40ref_GPR50com×β-catenin

Between-Subjects Factors

		N
Dummy	.00	36
	1.00	36

Tests of Between-Subjects Effects

Dependent Variable:mBace1

Source	Type III Sum of Squares	df	Mean Square	F	Sig.	Partial Eta Squared
Corrected Model	4996.024[a]	3	1665.341	28.561	.000	.558
Intercept	26.980	1	26.980	.463	.499	.007
p40ref_GPR50com	72.106	1	72.106	1.237	.270	.018
β-catenin	4635.379	1	4635.379	79.498	.000	.539
p40ref_GPR50com × β-catenin	154.730	1	154.730	2.654	.108	.038
Error	3964.958	68	58.308			
Total	13960.982	72				
Corrected Total	8960.982	71				

a. R Squared = .558 (Adjusted R Squared = .538)

Parameter Estimates

Dependent Variable:mBace1

Parameter	B	Std. Error	t	Sig.	95% Confidence Interval	
					Lower Bound	Upper Bound
Intercept	-.532	1.703	-.312	.756	-3.929	2.866
p40ref_GPR50com=.00	2.739	2.463	1.112	.270	-2.176	7.654
p40ref_GPR50com=1.00	0[a]	.	.	.	.	.
β-catenin	1.064	.136	7.838	.000	.793	1.335
p40ref_GPR50com=.00× β-catenin	-.329	.202	-1.629	.108	-.731	.074
p40ref_GPR50com=1.00× β-catenin	0[a]	.	.	.	.	.

a. This parameter is set to zero because it is redundant.

According to the parameter estimates in Table 5.3, the predicted model is: mBace1=-0.532+2.739 p40ref_GPR50com+1.064 β-catenin-0.329 p40ref_GPR50com×β-catenin.

When p40ref_GPR50com=0, mBace1=-0.532+1.064 β-catenin.

When p40ref_GPR50com=1, mBace1=-0.532+2.739+1.064 β-catenin-0.329 β-catenin

Thus, for p40 group, the intercept is -0.532 and the slope is 1.064; for GPR50 group, the intercept is -0.532+2.739 and the slope is 1.064-0.329. SPSS calculates the significance of differences in intercepts (+2.739) and slopes (-0.329) that occur in the two groups. These two parameters reflect the basic levels of the dependent variable and the effect size of a predictor respectively.

Table 5.4 A summary of the general linear model for the example: mBace1=-0.532+2.739 p40ref_GPR50com+ 1.064 β-catenin-0.329 p40ref_GPR50com×β-catenin

a. Adjusted r^2=0.538	**F**	**P-value**	**Partial Eta Squared**
Corrected model [a]	28.561	**4.6×10^{-12}****	0.558
p40ref_GPR50com	1.237	**0.270**	0.018
β-catenin	79.498	**4.8×10^{-13}****	0.539
p40ref_GPR50com × β-catenin	2.654	**0.108**	0.038
Predicted slopes	**P40: 1.064; GPR50: 0.735**		

**** p<0.01**

5.3 Results

5.3.1 The relation between endogenous GPR50 and cell-surface BACE1

In chapter 3, I showed that, in HEK293 cells, endogenous GPR50 was co-localised with endogenous cell surface BACE1. It was also seen that, in a group of cells, there were more cells singly labelled with GPR50 or surface BACE1 than cells that expressed both of them. Here I wanted to investigate whether the expression of GPR50 reduced the amount of BACE1 at the cell surface.

5.3.1.1 Intensity correlation analysis of staining patterns of endogenous GPR50, cell surface BACE1 and total BACE1 in HEK293 cells

As HEK293 cells grow in clumps and single cells seem not to survive the cell surface labelling at a low temperature, it is very difficult to statistically quantify the

relationship between GPR50 and surface BACE1 in single cells. Thus, the intensity correlation analysis of co-localisation between the two proteins in a group of cells was carried out.

It was mentioned in chapter 3 that intensity correlation analysis (ICA) plot of correlated staining generates an hourglass figure with a positive skew, while that of segregated staining yields one with a negative skew (see 3.2.3). The values for Pearson's correlation coefficient (Rr) range from 1 to -1. A value close to 1 indicates reliable correlation, while negative values and those close to zero can be resulted from mixed patterns. Mander's overlap coefficients (R, M1, and M2) are adopted to explain the identical location of the two intensity sets. Finally, intensity correlation quotient (ICQ) is used to identify whether the staining intensities are associated in a random (ICQ~=0), dependent (0 <ICQ ≤0.5) or segregated (0>ICQ≥ -0.5) manner. Nonparametric sign test is carried out to judge whether the median of differences between two sets of intensity values equals 0 (ICQ=0) (Li et al, 2004).

In a group of cells, ICA plots for GPR50 and surface BACE1 (Figure 5.4.A) exhibited a random staining (mixed with dependent and segregated manners) with a slightly negative skew. This pattern indicates that GPR50 and surface BACE1 tended to localise in different cells in this group. The Pearson's correlation coefficient (Rr=0.08, Table 5.5.A) supported the hypothesis that these two proteins had very low correlation. However, Mander's overlap coefficient (R=0.432) demonstrated that there were cell parts retained with both GPR50 and surface BACE1. 68.4% of pixel intensities in GPR50 channel matched those in surface BACE1 channel, while 16.6% in the latter matched with those in the former. The ICQ value revealed a significant positive correlation between the two, but the possibility cannot be ruled out that GPR50 and surface BACE1 from two adjacent cells might come into contact at the indivisible conjunction sites of the cells, and this is the main concern when investigating co-localisation in a clump of cells.

With respect to GPR50 and total BACE1 in this group of cells (Figure 5.4.B, Table 5.5.B), it was shown that the staining of GPR50 was likely to be dependent on that of total BACE1 (with ICA plot positively skewed), but there were pixels of GPR50 below the average value that segregated with their paired total BACE pixels. This was because there were some BACE1-expressing cells with no endogenous GPR50 and this resulted in a percentage of pixel pairs as {GPR50=0, total BACE1=Y}.

Correspondingly, the staining of total BACE1 somehow depended on that of GPR50, but a part of the above average pixels excluded with their GPR50 partners (again, these are {GPR50=0, total BACE1=Y}). This observation reflected an imbalance of the total pixel quantities and intensity strength between GPR50 and total BACE1, which was indeed the case with this group of cells. All GPR50 intensities matched those of total BACE1 (M1=1), while only 32.1% of the latter matched with the former. The significant positive ICQ (0.029) indicated very low co-localisation, largely due to the fact that the amount of total BACE1 outweighed that of GPR50 in cell groups.

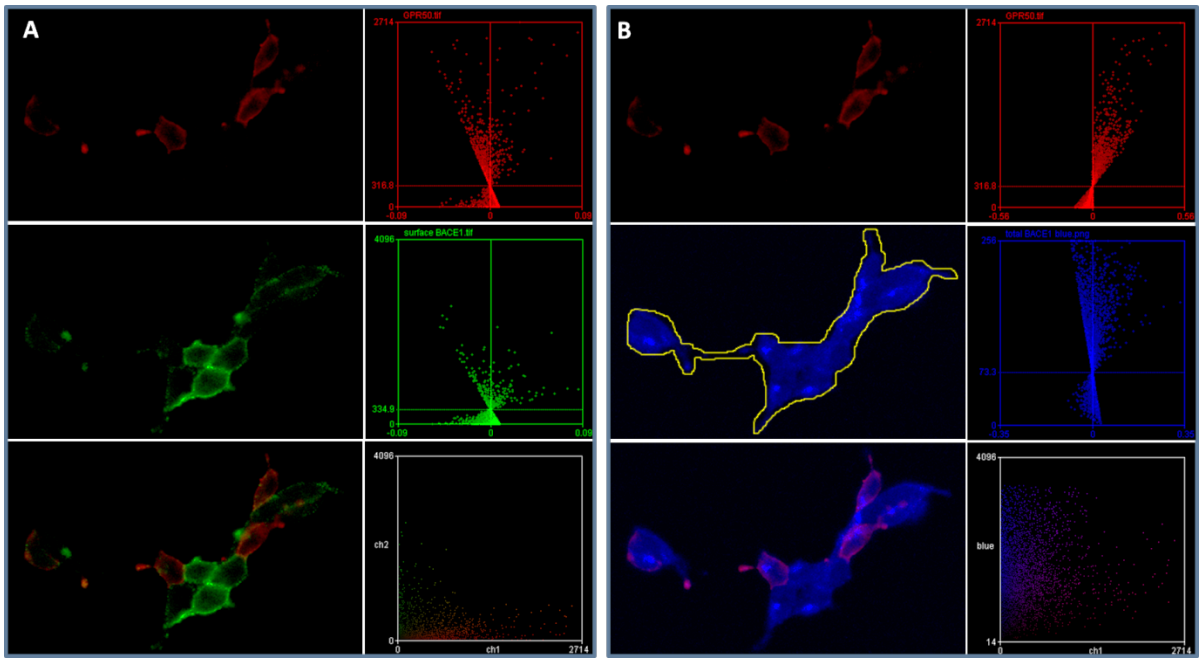

Figure 5.4 Intensity correlation analysis of GPR50 with surface BACE1 or total BACE1 in a cluster of cells. A) GPR50 (red) and surface BACE1 (green); B) GPR50 (red) and total BACE1 (blue), represented by their split ICA plots and scatter-plot of intensities. The yellow shut line indicated region of interest (ROI) that was analysed.

Table 5.5 ICA parameters for co-localisation analysis of GPR50 with surface BACE1 or total BACE1. A) GPR50 and surface BACE1; B) GPR50 and total BACE1 in a cluster of cells

Co-localisation parameters	Rr	R	ch1:ch2	M1	M2	ICQ	P-value
A)GPR50 V.S. surface BACE1	0.08	0.432	0.515	0.684	0.166	0.104	<0.05
B)GPR50 V.S. total BACE1	0.046	0.622	0.05	1	0.321	0.029	<0.05

In conclusion, the correlation between paired pixel intensities of GPR50 and cell surface BACE1 in a cell group was very weak. Even though there were overlapping pixels in the two channels, the staining pattern of GPR50 and cell surface BACE1 in a cell group was not dependent. However, in a single cell expressed with both

GPR50 and cell surface BACE1, their staining patterns were significantly dependant (see chapter 3, Figure 3.11). Thus, the correlation of the two proteins' staining in a cell group was largely averaged by their exclusive expression pattern.

5.3.1.2 Intensity Profiles of endogenous GPR50, cell surface BACE1 and total BACE1 in HEK293 cells

To better address the observation that GPR50 and surface BACE1 seem to not co-localise in a group of cells, intensity profiles were generated cell by cell (Figure 5.5), and the cell-cell adhesion sites were avoided when plot lines were drawn across the cells. The red and green profiles for GPR50 and cell surface BACE1 normally had two peaks at both ends, indicating the sites of the plasma membrane on the two sides of cells. The blue profile for total BACE1 included continuous contents in the middle, which reflects that BACE1 was also expressed in the intracellular organelles, presumably in the Golgi, the early endosomes and the late endosomes or cytosolic sites (see chapter 2, Figure 2.10). It was confirmed that in this group, cells expressed with endogenous GPR50 tended to have no or very little surface BACE1 (cells 3 and 8), and vice versa (cells 2, 4, 5, 6 and 9). Cells 1 and 7 had peaks of red and green at the same position (indicated by an open arrow), so they were potential cells that might show co-localisation of GPR50 and cell surface BACE1. Yet, even in these two cells, there were high levels of GPR50, but low levels of surface BACE1. Thus, in a group of cells, GPR50 and cell surface BACE1 appeared to localise in an exclusive manner. A possible explanation for this observation is that in cells endogenously expressed with GPR50, more BACE1 was internalised from the cell surface.

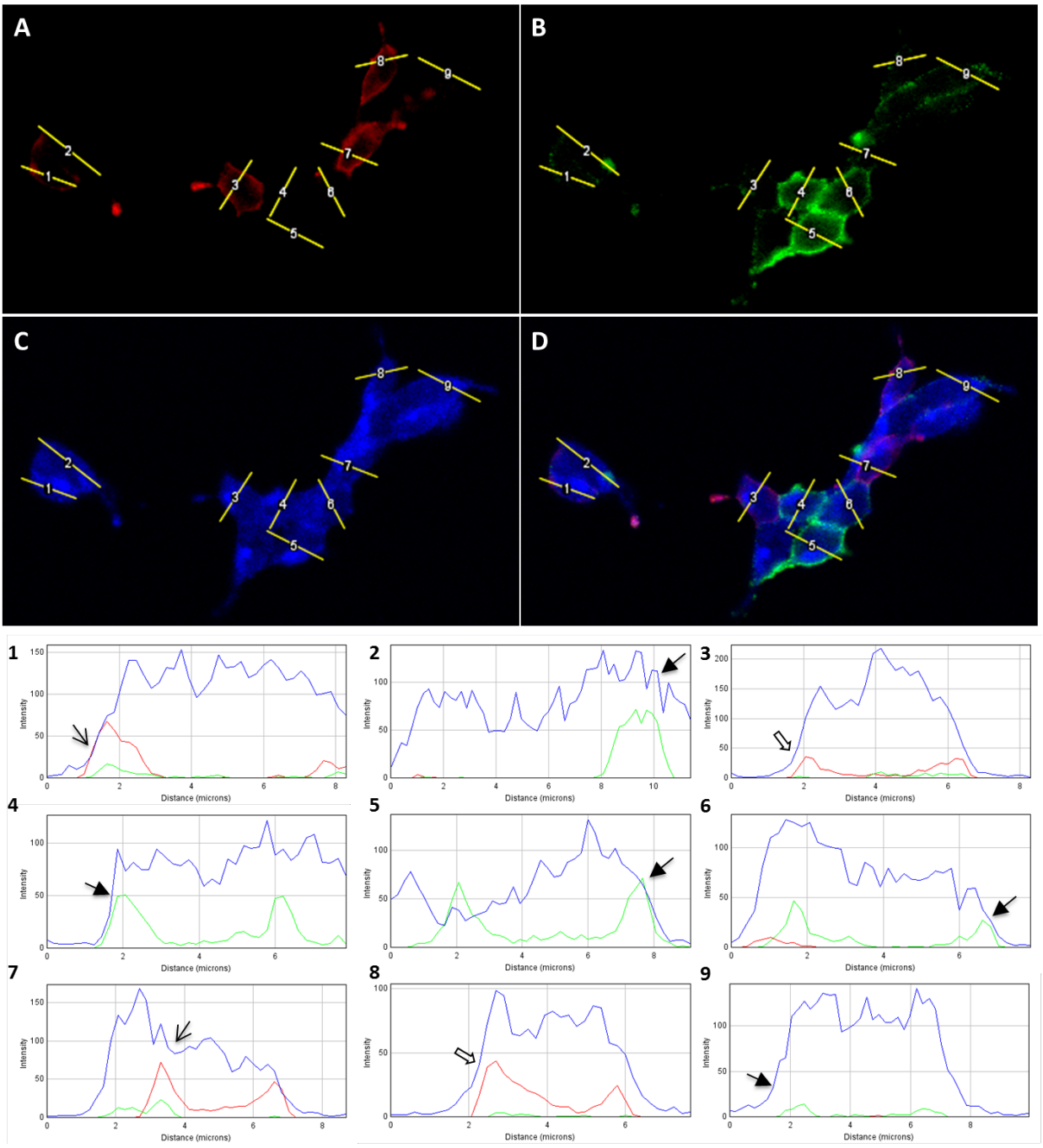

Relation between GPR50 and surface BACE1	Cell number	Symbol in the figure
GPR50 with little or no surface BACE1	3,8	⇨
Surface BACE1 with little or no GPR50	2,4,5,6,9	→
Potential co-localisation	1,7	→

Figure 5.5 Intensity profiles of GPR50, cell surface BACE1 and total BACE1 in HEK293 cells of a group. A) GPR50 (red); B) surface BACE1 (green); C) total BACE1 (blue); D) merged signal. 1-9: cell numbers labelled in pictures A-D.

5.3.1.3 Correlation of expression levels of GPR50 to the percentage of cell surface BACE1 in clustered HEK293 cells

Results by immunocytochemistry suggested that HEK293 cells endogenously expressing a high level of GPR50 tended to have a low level of BACE1 at the cell surface. To further investigate this, statistical analysis was performed to assess the relationship between the level of endogenous GPR50 and the percentage of cell surface BACE1 in groups of cells.

1) Cell number optimisation

The number of HEK293 cells cultured on the coverslips has a strong effect on the performance of the cell surface labelling technique. Therefore, the cell plating density was explored, initially by plating the normal number of cells into in a 12-well plate (Trial 1, 5×10^4 cells/coverslip, Table 5.6). The cells formed clusters due to the fast-growing nature of HEK293. Then, there were several attempts to keep HEK293 more scattered by reducing the cell number, but there was a strikingly increased degree of cell death as the cells were more diluted. The minimum number for the cells to survive the surface labelling was 1×10^4 cells/coverslip, in which only 20 photos were obtained due to poor cell viability. It was also noticed that the decreasing cell number led to more dead cells, and this did not prevent the remaining cells from forming clusters. Therefore, there were a minimum number of cells needed to guarantee a healthy pool of cells, and to allow successful cell surface labelling and the possibility of running a statistical analysis. Finally, the ideal cell number was confirmed (Optimised, Table 5.6), which was 2×10^4 cells/coverslip.

2) Statistical analysis

The area with GPR50 expression (red channel, GPR50Area) was calculated, indicating its expression level in each cell cluster. The area of cell surface BACE1 (green channel) divided by that of total BACE1 (blue channel) was computed as the proportion of BACE1 located at cell surface (BACE1Sur.Per). The areas with protein expression were masked according to the given values of threshold automatically calculated by ImageJ. The calculation of the masked areas was run through the measurement command in a batch to avoid bias.

Firstly, Pearson's correlation analysis was run to analyse the relationship between GPR50Area and BACE1Sur.Per. There was a significant negative correlation between the two proteins only under the optimised condition (Table 5.6). This means that there is a small percentage of endogenous BACE1 located at the plasma membrane in cells expressed with endogenous GPR50, which supports the ICA results from the images and might indicate that endogenous GPR50 facilitates BACE1 internalisation. Further statistical analysis was performed on data obtained under the optimised condition.

Table 5.6 Pearson's correlation between GPR50 expression level and cell surface BACE1 proportion

Correlations		GPR50Area		
		Trial 1	Trial 2	Optimised
BACE1Sur.Per	Starting cell number	5×10^4	1×10^4	2×10^4
	Cluster number	50	20	50
	Cell number in a cluster	20-127	1-14	3-30
	Pearson Correlation	-.072	.173	-.470
	Sig. (2-tailed)	.620	.465	.001**

**. Correlation is significant at the 0.01 level (2-tailed).

GPR50Area: the area with GPR50 expression in each cell group

BACE1Sur.Per: the percentage of cell surface BACE1 as a fraction of total BACE1 in each cell group

It was noticed that even in the optimised experiment, the cell number in a cluster was not stable, ranging from 3 to 30. Thus, I tested whether cell number was one of the factors affecting BACE1Sur.Per (Figure 5.6). It was found that the more cells there were in a cluster, the higher the expression level of endogenous GPR50 was. Surprisingly, there was a significant decrease of BACE1 proportion at the cell surface with the cell number increasing. In order to find out if the negative effect of GPR50Area on BACE1Sur.Per could be attributed to the increasing cell number, a general linear model was run including 3 predictors: cell number, GPR50Area, and cell number×GPR50Area. As is shown in Table 5.7, both cell number and GPR50Area had significant negative effects on BACE1Sur.Per, while cell number×GPR50Area contributed a small positive trend. This indicates that the more cells there were in a cluster, the more likely the cell number and GPR50 expression level had a combined impact on BACE1 proportion located at cell surface. The equation of the model is: BACE1Sur.Per=17.689-0.647 CellNumber-0.110 GPR50Area+0.006 CellNumber×GPR50Area. Thus, endogenous GPR50 does have

an effect on the percentage of endogenous BACE1 localised at the surface of HEK293 cells, even after accounting for the effect of the cell number.

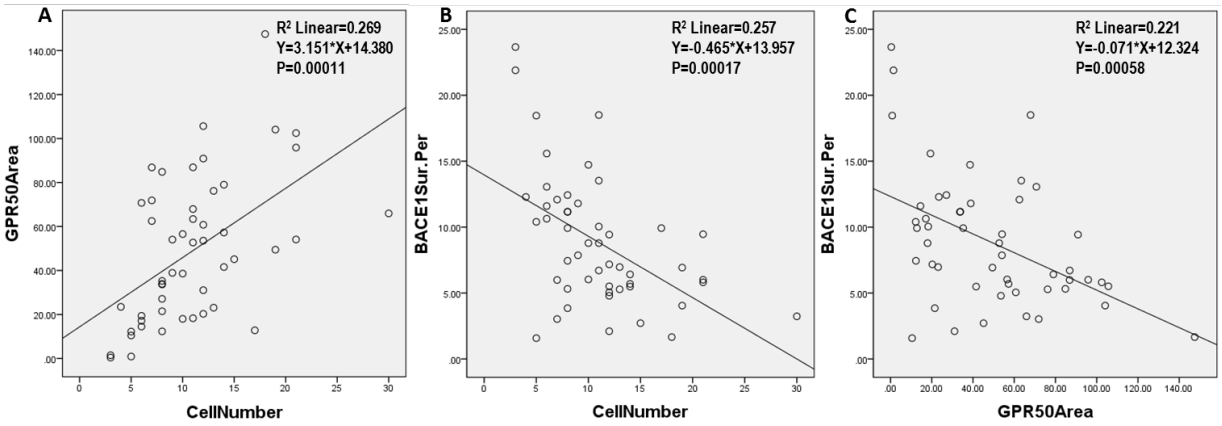

Figure 5.6 Scatter plots for GPR50 expression level, cell surface BACE1 proportion and cell number. A) GPR50Area~ CellNumber, B) BACE1Sur.Per~ CellNumber and C) BACE1Sur.Per~ GPR50Area under optimised condition

Table 5.7 Predication of the general linear model for cell surface BACE1 proportion
BACE1Sur.Per=a+b× CellNumber+c× GPR50Area+d× CellNumber ×GPR50Area

	F	P-value	B
Corrected model [a]	8.534	**0.00013****	
Cell number	8.514	**0.005****	**-0.647**
GPR50	6.293	**0.016***	**-0.110**
Cell number× GPR50	3.035	**0.088**[$]	**0.006**
a. Adjusted r^2=0.316 ** p<0.01, *p<0.05, [$]p<0.1,			

This result suggests a possibility that GPR50 may affect BACE1 trafficking. However, I am aware that this is an incomplete experiment, due to lack of proper replicates. Therefore, none of these data can be drawn into a conclusion without further investigation.

5.3.2 The effect of exogenous GPR50 on the subcellular localisation of endogenous BACE1

It was analysed in 5.3.1 that GPR50 is possibly playing a role in the sorting system of BACE1. This hypothesis was further investigated by looking at the distribution of BACE1 in different organelles with or without the overexpression of GPR50 or GPR50del. The same amount and volume of empty vector pDEST40 was transfected as control. Three identical replicates were performed for both cell types: HEK293

and primary cortical neurons, in which endogenous levels of β-secretase activity were found (Kao et al, 2004; Lefranc-Jullien et al, 2005). The percentage of BACE1 in different subcellular compartments was predicted by that of subcellular markers and was compared between different conditions in pair (p40 VS GPR50; p40 VS GPR50del; GPR50 VS GPR50del).

5.3.2.1 The subcellular fractionation of endogenous BACE1/Bace1 and subcellular compartment markers

Mature BACE1 (mBACE1, 65 kDa) in HEK293 cells was detected in bottom fractions, and sometimes there were two bands, which might be different intermediate forms of BACE1 in the process of secondary modifications (Figure 5.7.A). These doublets were quantified together as mature BACE1, and they were mainly co-fractionated with the plasma membrane marker VLA-2α and the ER marker calreticulin (Figure 5.8). Immature BACE1 (imBACE1, 55 kDa) were found in lighter fractions that contained the early endosomes and the microsomes (fragmented ER).

Endogenous Bace1 detected in the primary cortical neurons (E18, DIV3) is identical to that observed in E18 mouse brain (see chapter 2) (Figure 5.7.B). The majority of Bace1 in cultured neurons was mature Bace1 (mBace1), at around 65 kDa and appeared highly glycosylated. It was generally located across all the fractions, but was enriched in middle fractions, where β-catenin was found (Figure 5.9). The 55 kDa immature Bace1 (imBace1) was mainly dispersed in heavier fractions, which were dominated by the ER marker calreticulin.

It is interesting that BACE1 in HEK293 cells and Bace1 in neurons seemed to be localised at different ends of the fractions. This indicates that the allocation of mature β-secretase/immature β-secretase among light membranes and heavy membranes is not identical in the two cell types, which might result in different trafficking systems of BACE1/Bace1, distinct distribution of β-secretase activity and diversified substrate cleavage.

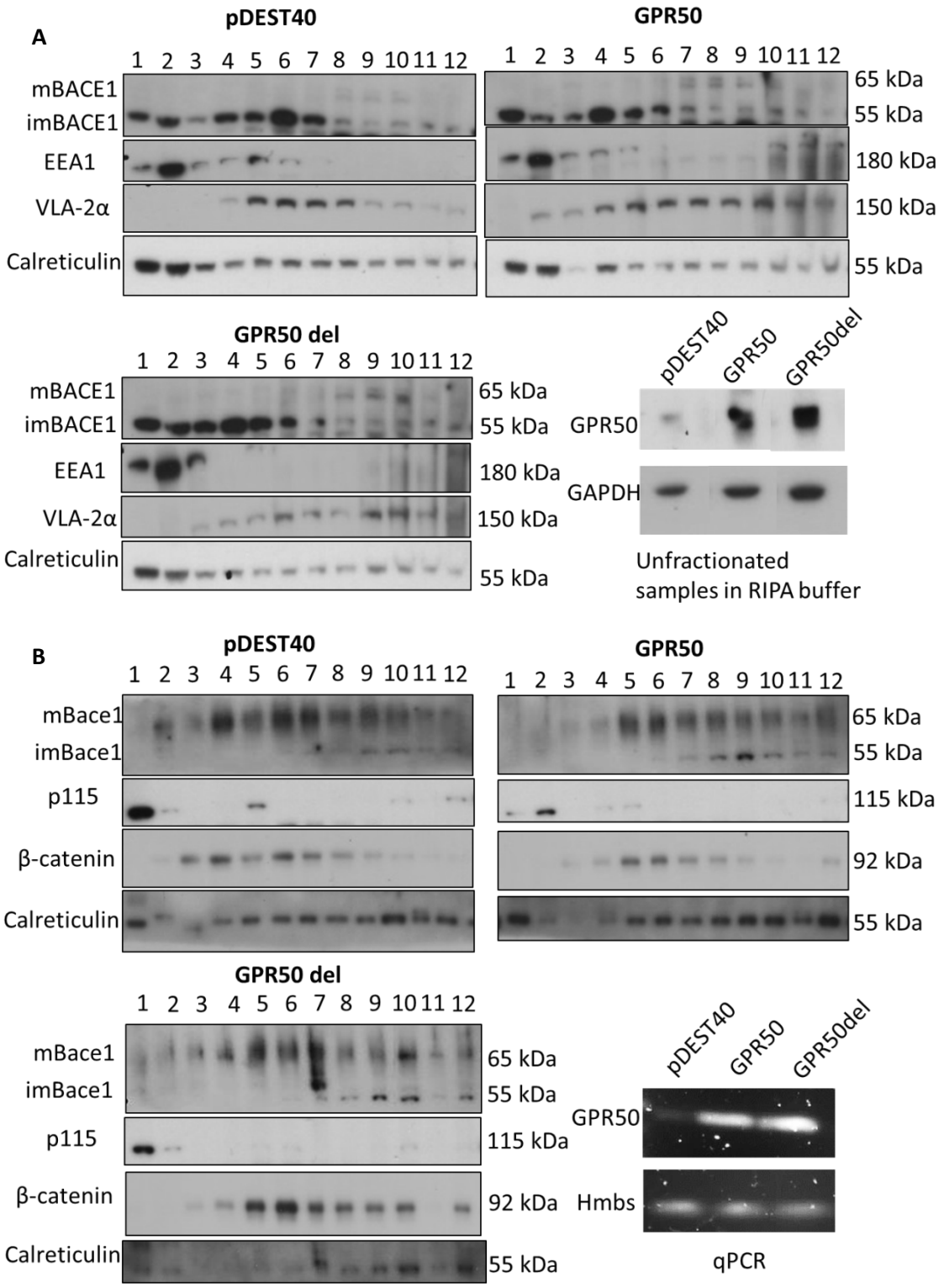

Figure 5.7 Subcellular fractionation of cell lysates transfected with pDEST40, GPR50 or GPR50del in A) HEK293 cells; B) primary cortical neurons. Subcellular compartment markers: VLA-2α for plasma membrane, EEA1 for early endosomes, calreticulin for ER, β-catenin for external organelles and p115 for cis-Golgi. For HEK293 cells, western blotting was performed to confirm that the plasmids were successfully transfected and expressed. For primary cortical neurons, qPCR was performed to confirm that GPR50 and GPR50del were overexpressed.

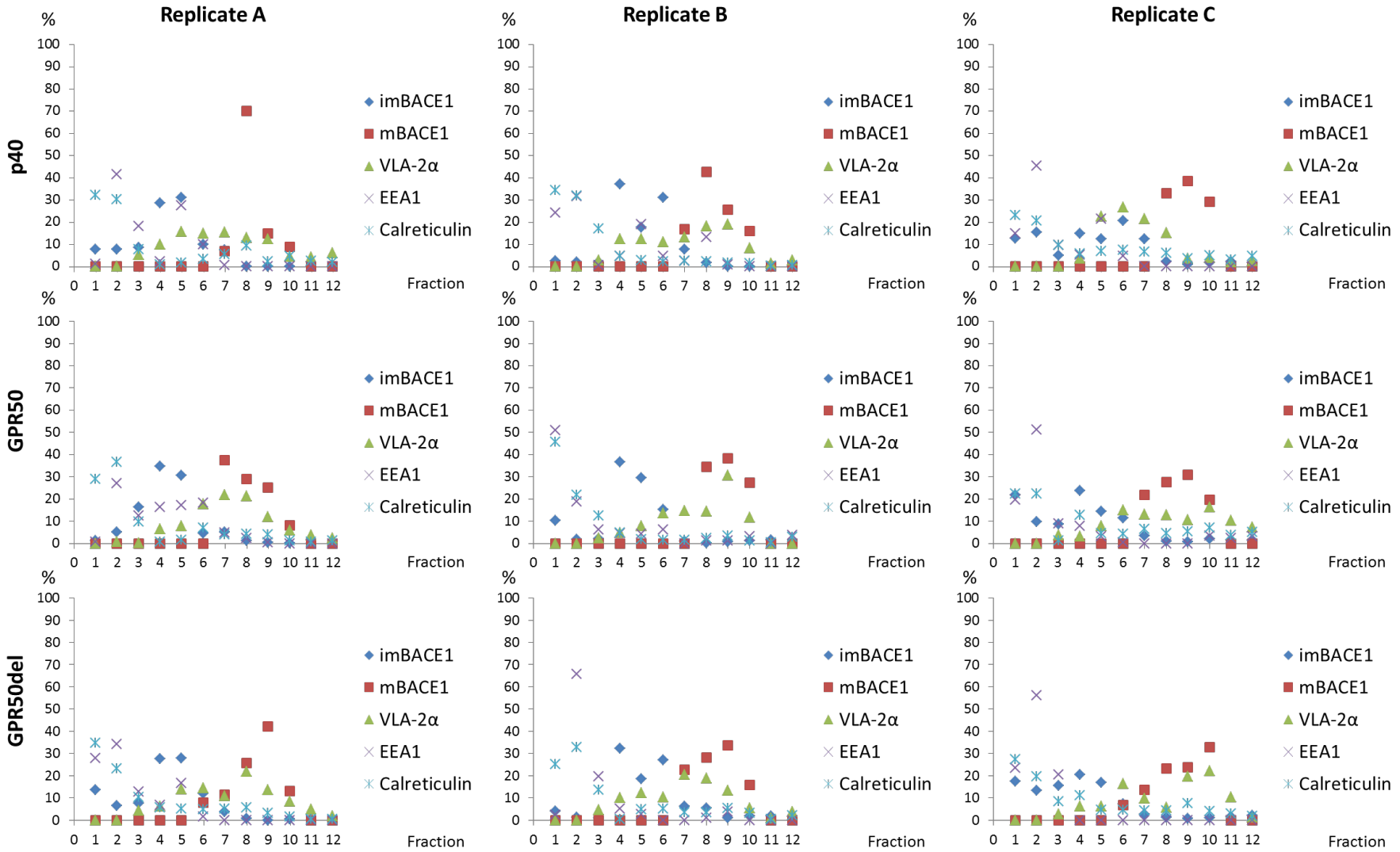

Figure 5.8 The distribution proportion of immature BACE1, mature BACE1, VLA-2α, EEA1 and calreticulin in each sucrose fraction in HEK293 cells. ImBACE1: immature BACE1; mBACE1: mature BACE1.

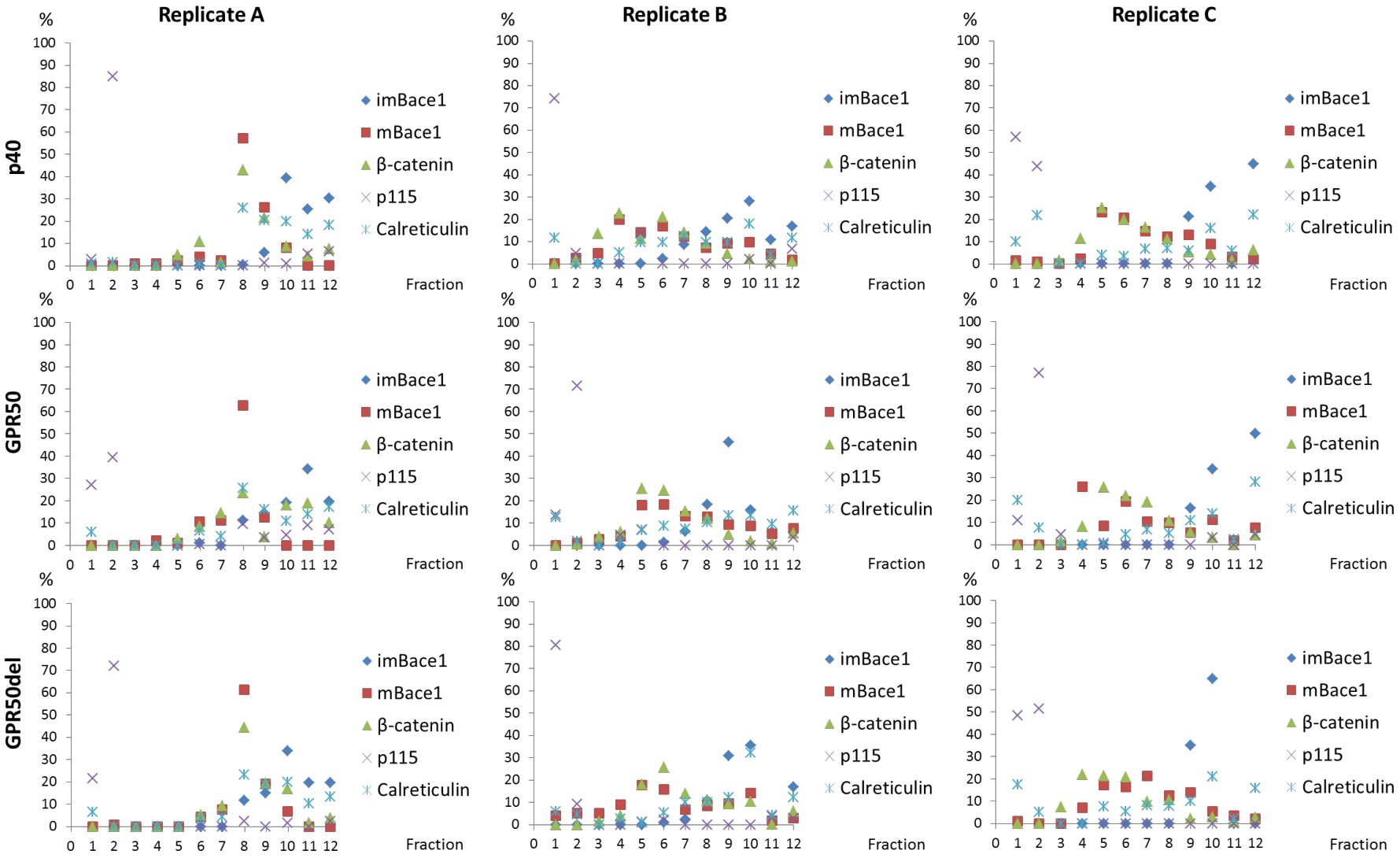

Figure 5.9 The distribution proportion of immature Bace1, mature Bace1, β-catenin, p115 and calreticulin in each sucrose fraction in mouse primary cortical neurons. ImBace1: immature Bace1; mBace1: mature Bace1.

To answer the question whether GPR50/GPR50del are involved in BACE1/Bace1 trafficking, statistical analysis were applied by correlating the percentages of BACE1/Bace1 to those of different compartment markers under the conditions overexpressing GPR50/GPR50del, compared with the control condition p40.

5.3.2.2 Comparing interaction terms of the general linear models

The general equation of the general linear model was BACE1/Bace1 = a+ b×marker+c×dummy variable+d×dummy variable×marker. This model tested whether BACE1/Bace1 fractionated with a particular subcellular compartment and whether BACE1/Bace1 fractionation with a particular subcellular marker was changed by overexpressing GPR50 or GPR50del.

1) HEK293 cells

Predictors of general linear model for mBACE1/imBACE1 in HEK293 cells included subcellular markers for the early endosome, plasma membrane and ER (EEA1, VLA-2α and calreticulin), group membership (p40, GPR50, GPR50del transfected groups) and the interaction term (the products of subcellular markers and group membership). The test results of the fitted model for BACE1 in HEK293 cells are listed in Table 5.8-5.9. The observed significance or trend of significance of each predictor, together with the predicted effects for the interaction terms of significance or with a trend of significance are summarised in Table 5.10.

As GPR50 is able to increase BACE1 activity in HEK293 cells (Grünewald, 2011), it was hypothesised that GPR50 overexpression would facilitate the co-fractionation of mBACE1 with the plasma membrane or the early endosomes, the two putative sites for BACE1 activity. GPR50del does not have the same effect on BACE1 activity as GPR50, so a different influence between the two on BACE1 fractionation was expected.

According to the general linear model, in HEK293 cells, the percentage of mBACE1 distributed in the sucrose fractions were significantly correlated with all the three markers for the plasma membrane (positive), the early endosomes (negative) and the ER (negative). ImBACE1 distribution had a trend of association only with the early endosomes (positive) (Table 5.10). As mBACE1 has much higher activity than imBACE1 (Zhong et al, 2007), my results indicated that BACE1 activity mainly occurred in the plasma membrane.

Compared with the p40 control, the overexpression of either GPR50 or GPR50del resulted in a trend of more mBACE1 co-fractionated with VLA-2α (Table 5.10), suggesting a larger percentage of mBACE1 distributed at the plasma membrane. Yet, there was an opposite direction for imBACE1 only in GPR50 overexpressed cells, in which imBACE1 was less associated with the plasma membrane. Thus, GPR50 had an additional effect on imBACE1 distribution compared with GPR50del. There was no significant difference of BACE1 percentage in any compartment between groups GPR50 and GPR50del. However, the predicted slopes suggested that the ratio of mBACE1/imBACE1 associated with the plasma membrane in GPR50-transfected HEK293 cells was apparently larger than that in p40-transfected or GPR50del-transfected cells. Thus, my observation supported the hypothesis that the increase of BACE1 activity upon GPR50 overexpression in HEK293 cells is at least partly attributed to a higher ratio of mBACE1/imBACE1 distributed in the plasma membrane.

Table 5.8 A summary of the general linear model for mature BACE1 in HEK293 cells

mBACE1, GPR50× VLA-2α			**mBACE1, GPR50del× VLA-2α**			**mBACE1, (GPR50 VS GPR50 del)×VLA-2α**		
Adjusted r^2=0.215	Partial Eta Squared	P-value	Adjusted r^2=0.180	Partial Eta Squared	P-value	Adjusted r^2=0.475	Partial Eta Squared	P-value
Corrected model	0.248	**0.00022****	Corrected model	0.215	**0.001****	Corrected model	0.497	**3.4×10^{-10}****
GPR50	0.027	0.172	GPR50del	0.024	0.205	GPR50 VS GPR50del	0.000	0.909
VLA-2α	0.218	**0.000046****	VLA-2α	0.199	**0.00011****	VLA-2α	0.494	**1.2×10^{-11}****
GPR50 × VLA-2α	0.048	**0.069$**	GPR50del×VLA-2α	0.040	**0.097$**	(GPR50 VS GPR50del) ×VLA-2α	0.000	0.881
Predicted slopes	P40: 0.519; GPR50: 1.286		Predicted slopes	P40: 0.519; GPR50del : 1.239		Predicted slopes	GPR50: 1.286; GPR50del : 1.240	
mBACE1, GPR50× EEA1			**mBACE1, GPR50del× EEA1**			**mBACE1, (GPR50 VS GPR50 del)×EEA1**		
Adjusted r^2=0.049	Partial Eta Squared	P-value	Adjusted r^2=0.049	Partial Eta Squared	P-value	Adjusted r^2=0.074	Partial Eta Squared	P-value
Corrected model	0.089	**0.095$**	Corrected model	0.089	**0.093$**	Corrected model	0.113	**0.042***
GPR50	0.000	0.993	GPR50del	0.001	0.852	GPR50 VS GPR50del	0.001	0.825
EEA1	0.089	**0.012***	EEA1	0.088	**0.012***	EEA1	0.113	**0.005****
GPR50× EEA1	0.000	0.987	GPR50del× EEA1	0.002	0.721	(GPR50 VS GPR50del) ×EEA1	0.003	0.670
Predicted slopes	P40: -0.352; GPR50: -0.357		Predicted slopes	P40: -0.352; GPR50del : -0.266		Predicted slopes	GPR50: -0.357; GPR50del : -0.266	
mBACE1 GPR50 × Calreticulin			**mBACE1 GPR50del × Calreticulin**			**mBACE1, (GPR50 VS GPR50 del)×Calreticulin**		
Adjusted r^2=0.008	Partial Eta Squared	P-value	Adjusted r^2=0.017	Partial Eta Squared	P-value	Adjusted r^2=0.035	Partial Eta Squared	P-value
Corrected model	0.050	0.322	Corrected model	0.058	0.250	Corrected model	0.076	0.144
GPR50	0.000	0.998	GPR50del	0.000	0.879	GPR50 VS GPR50del	0.000	0.861
Calreticulin	0.049	**0.064$**	Calreticulin	0.058	**0.044***	Calreticulin	0.076	**0.021***
GPR50×calreticulin	0.000	0.997	GPR50del× Calreticulin	0.001	0.819	(GPR50 VS GPR50del)× Calreticulin	0.001	0.788
Predicted slopes	P40: -0.321; GPR50:- 0.322		Predicted slopes	P40: -0.321; GPR50del : -0.402		Predicted slopes	GPR50: -0.320; GPR50del : -0.403	

**** p<0.01, * p<0.05, $p<0.1**

Table 5.9 A summary of the general linear model for immature BACE1 in HEK293 cells

imBACE1, GPR50× VLA-2α			**imBACE1, GPR50del× VLA-2α**			**imBACE1, (GPR50 VS GPR50 del)×VLA-2α**		
Adjusted r^2=0.215	Partial Eta Squared	P-value	Adjusted r^2=0.014	Partial Eta Squared	P-value	Adjusted r^2=-0.016	Partial Eta Squared	P-value
Corrected model	0.072	0.163	Corrected model	0.055	0.272	Corrected model	0.027	0.599
GPR50	0.040	0.095	GPR50del	0.020	0.241	GPR50 VS GPR50del	0.004	0.596
VLA-2α	0.002	0.706	VLA-2α	0.018	0.268	VLA-2α	0.018	0.270
GPR50 × VLA-2α	0.070	**0.027***	GPR50del×VLA-2α	0.040	0.125	(GPR50 VS GPR50del) ×VLA-2α	0.007	0.486
Predicted slopes	P40: 0.431; GPR50: -0.308		Predicted slopes	P40: 0.431; GPR50del : -0.071		Predicted slopes	GPR50: -0.308; GPR50del : -0.070	
imBACE1, GPR50× EEA1			**imBACE1, GPR50del× EEA1**			**imBACE1, (GPR50 VS GPR50 del)×EEA1**		
Adjusted r^2=0.025	Partial Eta Squared	P-value	Adjusted r^2=-0.001	Partial Eta Squared	P-value	Adjusted r^2=-0.004	Partial Eta Squared	P-value
Corrected model	0.066	0.197	Corrected model	0.041	0.408	Corrected model	0.046	0.357
GPR50	0.000	0.958	GPR50del	0.002	0.694	GPR50 VS GPR50del	0.003	0.662
EEA1	0.066	**0.032***	EEA1	0.040	**0.099$^{\$}$**	EEA1	0.043	**0.085$^{\$}$**
GPR50× EEA1	0.000	0.925	GPR50del× EEA1	0.008	0.452	(GPR50 VS GPR50del) ×EEA1	0.010	0.399
Predicted slopes	P40: 0.207; GPR50: 0.226		Predicted slopes	P40: 0.207; GPR50del : 0.078		Predicted slopes	GPR50: 0.225; GPR50del : 0.078	
imBACE1 GPR50 × Calreticulin			**imBACE1 GPR50del × Calreticulin**			**imBACE1, (GPR50 VS GPR50 del)×Calreticulin**		
Adjusted r^2=-0.041	Partial Eta Squared	P-value	Adjusted r^2=-0.037	Partial Eta Squared	P-value	Adjusted r^2=-0.041	Partial Eta Squared	P-value
Corrected model	0.003	0.973	Corrected model	0.007	0.921	Corrected model	0.003	0.976
GPR50	0.001	0.825	GPR50del	0.003	0.646	GPR50 VS GPR50del	0.001	0.821
Calreticulin	0.002	0.725	Calreticulin	0.000	0.999	Calreticulin	0.002	0.730
GPR50×calreticulin	0.002	0.728	GPR50del× Calreticulin	0.007	0.488	(GPR50 VS GPR50del)× Calreticulin	0.002	0.727
Predicted slopes	P40: -0.087; GPR50:- 0.001		Predicted slopes	P40: -0.087; GPR50del : 0.087		Predicted slopes	GPR50: 0.000; GPR50del : 0.088	

**** p<0.01, * p<0.05, $^{\$}$p<0.1**

Table 5.10 A summary of the predictors of significance or with a trend of significance in the general linear model for mature BACE1 and immature BACE1 in HEK293 cells

HEK293 cells		GPR50		GPR50del		GPR50 v GPR50del	
		Marker correlation (p-value)	Interaction effect on co-fractionation (p-value)	Marker correlation (p-value)	Interaction effect on co-fractionation (p-value)	Marker correlation (p-value)	Interaction effect on co-fractionation (p-value)
mBACE1	Plasma membrane	+ve (0.000046)**	Increased (0.069)$	+ve (0.00011)**	Increased (0.097)$	+ve (1.2×10^{-11})**	NS
	Early endosome	-ve (0.012)*	NS	-ve (0.012)*	NS	-ve (0.005)**	NS
	ER	-ve (0.064)$	NS	-ve (0.044)*	NS	-ve (0.021)*	NS
imBACE1	Plasma membrane	NS	Reversed +ve→-ve (0.027)*	NS	NS	NS	NS
	Early endosome	+ve (0.032)*	NS	+ve (0.099)$	NS	+ve (0.085)$	NS
	ER	NS	NS	NS	NS	NS	NS

****p<0.01, *p<0.05, 0.05<$P<0.1, NS: not significant, +ve: positive, -ve,negative, reference group = p40, the predicted slopes for the interaction terms of significance or with a trend of significance are listed.**

2) Primary cortical neurons

Predictors of general linear model for mBace1/imBace1 in primary cortical neurons included subcellular markers (β-catenin, p115 and calreticulin), group membership (p40, GPR50, GPR50del transfected groups) and the interaction term (the products of subcellular markers and group membership). The test results of the fitted model for Bace1 in primary cortical neurons are listed in Table 5.11-5.12. The observed significance or trend of significance of each predictor, together with the predicted effect for the interaction terms of significance or with a trend of significance are summarised in Table 5.13.

In primary cortical neurons, GPR50del overexpression had a trend of decreasing Bace1 activity compared with the control and a significant suppressing effect compared with GPR50 overexpression (see chapter 4). Overexpressed GPR50 had no effect compared with the control. Therefore, it was hypothesised that, compared with p40 or GPR50, the transfection of GPR50del would decrease the association of mBace1 distribution with that of the plasma membrane or the early endosomes, or would enhance the association of imBace1 distribution with that of the ER.

In this general linear model, the distribution percentage of mBace1 was significantly correlated to β-catenin (positive) and p115 (negative) no matter which two groups were compared. ImBace1 was always associated with calreticulin (positive). This indicates that, in primary cortical neurons, mBace1 was co-fractionated with the plasma membrane but excluding cis-Golgi, while imBace1 was co-fractionated with calreticulin. The interaction term had a trend of significance when correlation between both forms of Bace1 and calreticulin in groups p40 and GPR50del was compared. The trends for mBace1 (decreased) and imBace1 (increased) were opposite, which meant that in neurons transfected with GPR50del, there was a trend of less mBace1 but more imBace1 co-fractionated with the ER marker calreticulin, compared with the control group p40. Thus, GPR50del overexpression appeared to retain imBace1 in the ER and to impede Bace1 maturation, which will decrease BACE1 activity. This effect was unique to GPR50del, even though there were no significant differences of Bace1 distribution between cell groups with overexpressed GPR50 and overexpressed GPR50del. This observation supported the hypothesis that the potential of GPR50del but not GPR50 in decreasing Bace1 activity in primary cortical neurons is partly explained by causing less Bace1 undergoing maturation.

Table 5.11 A summary of the general linear model for mature Bace1 in primary cortical neurons

mBace1, GPR50× β-catenin			**mBace1, GPR50del× β-catenin**			**mBace1, (GPR50 VS GPR50 del)×β-catenin**		
Adjusted r^2=0.538	Partial Eta Squared	P-value	Adjusted r^2=0.757	Partial Eta Squared	P-value	Adjusted r^2=0.478	Partial Eta Squared	P-value
Corrected model	0.558	**4.6×10^{-12}****	Corrected model	0.768	**1.7×10^{-21}****	Corrected model	0.500	**2.7×10^{-10}****
GPR50	0.018	0.270	GPR50del	0.005	0.568	GPR50 VS GPR50del	0.007	0.500
β-catenin	0.539	**4.8×10^{-13}****	β-catenin	0.767	**3.2×10^{-23}****	β-catenin	0.484	**2.4×10^{-11}****
GPR50 × β-catenin	0.038	0.108	GPR50del×β-catenin	0.011	0.385	(GPR50 VS GPR50del) ×β-catenin	0.015	0.320
Predicted slopes	P40: 1.064; GPR50: 0.735		Predicted slopes	P40: 1.064; GPR50del : 0.947		Predicted slopes	GPR50: 0.735; GPR50del : 0.946	
mBace1, GPR50× P115			**mBace1, GPR50del× P115**			**mBace1, (GPR50 VS GPR50 del)×P115**		
Adjusted r^2=0.030	Partial Eta Squared	P-value	Adjusted r^2=0.027	Partial Eta Squared	P-value	Adjusted r^2=0.023	Partial Eta Squared	P-value
Corrected model	0.071	0.169	Corrected model	0.068	0.183	Corrected model	0.064	0.207
GPR50	0.000	0.963	GPR50del	0.000	0.956	GPR50 VS GPR50del	0.000	0.993
P115	0.071	**0.026***	P115	0.068	**0.029***	P115	0.064	**0.034***
GPR50× P115	0.000	0.906	GPR50del× P115	0.000	0.889	(GPR50 VS GPR50del) ×P115	0.000	0.982
Predicted slopes	P40: -0.159; GPR50: -0.143		Predicted slopes	P40: -0.159; GPR50del : -0.140		Predicted slopes	GPR50: -0.143; GPR50del : -0.140	
mBace1 GPR50 × Calreticulin			**mBace1 GPR50del × Calreticulin**			**mBace1, (GPR50 VS GPR50 del)×Calreticulin**		
Adjusted r^2=0.025	Partial Eta Squared	P-value	Adjusted r^2=0.026	Partial Eta Squared	P-value	Adjusted r^2=-0.031	Partial Eta Squared	P-value
Corrected model	0.066	0.199	Corrected model	0.068	0.187	Corrected model	0.013	0.827
GPR50	0.003	0.628	GPR50del	0.027	0.176	GPR50 VS GPR50del	0.008	0.466
Calreticulin	0.044	**0.081$^{\$}$**	Calreticulin	0.010	0.409	Calreticulin	0.000	0.932
GPR50×calreticulin	0.006	0.523	GPR50del× Calreticulin	0.050	**0.063$^{\$}$**	(GPR50 VS GPR50del)× Calreticulin	0.013	0.350
Predicted slopes	P40: 0.440; GPR50:0.206		Predicted slopes	P40: 0.440; GPR50del : -0.171		Predicted slopes	GPR50: 0.206; GPR50del : -0.171	

**** p<0.01, * p<0.05, $^{\$}$p<0.1**

Table 5.12 A summary of the general linear model for immature Bace1 in primary cortical neurons

imBace1, GPR50× β-catenin			**imBace1, GPR50del× β-catenin**			**imBace1, (GPR50 VS GPR50 del)×β-catenin**		
Adjusted r^2=-0.012	Partial Eta Squared	P-value	Adjusted r^2=-0.022	Partial Eta Squared	P-value	Adjusted r^2=-0.042	Partial Eta Squared	P-value
Corrected model	0.031	0.543	Corrected model	0.021	0.692	Corrected model	0.002	0.989
GPR50	0.008	0.458	GPR50del	0.002	0.688	GPR50 VS GPR50del	0.001	0.838
β-catenin	0.011	0.385	β-catenin	0.016	0.290	β-catenin	0.000	0.900
GPR50 × β-catenin	0.017	0.278	GPR50del×β-catenin	0.005	0.542	(GPR50 VS GPR50del) ×β-catenin	0.001	0.762
Predicted slopes	P40: -0.310; GPR50: 0.034		Predicted slopes	P40: -0. 310; GPR50del : -0.084		Predicted slopes	GPR50: 0.034; GPR50del : -0.084	
imBace1, GPR50× P115			**imBace1, GPR50del× P115**			**imBace1, (GPR50 VS GPR50 del)×P115**		
Adjusted r^2=0.006	Partial Eta Squared	P-value	Adjusted r^2=-0.012	Partial Eta Squared	P-value	Adjusted r^2=0.002	Partial Eta Squared	P-value
Corrected model	0.048	0.341	Corrected model	0.031	0.543	Corrected model	0.044	0.376
GPR50	0.000	0.902	GPR50del	0.000	0.907	GPR50 VS GPR50del	0.000	0.983
P115	0.045	**0.079$^{\$}$**	P115	0.029	0.157	P115	0.044	**0.080$^{\$}$**
GPR50× P115	0.001	0.752	GPR50del× P115	0.001	0.768	(GPR50 VS GPR50del) ×P115	0.000	0.957
Predicted slopes	P40: -0.104; GPR50:- 0.149		Predicted slopes	P40: -0.104; GPR50del : -0.158		Predicted slopes	GPR50: -0.149; GPR50del : -0.158	
imBace1 GPR50 × Calreticulin			**imBace1 GPR50del × Calreticulin**			**imBace1, (GPR50 VS GPR50 del)×Calreticulin**		
Adjusted r^2=0.434	Partial Eta Squared	P-value	Adjusted r^2=0.400	Partial Eta Squared	P-value	Adjusted r^2=0.405	Partial Eta Squared	P-value
Corrected model	0.458	**4.1×10^{-9}****	Corrected model	0.426	**2.9×10^{-8}****	Corrected model	0.431	**2.2×10^{-8}****
GPR50	0.012	0.368	GPR50del	0.021	0.230	GPR50 VS GPR50del	0.003	0.667
Calreticulin	0.451	**2.0×10^{-10}****	Calreticulin	0.424	**1.0×10^{-9}****	Calreticulin	0.416	**1.7×10^{-9}****
GPR50×calreticulin	0.021	0.236	GPR50del× Calreticulin	0.040	**0.098$^{\$}$**	(GPR50 VS GPR50del)× Calreticulin	0.005	0.581
Predicted slopes	P40: 0.920; GPR50:1.270		Predicted slopes	P40: 0.920; GPR50del : 1.490		Predicted slopes	GPR50: 1.270; GPR50del : 1.490	

**** p<0.01, * p<0.05, $^{\$}$p<0.1**

Table 5.13 A summary of the predictors of significance or with a trend of significance in the general linear model for mature Bace1 and immature Bace1 in primary cortical neurons

primary cortical neurons		GPR50		GPR50del		GPR50 v GPR50del	
		Marker correlation (p-value)	Interaction effect on co-fractionation (p-value)	Marker correlation (p-value)	Interaction effect on co-fractionation (p-value)	Marker correlation (p-value)	Interaction effect on co-fractionation (p-value)
mBace1	Plasma membrane	+ve (4.8×10^{-13})**	NS	+ve (3.2×10^{-23})**	NS	+ve (2.4×10^{-11})**	NS
	Cis-Glogi	-ve (0.026)*	NS	-ve (0.029)*	NS	-ve (0.034)**	NS
	ER	+ve (0.081)$	NS	NS	Reversed +ve→-ve (0.063)$	NS	NS
imBace1	Plasma membrane	NS	NS	NS	NS	NS	NS
	Cis-Glogi	-ve (0.079)$	NS	NS	NS	-ve (0.080)$	NS
	ER	+ve (2.0×10^{-10})**	NS	+ve (1.0×10^{-9})**	Increased (0.098)$	+ve (1.7×10^{-9}) **	NS

****p<0.01, *p<0.05, 0.05<$P<0.1, NS: not significant, +ve: positive, -ve,negative, reference group = p40, the predicted slopes for the interaction terms of significance or with a trend of significance are listed.**

5.4 Discussion

In this chapter, the relationship between endogenous GPR50 level and the percentage of endogenous BACE1 at the surface of HEK293 group cells was investigated. In most of the cells, GPR50 and cell surface BACE1 seemed to express in an exclusive manner. Statistical analysis showed that endogenous GPR50 expression level in HEK293 cells was negatively correlated with the proportion of cell surface BACE1 level against total BACE1 level. This indicates that GPR50 is likely to be involved in the trafficking of BACE1 at the endogenous level. However, this result requires replication before a solid conclusion can be drawn.

Further investigation demonstrated that GPR50 plays a part in the subcellular localisation of BACE1, and that GPR50 and its deletion/SNP variant (GPR50del) may have differential effects in different cell lines.

In HEK293 cells, GPR50 transfection resulted in a trend of more mature BACE1 (mBACE1) and less immature BACE1 (imBACE1) associated with the plasma membrane (VLA-2α). GPR50del had a similar positive trend of significant effects on the correlation between mBACE1 and the plasma membrane, but had no effect on imBACE1, compared to either p40 or GPR50. The plasma membrane is one of the putative sites of BACE1 activity, and imBACE1 has much less β-secretase activity than mBACE1 (Zhong et al, 2007). Thus, my observations are in agreement with the BACE1 activity assay results that GPR50, but not GPR50del increases BACE1 activity in HEK293 cells (Grünewald, 2011). One potential mechanism is that GPR50 helps to adjust the ratio of mBACE1/imBACE1 at the plasma membrane. This ability of GPR50 has already been suggested by the result of correlation between the level of endogenous GPR50 and the ratio of cell surface BACE1/total BACE1. The traditional theory is that BACE1 becomes mature once the protein moves out of the trans-Golgi network (TGN), and then cycles between the TGN, the plasma membrane and the early endosomes (Huse et al, 2000). My results also demonstrated that imBACE1 in HEK293 cells was not significantly associated with the plasma membrane. However, GPR50 overexpression significantly reduced the variance of imBACE1 distribution explained by that of the plasma membrane marker. Thus, the decreased amount of BACE1 at the cell surface when the cells are expressed with GPR50 might be the immature isoform of BACE1. This is interesting and more investigation on the distribution of mBACE1 and imBACE1 in different

cellular compartments may help to understand the complicated trafficking network of BACE1 and its sites of functional cleavage.

In primary cortical neurons, GPR50del overexpression appears to alter Bace1 distribution to a larger extent than GPR50 overexpression, reflected by more immature Bace1 correlated with the ER (calreticulin), compared with the control condition. This indicates that more pro-Bace1 is likely to be retained in the ER in GPR50del transfected cells, thus less Bace1 becomes mature and enzymatically active. The potential effect of GPR50del in Bace1 maturation might explain the result that GPR50del overexpression in neurons shows a trend of reducing Bace1 activity (chapter 4), because less mature Bace1 is transported to Bace1 cleavage sites.

In summary, I have found that GPR50/GPR50del might be one of the regulators involved in the complex network of the BACE1/Bace1 trafficking system. Also, my results demonstrated how complicated the network of β-secretase trafficking could be, and it could even be diversified and associated with different modulators affecting different isoforms of BACE1 (immature and mature) during the cleavage of different substrates in different cell lines.

5.4.1 The GPR50 C-terminal tail might be a key region that mediates the role of GPR50 in β-secretase trafficking

I and others have shown that GPR50 and the variant GPR50del demonstrate diversity in the regulation of BACE1 activity, not only in HEK293 cells, but also in mouse primary cortical neurons. Interestingly, in the trafficking experiment of BACE1 demonstrated in this chapter, the two isoforms of GPR50 seem to have effects that are consistent with their effects, in the corresponding cell types, in the BACE1 activity assays {(Grünewald, 2011), my chapter 4}. My results provide insights for the discussion about the close relation between β-secretase trafficking system and its activity levels.

It is notable that the variation in the peptide sequence of GPR50del is confined to the C-terminal domain, a structure that is believed to be a key region for G-protein coupled receptors to exert their functions, including modification during activation and protein-protein interaction. GPR50 has a long C-terminal domain (CTD), occupying over half of its protein sequence (residues 295 – 617). Deleting either the N-terminal or the C-terminal of GPR50 changes its subcellular location, with more

protein retained in the internal compartments (Grünewald, 2011; Li et al, 2011). Full length GPR50 and the CTD can be translocated to the perinuclear area and nuclear compartment respectively by co-expressing with TIP60, while GPR50 lack of CTD is not affected (Li et al, 2011). In addition, deletion of GPR50 CTD suppresses the inhibitory effect of GPR50 on the melatonin receptor MT1 signalling without affecting their heterodimerisation, suggesting that the GPR50 CTD modifies the interaction of other binding partners to MT1 (Levoye et al, 2006). GPR50 del does not display an altered localisation pattern compared to GPR50 (Grünewald, 2011), but the deletion/SNP in the CTD of this variant may damage or modify the interaction between GPR50 and its interactors.

The yeast two-hybrid study using both the CTDs of GPR50 and GPR50del as bait identified overlapping interactors of the two, but also potentially unique binders, for example SNX6 of GPR50 CTD and RTN3 of GPR50del CTD (Grunewald et al, 2009). BACE1 was not identified in the screen, and there is no direct evidence showing that an altered interaction exists between GPR50-BACE1 and GPR50del-BACE1. Therefore, it is also possible that GPR50 and GPR50del influence the trafficking of BACE1 by interacting with its known sorting regulators, such as SNX6 and RTN3, which are both proved transporters of BACE1 (Okada et al, 2010; Shi et al, 2009). However, the initial association between GPR50/GPR50del and their differentiated interactors needs to be verified.

5.4.2 Summary

Here I showed that in HEK293 cells, GPR50 seems to increase the ratio of mBACE1/imBACE1 at the cell surface, opposite to the sorting direction of RTN3 on BACE1 (Deng et al, 2013; Shi et al, 2009), which may correspond to their opposite effects on BACE1 activity. In neuronal cells, GPR50del overexpression appears to favour mature Bace1 exit from the external compartments and immature Bace1 retaining in the ER, which is identical to the transporting orientation of RTN3 on BACE1 (Deng et al, 2013; Shi et al, 2009) and RTN3 on GPR50del (Grünewald, 2011). This suggests that the regulative effects on BACE1 localisation and activity by GPR50/GPR50del might be RTN3-related. The connection between GPR50 and BACE1 transporters is interesting and requires further investigation.

5.4.3 Further experiments

In this chapter, I have found the answer to my original question: GPR50/GPR50del indeed has a role in regulating BACE1 trafficking. However, there is seemingly a discrepancy in the results obtained by the cell surface labelling technique and the subcellular fractionation. It appears that in HEK293 cells, cells expressed with endogenous GPR50 have reduced ratio of cell surface BACE1/total BACE1 (cell surface labelling technique), while GPR50 overexpression has a potential in increasing the ratio of mBACE1/imBACE1 in the plasma membrane (subcellular fractionation). These two observations are not necessarily contradictory. On the one hand, the cell surface labelling technique did not distinguish mBACE1 from imBACE1; on the other hand, and more importantly, there are two putative functional sites of BACE1 activity: one on the cell surface and the other in the internal compartment-the endosomes. There is a dynamic circulation of BACE1 between the two sites. Locating at the cell surface is not the opposite of being localised in the endosomes. Instead, accumulation in the one site might lead to accumulation in the other site. Even if the majority of cell surface BACE1 is mature, it can undergo internalisation to the endosomes, while BACE1 in the endosomes can also be recycled to the cell surface. To further clarity this situation, the next step is to use imBACE1/mBACE1-specific antibody to examine which isoform(s) can be localised at the cell surface. Then, a time-lapse internalisation experiment of cell surface BACE1, with or without the overexpression of GPR50, could be performed. Specific organelle markers are required to identify where BACE1 is directed to after internalisation and recycling.

6 Co-expression of GPR50 and BACE1 in the brain

6.1 Introduction

In previous chapters, the subcellular sites at which GPR50 potentially interacts with BACE1 were identified. Next, I wanted to investigate in which regions the interaction between GPR50 and BACE1 could occur. As BACE1 has high activity levels in the brain, I investigated the relationship between mRNA levels of GPR50 and BACE1 in brain regions of human and mouse using data from public resources (BrainCloud for human; BrainStars for mouse). Then, I sought to look at the protein expression of endogenous Gpr50 and Bace1 in adult mouse brain. Identification of co-localisation regions of the two may indicate a regulatory role of Gpr50 on Bace1 function, or vice versa.

6.1.1 GPR50 distribution in the sub-regions of brain tissue

GPR50 was originally cloned from a human pituitary cDNA library (Reppert et al, 1996). GPR50 protein is detected consistently in the pituitary and hypothalamic regions of adult human, sheep, rat, mouse and hamster by immunohistochemistry (Drew et al, 2001; Drew et al, 1998; Sidibe et al, 2010). Recently, immunohistochemistry and real-time qPCR studies have revealed an enlarged distribution of Gpr50 in several new brain areas of rodents (Batailler et al, 2012; Grunewald et al, 2012), including some sub-regions of the cortex (i.e. entorhinal cortex), the hippocampus (i.e. CA1), and the amygdala. These observations suggest that, apart from being potentially functional in the neuroendocrine system, GPR50 may play a role in the memory processing and storage.

Our group has published a thorough report on the mRNA levels and protein levels of Gpr50 in mouse brain during embryonic development and in the early adulthood when brain development continues through puberty (Grunewald et al, 2012). Gpr50 mRNA was detected with low expression levels from E13, peaked at E18 and increased again at week 5. At the developmental time-points E18 and P7, Gpr50 appeared to be highly expressed in specific regions, such as in the thalamus, the hypothalamus, the midbrain, the pons and the medulla. In particular, Gpr50 mRNA was more highly expressed in the frontal regions (i.e. the entorhinal cortex, the olfactory bulb) at week 5 only.

In E18 mouse brain, Gpr50 protein expression had high levels in the frontal cortex, the posterior cortex and the hypothalamus; moderate levels in the thalamus and the

medulla; and minor levels in the midbrain and the pons (Grunewald et al, 2012). In adult mouse brain, the expression sites of Gpr50 protein were the neurons in the hypothalamus, the cortex, the dentate gyrus, the superior colliculus, the pons; the vimentin-negative cells in the hypothalamic regions; and the neurotransmitter-related cells in the brain stem, such as the noradrenergic nuclei in the locus coeruleus, the serotonergic nuclei in the pontine grey and the dopaminergic nuclei in the substantia nigra. Other researchers have revealed slightly different sites of Gpr50 protein distribution in mouse brain. For instance, Sidibe and Batailler reported that there was no immunoreactivity of Gpr50 in the mouse hippocampus (Batailler et al, 2012; Grunewald et al, 2012; Sidibe et al, 2010). This might be attributed to the different strains and sexes of the mice used for investigation.

6.1.2 BACE1 distribution in the sub-regions of brain tissue

BACE1 is abundantly expressed in brains of both normal human and Alzheimer's disease (AD) patients (Coulson et al, 2010; Vassar et al, 1999). In human, BACE1 transcripts were found with robustly higher expression in various brain sub-regions and the pancreas than other peripheral tissues. *In situ* hybridisation signal of Bace1 was observed in multiple regions of the adult rat brain, with the strongest signal in the hippocampus, the cortex, and the cerebellum (Vassar et al, 1999). In mouse, during the prenatal and postnatal stage, Bace1 mRNA was detected in the rudimental brain, cranial and spinal ganglia, kidney, and developing hematopoietic organs (Marcinkiewicz & Seidah, 2000). In adult mouse brain, Bace1 mRNA had high levels in the pyramidal cells in layers III and V of the cortex and in the dorsal thalamus, and peaked in the CA1 and dentate gyrus of the hippocampus (Marcinkiewicz & Seidah, 2000).

The expression of Bace1 protein in mouse brain was robust during the prenatal stage, and was enhanced after birth, especially during the first postnatal week (Hebert et al, 2008). The protein level of mouse Bace1 in the brain lysates was decreased after 4 weeks and remained stable up to 1 year old. Bace1 was widely distributed in the adult mouse brain, with the highest protein level detected in the cerebellum (Hebert et al, 2008). Yet, Bace1 protein was predominantly expressed in the mouse primary cultured neurons, with a very weak level in the primary cultured glia (Hebert et al, 2008).

6.1.3 Introduction to experiments

In this chapter, I investigated the mRNA levels of GPR50 and BACE1, as well as where their expression is correlated, using publicly available data (BrainCloud, BrainStars). The protein levels of Gpr50 and Bace1 in the key brain regions of adult C57BL/6 mouse were further analysed by fluorescent immunohistochemistry.

6.2 Materials and methods

6.2.1 Summary of expression data from public database

6.2.1.1 The mRNA expression data of human GPR50 and BACE1 from BrainCloud

The BrainCloud database (Colantuoni et al, 2011) provides data of genome-wide gene expression in the human post-mortem dorsolateral prefrontal cortex (DLPFC) grey matter of normal subjects across the lifespan (PFC for prenatal subjects). The 269 samples were collected from both male (N=177) and female (N=92), with an age range from -0.50 to 78.23 years (negative numbers refer to the prenatal age calculated back from day 0). The ethnicity of the subjects includes Caucasian (N=112), African American (N=147), Asian (N=6) and Hispanic (N=4).

The normalised expression levels of selected genes (GPR50 and BACE1) are log2 of the ratio of sample signal to the reference signal (reference: pooled RNA from all the subjects). The length of the probes is 70 bp. The probe for GPR50 (Illumina 22996) is located within exon 2, from 1472 bp to 1541 bp, recognising both variants: GPR50 and GPR50del. The probe ID for BACE1 (Illumina 1634) is located within exon 1, from 17 bp to 86 bp, recognising all the five known variants: BACE1 a-e (see chapter 2, Figure 2.1). Statistical analysis was performed using SPSS 19 software (IBM Armonk, New York). Comparisons of expression levels for each gene among categorical factors were made with a general linear model. Findings where $p<0.05$ were considered significant. Correlation between expression levels of GPR50 and BACE1 were tested by Pearson's correlation analysis or by fitting the general linear model with the main effects and/or the interaction effect of the significant factors.

6.2.1.2 The mRNA expression data of mouse Gpr50 and Bace1 from BrainStars

The BrainStars (or B*) database (Kasukawa et al, 2011) has a genome-wide expression profile in 51 adult mouse CNS regions (Table 6.1). All the mice were

male 5-week old Balb/c mice. Each CNS region was collected from 30-150 mice and was sampled every 4 hours (5-25 mice at each time point). The RNA of pooled samples from the 6 time points was purified and measured with Affymetrix GeneChip Mouse Genome 430 2.0 arrays. Every CNS region was independently sampled twice (N=2). All expression values were log2-transformed. The probe IDs for Gpr50 and Bace1 analysed in this chapter were "1450346_at" and "1455826_a_at", the basic description of which can be found in NetAffx™ Analysis Centre (http://www.affymetrix.com/analysis/index.affx). Probe 1450346_at detects one isoform of mouse Gpr50 (Ensembl ID: ENSMUST00000070449), and probe 1455826_a_at detects two isoforms of mouse Bace1 (Ensembl ID: ENSMUST00000034591; ENSMUST00000078111). The analysis of expression levels of Gpr50 and Bace1 and their correlation was assessed by the general linear model.

Table 6.1 The 51 adult mouse CNS regions investigated in BrainStars database

Region Name	Region Abbreviation	Region Classification	Gpr50*	Bace1*
lateral septal nucleus	LS	Telencephalon	6.1318	10.3178
retrosplenial cortex	RS	Telencephalon	6.3180	9.6215
cerebral cortex motor	Cx motor	Telencephalon	6.3941	9.7967
cerebral cortex cingulate	Cx cingulate	Telencephalon	6.3210	10.1160
olfactory bulb anterior	OB anterior	Telencephalon	6.7000	9.7020
olfactory bulb posterior	OB posterior	Telencephalon	6.5443	9.7473
piriform cortex	Pir	Telencephalon	6.7011	9.3700
olfactory tubercle	Tu	Telencephalon	6.5230	9.3621
ventral subiculum	ventral S	Telencephalon	6.6795	9.5336
CA1 (hippocampus)	CA1	Telencephalon	6.3631	9.1722
CA2 / CA3 (hippocampus)	CA2/CA3	Telencephalon	6.4274	9.3791
dentate gyrus (hippocampus)	DG	Telencephalon	6.3326	9.6029
amygdala anterior	A anterior	Telencephalon	6.3624	9.8866
amygdala posterior	A posterior	Telencephalon	6.5208	9.7353
globus pallidus	GP	Telencephalon	6.4735	9.5616
caudate putamen lateral	CPu lateral	Telencephalon	6.4077	9.8646
caudate putamen medial	CPu medial	Telencephalon	6.2898	9.7176
mediodorsal thalamic nucleus	MD	Thalamus	6.3562	9.4823
ventral anterior thalamic nucleus / ventrolateral thalamic nucleus	VA/VL	Thalamus	6.3335	10.2648
ventral posteromedial thalamic nucleus / ventral posterolateral thalamic nucleus	VPM/VPL	Thalamus	6.2017	9.8543

lateral geniculate body	LG	Thalamus	6.4602	9.9836
medial geniculate nucleus	MG	Thalamus	6.2462	9.5314
habenular nucleus	Hb	Thalamus	6.4523	8.8036
mammillary body	M	Hypothalamus	7.1142	9.7956
median eminence	ME	Hypothalamus	9.4463	8.8700
suprachiasmatic nucleus	SCN	Hypothalamus	6.5090	9.2723
medial preoptic area	MPA	Hypothalamus	7.0264	9.5304
supraoptic nucleus	SO	Hypothalamus	6.5360	10.5202
paraventricular hypothalamic nucleus	Pa	Hypothalamus	6.5810	9.2265
subparaventricular zone ventral	SPa ventral	Hypothalamus	6.9833	9.1177
subparaventricular zone dorsal	SPa dorsal	Hypothalamus	7.4874	9.5330
dorsomedial hypothalamic nucleus	DM	Hypothalamus	7.7009	8.9431
ventromedial hypothalamic nucleus	VMH	Hypothalamus	6.5731	10.1043
arcuate hypothalamic nucleus	Arc	Hypothalamus	9.0252	9.3724
lateral hypothalamus	LH	Hypothalamus	6.5443	9.7238
periaqueductal gray	PAG	Mesencephalon	6.2105	9.5862
superior colliculus	SC	Mesencephalon	6.6232	9.3494
inferior colliculus	IC	Mesencephalon	6.2050	9.6536
ventral tegmental area	VTA	Mesencephalon	6.5783	9.4713
substantia nigra	SN	Mesencephalon	6.3696	9.9221
dorsal tegmental nucleus	Tg	Mesencephalon	6.5031	9.5541
pontine nucleus	Pn	Pons	6.5253	9.6754
medial vestibular nucleus	MVe	Pons	6.3779	9.7901
cerebellar cortex vermis	Cb vermis	Cerebellum	6.3211	9.5993
cerebellar cortex lobe	Cb lobe	Cerebellum	6.2273	9.5838
cerebellar nucleus	Cb nucleus	Cerebellum	6.1686	10.2940
spinal cord anterior	spinal cord anterior	spinal cord	6.2284	10.0596
spinal cord posterior	spinal cord posterior	spinal cord	6.2664	9.9500
retina	Retina	Misc	6.1448	9.6205
corpus pineal	Pineal	Misc	6.3815	8.9608
pituitary	Pituitary	Misc	6.5628	8.6560

***Each value was the mean of the two replicates.**

6.2.2 Immunohistochemistry (IHC)

The 12-week old female C57BL/6 mice were killed by cervical dislocation. This was performed by the technicians in Biomedical Research Resources Unit, Western General Hospital, Edinburgh. The mouse brains were immediately transferred to ice cold PBS, followed by the fixation in 70% ethanol at 4^{o}C for 12 hr (Grunewald et al, 2009; Grunewald et al, 2012). The fixed brains were embedded in paraffin wax and cut into 6 μm coronal sections (Bregma: -1.64 mm) on a Leica microtome. Sections were placed onto microscope slides (Superfrost Plus adhesion, 25 mm×75 mm×1 mm, Fisher Scientific) and dried at 37^{o}C overnight.

Sections were de-waxed through a series of alcohols: 100% xylene 5 min×2, 100% ethanol 5 min×2, 70% ethanol 5 min×2, running tap water 5 min, dH_2O 5 min. The sections were loaded onto the Shandon Sequenza slide racks (Thermo Scientific) and washed with PBS for 5 min. Tissues were permeabilised with 0.1% Triton X-100 (Sigma) in PBS for 30 min, followed by two washes with PBS/0.02% BSA. Proteins were denatured by 6 M guanidine hydrochloride in 50 mM Tris-HCl (pH 7.4) for 10 min, followed by three washes with PBS/0.02% BSA. Then sections were incubated with 10% donkey serum (from secondary antibody host, Sigma) in PBS/0.02% BSA for 1 hr. All the above mentioned steps were performed at room temperature. After the blocking, slides were incubated with the primary antibodies diluted in PBS at 4^{o}C for 16 hr. The primary antibodies used in this chapter include: GPR50 goat (1:10, Santa Cruz), BACE1 rabbit2 (1:300, Covance), BACE1 goat (1:50, R&D) (See Table 2.2 for details). Slides were washed three times with PBS/0.02% BSA and blocked again with 10% donkey serum in PBS/0.02% BSA at room temperature for 30 min. Sections were incubated at room temperature for 1 hr with fluorescent secondary antibodies (Alexa Fluor® donkey-anti-goat/rabbit 488/594, Invitrogen, see Table 2.3) diluted in PBS/0.02% BSA/10% donkey serum, followed by three washes with PBS/0.02% BSA. Coverslips were mounted onto slides using Mowiel/DAPI (Vector labs) and stored at 4^{o}C before viewing.

6.3 Results

6.3.1 The mRNA expression levels of GPR50 and BACE1 in human DLPFC

As the samples of human post-mortem DLPFC grey matter (PFC for prenatal subjects) collected in BrainCloud came from individuals with different ages, each

data point was viewed as a single case, irrespective of gender or ethnic background. Therefore, outliers were not removed from the dataset. The mRNA expression profiles of human GPR50 and BACE1 are shown in Figure 6.1. The fitted curves represented by the red dots were generated by local regression analysis (adapted from BrainCloud).

The most significant changes of expression for both genes occurred during the prenatal stage (week 14-20). In particular, there was a peak of GPR50 level at foetal week 17. BACE1 mRNA level appeared to increase continuously during the prenatal period. Both of the two genes were stably expressed on average after birth, but with great variance among individuals.

Then two factors were taken into account that might influence the expression levels of GPR50 or BACE1 thus contributing to the covariance of the correlation between the two genes:

1) Age. GPR50 expression was identified in the dentate gyrus of elderly individuals and AD patients (Hamouda et al, 2007). BACE1 is the key enzyme in the pathology of age-dependent AD (Vassar et al, 1999).
2) Sex. GPR50 has been identified as a risk factor for bipolar disorder in female subjects (Thomson et al, 2005). BACE1 levels in human hippocampus were found correlated with sex (Marballi et al, 2012).

Meanwhile, because the expression patterns of GPR50 and BACE1 have shown obvious differences between gestational period and the period after birth, the data were split into two categories ("prenatal" and "after birth") and were analysed separately.

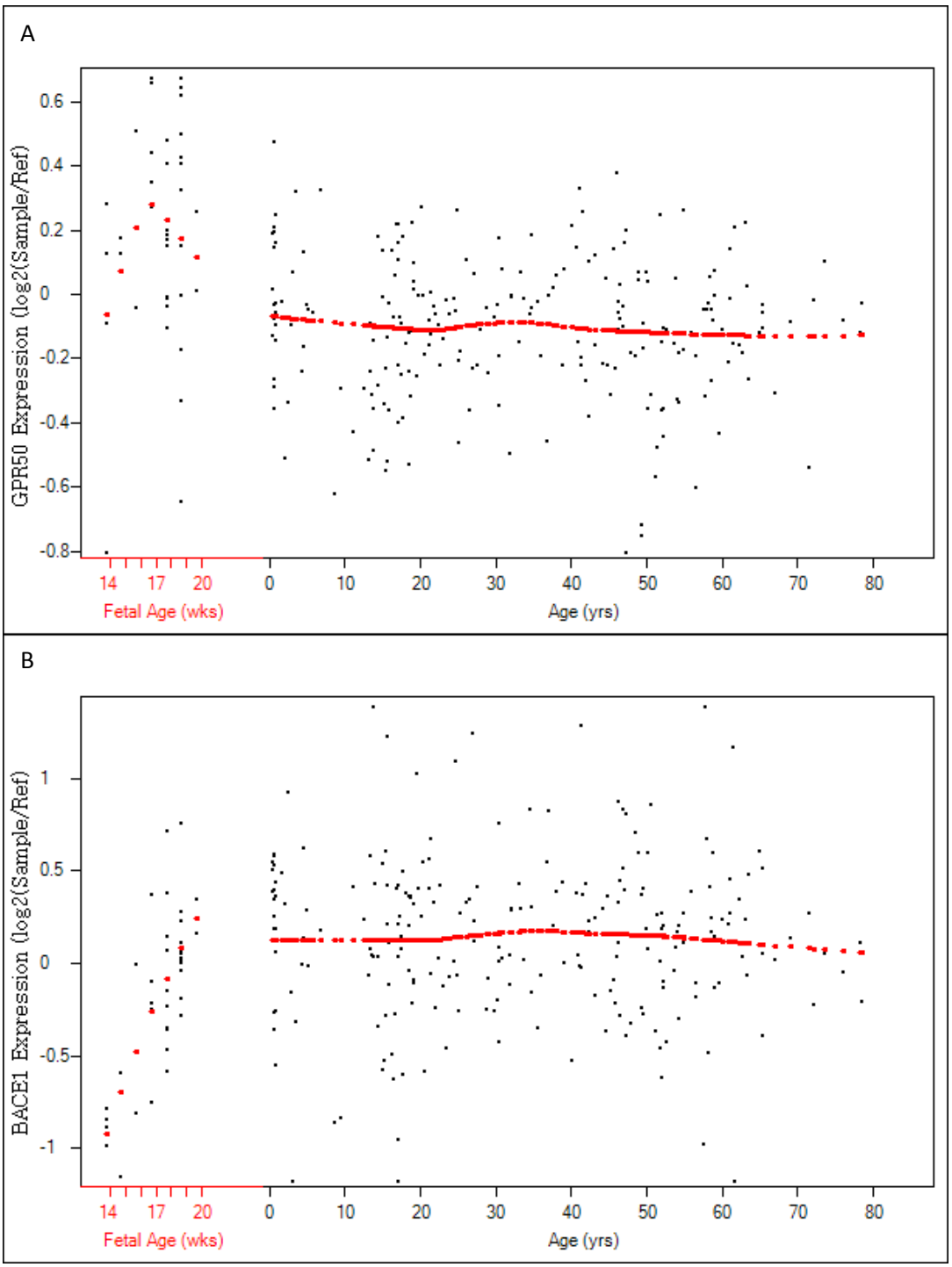

Figure 6.1 The mRNA expression profiles of GPR50 and BACE1 in human DLPFC, adapted from BrainCloud. The corresponding region of foetal samples was PFC. 500 ng of each total RNA sample was used for transcription to obtain the mRNA expression level. The age scale was demonstrated differently for prenatal subjects (in gestational weeks) than in all the other subjects who were sampled after birth (in years). Each black dot represents an individual subject. The red dots represent Loess fit (separate fit for foetal data and for the data sampled after birth).

6.3.1.1 Correlation between mRNA expression levels of GPR50 and BACE1 in human PFC during the prenatal stage

The timespan of prenatal stage in this dataset was from 14 to 20 weeks of gestation. The age of the prenatal subjects was not correlated with sex (p=0.266). The general linear model was run to assess the main effects of age and sex on GPR50 and BACE1 mRNA levels (Table 6.2). The ANOVA/ANCOVA analysis was used to test for differences. It is revealed that GPR50 levels were not affected by the foetal age (p=0.312) or sex (p=0.613). The prenatal BACE1 level was significantly associated with age ($p=3.2\times10^{-7}$), but not affected by sex (p=0.892). BACE1 mRNA level in PFC was positively correlated with the foetal age (r=0.736, $p=1.4\times10^{-7}$, Figure 6.2). Further, there was a trend of positive correlation between the mRNA levels of prenatal GPR50 and BACE1 in human PFC during the gestational week 14-20 (r=0.271, p=0.1, Table 6.3).

Table 6.2 The general linear model using gestational week and sex to predict prenatal GPR50 and BACE1 mRNA level in human PFC

A) GPR50	**F**	**P-value**	**Partial Eta Squared**	**B**
Corrected model Adjusted r^2=-0.023	0.580	0.565	0.032	
Week	1.054	0.312	0.029	1.761
Sex	0.260	0.613	0.007	0.075
B) BACE1	**F**	**P-value**	**Partial Eta Squared**	**B**
Corrected model Adjusted r^2=0.515	20.066	**1.2×10^{-6}****	0.541	
Week	39.581	**3.2×10^{-7}****	0.531	10.094
Sex	0.019	0.892	0.001	-0.014

**** p<0.01**

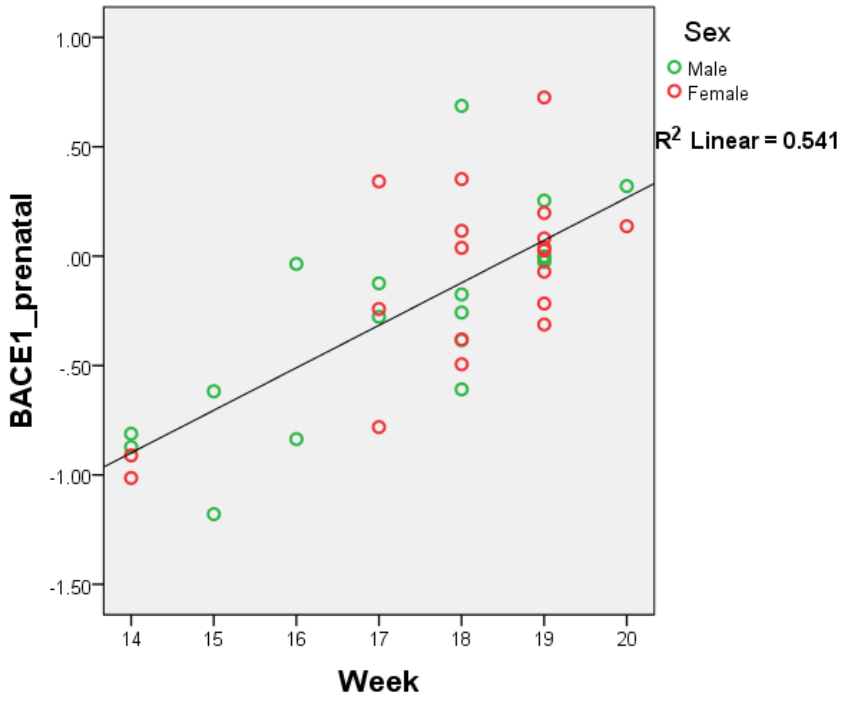

Figure 6.2 The scatterplot of prenatal BACE1 mRNA level and gestational week in human PFC

Table 6.3 The Pearson's correlation analysis of prenatal GPR50 and BACE1 mRNA levels during the gestational week 14-20 in human PFC

Correlations

Week 14-20		BACE1_prenatal
GPR50_prenatal	Pearson Correlation	0.271
	Sig. (2-tailed)	**0.100**
	N	38

6.3.1.2 Correlation between mRNA expression levels of GPR50 and BACE1 in human DLPFC sampled after birth

The age of subjects sampled after birth ranged from 2 days to 78.23 years. The age of the "after birth" subjects was not correlated with sex (p=0.191). The general linear model was run to assess the main effects of age and sex on GPR50 and BACE1 mRNA levels. The ANOVA/ANCOVA analysis was used to test for differences. The mRNA expression of neither GPR50 nor BACE1 was affected by age or sex (p>0.05, Table 6.4). However, the levels of GPR50 and BACE1 mRNA after birth were negatively correlated, even though the correlation was very week (r=-0.140, p=0.033, Table 6.5, Figure 6.3).

Table 6.4 The general linear model using age and sex to predict GPR50 and BACE1 mRNA level in human DLPFC sampled after birth

A) GPR50	F	P-value	Partial Eta Squared	B
Corrected model Adjusted r^2=-0.004	0.559	0.573	0.005	
Age	0.855	0.356	0.004	-0.001
Sex	0.185	0.667	0.001	0.013
B) BACE1	**F**	**P-value**	**Partial Eta Squared**	**B**
Corrected model Adjusted r^2=-0.008	0.061	0.940	0.001	
Age	0.002	0.968	0.000	5.6×10^{-5}
Sex	0.123	0.726	0.001	0.022

Table 6.5 The Pearson's correlation analysis of GPR50 and BACE1 mRNA levels in human DLPFC sampled after birth

Correlations

		BACE1_after birth
GPR50_after birth	Pearson Correlation	-0.140
	Sig. (2-tailed)	**0.033***
	N	231

*. Correlation is significant at the 0.05 level (2-tailed).

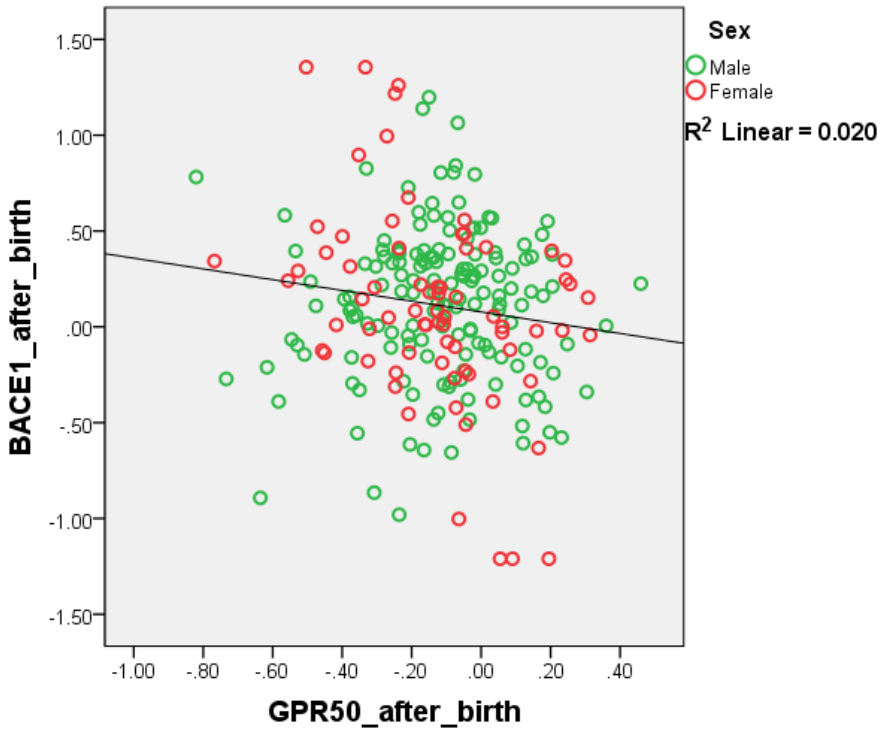

Figure 6.3 The scatterplot of mRNA levels of GPR50 and BACE1 in human DLPFC sampled after birth

Next, a general linear model to predict BACE1 mRNA level after birth (BACE1_*after birth*) was fitted using sex, age and GPR50 mRNA level after birth (GPR50_ *after birth*) as main effects and including the interaction term of sex and GPR50_ *after birth*, age and GPR50_ *after birth* (Table 6.6). The age of the subjects or the interaction of age and GPR50_ *after birth* did not have significant effects ($p>0.05$), while the sex had a trend of influencing BACE1_ *after birth* ($p=0.054$). Interestingly, both GPR50_ *after birth* ($p=0.029$) and the interaction of sex and GPR50_ *after birth* had a significant effect on BACE1_ *after birth* ($p=0.002$). Importantly, the correlation between GPR50_ *after birth* and BACE1_ *after birth* occurred in female subjects ($r=-0.372$, $p=0.001$), but not in male subjects ($r=0.0024$, $p=0.977$) (Figure 6.4).

Table 6.6 The general linear model with the interaction term to predict BACE1 mRNA level in human DLPFC sampled after birth

BACE1_after birth	F	P-value	Partial Eta Squared	B
Corrected model Adjusted r^2=0.041	2.962	**0.013***	0.062	
Age	0.060	0.806	0.000	0.000
Sex	3.761	**0.054$^{\$}$**	0.016	0.136
GPR50_ after birth	4.807	**0.029***	0.021	-0.968
Age × GPR50_ after birth	0.338	0.562	0.001	0.863
Sex ×GPR50_ after birth	9.849	**0.002****	0.042	0.004

**** p< 0.01 level, * p< 0.05, $^{\$}$p< 0.1.**

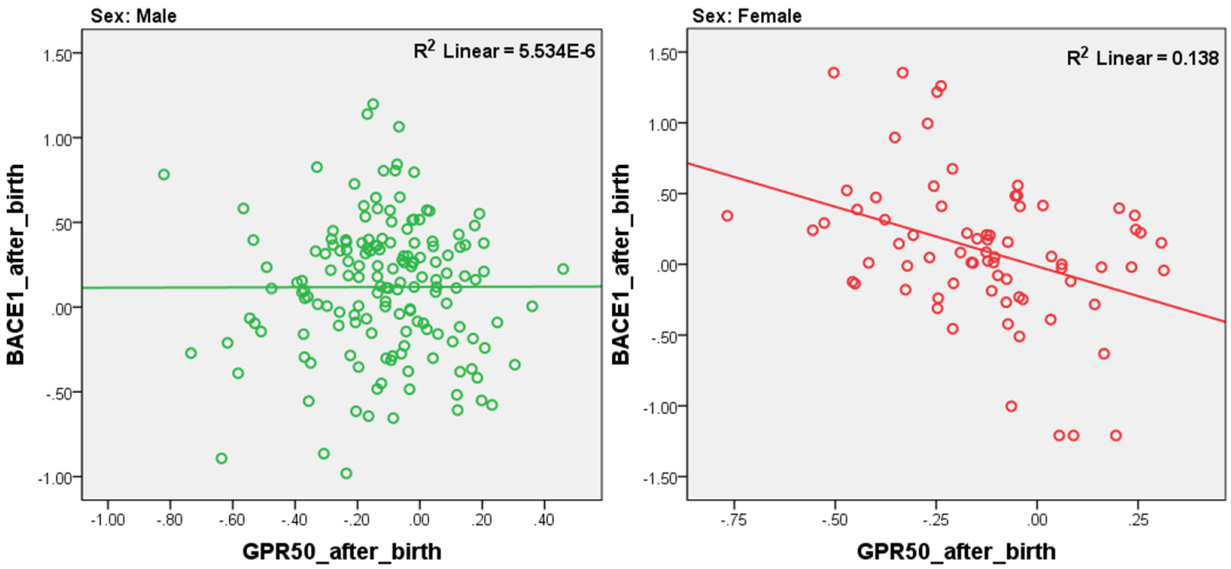

Figure 6.4 The scatterplot of mRNA levels of GPR50 and BACE1 in human DLPFC sampled after birth in male and female subgroups

6.3.2 The mRNA levels of Gpr50 and Bace1 in Balb/c mouse

Next, the mRNA expression of Gpr50 and Bace1 in mice was investigated using the data retrieved from the BrainStars database. All these mice had the same strain (Balb/c), age (5 weeks, adult) and sex (male). The analysis was designed to study the mRNA levels of Gpr50 and Bace1 across sub-regions of the mouse brain. The mRNA expression profiles of Gpr50 and Bace1 in 51 CNS regions of adult Balb/c mouse (Table 6.1) are shown in Figure 6.5 and 6.7 (adapted from BrainStars). Gpr50 mRNA was expressed with dominant levels in the median eminence (ME) and the arcuate hypothalamic nucleus (Arc). Bace1 mRNA had expression in multiple brain regions, with the highest levels in the lateral septal nucleus (LS), the supraoptic nucleus (SO) and the cerebellar nucleus (Cb nucleus). Interestingly, these three areas with robust Bace1 expression had lowest Gpr50 levels, while some other areas with high Gpr50 expression, for instance the median eminence, had minor Bace1 levels.

The mRNA levels of Gpr50 and Bace1 across all the 51 CNS regions of adult Balb/c mouse were negatively correlated in general, revealed by Pearson's correlation analysis ($r=-0.398$, $p=0.004$, Table 6.7, Figure 6.7.A). Further analysis showed that, there was a significantly negative correlation between the mRNA levels of the two genes across the telencephalon sub-regions ($r=-0.496$, $p=0.043$, Figure 6.7.B). A trend of significance was identified across the sub-regions of hypothalamus ($r=-0.523$, $p=0.081$). No significant correlation of Gpr50 and Bace1 mRNA was found across the thalamus ($p=0.570$) or the mesencephalon ($p=0.239$). The relationship between the levels of the two genes was not investigated in sub-regions (pons, cerebellum, spinal cord, misc) with less than 4 data points.

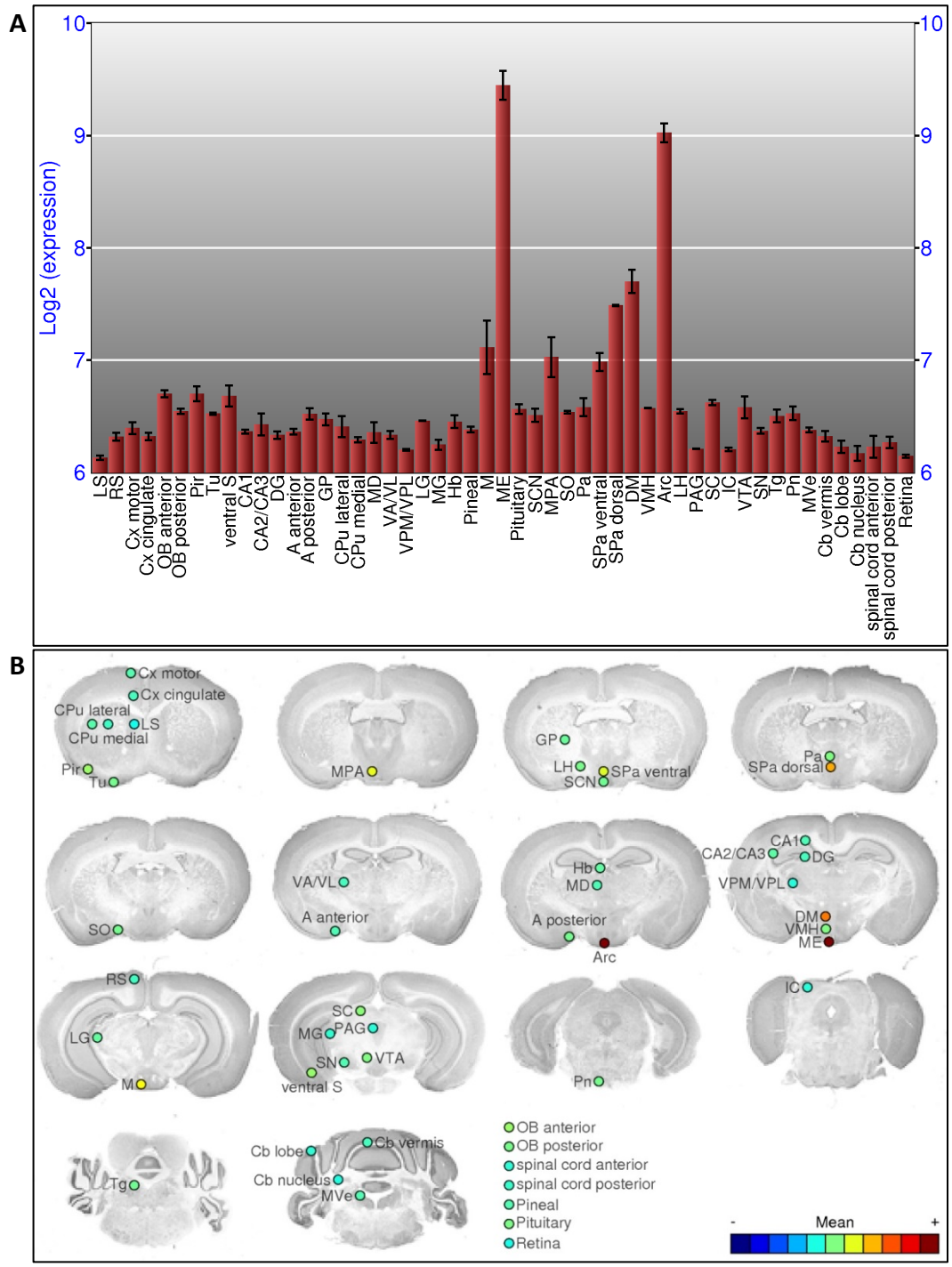

Figure 6.5 The expression profile and distribution map of Gpr50 mRNA in 51 CNS regions of adult Balb/c mouse. The figures were cited from BrainStars. For abbreviations of the brain regions, see Table 6.1.

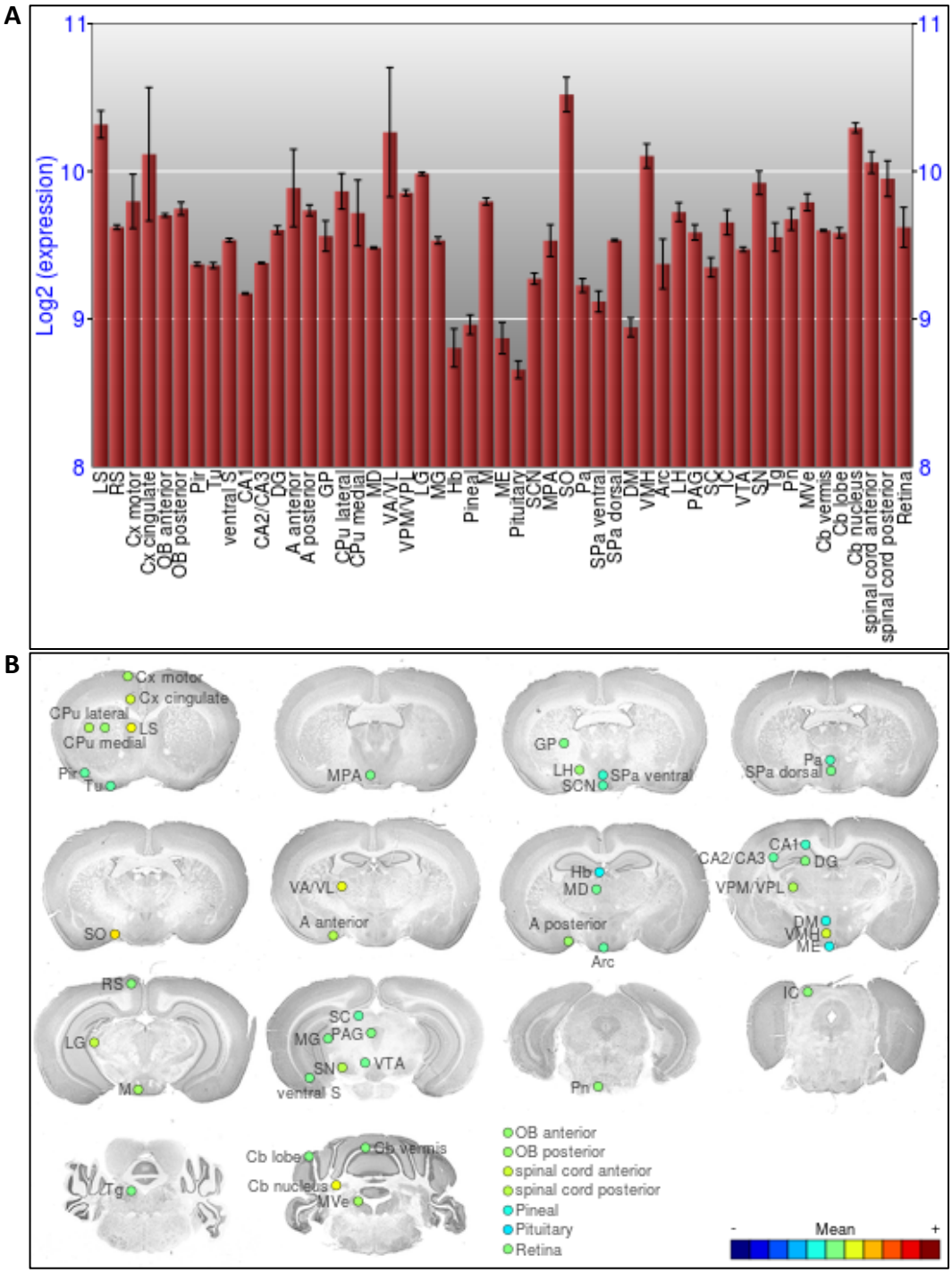

Figure 6.6 The expression profile and distribution map of Bace1 mRNA in 51 CNS regions of adult Balb/c mouse. The figures were cited from BrainStars. For abbreviations of the brain regions, see Table 6.1

Table 6.7 The Pearson's correlation analysis of adult mouse Gpr50 and Bace1 mRNA levels across 51 CNS regions and across CNS sub-regions of adult Balb/c mouse

	N	r	P-value
All 51CNS regions	51	-0.398	**0.004****
Telencephalon	17	-0.496	**0.043***
Thalamus	6	-0.296	0.570
Hypothalamus	12	-0.523	**0.081**$**
Mesencephalon	6	-0.569	0.239
Pons	2	-	-
Cerebellum	3	-	-
spinal cord	2	-	-
Misc	3	-	-

**** p< 0.01 level, * p< 0.05, $p< 0.1, - not tested (N<4)**

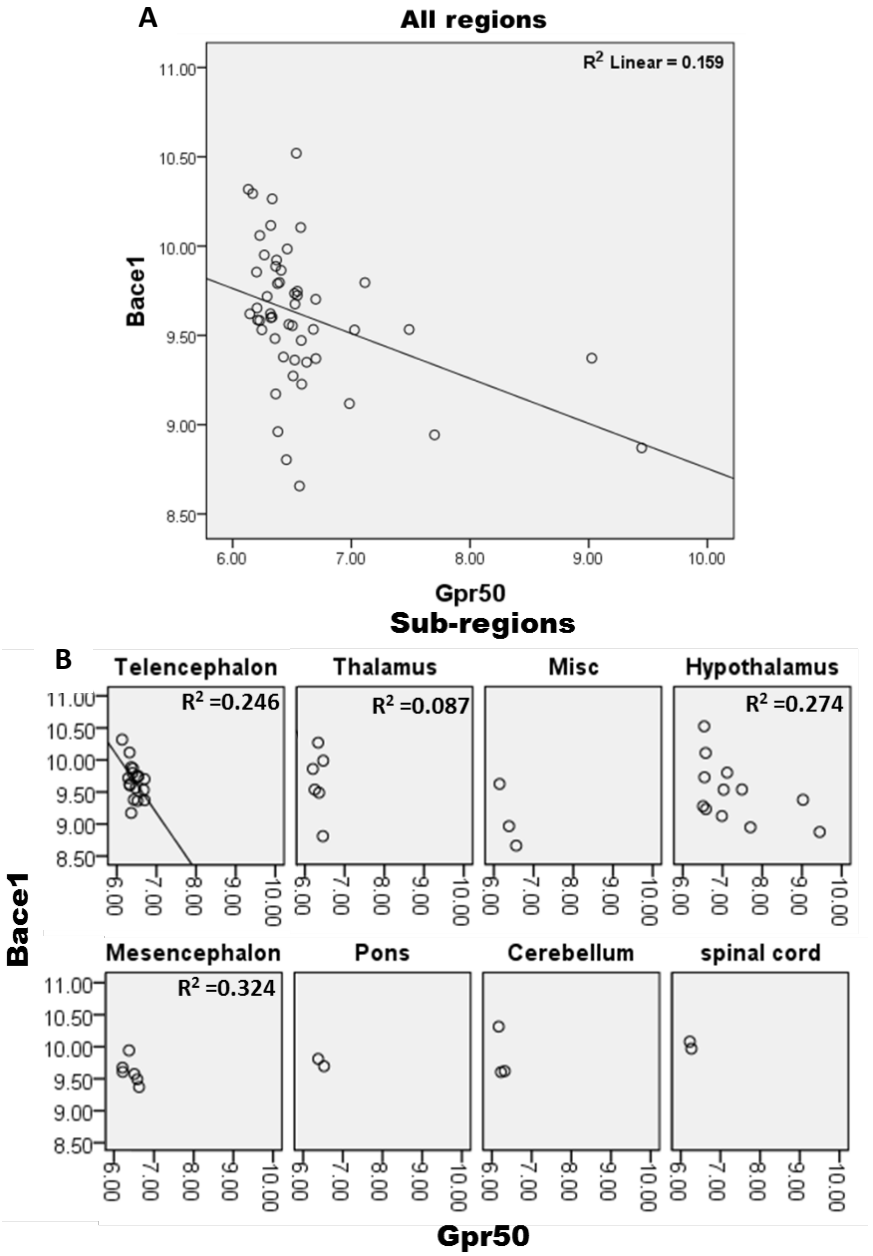

Figure 6.7 The scatterplots of mRNA levels of Gpr50 and Bace1 across different CNS regions of adult Balb/c mouse in A) all 51 CNS regions and B) sub-regions of CNS. Misc: retina, pineal and pituitary.

6.3.3 The protein levels of endogenous Gpr50 and Bace1 across the brain regions of wild-type C57BL/6 mice

Three brains of female adult C57BL/6 mice were used to investigate the protein levels of endogenous Gpr50 and Bace1 by fluorescent immunohistochemistry (IHC).

6.3.3.1 The detection of Bace1 protein in adult mouse brain by immunohistochemistry

The specific staining by the BACE1 rabbit2 antibody in adult mouse brain was verified through the pre-absorption with its blocking peptide (Figure 6.8). The BACE1 goat antibody co-localised with the BACE1 rabbit2 antibody in most of brain regions (Figure 6.9.A, an example of the cortical area). However, an additional signal was detected only by the BACE1 goat antibody in the thalamic region (Figure 6.9.B). The difference in the detection by these two antibodies might be related to their different antigens, as the antigen of BACE1 rabbit2 antibody is within the cytosolic C-terminal, while the antigen of BACE1 goat antibody is located at the extracellular N-terminal. The peptide for the goat antibody was not available to further test its specificity in the IHC application. Therefore, the BACE1 rabbit2 antibody was used in the following IHC experiments.

It was found that Bace1 protein was widely distributed across the coronal section of adult mouse brain (Figure 6.10), with high expression levels at the amygdalar nucleus, the endopiriform nucleus, the neuronal layer II/III/V of isocortex, the CA2 of hippocampus, the arcuate nucleus and the dorsomedial nucleus of the hypothalamus; moderate levels in layer IV of the isocortex, the CA1/CA3 and the dentate gyrus of the hippocampus, the ventromedial hypothalamic nucleus and the lateral hypothalamic area; nearly not detectable in the thalamic region (by the BACE1 rabbit2 antibody). The olfactory bulb and the cerebellum were not tested in this experiment. The high levels of Bace1 protein in the cortex and hippocampus of C57BL/6 mice was in line with the robust expression of Bace1 mRNA in these areas.

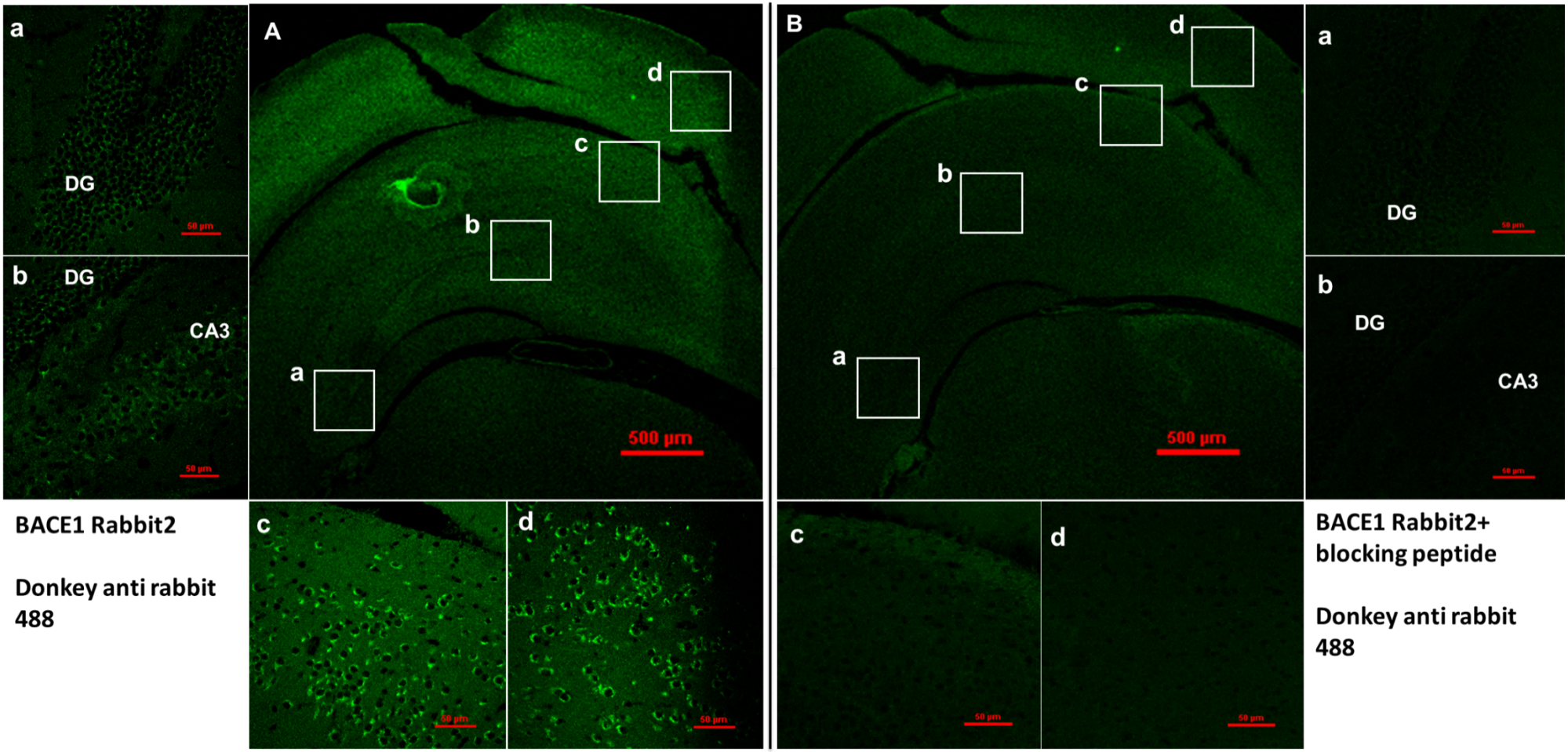

Figure 6.8 Immunostaining of Bace1 in adult mouse brain by A) BACE1 rabbit2 antibody; B) BACE1 rabbit2 antibody pre-incubated with its blocking peptide. This was a coronal section of a female C57BL/6 mouse brain. The dissected position was roughly at Bregma: -2.75 mm. a-c: hippocampal sub-fields; d: cortex. CA3: Cornu Ammonis region 3 of hippocampus; DG: dentate gyrus region of hippocampus.

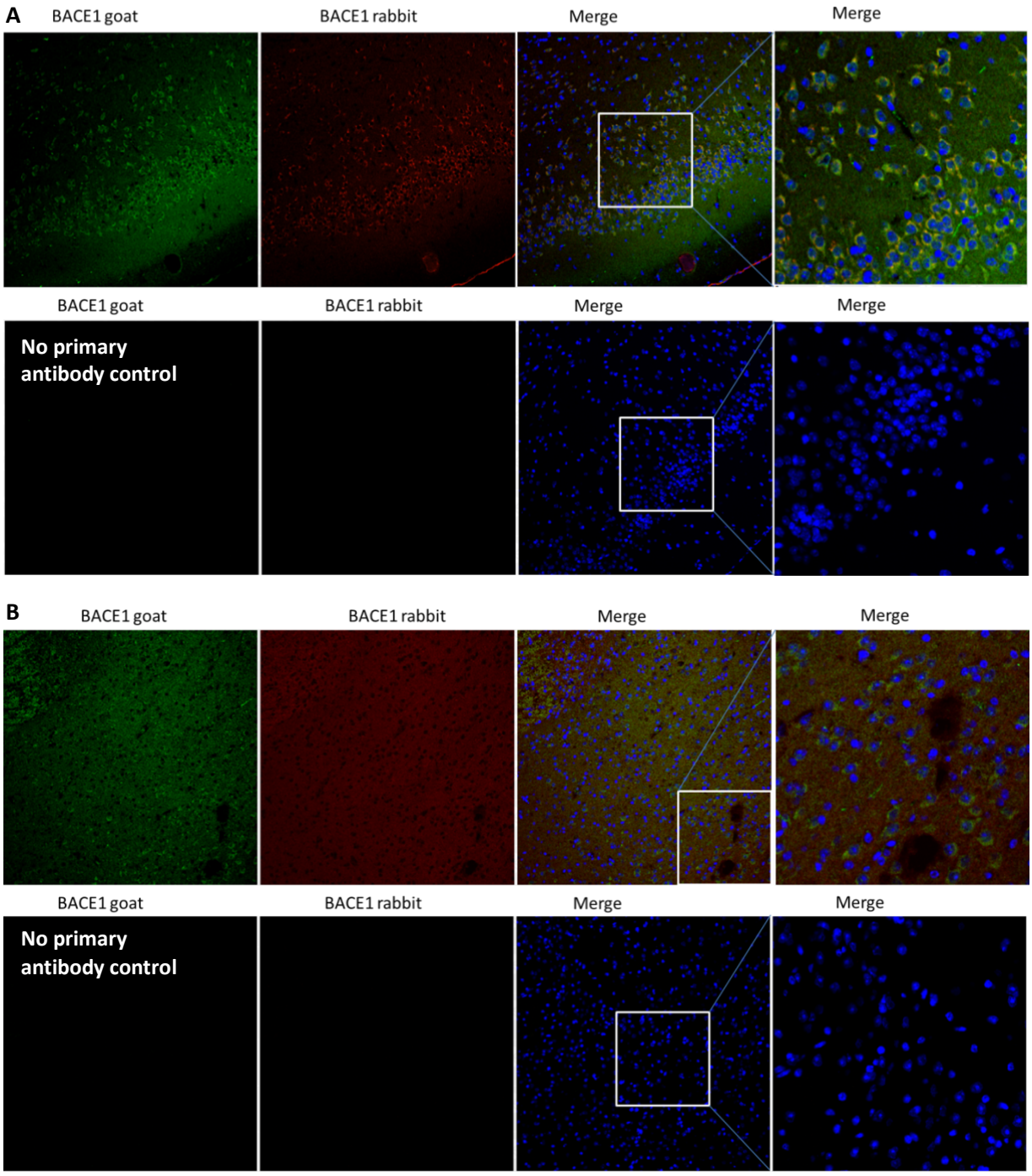

Figure 6.9 Bace1 co-staining by rabbit2 and goat antibodies in A) cortex and B) thalamus of a coronal slice of adult mouse brain.

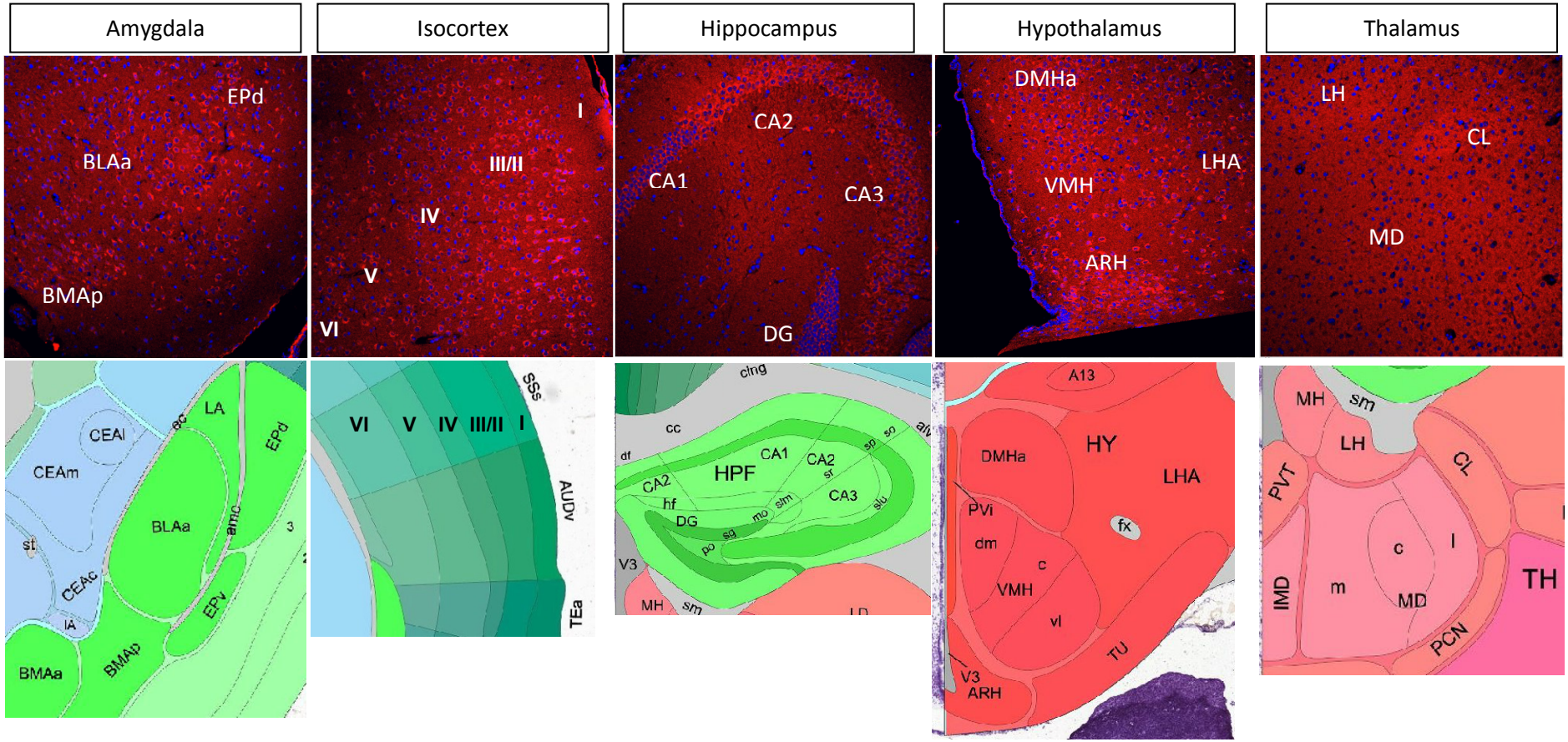

Figure 6.10 The expression of Bace1 protein in adult mouse brain. BLAa: basolateral amygdalar nucleus, anterior part; BMAp: basomedial amygdalar nucleus, posterior part; EPd: endopiriform nucleus, dorsal part; I-VI: layer I-VI of cortex; CA1-3: Cornu Ammonis 1-3; DG: dentate gyrus; ARH: arcuate hypothalamic nucleus; DMHa: dorsomedial nucleus of the hypothalamus, anterior part; VMH: ventromedial hypothalamic nucleus; LHA: lateral hypothalamic area; LH: lateral habenula; MD: mediodorsal nucleus of the thalamus; CL: central lateral . The map in the bottom panel was adapted from the Allen Brain Atlas.

6.3.3.2 The co-localisation of Gpr50 and Bace1 in the brain of female adult C57BL/6 mouse

The expression levels of Gpr50 protein in female CD1 adult mouse have been investigated previously (Grunewald et al, 2012). I repeated this experiment using the same IHC protocol and the same GPR50 goat antibody in female C57BL/6 adult mouse brain (olfactory bulb and cerebellum not included). I found similar expression pattern and distribution of endogenous Gpr50 in C57BL/6 mice although with several differences from CD1 mice (Table 6.8). The high level of Gpr50 protein in the hypothalamus of C57BL/6 mice was identical to what was observed for CD1 mice (Grunewald et al, 2012). Gpr50 was also found strongly expressed in the cortical region, especially in the entorhinal cortex, piriform cortex and amygdala. While Gpr50 expression was only identified in the dentate gyrus (DG) of the hippocampus in CD1 mice (Grunewald et al, 2012), I also saw highly expressed Gpr50 in the pyramidal layer of CA1, CA2 and CA3 in C57BL/6 mice. Previously, it was reported that Gpr50 is expressed in the pyramidal layer of CA1 in female Wistar rat, but not in male C57BL/6 mouse using a different antibody (Batailler et al, 2012). Therefore, there might be differences in expression levels of Gpr50 protein between species, strains or sexes.

Next, Gpr50 and Bace1 were doubly immunostained in adult mouse brain. There was no cross-immunoreactivity between primary antibodies GPR50 goat/BACE1 rabbit2 and the secondary antibodies for other species (shown by immunocytochemistry in chapter 2, Figure 2.22). Here, the no primary antibody control showed a clean background (Figure 6.11), which guaranteed that there was no unspecific staining from the secondary antibodies or auto-fluorescence in the brain tissue.

The co-labelling of the two proteins was found in several areas (Figure 6.12, Table 6.8). The strongest co-localisation occurred in the CA2 pyramidal neurons of hippocampus, the neuronal layer II/III/V of isocortex and the dorsomedial nucleus of the hypothalamus. Weaker co-localisation of Gpr50 and Bace1 was found at the basolateral amygdalar nucleus and the ependymal layer of the third ventricle. Interestingly, Gpr50 and Bace1 appeared to only co-localise in a certain type of cells in the basolateral amygdala (BLA). BLA contains two main cell types (Pare & Gaudreau, 1996). The most common type is a spiny multipolar neuron with a dominant dendrite giving it a pyramidal appearance. These cells are excitatory

projection neurons because they have long axons. Gpr50 and Bace1 seemed to co-localise in this type of neurons. The second cell type consists of a morphologically heterogeneous group of less spiny neurons with a locally ramifying axon (Pare & Gaudreau, 1996). There were particularly high levels of Gpr50 in the second type of neurons. This is intriguing, as these neurons are immunoreactive for GABA (McDonald & Augustine, 1993), and thus may be the site where GPR50 interacts with proteins related to GABA transmission such as PICK1, SLC12A5/ KCC2, MADD, identified by the yeast two-hybrid study (Grunewald et al, 2009). In addition, there was no clear co-localisation in the thalamus, as very little if any Bace1 was detected.

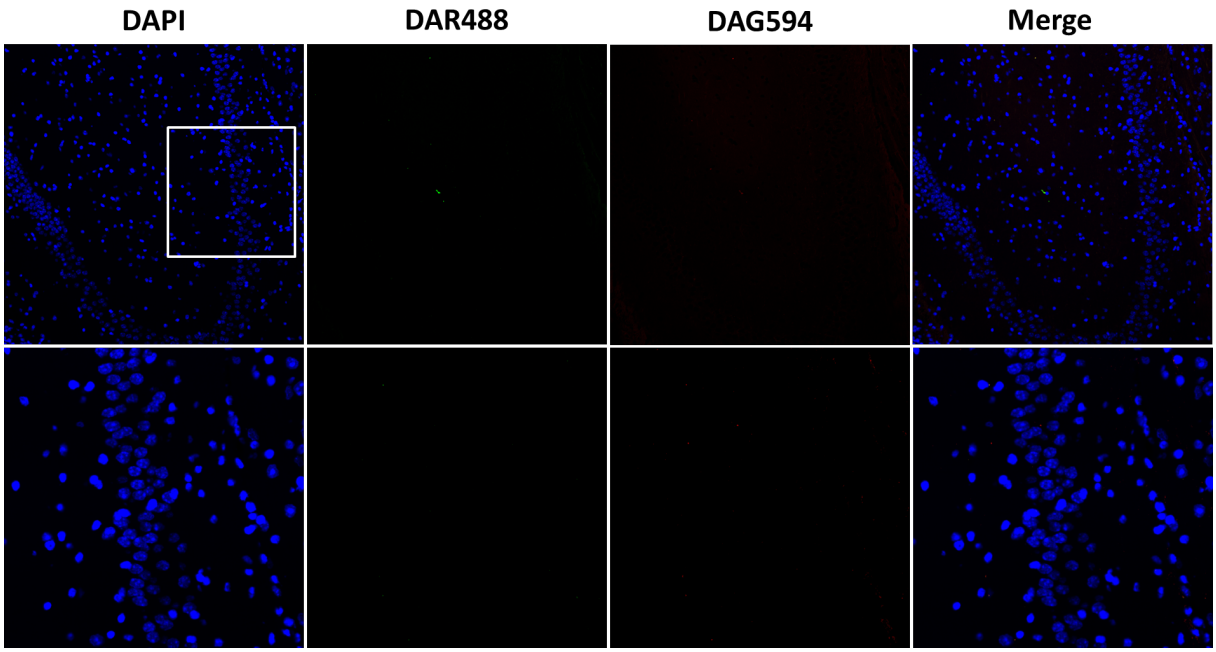

Figure 6.11 No primary antibody control for fluorescent IHC in adult mouse brain. The brain section was stained according to the normal IHC protocol. The incubation of primary antibodies GPR50 goat and BACE1 rabbit2 were skipped. DAR488: secondary antibody donkey-anti-rabbit 488; DAG594: secondary antibody donkey-anti-goat 594. The white square in the top panel indicated an enlarged area represented in the bottom panel.

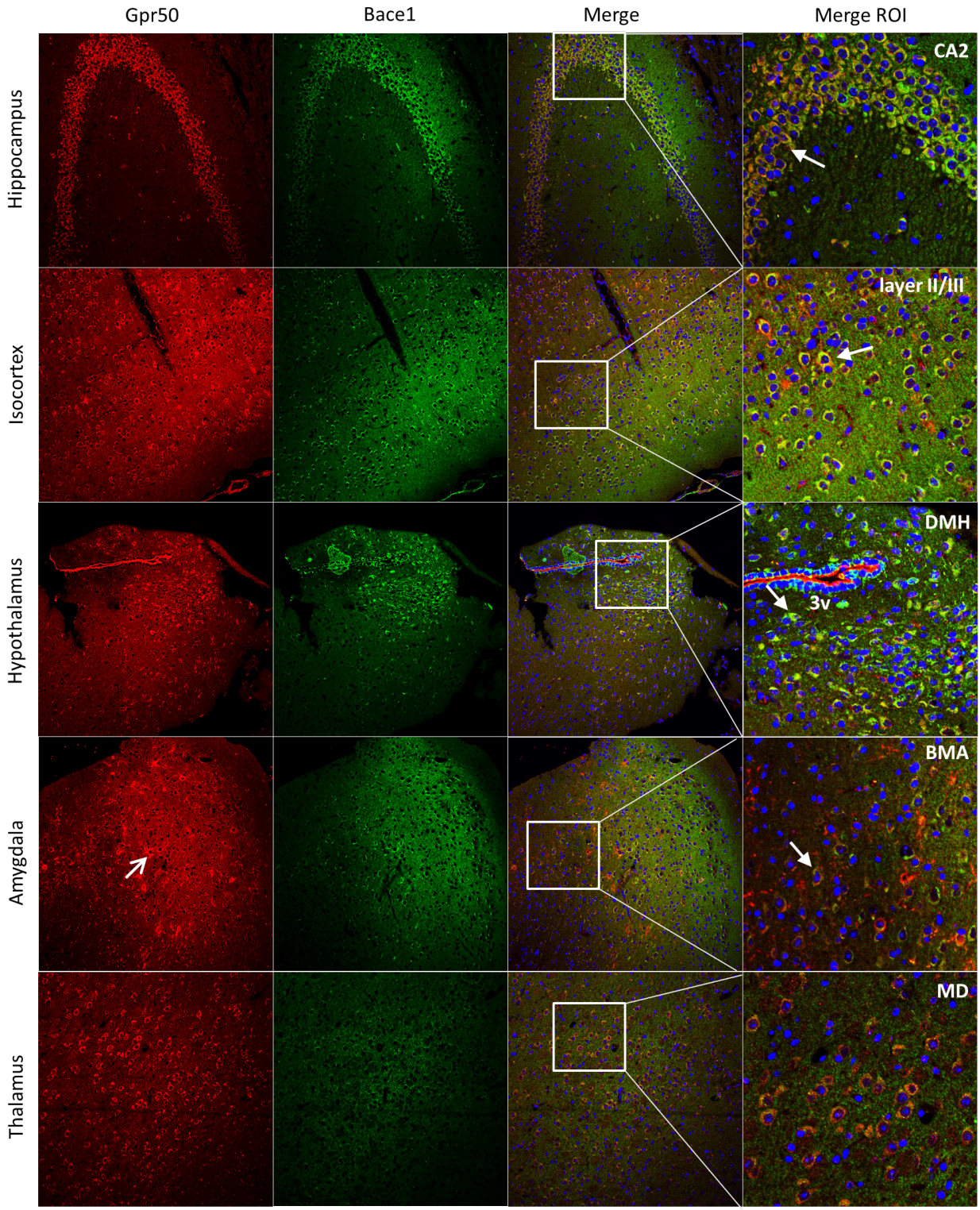

Figure 6.12 Co-localisation of Gpr50 and Bace1 in C57BL/6 mouse brain. CA2: Cornu Ammonis region 2 of hippocampus; layer II/III: neuronal layer II/III of isocortex; BLA: basolateral amygdalar nucleus; DMH: dorsomedial nucleus of the hypothalamus; 3v: the third ventricle; MD: mediodorsal nucleus of the thalamus. The solid-head arrows indicated potential cells with co-localisation of Gpr50 and Bace1. The open-head arrow indicated a type of neurons in BLA with particularly high levels of Gpr50.

Table 6.8 The distribution of endogenous Gpr50 and Bace1 in adult female C57BL/6 mouse brain and the co-localisation between the two proteins

Region	Gpr50 protein level*	Bace1 protein level	Co-localisation
Isocortex	**++**	**+++**	√
Frontal cortex	×	++	×
Posterior cortex	×	++	×
Motor cortex	+	++	×
Somatosensory cortex	++	+++	√
Visual cortex	++	+++	√
Entorhinal cortex	++ (→ +++)	+++	√
Piriform cortex	++ (→ +++)	+++	√
Olfactory Bulb	***NA***	***NA***	***NA***
Hippocampus	**+ (→ +++)**	**+++**	√
Dentate gyrus medial blade polymorph layer	+ (→ ++)	++	√
CA1 pyramidal layer	- (→ +++)	++	√
CA2 pyramidal layer	- (→ +++)	+++	√
CA3 pyramidal layer	- (→ +++)	++	√
Amygdala	**++ (→ +++)**	**++**	√
Striatum	**-**	**-**	**×**
Thalamus	**++**	**-**	**×**
Hypothalamus	**+++**	**+++**	√
suprachiasmatic nucleus	++	NA	NA
paraventricular nucleus	+	+	×
ependyma of 3rd ventricle	+++	+	√
dorsomedial hypothalamus	++ (→ +++)	+++	√
ventromedial hypothalamus	++	++	√
lateral hypothalamus	+	++	√
arcuate nucleus	++	+++	√
median eminence	++	+	NA
Cerebellum	**+**	***NA***	***NA***
Purkinje cell layer	+	NA	NA
Cerebellum other	-	NA	NA

* The protein levels of Gpr50 in female CD1 adult mouse were adapted from (Grunewald et al, 2012). Similar expression levels were observed in C57BL/6 mouse (using the same IHC protocol and GPR50 goat antibody). Alterations were marked by symbols in the parentheses.
+++: strong expression, ++: moderate expression, +: low expression, -: no expression, NA: not investigated, √: co-localised, ×: not co-localised.

6.4 Discussion

In this chapter, I investigated the expression patterns of GPR50 and BACE1, as well as the correlation of their levels in human brain and mouse brain. In human prefrontal cortex (PFC) during the prenatal stage (week 14-20), the mRNA levels of GPR50 and BACE1 appeared to have a trend of positive correlation. This is expected, as multiple genes with neuronal functions are up-regulated during the foetal development. Yet, the expression of the two genes was negatively correlated in human dorsolateral prefrontal cortex (DLPFC) of subjects sampled after their birth, and this suggests additional roles of GPR50 and BACE1 across the life span, apart from their overlapping function in neuronal development. The negative correlation between the mRNA levels of the two genes was also seen across the central nervous system (CNS) in male Balb/c mice at a time point of 5 weeks (early adolescence for mice). Interestingly, this negative co-regulation of Gpr50 and Bace1 seems to be enriched in the telencephalon and the hypothalamus sub-regions, in which the co-localisation of their proteins was found in adult C57BL/6 mice.

6.4.1 The co-expression of GPR50 and BACE1 in human PFC

Human PFC has been widely investigated due to its crucial role in memory, personality, social behaviour and executive function. The expression correlation of certain genes in this region can provide clues to understanding its development, functions and related disorders. For instance, *De novo* mutations in a number of genes that function in the neurogenesis in the foetal prefrontal cortex (dorsolateral and ventrolateral) are critical to the pathophysiology of schizophrenia, and these genes formed a network significantly enriched for transcriptional co-expression and protein-protein interaction (Gulsuner et al, 2013).

6.4.1.1 GPR50 and BACE1 in human PFC during the prenatal stage

The function of GPR50 might be implicated in the physiological activities that occur during the foetal week 17, as its mRNA level reached a peak in this week. In the PFC at 17 weeks of gestation, large mature pyramidal neurons appeared in the interface of the middle and low third of the cortical plate (Mrzljak et al, 1988). These neurons had basal dendrites with growing secondary structures and apical dendrites extending to the outer part of the marginal zone. Therefore, the peak of prenatal GPR50 expression might be associated with the maturation, in particular the extension of the

pyramidal neurons in the cortical plate of the PFC. This is in line with the function of GPR50 in promoting neurite outgrowth (Grunewald et al, 2009). Also, the week 17 of human gestation is a time point when additional types of neurons was seen in the subplate zone of the PFC, such as the inverted pyramidal neurons (Mrzljak et al, 1988). Hence, GPR50 may be also related to certain processes of neurogenesis.

The BACE1 mRNA level in human PFC increased persistently during the gestational weeks 14-20. The cellular growth in the human foetal forebrain can be divided to two-phases, an exponential phase from 13 to 20 weeks of gestation and a linear increasing phase from approximately 22 weeks of gestation to term (Samuelsen et al, 2003). The exponential phase appeared to correspond to a robust process of neurogenesis before gestational week 20 (Malik et al, 2013). Therefore, my observation supports a role of BACE1 in neuronal development, which has been suggested by its cleavage of neural cell adhesion molecules (Hitt et al, 2012). Furthermore, this function of BACE1 is most likely to be related to Notch signalling, which controls the balance of neurogenesis and astrogenesis in the hippocampus during early development and can be induced by BACE1 cleavage of Jagged1 (Hu et al, 2013a).

GPR50 and BACE1 have overlapping roles in neuronal development. This agrees with my finding that their RNA levels in PFC demonstrated a trend of positive correlation during gestational weeks 14-20. As GPR50 is involved in the regulation of β-secretase activity {(Grünewald, 2011); my chapter 4}, it is worthwhile to further investigate if GPR50 has a role in balancing the release of active neural cell adhesion molecules.

6.4.1.2 GPR50 and BACE1 in human DLPFC sampled after birth

In subjects whose samples were collected after birth, the mRNA levels of GPR50 and BACE1 in DLPFC were negatively correlated, opposite to the trend in the prenatal subjects. Interestingly, this negative correlation was contributed by their levels in females. Therefore, the co-regulation of GPR50 and BACE1 expression in human DLPFC from the period of postnatal development to adulthood was sex-specific.

Previous studies have shown that the functions of both GPR50 and BACE1 are related to females. The association of GPR50 gene polymorphism with mental

disorders increased in significance in female subjects (Thomson et al, 2005). Elsewhere, the regulation of BACE1 expression and function has a link to females, as a recent study showed that BACE1 mRNA and protein levels could be down-regulated, thus reducing amyloid plaque formation in the brain of aromatase-deficient APP transgenic mice after estrogen treatment (Li et al, 2013). Thus, my results strengthened the importance of investigations on the function of GPR50 and BACE1 in terms of the striking physiological differences between sexes. For example, studies of the signalling system mediated by sex hormones are helpful to elucidate the roles of GPR50 and BACE1, as well as their association in brain illnesses. Further analysis of the correlation between GPR50 and BACE1 expression can be performed in the female "after birth" subset with the life scale being divided into periods related to estrogen, such as before menstrual onset, during menstrual period and after menopause.

6.4.2 The co-expression of Gpr50 and Bace1 in mouse brain

In Balb/c adult mouse, the mRNA levels of Gpr50 and Bace1 were negatively correlated across multiple CNS regions. This correlation appeared to result from their levels across the telencephalon and the hypothalamus. The co-regulation of these two genes might be associated with their functional interaction in relevant areas, such as in the brain sub-regions observed with co-localisation of their proteins in C57BL/6 mouse.

6.4.2.1 The co-expression of Gpr50 and Bace1 in the CA2 region of mouse brain

GPR50 and BACE1 may have cooperating functions in the brain activities that are related to memory, as the two proteins are strongly co-localised in the hippocampus of the adult mouse brain, especially the CA2 sub-field. CA2 appears to be located at the key position of the cortico-hippocampal disynaptic circuit, as its pyramidal neurons are strongly excited by their distal dendritic inputs from the entorhinal cortex, and in turn excite the neurons in CA1 (Chevaleyre & Siegelbaum, 2010). Recent studies showed that the regulation of plasticity at CA2 synapses might play a role in different sorts of learning and memory, including the hippocampus-dependent spatial memory, contextual learning and social recognition memory (Chevaleyre & Siegelbaum, 2010; Hitti & Siegelbaum, 2014; Wintzer et al, 2014).

My results showed that BACE1 is a CA2-enriched molecule. Even though BACE1 overexpression caused damage to memory in BACE1 transgenic mice and BACE1 deletion seems to rescue those deficits in AD mice (Ohno et al, 2007; Ohno et al, 2004), it is not clear whether the phenotypes are related to BACE1 levels or Aβ amounts. BACE1 knockout mice exhibited an age-dependent deficit in spatial reference memory and had synaptic dysfunctions in the CA1 and the CA3 (Laird et al, 2005; Wang et al, 2014a; Wang et al, 2008a). Therefore, the normal function of BACE1 is related to cognition. No BACE1 loss-of-function studies so far have been performed in the CA2 region, possibly because of the difficulty in distinguishing this structure. However, it will be interesting to do so, as the high expression level in CA2 may reveal new explanations for the link of BACE1 function to different sorts of memory. Gpr50 expression is almost equally high in the pyramidal neurons of CA1, CA2 and CA3. The protein of GPR50 was found in postsynaptic densities {(Grunewald et al, 2012); my chapter 3}, the components of which are closely related to the molecular mechanisms of learning and memory (Nagura et al, 2012; Nicholson et al, 2004). Thus, the hippocampal expression of GPR50 may suggest that the function of this protein is associated with the maintenance of memory and learning ability and its interaction with BACE1 in CA2 relating to synaptogenesis and synaptic plasticity is a good start to study this hypothesis. This will help to understand the role of GPR50 and BACE1 in neuronal development in a later postnatal stage.

6.4.2.2 The co-expression of Gpr50 and Bace1 in the hypothalamus of mouse brain

The hypothalamic co-expression of Gpr50 and Bace1 proteins in C57BL/6 mice was mainly observed in the arcuate nucleus (ARH) and the dorsomedial nucleus (DMH). One should be aware that the Bace1 mRNA level in the DMH of Balb/c mice was relatively low compared to C57BL/6 mice. This genetic diversity might reflect a behavioural or physiological difference in relation to the function of DMH between the two strains.

The level of corticosterones in GPR50 knockout (KO) mice was elevated (Ivanova et al, 2008), which indicates that GPR50 expression under normal conditions might be associated with the suppression of glucocorticoid overproduction, which is stimulated by corticotropin. Proopiomelanocortin (POMC) is the precursor molecule of intermedin, corticotropin, β-endorphin and Met-enkephalin. A previous study in

C57BL/6 mice showed that Bace1 in ARH was expressed in 30% POMC neurons (Meakin, 2013). Thus, the co-localisation of Gpr50 and Bace1 in ARH may suggest that the physical association of the two proteins is correlated with the hormone releasing in the hypothalamic-pituitary-adrenal (HPA) axis. Bace1 was not co-localised with appetite-inducing neuropeptide Y (NRY) or agouti-related peptide (AgRP) (Meakin, 2013). However, the deletion of Bace1 gene resulted in an enhanced expression of NRY/AgRP, which might be associated with the increasing appetite in BACE1 KO mice (Meakin et al, 2012). Interestingly, the deletion of Gpr50 gene did not have effects in the levels of NRY/AgRP (Bechtold et al, 2012). This may indicate that the putative interaction of Gpr50 and Bace1 in ARH is less associated with food intake.

The high expression level of GPR50 in the DMH is closely related to the regulation of leptin signalling, as leptin deficient mice had decreased level of Gpr50 in the DMH, which is recovered by leptin feeding (Bechtold et al, 2012). This function of GPR50 in the maintenance of leptin efficacy is specific to thermogenesis, as GPR50 KO mice had lower expression of a thermogenin, uncoupling protein 1 and entered a state of topor when fasted (Bechtold et al, 2012). BACE1 KO mice also had alterations in leptin signalling. When on a high-fat diet, BACE1 KO mice were protective against the metabolic inefficiency in wild-type mice, as they were observed with improved glucose disposal and insulin sensitivity, and reduced leptin levels (Meakin et al, 2012). These measures of increased energy expenditure may be related to an increased thermogenesis, which could be suggested by the increased expression of uncoupling proteins in the brown adipose tissue and skeletal muscle. This apparent opposite role of GPR50 and BACE1 in energy expenditure might be associated with their negatively correlated trend of mRNA expression across the hypothalamus. In particular, the co-localisation of Gpr50 and Bace1 in the DMH may be linked with a balanced status of the leptin signalling in the process of thermogenesis.

6.4.3 Further studies

My results demonstrated that GPR50 and BACE1 have correlated expression with overlapping functions in certain areas of the brain, and this extends the findings in previous chapters that the two proteins interact putatively in cells. To reveal more evidence of the association between GPR50 and BACE1, it would be beneficial to

determine and correlate the expression levels and properties of the two proteins in human post-mortem brains of mentally related illnesses (i.e. AD, bipolar disorder, schizophrenia) or relevant animal models. By comparing with healthy/wild-type control, we may evaluate the possible modification of GPR50 and BACE1 as individual factors, as well as their co-operational effects upon development of brain diseases, thus the pathology related to the two factors will be better understood.

7 The investigation of Gpr50 expression in Alzheimer's disease model TgSwDI mice

7.1 Introduction

Results in previous chapters have provided clues for the function of GPR50 through its potentials in the regulation of BACE1 expression and activity in cultured cells, as well as their co-regulated expression pattern and co-localisation in the brain. To further investigate the role of GPR50 in the pathology of brain diseases, in this chapter, I made use of an Alzheimer's disease (AD) mouse model and examined the characteristics of Gpr50 expression during the process of Aβ deposition, which is one of the hallmarks of AD.

7.1.1 The investigation of AD in mouse models

During the last two decades, a number of AD mouse models have been generated in order to understand the etiological mechanism of AD, and to look for effective treatments of relative symptoms, as well as to perform preclinical tests of new drugs. These models have generally been created to recapitulate the known processing features of AD, together with the introduction of genetic risk factors to promote earlier pathology. Most models showed functionally defective cognition and amyloid plaques aggregation in the brain, but none of them exhibit the full range of human AD properties, particularly the occurrence of neuronal loss. Moreover, neurofibrillary tangles were generated only when human tau was overexpressed or mutant tau with a greater likelihood of forming tangles was used. The AD mouse models generally used can be divided into the following types {summarised from reviews (Chin, 2011; Hall & Roberson, 2012)}.

a) Human APP transgenic models

Both mutations in the APP sequence and a copy number increase of the APP gene can lead to the pathogenesis of AD. Aggregation of mouse Aβ is not as effective as that of human Aβ, probably because of the sequence differences of APP within the Aβ section between the two species (Hall & Roberson, 2012). Also, mouse Aβ is less efficient in causing cognitive deficits (Hall & Roberson, 2012). Overexpression of human APP, particularly with mutations is one of the most frequently used measures to develop AD phenotypes in mice. The commonly adopted APP mutations include: Swedish (K670N/M671L) (Haass et al, 1995) located at BACE1 cleavage site, which is more likely to be processed via the amyloidogenic pathway; London (V717I) (Goate et al, 1991) and Indiana (V717F) (Murrell et al, 1991) within the γ-secretase

cleavage site, favouring the production of Aβ42; Dutch (E693Q) (Levy et al, 1990) and Iowa (D694N) (Grabowski et al, 2001), within the Aβ region, elevating generation of Aβ40 and inducing hereditary cerebral haemorrhage; Arctic (E693G) (Nilsberth et al, 2001), decreasing α-secretase processing of APP.

b) Presenilin mutant models

Presenilin functions as the subunit of γ-secretase and mutations in the two presenilins PS1 and PS2 (i.e. PSEN1-M146V) lead to familial early-onset AD (Tokuhiro et al, 1998), which has identical symptoms and neuropathology to more commonly seen sporadic AD. The introduction of presenilin mutations in mice accelerated the production of Aβ42 without affecting levels of Aβ40 (Jankowsky et al, 2004). Furthermore, familial early-onset AD is a relatively rare form and only accounts for less than 6% of all AD cases (Hausner et al, 2014), so a presenilin mutant is normally combined with APP to produce double or multiple transgenic models (Holcomb et al, 1998; Lok et al, 2013).

c) Aβ transgenic model

Directly expressing Aβ peptide in mice can exclude the effects of APP overexpression, so the pathological features of these mice derive purely from the deposition of amyloid plaques. However, although this model successfully demonstrates amyloid pathology, there is no literature reporting the deficits in memory and learning ability of these mice (McGowan et al, 2005). It will be controversial if a supposed AD model fails to show loss-of-function behavioural symptoms.

d) Apolipoprotein E models

The E4 variant apolipoprotein E (APOE-e4) is known as a genetic risk factor for late-onset sporadic AD (Sadigh-Eteghad et al, 2012). In the human general population, there are three major alleles of the gene for Apolipoprotein E, APOE-e3 (77%), APOE-e4 (15%) and APOE-e2 (8%) (Tai et al, 2011). Compared to individuals with no APOE-e4, the risk for developing AD is 2-3 fold in those with one copy of APOE-e4 and 12-fold in people with two copies of this allele (Kim et al, 2009). Human APOE knock-in (KI) mice have been generated to investigate the effect of APOE on Aβ deposition (Mann et al, 2004). Crossing APOE-e4 KI mice

with different APP transgenic mice could alter the ratio of Aβ40:Aβ42 (Fryer et al, 2005), or enhance Aβ generation at a young age (Bales et al, 2009). Moreover, the cholesterol levels in APOE-e4 KI mice were greatly altered, which is closely related to the production and clearance of Aβ (Mann et al, 2004). Thus, APOE-e4 KI/APP mice might be also useful in the elucidation of the lipid metabolism state in AD.

e) Multi-transgenic models

As mentioned above, presenilin mutation does not account for more prevalent sporadic AD, and is not sufficient for the mice to develop cognitive deficits and amyloid plaques. Therefore, the double transgenic model APP/PS1 is more usually generated to develop AD symptoms, as well as to increase the Aβ42/Aβ40 ratio to enhance pathological toxicity. Additionally, tau pathology may be developed in these models by introducing human tau mutation. The triple transgenic mice (APP/PS1/tau) demonstrated aggravated tau formation and neuronal loss compared to tau mice (Oddo et al, 2003; Wirths & Bayer, 2010). The latter is normally used as a frontotemporal dementia model rather than an AD model, because the tau mutation does not lead to AD pathology as the deposition of amyloid plaques and tau aggregation seem to be two independent processes. Double transgenic mouse APP/tau is also available, with more severe tau pathology than tau mice (Perez et al, 2008).

Although these mice only show the main pathological hallmarks of AD, the diversity of different transgenic lines provides powerful tools for research in various aspects, with varying degrees of phenotypes and specific combinations. Moreover, AD mice can be crossed with other mouse models to investigate the function of a particular protein involved in AD, for example, APP transgenic mice crossbred with GPR50 knockout mice will be useful to study the side effects of the complete wipe-out of this protein under AD conditions. Other considerations when selecting an AD mouse model include: gene promoters, mice strain background, transgenic techniques (for instance, knock-in technology can be applied).

7.1.2 TgSwDI AD mouse model

The AD model TgSwDI used in this chapter is APP transgenic mice with a pure C57BL/6 background (Davis et al, 2004a). Swedish double mutation (K670N/M671L) and vascular Aβ-associated Dutch (E693Q)/Iowa (D694N) were

introduced to the longest isoform APP770, as a gene cassette by promoter Try 1.2, which induces high levels of neuron-specific expression and is expressed from postnatal day 7, preventing potential early neurodevelopmental impairments.

The cleavage of the Swedish-APP results in a global elevation of both Aβ42 and Aβ40 (Gau et al, 2002). The Dutch mutation is protective of Aβ40 from proteolysis and renders APP a highly fibrillogenic feature (Kumar-Singh, 2009). The Iowa mutation has similar properties of cytotoxicity and aggregation as the Dutch mutation (Van Nostrand et al, 2001). The Dutch/Iowa mutant showed with a reduced clearance of amyloid across the blood-brain barrier, leading to cerebrovascular amyloidosis in blood vessel walls (Davis et al, 2006). These mice developed abundant diffuse but non-fibrillar plaques in the cortical parenchyma and compact fibrillar microvascular deposits in the thalamus (Davis et al, 2004a). Diffuse plaques mainly consist of neuritic Aβ42 which exist also in the healthy aged brain but are more abundant in the AD brain (Bengtsson et al, 2013), while the main component of cerebrovascular plaques is neuritic and non-neuritic Aβ40 (Xu, 2011). The Dutch/Iowa mutation favours the production of Aβ40 and the overall ratio of Aβ40:Aβ42 in TgSwDI mice is approximately 10:1 (Davis et al, 2004a).

The pathological feature of this AD mouse is early-onset with accumulation of amyloid plaques and severe cerebral amyloid angiopathy as age increases. These mice develop Aβ plaque-like deposits from the age of 3 months, with a progressive and widespread accumulation up to 12 months. The vascular Aβs are fibrillar, with strong thioflavin S staining, and occasionally showing signs of micro-haemorrhage. The initial regions with the appearance of Aβ are the subiculum, the hippocampus, and the cortex at the age of 3 months. As the TgSwDI mice grow to 6 months, the affected areas extend to the olfactory bulb and the thalamus. By the age of 12 months, the Aβ deposition spreads throughout most of the forebrain. Accordingly, ELISA quantification of vascular Aβ showed that the levels of Aβ40 and Aβ42 are 12- and 14- fold higher respectively in the forebrain micro-vessels than in the whole forebrain tissue homogenates of TgSwDI mice at the age of 12 months.

Deficits in spatial reference memory (performance in Barnes maze) were found in TgSwDI mice from 3 months old (Xu et al, 2007). Impairments in novel object recognition, social recognition memory (intruder test) and contextual fear conditioning (electric foot shock test) were identified at 9 months (Medeiros et al,

2011). No differences in mobility and coordination (Rotarod), strength (inverted crawl test), muscle endurance (wirehang test), or anxiety (light/dark box test) were shown in these animals (Xu et al, 2007).

The TgSwDI mouse is an AD model that can be adopted to investigate different degrees of severities of AD, the pathological mechanism that develops with age, as well as distinct phenotypes related to either diffuse Aβ peptides in the cerebral parenchyma or fibrillar plaques in the cerebral vasculature.

7.1.3 Introduction to experiments

One study showed that GPR50 was expressed in the neurodegenerative neurons in the brains of elderly individuals and AD patients (Hamouda et al, 2007). Therefore, in this chapter, I examined if Gpr50 had any meaningful characteristics of expression in an AD model TgSwDI mice. The expression pattern and levels of Gpr50 in both young (3 months) and old (9 months) TgSwDI mice and their wild-type littermates were investigated by immunohistochemistry, focusing on AD-affected brain regions, the entorhinal cortex and the hippocampus. Correlation analysis between Gpr50 levels and Aβ deposits were performed to further answer the question whether Gpr50 is correlated with AD.

The two brain areas I selected are essential parts of the system that control memory. The hippocampus works as a sorting centre for the information to be memorised, processed and passing through, while the actual memory codes are recorded at various regions of the cortex (Insausti, 1993; Insausti et al, 1993). The entorhinal cortex (EC) is considered to be the interface between the neocortex and the hippocampus. On the one hand, the output of the EC, through the perforant pathway, is the main cortical source of input into the hippocampus; on the other hand, EC, together with the subiculum, provides the major output of the hippocampus (van Groen et al, 2003). EC is believed to receive highly-processed inputs from sensory processes and cognitive functions. Neurons in different layers of the EC project to subdivisions of the hippocampal formation, providing the input from the cortical region. The deep layers, especially layer V, receive one of the three main outputs of the hippocampus and, in turn, reciprocate connections from other cortical areas that project to superficial EC (Czajkowski et al, 2013). The output of the hippocampus particularly targets deep layers V and VI of EC, which consecutively are the source

of far-reaching reciprocal projections in the cortex and the subcortical projections to the septum, the striatum, the amygdala and the thalamus. Each of the responding pyramidal cells in layer V has an axon reaching toward the white matter, with half of these neurons also extending an axon to superficial layers II and III. Hence, neuronal cells in layer V of EC play a role of transition station in the cortical functional network. To specify the expression of Gpr50 in the cortex, I concentrated on the layer V of EC.

Both the hippocampus and the entorhinal cortex are among the first regions of the brain to suffer damage in AD (Van Hoesen et al, 1991) and were found abundantly harboured with Aβs in TgSwDI mice (Davis et al, 2004a). Furthermore, they are amongst the areas in which I found the co-localisation of Gpr50 and Bace1 in wild type adult mouse brain (see chapter 6), so investigating these areas could be relevant to my studies.

7.2 Materials and methods

7.2.1 Alzheimer's disease mouse model TgSwDI

The TgSwDI mice (Tg) and wild-type (WT) control mice were littermates with a C57BL/6 background. The mouse brain sections were kindly provided by Professor Karen Horsburgh (University of Edinburgh). The hemi-brains of 3 months and 9 months animals were fixed with 4% paraformaldehyde and were paraffin-embedded. All cohorts (WT3, Tg3, WT9 and Tg9) contained 8 animals. Two consecutive sections for each animal were placed on one glass slide (6 μm, coronal, Bregma:-1.28 mm). Two sets of slides (for Aβ and GPR50 separately) including consecutive and non-consecutive sections were used (Table 7.1).

Table 7.1 The two sets of slides for staining Aβ and Gpr50

Slides	WT3	Tg3	WT9	Tg9
Consecutive	N=6	N=4	N=4	N=5
Not consecutive	N=2	N=4	N=4	N=3
Total	N=8	N=8	N=8	N=8

WT3: wild-type, 3 months; Tg3: transgenic, 3 months;
WT9: wild-type, 9 months; Tg9: transgenic, 9 months.

7.2.2 Immunohistochemistry

The method of immunohistochemistry was adapted from the protocol used in Professor Horsburgh's lab. The sections were incubated at 60^{o}C for 20 min to melt the wax, and then rehydrated through a series of alcohols: 100% xylene 15 min, 100% ethanol 10 min, 100% ethanol 5 min, 90% ethanol 5 min, 70% ethanol 5 min, running tap water 5 min, dH_2O 5 min. The set of slides for Aβ were subjected to wet-heat induced antigen retrieval in citrate buffer (pH 6.0). After an incubation of 20 min at 100^{o}C, the slides were cooled at room temperature for 10 min and washed in PBS. The other set of slides were kept un-retrieved for GPR50 staining, as I found this was better for the GPR50 antibody staining (shown later, Figure 7.5, 7.6). The sections were blocked in PBS+20% donkey serum (+1% BSA) at room temperature for 2 hr. 1% BSA was omitted for GPR50 sections in this case, where the goat antibody (G-15, Santa Cruz) was used, with a view of reducing the possibility of interference between goat polyclonal antibodies and BSA. After the blocking, the sections were incubated with primary antibodies overnight at 4^{o}C. Mouse monoclonal antibody Aβ 6E10 (SIG-39320, sigma) is reactive to amino acid residue 1-16 of Aβ and specific to human isoforms. Sections were washed 3×5 min with PBS, followed by incubation with secondary antibodies donkey-anti-mouse 488 and donkey-anti-goat 488 separately, for 2 hr at room temperature. Again, sections were washed 3×5 min with PBS before mounting with VECTASHIELD® HardSet Mounting Medium containing DAPI (Vector Laboratories, H-1500).

7.2.3 Imaging and statistical analysis

Two brain regions were selected and photographed. For the entorhinal cortex, layer V, confocal images were captured on a Nikon A1R confocal laser-scanning microscope (×60, oil) with an image size of 512×512 using the software NIS elements. The hippocampal region was photographed on a Zeiss Britmac fluorescent microscope (×5, dry) with an image size of 1024×1024 using the software Envision. When more than one image was required to cover the hippocampal structure, photos were stitched by the software Adobe Photoshop CS2 (Figure 7.1.A). The whole hippocampus was identified as the region of interest (Figure 7.1.B) and subjected to quantification.

Total Aβ burden or Aβ-affected area was defined as the percentage of test area occupied by immunoreactive Aβ-like plaques (Abeta_Area). Gpr50 expression level was represented by the percentage of test area immunoreactive with the GPR50 goat antibody (Gpr50_Area). It is not recommended to use the intensity of Aβ/Gpr50 signals as the expression levels. On the one hand, it is difficult to distinguish the specific signal from cell to cell, especially those adjacent cells that were both expressed with Aβ; on the other hand, the calculation of fluorescence intensity is easily affected by the background, in particular the Gpr50 signal, which was not very strong. All the quantification was performed automatically with an ImageJ macro in order to standardise the analysis across sections/slides. For the auto-thresholding of Aβ, the Triangle algorithm (Zack et al, 1977) was used, while that of Gpr50 applied Tsai's method which attempts to preserve the moments of the original image in the thresholded result (Tsai, 1985). The two methods are auto-threshold procedures bundled in ImageJ as "Triangle" and "Moments". Values were averaged when duplicate sections were adopted. The statistical assessments were carried out in the software package SPSS 19.

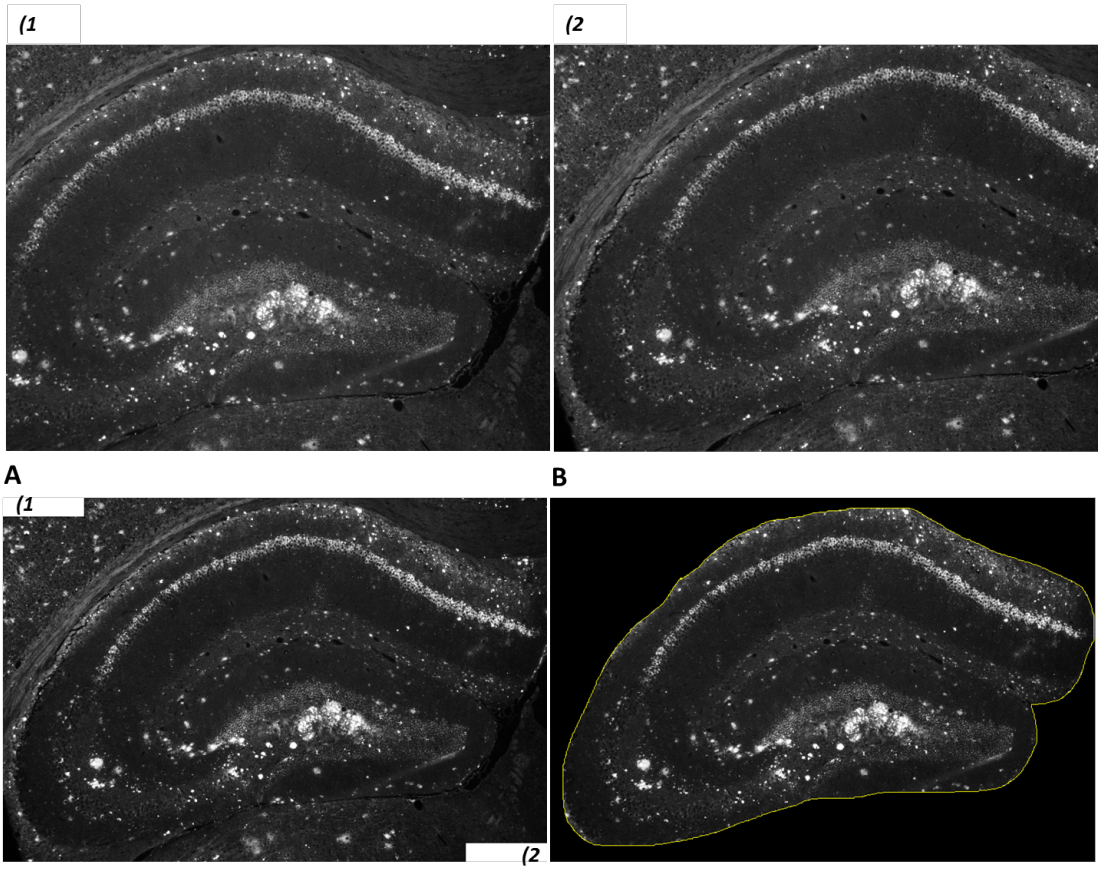

Figure 7.1 Preparation work for the quantification in the hippocampus. 1) A photo that covered the top side of the hippocampus; 2) a photo that covered the bottom side of the hippocampus in photo 1). A) Photos *(1* & *(2* were stitched together to cover the whole hippocampus; B) an example of the ROI for the hippocampus.

7.2.4 The removal of outlier data

Briefly, outliers are those data points that show extreme patterns to the rest of the dataset. There are two types of outliers: 1) they are generated during the process of collection, data conversion, methodology failure, initial determination mistake, etc. In this case, the aberrance is produced due to measurement errors and is not representative of extreme cases that may occur by chance. Therefore, the removal of these outliers is necessary; 2) they are caused by pure chance and can only be interpreted by randomness of sampling. In other words, there is no reason to exclude these deviated values from the analysis. Thus, the removal of outliers must be carefully considered, and evidence must be provided to fully explain the aberration.

All photos were renamed and quality checked. The ones with obvious crushed or damaged brains (Figure 7.2.B) were excluded. This was a process of removing potential outliers prior to the quantification and the analysis.

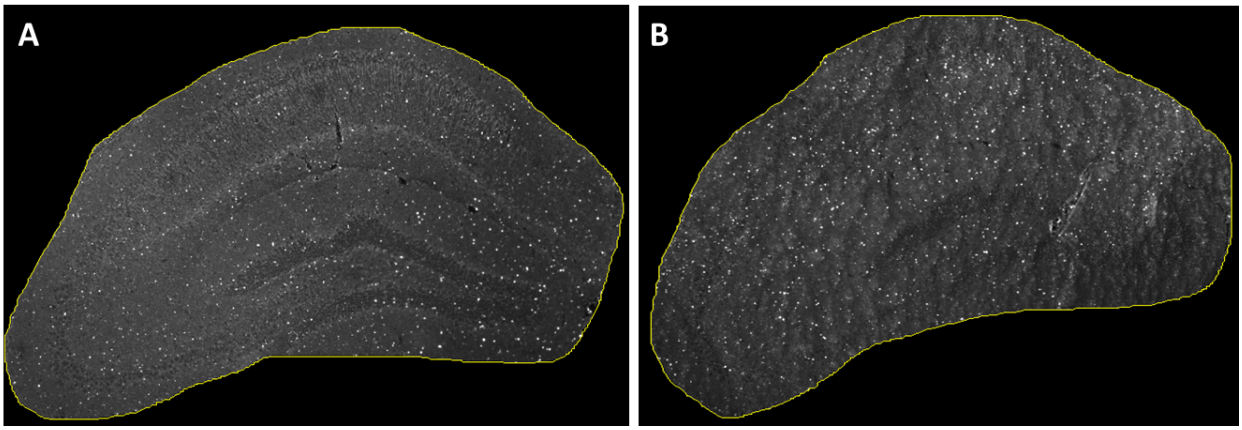

Figure 7.2 Quality checking of photos prior to the analysis. A) A normal brain suitable for assessment; B) a crushed brain to be excluded.

The post hoc method to identify outliers is Tukey's box and whisker plot, which sets the inner and outer fences of the dataset based on calculation of quartiles (Figure 7.3.A). Inner fences: [Q1-1.5 IQR, Q3+1.5IQR], outer fences: [Q1-3IQR, Q3+3IQR], Q1: the first quartile, Q3: the third quartile, IQR: Inter Quartile Range=Q3-Q1. A data point located between inner and outer fences is a possible outlier. An extreme value beyond the outer fences is a probable outlier.

The potential outliers were inspected cautiously. This included the setting of confocal parameters, the depths of tissue that were photographed, comparison with the other parts of the brain, comparison with the other replicate, comparison with

other animals in the same cohort, the automatic threshold used and the running of ImageJ macro. For the dataset of Abeta_Area, one outlier "#668 left" (labelled 13 in Figure 7.3.B) was removed due to its plaque like staining for 3 months wild-type mice. The other two large potential outliers in 9 months wild-type mice were kept, because they could be extreme values that might occur occasionally in old animals. No obvious mistake was identified in other checking-up processes. The same approach was applied to the dataset of Gpr50_Area as a variable (Figure 7.3.C). It was found that one Gpr50 value in cohort TgSwDI 9 months (10.976, #251 right, labelled 60 in Figure 7.3.C) was an extraordinarily large value compared to other animals in the same cohort (around 2.5-fold of most others), as well as to its own replicate (5.741, #251 left). More importantly, it seemed that this photo was over-thresholded which could not be avoided when using the auto-threshold (Figure 7.4). Therefore, this data point was omitted as an outlier and "#251 left" was used as the mean for animal 251. No other outliers were identified by the box plot after removal of this value. Brain sections that were excluded from analysis are summarised in Table 7.2.

There were 8 animals (maybe less after the outlier removal) in each of the four cohorts. Every data point came from the mean of two consecutive sections for each animal. If one section was identified as the origin of an outlier, the value of the other replicate was solely used to replace the mean.

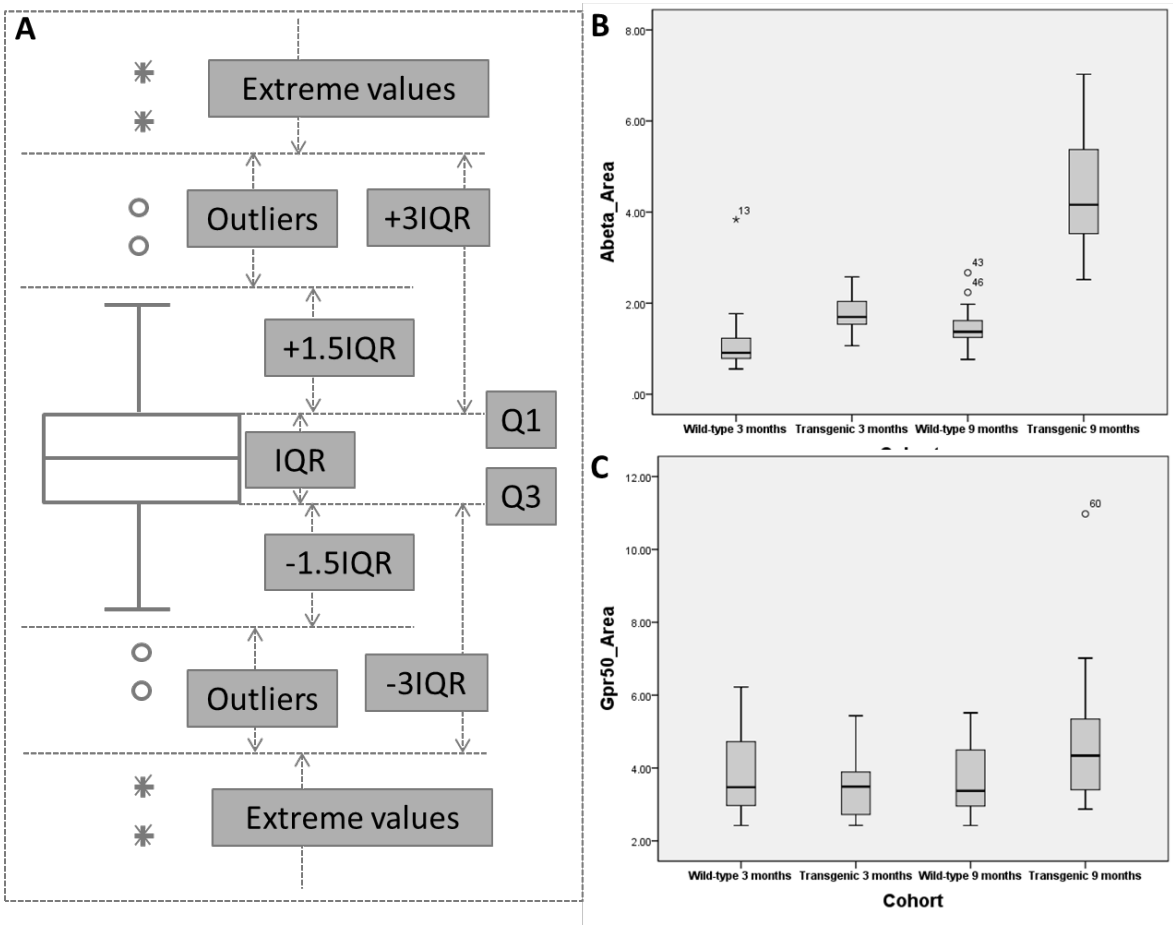

Figure 7.3 The method of identifying outliers. A, Tukey's box and whisker plot; tests of dataset B) Abeta _Area and C) Gpr50_Area of the entorhinal cortex, layer V as variables.

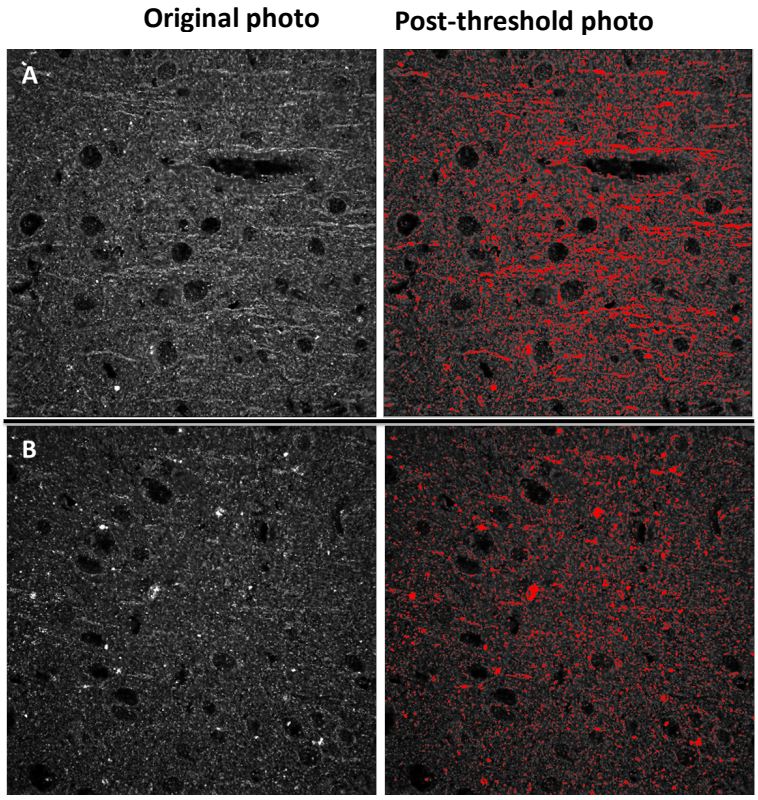

Figure 7.4 The original photos and post-threshold photos of Gpr50 in the entorhinal cortex layer V of animal 251. A) #251 right; B) #251 left. "Left" and "right" meant the two consecutive replicate sections on one slide for each animal.

Table 7.2 Brain sections excluded from the analysis

Aβ	Crushed structure		Absence of structure	Removed outlier		Final sample number for analysis
Cortex				WT3	668L	N=8 for each group
Hippocampus	WT3	663R, 664L, 664R, 665L, 667R, 668L, 668R				N=6
	Tg3	655R, 658L	660L, 660R			N=7
	WT9	265R, 266R				N=8
	Tg9	249L, 249R, 251L,251R				N=6
Gpr50	**Crushed structure**		**Absence of structure**	**Removed outlier**		
Cortex				Tg9	251R	N=8 for each group
Hippocampus	WT3	666L				N=8
	Tg3	655R, 658L	660L, 660R			N=7
	WT9	261L, 262L, 265R, 267R, 270R,				N=8
	Tg9	255R				N=8

L: left; R: right. "Left" and "right" meant the two consecutive replicates on one slide for each animal.

7.3 Results

7.3.1 Optimisation of Gpr50 staining in TgSwDI mice

In chapter 6, the expression pattern of Gpr50 in female mouse brain of the C57BL/6 strain was described and compared with previous publications. It was shown that the expression of mouse Gpr50 was mainly expressed in the cortex and the hippocampus in addition to the usually identified regions in the hypothalamus.

The brain sections used in this chapter were fixed with 4% paraformaldehyde, a fixation method that commonly requires antigen retrieval (D'Amico et al, 2009). However, our only applicable GPR50 antibody in immunohistochemistry, GPR50 goat failed to provide a quality staining after the heat-induced antigen retrieval, with diminished signal and unaccountable background (Figure 7.5, 7.6). On the contrary, the detection of Aβ requires antigen retrieval. Therefore, the staining of GPR50 and Aβ was performed separately in two sets of slides instead of co-labelling.

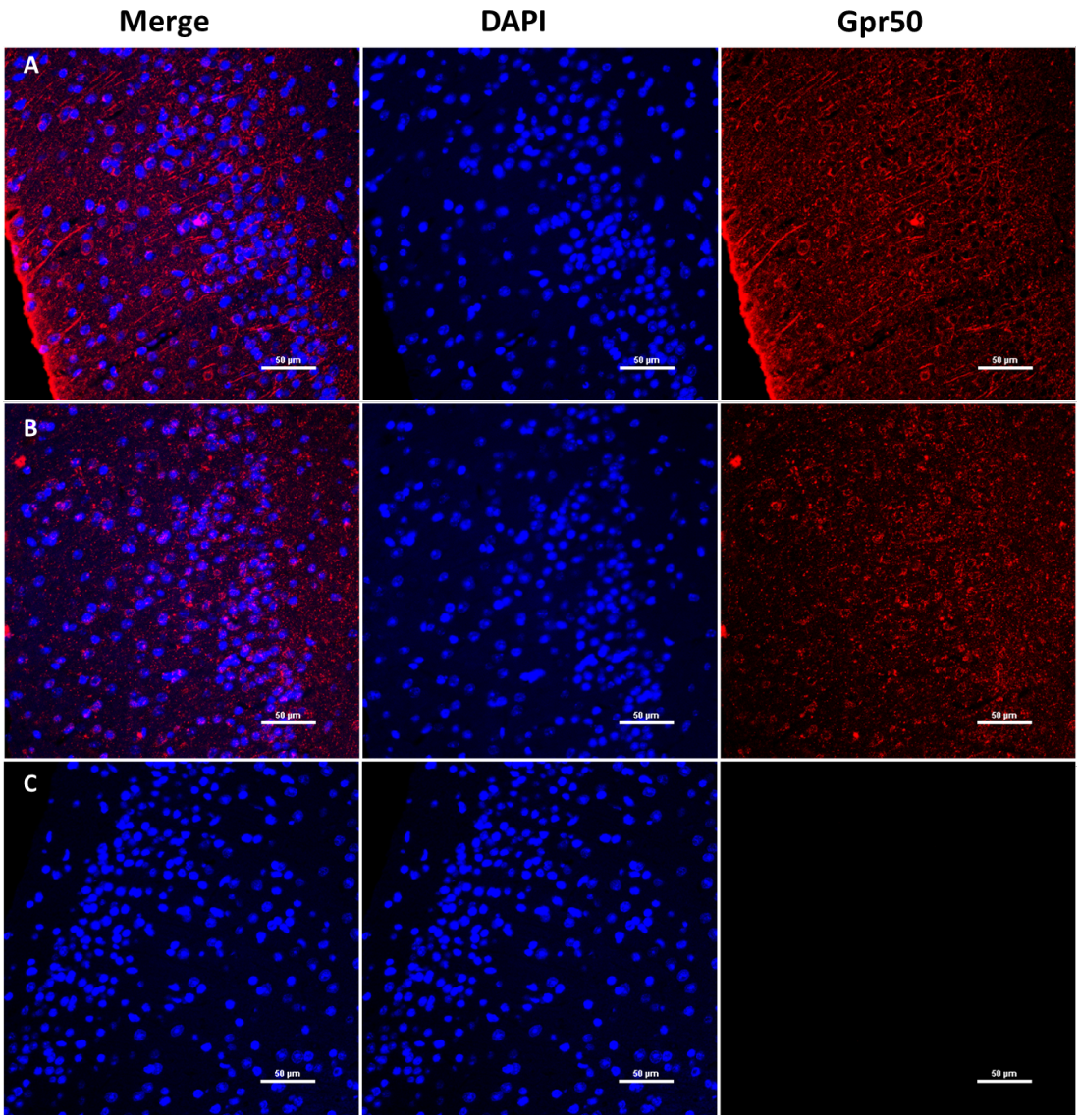

Figure 7.5 The cortex of 9 months TgSwDI mice stained with GPR50 goat antibody in A) a non-retrieved brain section and B) a heat retrieved brain section. C) No primary antibody control, non-retrieved. Scale bar: 50 µm.

Immunofluorescence labelling of Gpr50 in these sections was found in the cells of the third ventricle ependymal layer (Figure 7.6), but not as predominant in the hypothalamic region as in previously reported literature or my observation in chapter 6. It is possible that the fixation method caused differences in staining patterns, as was previously noted (Grunewald et al, 2012). However, the detection in the neuronal cells in the pyramidal layer of the hippocampus and the layers with neurons in cortex was not affected. Both soma and axons of the neurons were found with Gpr50 immunoreactivity (Figure 7.5). Additionally, there was dispersed punctuate staining detected throughout the section. This was not associated with any of the animal cohorts or any particular cell type, as this staining pattern was present in all the sections. I did not see the punctuate pattern in sections that were fixed by 70%

ethanol (see chapter 6), thus it is possible that these puncta were generated during the fixation or storage of the sections. Because the pattern was rather homogenous, the original photos were not modified and were subjected to quantification with the existence of this noise.

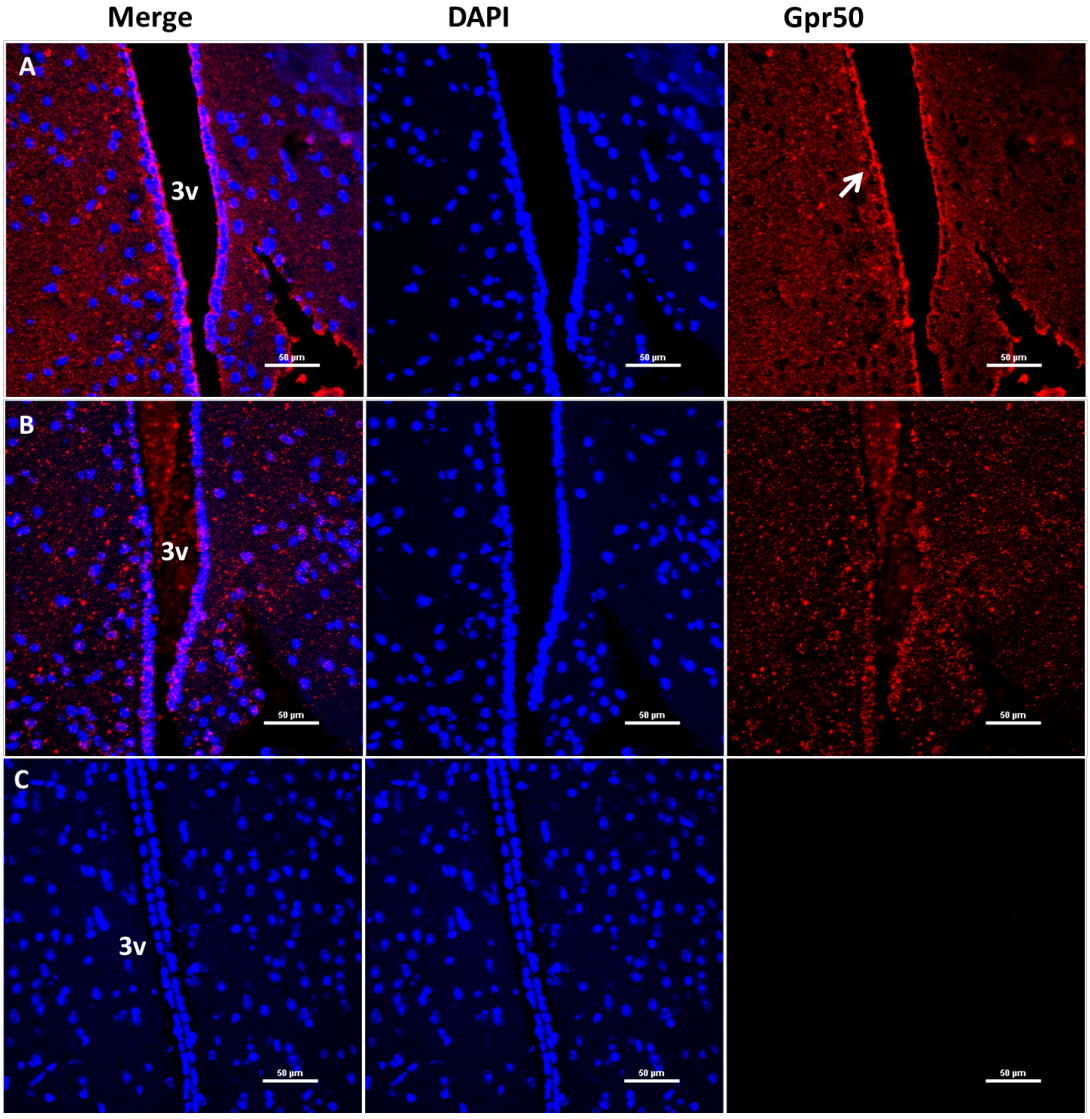

Figure 7.6 The hypothalamus of 9 months TgSwDI mice stained with GPR50 goat antibody in A) a non-retrieved brain section and B) a heat retrieved brain section. C) No primary antibody control, non-retrieved. Scale bar: 50 µm. 3v: the third ventricle. The white arrow indicated an ependymal cell expressed with Gpr50.

7.3.2 Aβ and Gpr50 in the entorhinal cortex

7.3.2.1 Aβ and Gpr50 in the layer V, entorhinal cortex of TgSwDI mice

Aβ and Gpr50 were both detected in the entorhinal cortex of 9 months TgSwDI mice (Figure 7.7). Diffuse Aβ plaques were detected in the layer V, which possibly indicates a damaged interchange of cortical-hippocampal system and may also eventually lead to an impaired memory. The signal of Gpr50 was seen mainly in the

pyramidal neurons, especially at the axons in layer II, III and V. It was not known if Aβ and Gpr50 were localised in the same neurons as the double staining was not available due to the failure of Gpr50 to be fully stained after the antigen retrieval (Figure 7.5, 7.6).

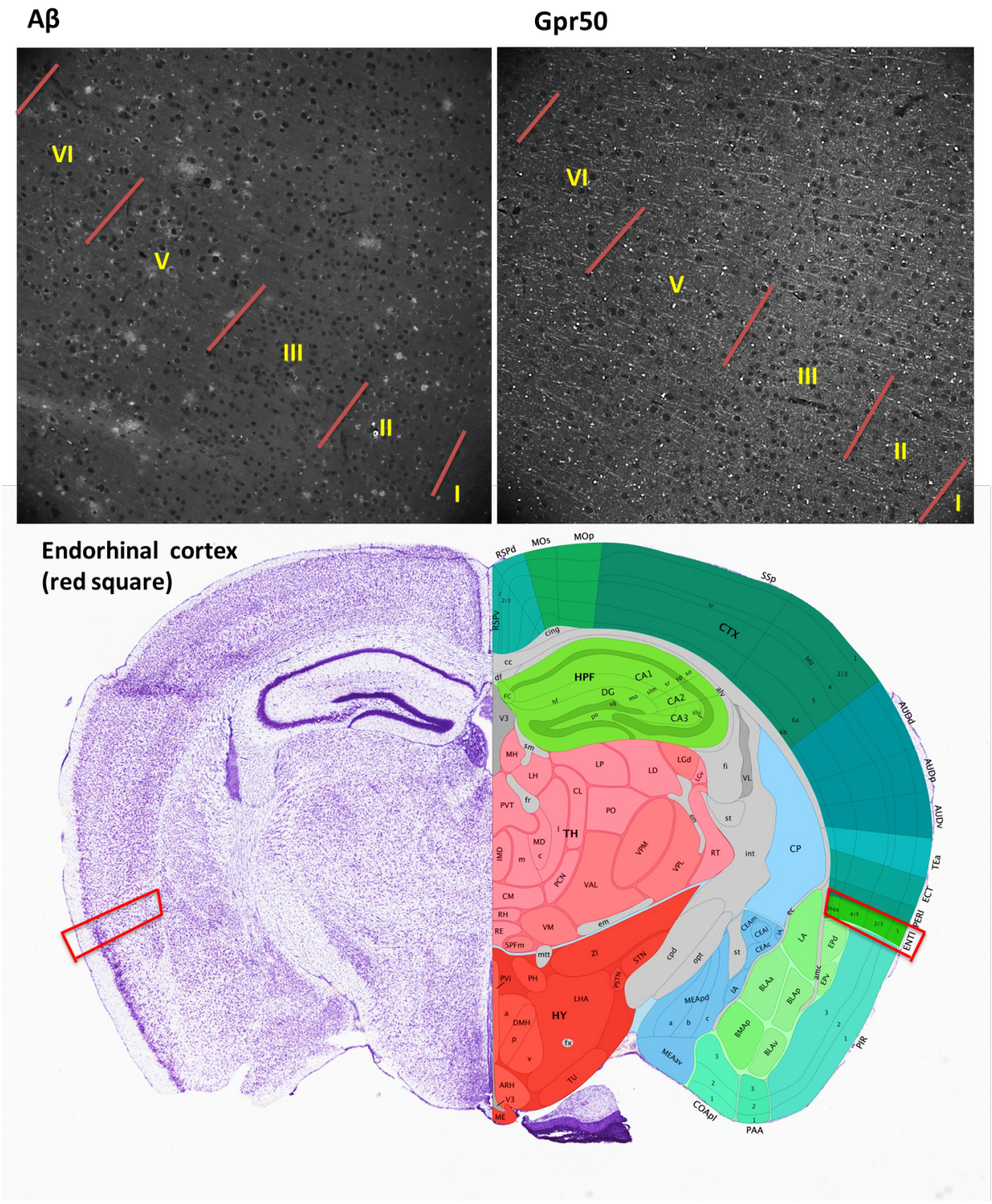

Figure 7.7 The immunofluorescence labelling of Aβ and Gpr50 in the entorhinal cortex of 9 months TgSwDI mice. I~VI refer to different layers of the entorhinal cortex (EC). One of the characteristics of EC is the lack of layer IV. The brain map was adapted from Allen brain atlas.

The expression levels were indicated by the percentage of targeting area with Gpr50 immunoreactivity (Gpr50_Area), in the same way as how Aβ burden (Aβ_Area) was calculated. Representative images of staining in the layer V of the entorhinal cortex and the analysed data obtained through ImageJ are presented in Figure 7.8, Table 7.3 and Table 7.4.

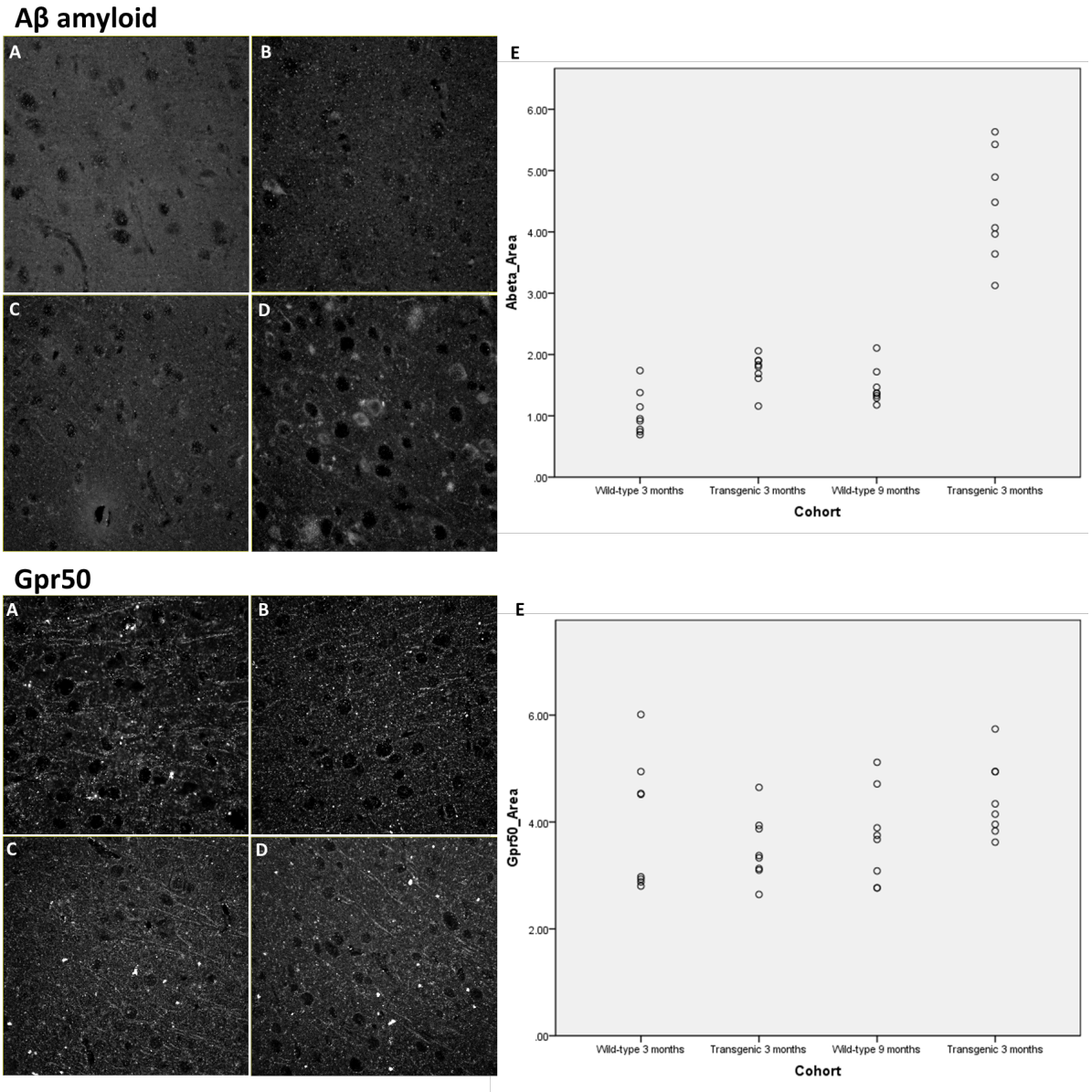

Figure 7.8 Representative photos of Aβ and Gpr50 in the entorhinal cortex layer V of the four mouse cohorts of A) 3 months wild-type; B) 3 months TgSwDI; C) 9 months wild-type; D) 9 months TgSwDI. E) Dot plots of expression percentages in each cohort.

Table 7.3 The expression percentage of Aβ and Gpr50 in the entorhinal cortex layer V

Animal number	Age	Phenotype	Entorhinal cortex, layer V	
			Aβ	GPR50
662	3 months	Wild-type	0.6915	4.5345
663	3 months	Wild-type	1.145	4.5175
664	3 months	Wild-type	1.378	2.8785
665	3 months	Wild-type	0.741	2.973
666	3 months	Wild-type	0.9525	4.944
667	3 months	Wild-type	0.778	2.8
668	3 months	Wild-type	1.738*	2.931
669	3 months	Wild-type	0.9165	6.0115
654	3 months	Transgenic	1.904	2.644
655	3 months	Transgenic	1.6885	3.13
656	3 months	Transgenic	1.16	3.329
657	3 months	Transgenic	2.0595	3.372
658	3 months	Transgenic	1.7995	3.8715
659	3 months	Transgenic	1.8975	4.647
660	3 months	Transgenic	1.611	3.9365
661	3 months	Transgenic	1.8305	3.0985
261	9 months	Wild-type	1.4675	4.712
262	9 months	Wild-type	1.3675	3.0845
263	9 months	Wild-type	1.37	3.891
264	9 months	Wild-type	1.329	3.7515
265	9 months	Wild-type	1.2915	2.7655
266	9 months	Wild-type	1.7175	3.6725
267	9 months	Wild-type	2.106	2.7685
270	9 months	Wild-type	1.176	5.1175
245	9 months	Transgenic	3.6395	3.6225
246	9 months	Transgenic	4.4825	4.1465
247	9 months	Transgenic	5.427	4.94
248	9 months	Transgenic	5.632	3.8315
249	9 months	Transgenic	3.965	4.3395
251	9 months	Transgenic	4.0665	5.741*
255	9 months	Transgenic	4.894	3.9565
257	9 months	Transgenic	3.125	4.945

***Single hemi-brain section used. All other data represent the mean of two consecutive hemi-brain sections.**

The percentage of test area occupied by the immunoreactivity of Aβ or Gpr50 was calculated as their expression levels in this area. All the quantification was performed automatically in ImageJ. Values were averaged from the duplicate sections. In case of an outlier identified in one animal, its replicate was used in replacement of the mean.

Table 7.4 A summary of expression percentage of Aβ and Gpr50 in the entorhinal cortex layer V

Age	Phenotype	Mean±Standard Deviation, N	
		Aβ	Gpr50
3 months	Wild-type	1.1737±0.6904, 8	3.9488±1.2169, 8
3 months	Transgenic	1.7438±0.2728, 8	3.5036±0.6234, 8
9 months	Wild-type	1.4781±0.2985, 8	3.7204±0.8610, 8
9 months	Transgenic	4.4039±0.8724, 8	4.7675±0.7138, 8

N: sample size

Next, a general linear model was fitted to analyse whether there were differences in the expression levels of Aβ and Gpr50 in the layer V of the entorhinal cortex among the four cohorts (3 months wild-type, 3 months TgSwDI, 9 months wild-type, 9 months TgSwDI). The main effects "Age", "Phenotype" and the interaction term of the two were examined as the category factors. The model performed a two way ANOVA (2×2 factorial ANOVA) to assess the differences of Aβ or Gpr50 levels.

As is shown in Table 7.5.A, this model fits well for Aβ levels ($F(3, 28) = 50.541$, Adjusted $R^2 = 0.827$, $p < 0.01$). The Aβ level was significantly associated with the age or phenotype of the mice (Age, $F(1, 30) = 50.173$, $p < 0.01$; Phenotype, $F(1, 30) = 69.771$, $p < 0.01$). There were also differences in Aβ levels in subgroups with the same age or the same phenotype (Age×Phenotype: $F(1, 30) = 31.680$, $p < 0.01$). According to Table 7.4, the Aβ amounts in the layer V of the entorhinal cortex were increased in TgSwDI mice compared with wild-type mice at both 3 months and 9 months; and were elevated with age, from 3 months to 9 months in both wild-type and TgSwDI mice. These results are in line with the known properties of Aβ deposition in this AD mouse model and the observation of increased Aβ levels during normal aging (Davis et al, 2004a; Mintun et al, 2006).

This model was not significant to account for the variance of Gpr50 levels in this region ($F(3, 28) = 1.654$, Adjusted $R^2 = 0.059$, $p = 0.200$, Table 7.5.B). This means that differences in age and phenotype did not account for the variance in Gpr50 levels. No significant differences in Gpr50 expression were identified between 3 months and 9 months (Age, $F(1, 30) = 1.287$, $p = 0.266$), or wild-type and transgenic animals (Phenotype, $F(1, 30) = 0.194$, $p = 0.663$). The interaction term of Age and Phenotype had a trend of significance (Age×Phenotype: $F(1, 30) = 3.481$, $p = 0.073$), indicating

that there might be differences in Gpr50 expression in subgroups such as between wild-type and TgSwDI mice at the same age, or between 3 months and 9 months mice with the same phenotype. Therefore, post hoc analysis was performed on Gpr50 levels in the entorhinal cortex layer V in pairwise comparisons using unpaired Student's t-test (see 7.3.2.2 and 7.3.2.3).

Table 7.5 The general linear model to predict the expression levels of Aβ and Gpr50 in the layer V of the entorhinal cortex among the four mouse cohorts

A) Aβ	**df**	**F**	**P-value**	**Partial Eta Squared**
Corrected model Adjusted r^2=0.827	3, 28	50.541	**2.0×10^{-11}****	**0.844**
Age	1, 30	50.173	**1.0×10^{-7}****	**0.642**
Phenotype	1, 30	69.771	**4.4×10^{-9}****	**0.714**
Age× Phenotype	1, 30	31.680	**5.0×10^{-6}****	**0.531**
B) Gpr50	**df**	**F**	**P-value**	**Partial Eta Squared**
Corrected model Adjusted r^2=0.059	3, 28	1.654	0.200	**0.151**
Age	1, 30	1.287	0.266	**0.044**
Phenotype	1, 30	0.194	0.663	**0.007**
Age×Phenotype	1, 30	3.481	**0.073$^{\$}$**	**0.111**

$^{\$}$ p<0.1, ** p<0.01.
df: degrees of freedom (between-groups df, within-groups df)

7.3.2.2 Is the expression level of Gpr50 altered in the layer V of the entorhinal cortex in TgSwDI mice compared to the wild-type control?

In the layer V of the entorhinal cortex, it was found that there was no significant alteration of Gpr50 expression in young TgSwDI mice compared to wild-type littermates at the age of 3 months (Figure 7.9.A, p=0.378). Diffuse plaques of Aβ were not abundant in the cortex at this stage (see Table 7.4). However, in older animals at the age of 9 months, there was a trend of elevation identified of Gpr50 expression in TgSwDI mice compared to the wild-type control (Figure 7.9.B, p=0.091).

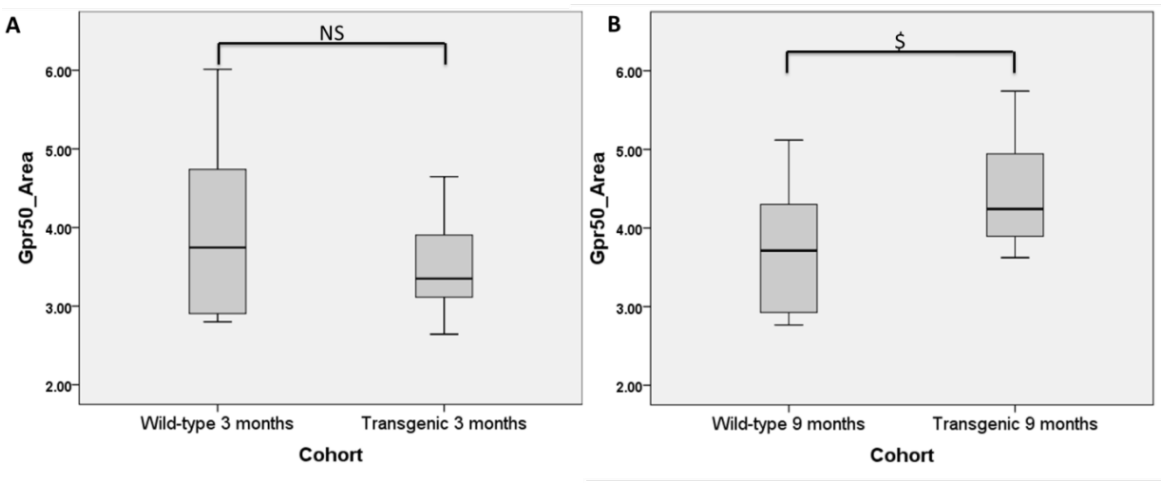

NS: not significant, p= 0.378>0.1; $: a trend of significance, 0.05< p=0.091<0.1; N=8

Figure 7.9 Comparison of Gpr50 expression in the entorhinal cortex layer V of TgSwDI mice with that of wild-type mice at 3 months or 9 months. The differences in means were tested using the unpaired Student's t-test.

7.3.2.3 Is the expression level of Gpr50 in the layer V of the entorhinal cortex related to age?

No significant alteration of Gpr50 expression in the layer V of the entorhinal cortex was identified between 3 months and 9 months wild-type mice (Figure 7.10.A, p=0.672). Yet, there was a significant increase of Gpr50 levels in this region of 9 months transgenic mice compared to their 3 months littermates (Figure 7.10.B, p=0.014). Thus, the expression level of Gpr50 in the layer V of the entorhinal cortex was related to age in transgenic animals only.

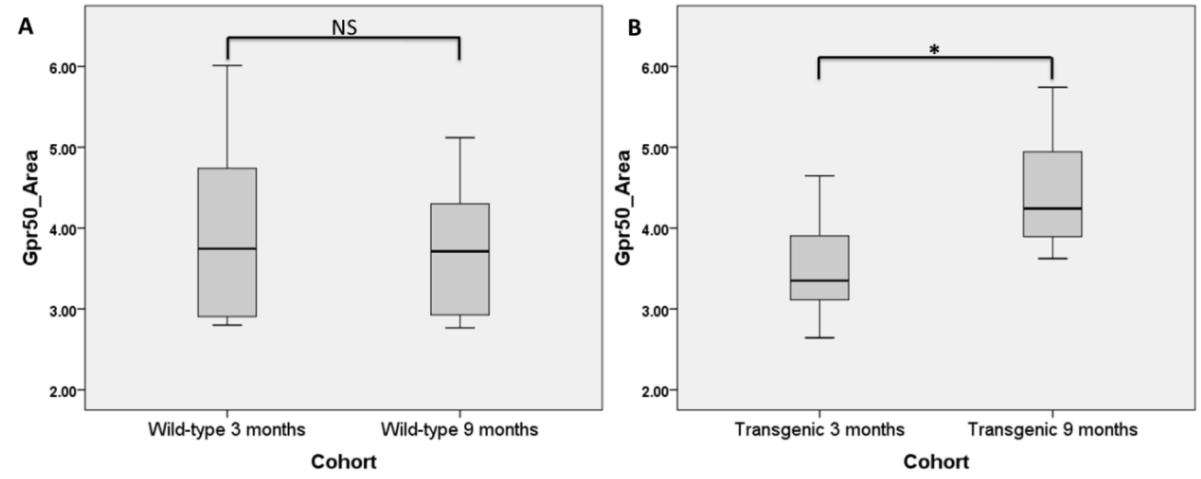

NS: not significant, p= 0.672>0.1; *: significant, p=0.014<0.05; N=8.

Figure 7.10 Comparison of Gpr50 expression in the entorhinal cortex layer V of mice between 3 months and 9 months in A) wild-type or B) TgSwDI. The differences in means were tested using the unpaired Student's t-test.

7.3.2.4 Is the expression level of Gpr50 in the layer V of the entorhinal cortex correlated to that of Aβ?

It was shown in the last section that in TgSwDI mice the expression level of Gpr50 was significantly higher in older animals than in young animals. This modulation was not totally contributed by age, because no significant alteration was found between young and old wild-type animals. To answer the question whether Gpr50 expression is associated with the AD pathogenesis, Pearson's correlation analysis was performed to evaluate the potential link between Aβ and GPR50 in TgSwDI mice by using a combined dataset of 3 months and 9 months animals. As expected, there was a positive correlation between the expression levels of Aβ and Gpr50 in the entorhinal cortex, layer V (Figure 7.11, r=0.498, p=0.050).

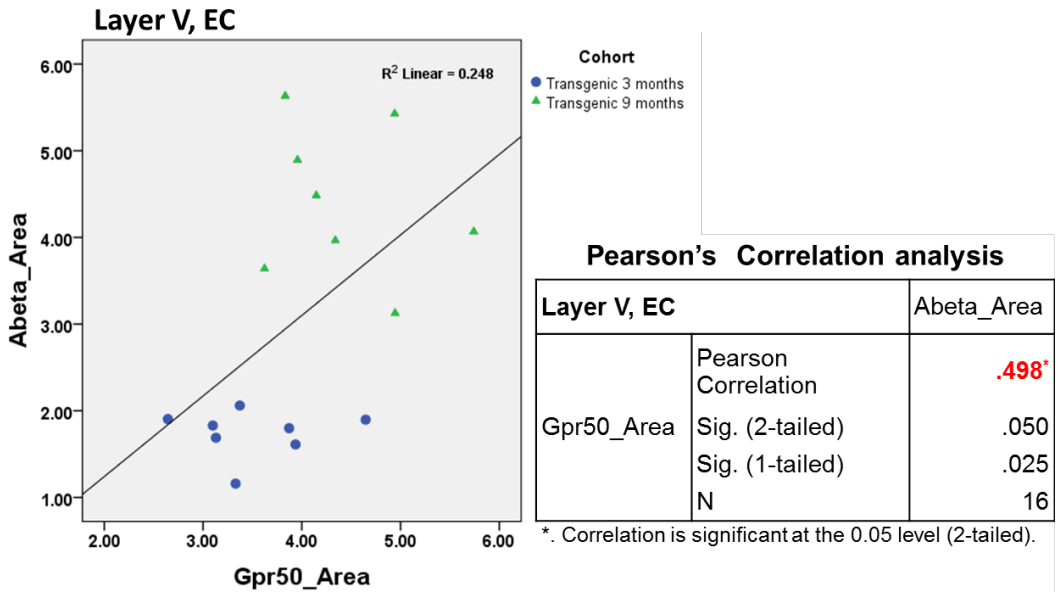

Pearson's Correlation analysis

Layer V, EC		Abeta_Area
Gpr50_Area	Pearson Correlation	.498*
	Sig. (2-tailed)	.050
	Sig. (1-tailed)	.025
	N	16

*. Correlation is significant at the 0.05 level (2-tailed).

Figure 7.11 Correlation between the expression levels of Aβ and Gpr50 in the layer V of the entorhinal cortex of TgSwDI mice. EC: entorhinal cortex.

7.3.3 Aβ and Gpr50 in the hippocampus

7.3.3.1 Aβ and Gpr50 in the hippocampus of TgSwDI mice

There were two distinguished staining patterns of Aβ in the hippocampus, revealed by the mouse monoclonal antibody Aβ 6E10 (Figure 7.12.A). The commonly identified plaques were localised mainly in the polymorph layer of the dentate gyrus and occasionally in the molecular layer of the dentate gyrus, the lacunosum-moleculare stratum and the oriens layer of CA1, as well as the stratum radiatum of CA2 and CA3 (Figure 7.12.A, 7.13.D). There was also a perinuclear cytoplasm-like neuronal staining in the pyramidal layer of CA1. By comparing the observation with

other cohorts, it was found that there was no such signal identified in 3 months or 9 months wild-type groups (Figure 7.13.A, C), confirming that it was not endogenous mouse App. Yet, a moderate amount of a slightly punctate pattern was spotted in 3 months transgenic group in the pyramidal layer of CA1 (Figure 7.13.B). This implied that the signal was not human APP, but Aβ peptide, showing up early-onset accumulation at a young age and increasing with age.

Gpr50 was found allocated orderly in the pyramidal layer of CA1 with axons projecting to the stratum radiatum, while weaker signal was also detected in the pyramidal layer of CA2, CA3 and the granular layer of the dentate gyrus (DG) (Figure 7.12.B). The staining pattern of Gpr50 in other cohorts was rather similar (data not shown).

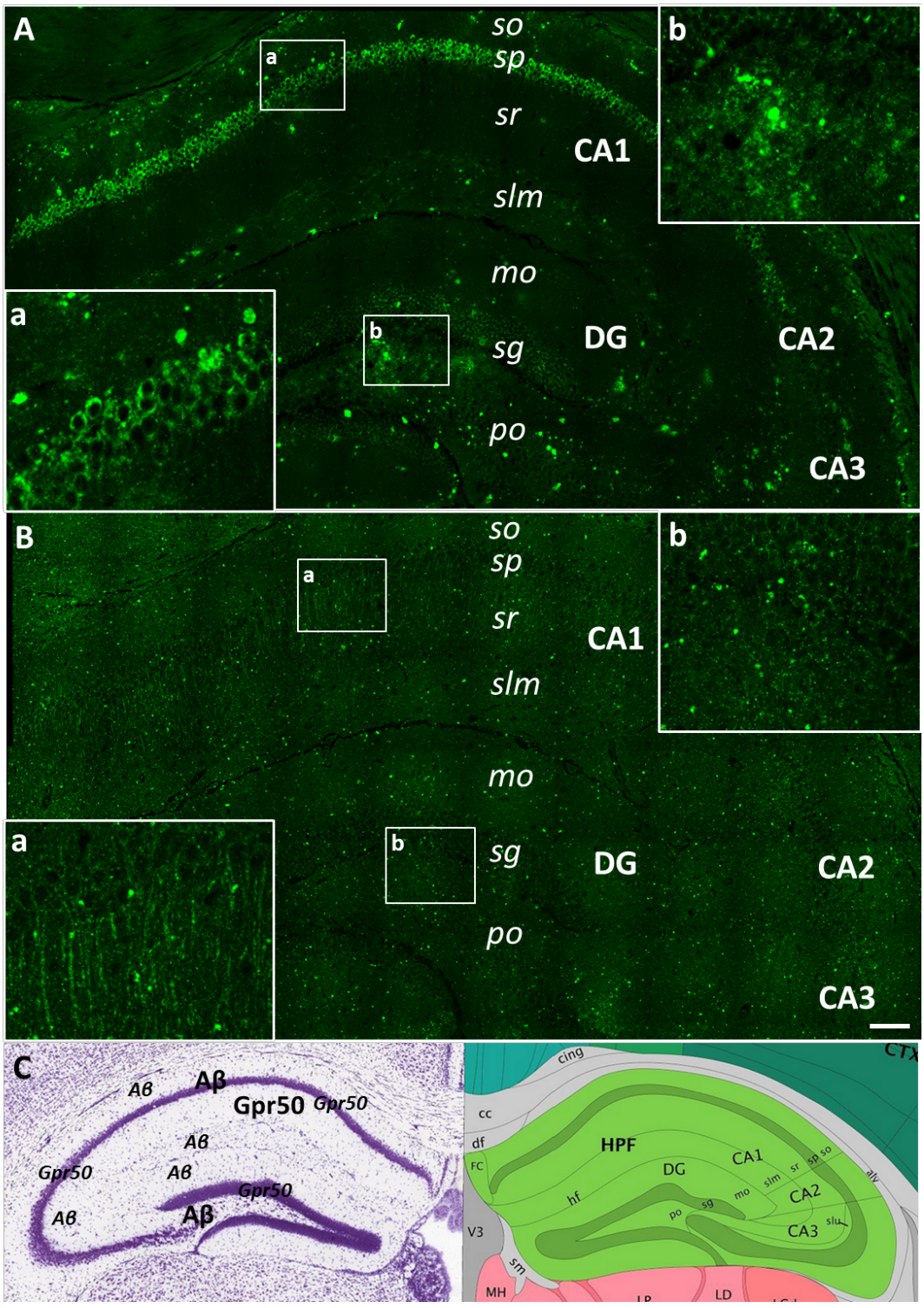

Figure 7.12 The immunofluorescence labelling of Aβ and Gpr50 the in the hippocampus of 9 months TgSwDI mice. A) Aβ, enlarged area: a) CA1, pyramidal layer, b) dentate gyrus (DG), Po, polymorph layer; B) Gpr50; C) a distribution map of hippocampal Gpr50 and Aβ (larger font indicates main sites). So/sp/sr/slm: oriens layer/pyramidal cell layer/stratum radiatum /lacunosum-moleculare stratum of CA1; mo/sg/po: molecular layer/granular layer/polymorph layer of DG. Scale bar: 100 µm. The map of mouse hipocampus was adapted from Allen brain atlas.

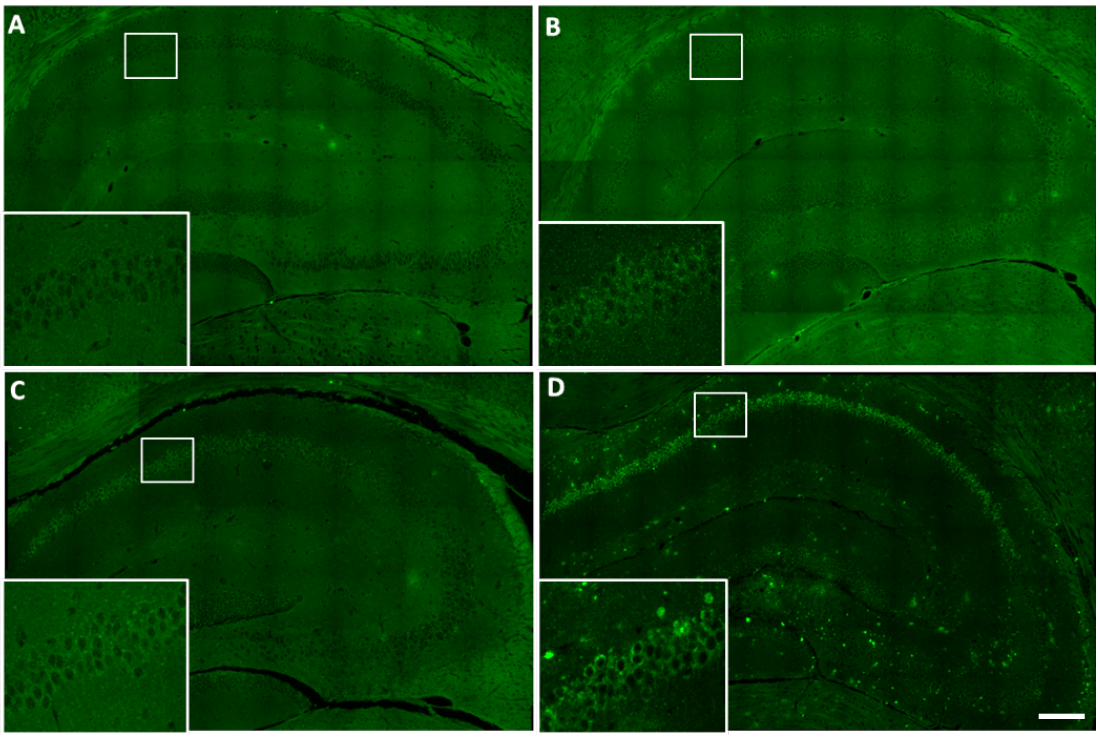

Figure 7.13 Aβ in the hippocampus of the four mouse cohorts. A) 3 months wild-type; B) 3 months TgSwDI; C) 9 months wild-type; D) 9 months TgSwDI. The white square indicated an enlarged region of the CA1 pyramidal layer. Scale bar: 200 µm.

Even though both Aβ and Gpr50 were identified in the hippocampus, they were predominantly located in different layers (see Figure 7.12.C). Therefore, the correlation between Aβ peptide and Gpr50 in the whole hippocampal region was analysed. Quantification of the percentage with protein expression in the hippocampus region was performed on areas with hand-drawn boundary according to Allen brain atlas (see Figure 7.1). This is similar to the method of correlating the protein levels in lysates by western blotting. The data of the expression percentage of Aβ and Gpr50 in the hippocampus (obtained through ImageJ) are presented in Table 7.6 and summarised in Table 7.7.

Table 7.6 The expression percentage of Aβ and Gpr50 in the hippocampus

Animal number	Age	Phenotype	Hippocampus	
			Aβ	GPR50
662	3 months	Wild-type	0.2325	3.465
663	3 months	Wild-type	0.18*	3.148
664	3 months	Wild-type	-	1.9675
665	3 months	Wild-type	0.665*	-
666	3 months	Wild-type	0.352	4.667*
667	3 months	Wild-type	-	1.5065
668	3 months	Wild-type	0.579*	3.615
669	3 months	Wild-type	0.339	3.701
654	3 months	Transgenic	3.796	3.4645
655	3 months	Transgenic	1.512	2.617*
656	3 months	Transgenic	2.5555	3.005
657	3 months	Transgenic	1.21	3.3055
658	3 months	Transgenic	2.2495	4.771*
659	3 months	Transgenic	1.2975	1.893
660	3 months	Transgenic	-	-
661	3 months	Transgenic	1.6035	1.332
261	9 months	Wild-type	0.116	4.35*
262	9 months	Wild-type	0.318	2.315*
263	9 months	Wild-type	0.1685	6.134*
264	9 months	Wild-type	0.404	2.0415
265	9 months	Wild-type	0.274*	3.329*
266	9 months	Wild-type	0.325*	-
267	9 months	Wild-type	0.3175	2.726*
270	9 months	Wild-type	0.481	3.857*
245	9 months	Transgenic	1.5905	1.5905
246	9 months	Transgenic	1.1645	1.1645
247	9 months	Transgenic	1.2965	1.2965
248	9 months	Transgenic	1.501	1.501
249	9 months	Transgenic	-	-
251	9 months	Transgenic	2.825	2.825
255	9 months	Transgenic	3.353	3.353*
257	9 months	Transgenic	2.281	2.281

*** Single hemi-brain section used; -Structure missing or damaged. All other data represent the mean of two consecutive hemi-brain sections.**

The percentage of the hippocampus (defined by hand-drawn shut lines) occupied by the immunoreactivity of Aβ or Gpr50 was calculated as their expression levels in this region. All the quantification was performed automatically in ImageJ. Values were averaged from the duplicate sections. In case of an outlier identified in one animal, its replicate was used in replacement of the mean.

Table 7.7 A summary of the expression percentage of Aβ and Gpr50 in the hippocampus

Age	Phenotype	Mean±Standard Deviation, N	
		Aβ	Gpr50
3 months	Wild-type	0.3913±0.1920, 6	3.1529±1.0816, 7
3 months	Transgenic	2.0320±0.9222, 7	2.9126±1.1215, 7
9 months	Wild-type	0.3005±0.1175, 8	3.5361±1.4106, 7
9 months	Transgenic	4.7459±0.7034, 7	2.0016±0.8366, 7

The general linear model analysed the main effects of age and phenotype, and the interaction effect of age and phenotype (age×phenotype) on the expression levels of Aβ and Gpr50 in the hippocampus among the four cohorts.

As is shown in Table 7.8.A, there were significant differences in the Aβ levels in the hippocampus between 3 months and 9 months mice (Age, $F(1, 23) = 29.645$, $p<0.01$), and between wild-type and TgSwDI mice (Phenotype, $F(1, 23) = 156.480$, $p<0.01$). The Aβ level in the hippocampus was also affected by "Age×Phenotype" ($F(1, 23) = 31.423$, $p<0.01$). Therefore, according to the means shown in Table 7.7, the Aβ level in the hippocampus of 3 months TgSwDI mice was significantly higher than 3 months wild-type mice and lower than 9 months TgSwDI mice. This confirmed previous reports that the hippocampus is one of the first regions that were affected by AD, and the Aβ deposition increases with age (Allen et al, 2007; Schuff et al, 2009).

The model was not sufficient to account for the variance of Gpr50 levels in the hippocampus ($F(3, 24) = 2.327$, Adjusted $R^2=0.128$, $p=0.100$, Table 7.8.B). The expression of hippocampal Gpr50 was not associated with age or age×phenotype (Age, $F(1, 26) = 0.381$, $p=0.543$; Age×Phenotype, $F(1, 26) = 2.291$, $p=0.143$), but was significantly related to phenotype ($F(1, 26) = 4.308$, $p=0.049$). This is interesting, so post hoc analysis was further performed on Gpr50 levels in the hippocampus in pairwise comparisons using the unpaired Student's t-test (see 7.3.3.2 and 7.3.3.3).

Table 7.8 The general linear model to predict the expression levels of Aβ and Gpr50 in the hippocampus among the four mouse cohorts

A) Aβ	df	F	P-value	Partial Eta Squared
Corrected model Adjusted r^2=0.898	3, 21	71.100	**3.6×10^{-11}****	**0.910**
Age	1, 23	29.645	**2.1×10^{-5}****	**0.585**
Phenotype	1, 23	156.480	**3.4×10^{-11}****	**0.882**
Age× Phenotype	1, 23	31.423	**1.5×10^{-5}****	**0.599**
B) Gpr50	**df**	**F**	**P-value**	**Partial Eta Squared**
Corrected model Adjusted r^2=0.128	3, 24	2.327	0.100	**0.225**
Age	1, 26	0.381	0.543	**0.016**
Phenotype	1, 26	4.308	**0.049***	**0.152**
Age×Phenotype	1, 26	2.291	0.143	**0.087**

*** p<0.05, ** p<0.01**
df: degrees of freedom (between-groups df, within-groups df)

7.3.3.2 Is the expression level of Gpr50 altered in the hippocampus of TgSwDI mouse compared to the wild-type control?

By the unpaired Student's t-test, no significant alteration of Gpr50 expression was observed between the wild-type mice and the TgSwDI mice in the 3 months cohorts (Figure 7.14.A), similar to what was observed in the layer V of the entorhinal cortex. Interestingly, there was a significant decrease of Gpr50 levels in the hippocampus of 9 months TgSwDI animals compared with their wild-type littermates. And this was opposite to the trend of Gpr50 expression alteration in the layer V of the entorhinal cortex.

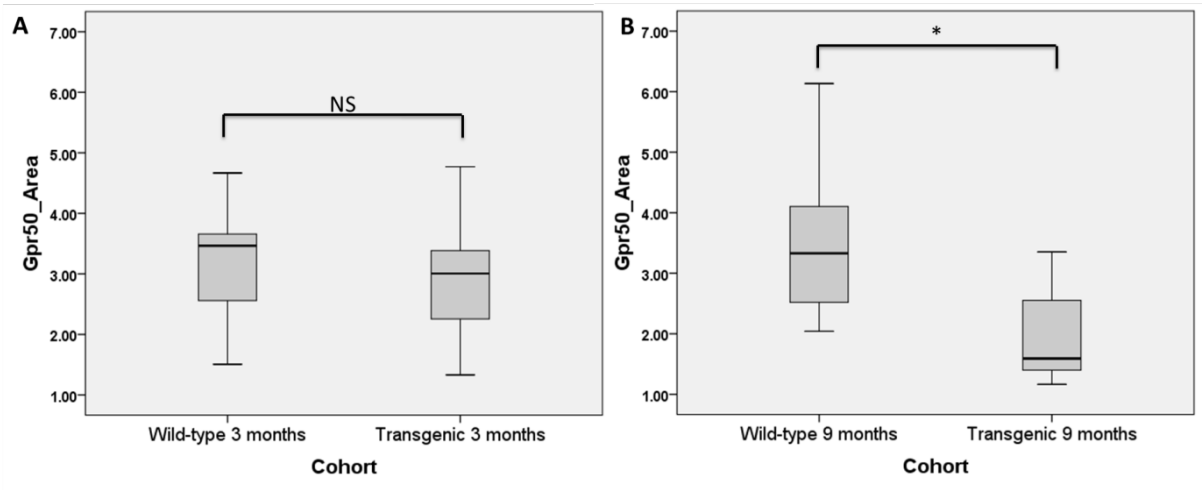

NS: not significant, p= 0.690>0.1; *: significant, p=0.033<0.05, N=7.

Figure 7.14 Comparison of Gpr50 expression in the hippocampus of TgSwDI mice with that of wild-type mice at 3 months or 9 months. The differences in means were tested using the unpaired Student's t-test.

7.3.3.3 Is the expression level of Gpr50 in the hippocampus related to age?

To determine whether Gpr50 expression in the hippocampus was regulated with the increasing age, Gpr50 levels were compared between 3 months and 9 months mice, in both wild-type and transgenic cohorts. No significant alteration of Gpr50 expression was identified in either phenotype (Figure 7.15), which agreed with the finding in the general linear model that age does not affect Gpr50 levels in the hippocampus (7.3.3.1).

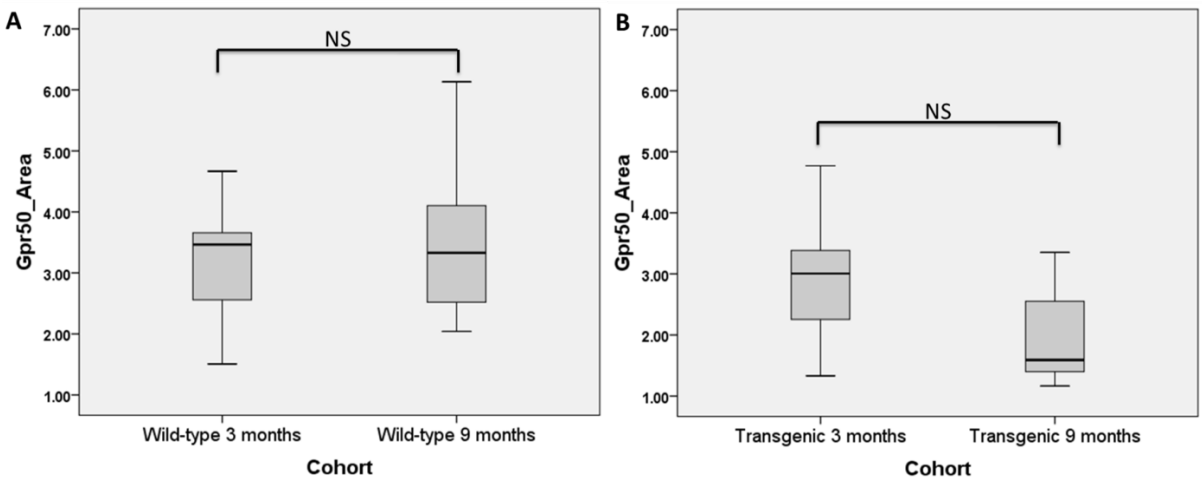

NS (left): not significant, p= 0.580>0.1; NS (right): not significant, p=0.113>0.1; N=7.

Figure 7.15 Comparison of Gpr50 expression in the hippocampus between 3 months and 9 months mice of A) wild-type or B) TgSwDI. The differences in means were tested using the unpaired Student's t-test.

7.3.3.4 Is the expression level of Gpr50 in hippocampus correlated to that of Aβ?

No significant correlation of Gpr50 levels and Aβ amounts was found in the hippocampus of TgSwDI mice (r=-0.394, p=0.183, Figure 7.16), which coincided with the observation that the expression level of Gpr50 in the hippocampus was unchanged in TgSwDI mice from 3 months to 9 months. Hence, the potential role of Gpr50 associated with AD may be related to certain brain regions, such as in the entorhinal cortex.

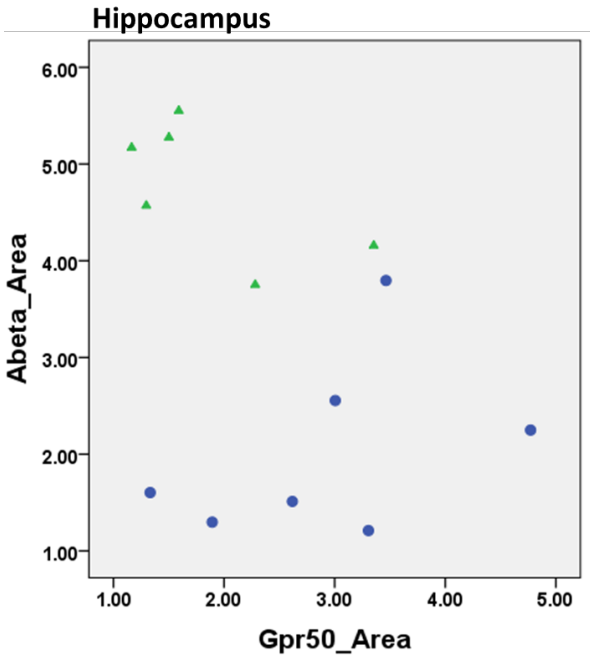

Pearson's Correlation analysis

Hippocampus		Abeta_Area
Gpr50_Area	Pearson Correlation	-.394
	Sig. (2-tailed)	.183
	Sig. (1-tailed)	.091
	N	13

Figure 7.16 Correlation between the expression levels of Gpr50 and Aβ in the hippocamous of TgSwDI mice

7.4 Discussion

In this chapter, I studied the expression levels of Gpr50 and its correlation with Aβ in an AD mouse model TgSwDI mice. My results showed that in the entorhinal cortex layer V, Gpr50 expression was significantly enhanced in older TgSwDI mice compared to younger TgSwDI mice, and showed a trend of elevation compared to wild-type littermates. Accordingly, a notable positive correlation between Gpr50 levels and Aβ deposition was identified in the entorhinal cortex layer V. In the hippocampus, Gpr50 expression was significantly decreased in older TgSwDI mice compared with age-matched wild-type control. No significant correlation of Gpr50 expression and Aβ deposition was found in the hippocampus.

My data provide further evidence for the association of GPR50 with AD, as it was confirmed that Gpr50 expression in the entorhinal cortex layer V was altered during a later stage of AD (9 months in TgSwDI mice), and its level was significantly elevated as the severity of the illness rose with age. Importantly, this response of Gpr50 was relevant to the major hallmark of AD pathology: the accumulation of amyloid plaques. Also, my results lead to a further speculation if the down-regulation of Gpr50 in the hippocampus is an indication of other aspects of AD, for instance the cognitive impairments, or whether it is involved with other complications of this disease that fail to exhibit in this model, for example, the neuronal loss.

7.4.1 What is the implication of the alteration of GPR50 expression in TgSwDI mice?

The parameter for assessing Gpr50 expression levels in this experiment is the percentage with Gpr50 immunoreactivity of certain regions (the entorhinal cortex layer V and the hippocampus). In wild-type C57BL/6 mice, Gpr50 was co-localised with mature neuronal marker NeuN, but not with GFAP, or O4 which marked astrocytes and oligodendrocytes respectively (Grunewald et al, 2012). This is further confirmed by my results that the staining of Gpr50 was mostly detected in neurons with apparent axons in both wild-type and TgSwDI mice, supporting the neuronal functions of Gpr50.

It is worth noting that 3 months old is referred to as the lower age limit of mature adult mice that are past development, while middle age group that begins to show senescent changes typically starts from 10 months old. The developmental features of cells especially neurons may be almost viewed as equal between 3 months and 9 months mice, as there would be no either further neuronal extension or neuronal damage in the span of the two ages. Also, there were no data about appreciable neuronal loss identified in TgSwDI mice up to 9 months. Therefore, an increase of Gpr50 levels in 9 months TgSwDI mice compared to 3 months in the entorhinal cortex, layer V indicated that there were more neurons activated to express Gpr50 in this area, rather than different cell sizes. This is interesting as Gpr50 in TgSwDI seems to follow the similar pattern to the accumulation of Aβ burden with increasing age, as well as a speculated elevation of Bace1 activity. As both Gpr50 and most of Bace1 seem to express in neuronal cells, more functional explanation might be achieved by correlating the "burden" of these two than that of Gpr50 and Aβ.

Note that the diffuse Aβ in the entorhinal cortex is not the major form of the extracellular Aβ plaques in this model, which is dominated by microvascular Aβ deposits in the thalamic region (Davis et al, 2004a). It will also be interesting to correlate the expression levels between Gpr50 and Aβ using quantitative real-time PCR to compare the mRNA level or using western blotting of brain sub-region homogenates to compare the protein level in their separately dominant areas.

Importantly, the decrease of Gpr50 expression in the hippocampus of 9 months TgSwDI animals may be related to different neurodegenerative processes between an elderly AD case and a normal aging case, while the cortex or at least the entorhinal cortex, layer V might be the area to investigate the pathological mechanism of this disease.

7.4.2 Is Gpr50 involved in the neurotransmitter signalling system in AD?

The endocrine system in AD patients is disturbed, as indicated by an increased level of glucocorticoids (GCs) circulation (de Quervain et al, 2004; Dhikav & Anand, 2007; Notarianni, 2013). GCs are synthesised in the adrenal cortex and highly responsive to chronic stress. These steroid hormones cause effects by coupling to the hippocampus-based glucocorticoid receptor (GR), which is activated after the binding and in turn boosts the up-regulation of anti-inflammatory factors and suppresses the pro-inflammatory factors. The function of hypothalamic-pituitary-adrenal (HPA) axis was disordered in AD, which triggered the adrenal cortex to release GCs in response to stress (Woulfe et al, 2002). Triple transgenic AD mice (3×TgAD) harbouring swAPP, PS1 (M146V) and tau (P301L) exhibited amyloid plaques and tangles with dysfunctional synapse. Administration of GR antagonist mifepristone (RU486) significantly improved the pathological and cognitive outcomes of these mice, indicating that the rescue of the glucocorticoid system highlights a ponderable effective treatment for AD (Baglietto-Vargas et al, 2013).

GPR50 has long been identified as having a potential to regulate the outputs of neuronal activity and hormone production in HPA axis, due to its high expression levels in the hypothalamic regions (Drew et al, 2001; Drew et al, 1998) and co-localisation with Nogo-A, Abca2 and Cdh8 in both adult and E18 mouse brain (Grunewald et al, 2012). Gpr50 knockout mice showed an elevated level of corticosterone circulation combined by *in vitro* data that Gpr50 knockdown in rat

pituitary cells attenuates TIP60-dependent GR signalling (Li et al, 2011). This suggests an impaired GCs feedback to GR, influenced by the lacking of Gpr50. A similar effect occurs in AD in terms of the GCs-GR interaction, exemplified by the hypercortisolemia and a GR-signaling insufficiency (Notarianni, 2013). I observed a down-regulation of Gpr50 in the hippocampus of old TgSwDI mice, and a trend of up-regulation in the entorhinal cortex, layer V. Therefore, the effect of Gpr50 on GCs-GR system in AD might be region-specific and highly responsive to other sites of the brain. In this case, the altered hippocampal Gpr50 may be linked with a dysfunctional GCs-GR system. Furthermore, the entorhinal cortex contributes the hippocampal inputs. Lesions of the enthorinal cortex resulted in a transient redistribution of GR expression in the hippocampus, a decrease in the dentate gyrus while an increase the CA1 sub-field (O'Donnell et al, 1993). The status of the entorhinal cortex seems to send signal to the regulation of GR. Thus, the observation that more neurons expressed with Gpr50 in the entorhinal cortex, layer V as AD develops might be a preliminary signal of rescue to the diminished GR signalling in the hippocampus. Further investigations are required to reveal the levels of GCs and GR in this transgenic model, hence to answer the question if Gpr50 is associated with the hypofunction of GCs-GR system in AD.

The melatonin-related receptor (MT) signalling pathway is also damaged in AD cases. Interestingly, the affected expression of MT1 is region-specific, with increased level in the hippocampus but decreased level in the cortical area (Brunner et al, 2006; Savaskan et al, 2001; Savaskan et al, 2002). These regulative effects are opposite to those on Gpr50 in TgSwDI mice. It is known that GPR50 can work as an antagonist to MT1, preventing its binding to agonist and G protein by forming heterodimer with it (Levoye et al, 2006). It is possible that Gpr50 expression changes under AD conditions are responsive to the dysregulation of MT1 functions, and related to the disrupted homeostasis of melatonin signalling in AD.

Other irregular endocrine activities recognised in AD patients include deficits in cholinergic, serotonergic, noradrenergic, dopaminergic, GABAergic and somatostatinergic neurotransmitter system (Reinikainen et al, 1990). For example, ablating muscarinic M_1 receptor (M_1R) in TgSwDI and 3×TgAD mice exacerbated AD pathological features and cognitive impairments (Medeiros et al, 2011). Elsewhere, increased binding to serotonin receptors (5-HT_{1A}, 5-HT_{2A}) was found in vascular AD brains compared with normally aged controls, and positively correlated

to cognition (5-HT_{1A}) (Elliott et al, 2009), while the density of 5-HT_{2A} and 5-HT_6 declined in neurons of AD brains compared with age-matched control (Lorke et al, 2006). Gpr50 was found co-localised with 5-hydroxytryptamine (5-HT, serotonin, serotonergic marker), tyrosine hydroxylase (dopaminergic and noradrenergic marker), and dopamine beta hydroxylase (noradrenergic neuronal marker) in the adult mouse brain stem, suggesting that it might function as a receptor for neurotransmitters (Grunewald et al, 2012). The yeast two-hybrid study also showed a potential role of GPR50 in the GABA transmission putatively via the interaction with PICK1, SLC12A5/ KCC2 or MADD (Grunewald et al, 2009).

The signal transduction of above-mentioned M_1R and 5-HT receptor is influenced by the regulator of G protein signalling (RGS) family (Muma et al, 2003). One of the members, RGS4 escalates the GTPase activity of Gi/o and Gq/11 proteins and the GTP hydrolysis in turn accelerates the termination of G protein-coupled receptor (GPCR) signalling. RGS4 is located in a major susceptibility locus (chromosome 1q21-q22) for schizophrenia identified by genetic linkage and association analysis, combined with quantitative studies showing a decreased RGS4 expression in the prefrontal cortex of schizophrenia patients (Chowdari et al, 2002; Gu et al, 2007; Morris et al, 2004). Down-regulated mRNA levels of RGS4 splice variants were also found in AD patients (Emilsson et al, 2006), which may be the explanation of reduced RGS4 protein levels in the AD parietal cortex, and responsible for the diminished M1 cholinergic signalling in AD. Interestingly, siRNA-mediated gene silencing of RGS4 resulted in the up-regulation of GPR50 (Vrajova et al, 2011), which might be related to my results of the enhanced Gpr50 expression in the entorhinal cortex of TgSwDI mice.

In summary, the alteration of Gpr50 expression in TgSwDI mice might be a response to a malfunctioning network of the signalling system in this AD-affected model.

7.4.3 Suggested future experiments

My results have demonstrated that Gpr50 expression level in the hippocampus is likely to be associated with certain aspects of AD pathogenesis, such as neurodegeneration. Its levels in the entorhinal cortex, layer V may indicate the severity of diffuse Aβ deposition. To further verify these observations, I emphasise that it is essential to investigate the putative interactors of Gpr50 observed in the

TgSwDI mouse model. The following additional experiments can be carried out to further reveal the causes or effects of altered GPR50 expression in AD:

1) Measure the levels of Bace1 expression and activity in the brain regions of TgSwDI mice where Gpr50 expression was found altered, and correlate the levels of the two proteins;
2) Perform immunoprecipitation between Gpr50 and potential interactors that are presumed to be affected in TgSwDI mice (Bace1);
3) Assess expression levels of interactors that are known to play a role in AD and might help to explain the alteration of Gpr50 expression in TgSwDI mice (GR, MT1, RGS4);
4) Cross TgSwDI mice with Gpr50 KO mice and monitor the body weight, body temperature, activity frequencies, cognitive function and pathological appearance of the animals;
5) Cross TgSwDI mice with GPR50 interactor-deficient mice (melatonin receptor) and study the levels of Gpr50;
6) Cross TgSwDI mice with BACE1 KO mice and study the expression patterns of Gpr50.

8 Discussion

In this thesis, my investigations expanded the knowledge of mental disorder risk factor GPR50, by linking its function with a key enzyme of major brain diseases BACE1 and by further revealing its altered expression during the progression of Alzheimer's disease (AD). I have shown that GPR50 is physically associated with BACE1, and has a potential in regulating the function of BACE1 at the cell surface and the synapse (chapter 3). The mechanism by which GPR50 modulates β-secretase activity may be different in non-neuronal cells compared to neuronal cells, as GPR50 overexpression demonstrated different regulatory trends on BACE1 expression and trafficking (chapter 2/5). Also, the C-terminal tail of GPR50 appears to be essential to its general function, because GPR50del reduced β-secretase activity in neurons in comparison to GPR50 (chapter 4). The protein levels of Gpr50 in AD model TgSwDI mice exhibited age-related region-specific alterations, and were correlated with the quantity of Aβ deposition in the entorhinal cortex layer V (chapter 7).

8.1 GPR50 co-localises with BACE1 at functional sites

Both GPR50 and BACE1 are membrane-bound proteins. GPR50 is primarily located at the cell surface. This feature is common to GPCRs, which sense molecules outside the cells and activate intracellular signal transduction pathways and ultimately trigger cell responses. The co-localisation sites of GPR50 and BACE1 are generally external. They are found co-localised at the cell surface and filopodia/lamellipodia-like structures in a subset of non-neuronal HEK293 cells, when endogenously expressed; at the cell surface and neurites in neuronal SH-SY5Y cells when exogenously expressed; and at spines and axonal terminals in primary neurons (chapter 3). This suggests potential roles for the interaction of GPR50 and BACE1 in neurodevelopment and cell signalling.

8.1.1 The cell surface

The cell surface is one of the putative BACE1 activity sites. It is still not clear whether the Aβ generation occurs at the plasma membrane or the early endosomes, but the shedding of CAMs is most likely to take place at the cell surface. For example, BACE1 selectively sheds contactin-2 at the cell surface, and tightly regulates the surface expression of this CAM (Gautam et al, 2014). Elsewhere, BACE1 cleavage of voltage-gated sodium channel β4 subunit ($Na_v\beta4$) accelerated neurite extension that could be promoted by $Na_v\beta4$ itself, but reduced the number of filopodia-like protrusions (Miyazaki et al, 2007). GPR50 and BACE1 have an over-

lapping role in extending neurites. Therefore, GPR50 may mediate BACE1 activity on molecules expressed at the cell surface or external compartments. Yet, GPR50 overexpression also resulted in an increase in filopodia formation, opposite to the effect of BACE1 on $Na_v\beta4$ shedding. This may suggest that neurite extension and filopodia protrusion are two independent processes.

8.1.2 The synapse

In the nervous system, synapse is the structure which passes signals from one neuron (or nerve cell) to another. BACE1 is present in presynaptic terminals, with a subset in close proximity to synaptic active zones (Kandalepas et al, 2013). In an AD mouse model and human AD brains, BACE1 accumulates at synaptophysin-positive dystrophic neurites around amyloid plaques, suggesting that Aβ is released from presynaptic terminals where BACE1 cleaves APP (Kandalepas et al, 2013). Other BACE1 substrates that may be processed in the presynaptic terminal include NRG1, Jagged 1 and CHL1.

Strong co-localisation of GPR50 and BACE1 at the dendritic spines and the axon terminals indicates that their interaction may be implicated in synapse functions. Specifically, endogenous Gpr50 and Bace1 co-fractionate in the synaptic vesicles from adult mouse brain (chapter 3). Gpr50 is also located in the post-synaptic densities, showed by myself and others (Grunewald et al, 2012). This expression profile is similar to that of Nogo-A and Nogo-A receptor, NgR, which are expressed at both pre-synaptic and post-synaptic sites (Grunewald et al, 2012; Wang et al, 2002). Contrary to NgR, GPR50 rescues the inhibitory effect on neurite outgrowth when interacting with Nogo-A. Also, the Nogo-A~NgR1 interaction limits synaptic plasticity in part by restricting the expression of glutamate receptors (NMDA/AMPA receptor) and GABA transmission (GABA B receptor/GIRK1) (Murthy et al, 2013; Peng et al, 2011), the processes that may be associated with GPR50 (Grunewald et al, 2009). In addition, NgR is able to trans-activate the phosphorylation of EGFR without binding to it, and this process is required for mediating the inhibition of axon regeneration and myelination (Koprivica et al, 2005). Hence, there is a possibility that the presynaptic pool of GPR50 takes a part in BACE1 activity, while the postsynaptic pool responds to the cleavage product of BACE1, for instance, the EGF-like domain of NRG1.

Furthermore, BACE1 cleavage-mediated NRG1/ErbB4 signalling is required for synaptic transmission (Savonenko et al, 2008). Reduced presynaptic cleavage of NRG1 upon BACE1 deletion impaired the regular signalling of postsynaptic ErbB4, which resulted in a decreased spine density and schizophrenia-like cognitive/behavioural deficits (Savonenko et al, 2008). In neuronal cells, alteration of GPR50 function (GPR50del) potentially affected neuronal β-secretase activity. Also, in mouse brain, the strongest co-localisation of Gpr50 and Bace1 was seen in CA2 pyramidal neurons (chapter 6), the synaptic plasticity of which is associated with different types of learning and memory (Chevaleyre & Siegelbaum, 2010; Hitti & Siegelbaum, 2014; Wintzer et al, 2014), and a region demonstrates abnormalities early in the onset of schizophrenia and bipolar disorder (Benes et al, 2001; Focking et al, 2011; Leranth & Ribak, 1991). Thus, the presynaptic interaction of GPR50 and BACE1 may suggest a coordinating role in synaptic functions and may be important in the maintenance of normal cognition.

8.2 GPR50 and its illness-related variant have distinct effects on β-secretase activity

In chapter 4, it was shown that GPR50del but not GPR50 potentially suppressed β-secretase activity in neuronal cells, which corresponds to an effect of impeding Bace1 maturation (chapter 5). This regulation trend is opposite to what was observed in HEK293 cells, in which GPR50 but not GPR50del is an effector of BACE1 activity (Grünewald, 2011), and this matches with a potentially increased ratio of mature BACE1/immature BACE1 in the plasma membrane fractions (chapter 5). Thus, the modulation direction of the two transcripts of GPR50 is consistent with their respective roles in the β-secretase trafficking system in respective cell lines. Interestingly, both cell lines showed higher activity when over-expressing GPR50 compared to GPR50del. As the BACE1 activity level in HEK293 cells is low, the putative supressing effect by GPR50del is probably difficult to detect; whereas the Bace1 activity in neurons is high, the up-regulating ability of GPR50 is not as obvious as in HEK293 cells.

Previous studies have reported that some GPCRs regulate the localisation of secretases in the amyloidogenic pathway, thus affecting the production of Aβ peptides. The overexpression of GPR3 led to an increased localisation of mature γ-secretase in the detergent resistant membranes at cell surface and this measure

promoted the generation of Aβ40/42 peptides (Thathiah et al, 2009). Activation of δ-opioid receptor caused enrichment of BACE1 and γ-secretase in the late endosomes/lysosomes, and enhanced the activities of both secretases specifically for Aβ production (Teng et al, 2010). Note that both cell surface and endocytic compartments are arguably the sites for β-/γ-secretase cleavage. In mouse primary cortical neurons overexpression of GPR50del seems to retain Bace1 in the ER, thus there is a trend of decreasing Bace1 activity; whereas, in HEK293 cells, GPR50 overexpression tends to result in a higher percentage of mature BACE1 but significantly less immature BACE1 distributed in the cell surface fractions. This observation in HEK293 cells may partly explain why BACE1 activity is up-regulated upon GPR50 transfection, as immature BACE1 is much less active than mature BACE1 (Zhong et al, 2007).

The C-terminal polymorphisms of GPCRs may affect their surface trafficking, secondary structure folding and responsiveness to ligand binding (Spomer et al, 2014). The C-terminal tail of GPR50 is required for its plasma membrane localisation and is essential for the binding of C-terminal interactors, i.e. TIP60 (Li et al, 2011). For GPR50 non-C-terminal interactors, for instance MT1, deletion of GPR50 C-terminal tail retained the ability to heterodimerise with MT1 but its inhibitory effect on MT1 was removed (Levoye et al, 2006). The deletion of residues 502-505 (TTGH) and Thr532Ala substitution do not affect the cellular localisation of GPR50, but enhanced its potential in neurite outgrowth (Grünewald, 2011). It has not been investigated which part of GPR50 physically binds to BACE1, but the two variations included in GPR50del are sufficient to affect its function by differentially regulating BACE1 activity in different cell lines.

The action of holding Bace1 in the ER by GPR50del may indicate a direct interaction with immature BACE1 and interrupt its maturation, a regulation mechanism that has been suggested for presenilin and the cellular prion protein (Griffiths et al, 2011; Hebert et al, 2003). While wild-type presenilin1 has a neuroprotective effect, mutant presenilin1 facilitates the generation of neurotoxic Aβ partly by increasing the transcription of BACE1 and correspondingly β-secretase activity (Giliberto et al, 2009). Thus, mutations in BACE1 regulators may imply an exchange between the neuroprotective and neurodegenerative roles. In this case, GPR50del seemingly has deleterious effects as it is associated with an increased susceptibility to bipolar disorder (BD) and schizophrenia. However, the negative effects represented by

presenilin1 mutations require the molecules in the amyloidogenic cascade, for instance APP and γ-secretase (Giliberto et al, 2009). On one hand, the inhibitory effect of GPR50del leads to insufficient BACE1 cleavage of neural CAMs, which may result in neuronal loss; on the other, excessive NRG1-ErbB4 signalling has been seen in BD and schizophrenia (Hahn et al, 2006; Wang et al, 2014b), thus the GPR50 variation (GPR50del) might be responsible for reducing NRG1-dependent ErbB4 activation . As it is not known which BACE1 substrate(s) GPR50 acts on, whether mutations in GPR50 generate adverse or favourable effects under diseased conditions has not been adequately investigated.

The positive impact of the GPR50 full-length isoform on BACE1 activity in HEK293 cells counteracted the negative effects of RTN3/Nogo-C (Grünewald, 2011), which may indicate that GPR50 and RTN3 bind to BACE1 in a competitive manner. This result is concomitant with the finding that in BACE1 trafficking network, RTN3 retains BACE1 in the ER, whereas GPR50 overexpression assists in more mature BACE1 releasing to the cell surface, two opposite directions of regulating β-secretase activity. Further investigation is called for on whether GPR50 and RTN3 form a complex with BACE1 at the same time and therefore cooperate to maintain the general activity level of β-secretase under healthy conditions. Malfunction of either GPR50 or RTN3 in mental diseases will affect BACE1-dependent cleavage. Dysregulation of GPR50 may include the variations in GPR50del that apparently facilitate the inhibitory effect of RTN3 (impeding BACE1 maturation).

8.3 What can we conclude from the investigation of GPR50 in the AD TgSwDI mouse model?

8.3.1 Why is GPR50 level regulated in AD mouse brain?

A unique feature of TgSwDI mice is that the brain parenchyma accumulates diffuse nonfibrillar plaques, while the thalamic microvessels harbour compact, fibrillar and thioflavine-S-positive amyloid deposits (Van Vickle et al, 2008). In chapter 7, I showed that in the entorhinal cortex layer V, Gpr50 expression level is increased with age in TgSwDI mice (transgenic, 3 months VS 9 months), but not in wild-type littermates, and the elevation is positively correlated with Aβ accumulation. Therefore, the expression level of Gpr50 might be responsive to that of Aβ level.

In the human brain and AD mouse models, diffuse plaques mainly consist of Aβ42 (Morrissette et al, 2009). Interestingly, Aβ42 itself is a transcription regulator. Aβ42, or its active fragment Aβ25-32, can stimulate the expression and function of several membrane receptors, including TrkA (Bulbarelli et al, 2009), p75 neurotrophin receptor (Chakravarthy et al, 2010), and insulin receptor (Bartl et al, 2013). This can potentially contribute to the pathogenesis of AD through downstream regulation cascades such as Akt/GSK3β, ERK/MAPK, NF-κB, Jun N-terminal kinase (JNK) and RhoA/ROCK signalling pathways. For instance, Aβ42 activates the expression of BACE1 via the JNK/c-jun signalling pathway and potential post-transcriptional mechanism (Guglielmotto et al, 2012; Sadleir & Vassar, 2012). It is possible that GPR50 is also a target of Aβ42 in the feedback loop of the amyloidogenic pathway during AD development. Additionally, the Swedish double mutation in APP is associated with increased β-secretase activity (Citron et al, 1992), so an increase of Bace1 activity is expected in TgSwDI mouse brain. Considering the interaction between Gpr50 and BACE1 revealed in this thesis, it will be interesting to test if the increased level of Gpr50 is required to coordinate with an inflated Bace1 activity in the entorhinal cortex.

Additionally, it is noted that in the hippocampus, there is no alteration of Gpr50 expression between young and old TgSwDI mice, and Gpr50 is not correlated to Aβ in density. This may be consistent with the observation that the immunoreactivity of Gpr50 and Aβ was detected in different sub-regions of the hippocampus. However, Gpr50 and Aβ were also located in different cell parts of the same cell layers (i.e. the CA1 sub-division). This implies that the putative association between Gpr50 and Aβ42 may be linked by a mediator, such as Bace1.

8.3.2 What do we know about the role of GPR50 in AD?

The level of Gpr50 in the hippocampus is down-regulated in older TgSwDI mice compared with the wild-type control (9 months, wild-type VS transgenic), and has a trend of elevation in the entorhinal cortex, the main input/output structure for the hippocampus (chapter 7). This asynchrony of Gpr50 regulation may indicate a dissociated role in the two brain regions, such as in learning ability and nonspatial memory (Ross & Eichenbaum, 2006; Shohamy et al, 2000). Hippocampus-dependent reference spatial memory (performance in Barnes maze) is found impaired in TgSwDI mice as early as 3 months old (Xu et al, 2007), a time point at which no loss

of Gpr50 was found in the hippocampus. The motor learning and coordination (rotarod analysis) showed no deficits in TgSwDI mice at an old age (12 months old), but they approached the novel object in an open field more quickly. This suggests that non-spatial memory is differentially affected from spatial memory in TgSwDI mice (Xu et al, 2007). Thus, it may be more practical to investigate the link of GPR50 to nonspatial memory, such as the object recognition memory, which may also be dependent on the hippocampus (Cohen et al, 2013). Moreover, Gpr50 expression in the hippocampus appears to respond to the severity of AD related to age and thus might be related to late-onset AD.

Levels of synaptophysin immunoreactive presynaptic terminals were found decreased in the hippocampus of different APP-overexpressing mice and this synaptotoxicity is believed to be independent of APP mutations (Mucke et al, 2000). Also, dentate gyrus neurons in the hippocampus of TgSwDI mice showed reduced frequency and amplitude of $GABA_A$ receptor-mediated miniature inhibitory postsynaptic currents, and decreased extrasynaptic tonic inhibitory current (Liang et al, 2014). In chapter 3, I showed that endogenous Gpr50 was present in presynaptic vesicles of adult mouse brain, and was suggested to mediate Bace1 cleavage which can occur in neural CAM-containing presynaptic terminals. Gpr50 was also localised in PSD-95 immunoreactive postsynaptic densities, the putative site where GPR50 counteracts the inhibiting effect of Nogo-A (Grunewald et al, 2009). Thus, the loss of Gpr50 in the hippocampus of 9 month-old TgSwDI mice may be associated with the hippocampal synaptotoxicity in these animals. This suggests that GPR50 might exert functions in maintaining the integrity and plasticity of synapses during the late adulthood, and this function broadens its role in the neuronal development (i.e. synapse formation) in postnatal stage. This function of GPR50 is supported by my finding that GPR50 and BACE1 putatively interact at synapse (chapter 3), as BACE1 is required for regulating synaptic inputs to hippocampal pyramidal neurons (Wang et al, 2014a). In particular, GABAergic synapses in the hippocampus are likely to be one of the major targets of GPR50, as some key proteins in GABA transmission (PICK1, SLC12A5/ KCC2, MADD) are putative GPR50 interactors (Grunewald et al, 2009).

8.3.3 How does the function of GPR50 in the hippocampus/entorhinal cortex link to that in HPA-axis?

TgSwDI mice, GPR50 KO mice and BACE1 KO mice share a range of metabolic deficits related to HPA-axis, including elevated levels of circulating glucocorticoids in serum, reflecting a response to stress (Freeman et al, 2012; Ivanova et al, 2008; Meakin et al, 2012). This may indicates that GPR50 and BACE1 have coincidental functions in maintaining HPA-axis activity.

Generally, the hippocampus undertakes the negative feedback mechanism to control the regular level of glucocorticoids secreted by the adrenal gland (Phillips et al, 2006). Glucocorticoid receptors (GR) are abundantly expressed in the hippocampus, while overactive glucocorticoid can cause damage to the hippocampus, which consequently results in insufficient GR signalling (Phillips et al, 2006). This regulative model fits with what was found about Gpr50 in TgSwDI mice. Gpr50 expression in the hippocampus may be diminished in response to abnormally high glucocorticoid levels (that can be induced by stress), a situation that will blunt the normal GR signalling activation mediated by Gpr50 (Li et al, 2011).

The entorhinal cortex receives one of the largest cortical projections of midbrain dopaminergic neurons (Loughlin & Fallon, 1984). Dopamine is released by the arcuate nucleus of the hypothalamus, an area that was seen with strong co-localisation of Gpr50 and Bace1 (chapter 6). Damage of dopamine systems has been observed in AD with Parkinsonism and in schizophrenia, such as the dysfunction of dopamine D2 receptor (Joyce et al, 1998a; Joyce et al, 1998b; Murray et al, 1995; Seeman, 1987). Dopamine is capable of facilitating or suppressing the synaptic responses in the entorhinal cortex depending on the concentration applied (Caruana et al, 2006). Higher concentrations of dopamine in the rat brain hyperpolarise responses in layer II neurons and depolarise responses in layer V neurons of the entorhinal cortex (Pralong & Jones, 1993). A recent study showed that rewarding stimulation of the lateral hypothalamus induces a dopamine-dependent suppression of synaptic responses in the entorhinal cortex (Hutter et al, 2013). Thus, the level of Gpr50 in the entorhinal cortex layer V of TgSwDI mice might be closely connected with its level in dopaminergic neurons of the hypothalamus, as the functional states of both areas are greatly influenced by the dopamine level.

Furthermore, Gpr50 and Bace1 mRNA levels appeared to be negatively correlated across the hypothalamic regions (chapter 6). This may indicate that GPR50 has a role in counteracting the deleterious aspects of BACE1 function in the endocrine system, such as the hyper-signalling through releasing the EGF-like domain from NRG1 cleavage. Subcutaneous injections of NRG1 especially EGF in rats resulted in hyperdopaminergic abnormalities, which were correlated with schizophrenia-like behavioural deficits, such as lower prepulse inhibition (Nawa et al, 2014). This neuropathological impairment was thought to result from the over-activation of ErbB receptors by EGF. Therefore, BACE1 has a potential to damage the homeostasis of dopamine synthesis and metabolism if its function is not restrained. GPR50 is expressed in dopaminergic neurons. In particular, Gpr50 strongly co-localises with Bace1 in the ARH and DMH, which are the hubs of the endocrine regulation, including the dopamine release and circulation. Thus, my findings have strengthened the crucial function of GPR50 in neurotransmitter signalling, probably by interacting with BACE1.

8.4 Future work

This thesis provides preliminary evidence for the interaction between GPR50 and BACE1. The regulation of GPR50 on neuronal β-secretase activity was highlighted. The potential of GPR50 in β-secretase activity-depending mechanisms (expression and trafficking) was demonstrated in both non-neuronal and neuronal cell lines, and primary neuronal cultures. The influence of GPR50-BACE1 interaction was confirmed by revealing the association of GPR50 with one of the medical-meaningful molecules from BACE1 cleavage-Aβ, which strengthened the link of GPR50 to brain diseases. The studies of GPR50's effects on BACE1 function reflect a new angle for investigating the pathogenesis of mentally related illnesses, but there are critical gaps to fill in. The most relevant points are addressed below.

1) **Does GPR50 C-terminal polymorphism affect its interaction with BACE1?**

   In chapter 3, the interaction between the insertion form of GPR50 and BACE1 was demonstrated, while in chapters 4 and 5, GPR50 deletion/SNP form (GPR50del) was shown with a differentiated potential in regulating BACE1 properties from the full-length form (GPR50). It is important to further investigate if the physical interaction of BACE1 with GPR50 is

altered upon deletion/SNP; for example, whether the co-immunoprecipitation of BACE1 and GPR50 is strengthened or weakened. This will partly explain the enrichment of GPR50del in BD patients.

2) **Is the regulative action of GPR50 on β-secretase activity substrate-specific?**

   BACE1 cleavage has multiple explanations with occasional contradictory effects in brain activity, reflected by its role in normal function maintenance and illness pathology. This performance is attributed to β-secretase activity on different substrates. Therefore, it is essential to assess which substrate cleavage is GPR50-dependent, so as to answer the question which part of, or direction of BACE1 function, is GPR50 involved in.

3) **Is the interaction of GPR50 and BACE1 supported by loss-of-function studies?**

   This thesis mainly focused on the effect of GPR50 gain-of-function on β-secretase activity. However, before we draw the conclusion that GPR50 is required for BACE1 function, it is essential to validate the results by loss-of-function studies (i.e. the Gpr50 RNAi studies attempted in chapter 4). It must be determined whether BACE1 activity and regulation are altered in GPR50 deletion cells or GPR50 KO animals. Also, the performance of Gpr50 in BACE1 KO and BACE1-overexpressing animals should be established, which will provide *in vivo* evidence for the involvement of GPR50 in BACE1 function.

4) **What part do co-interactors play in the interaction of GPR50 and BACE1?**

   The putative GPR50 interactors (i.e. RTN3/Nogo, SNX6) are important regulators of β-secretase activity, and have been functionally confirmed to be related to BACE1-dependent brain diseases. This link is emphasised as a part of the hypothesis in this thesis that the interaction between GPR50 and BACE1 is mediated via co-interactors. It will provide more validation by studying whether GPR50 plays a part in the biochemical function of RTN3/Nogo/SNX6 or vice versa, which is sequentially connected to the modulation of BACE1 activity. GPR50, BACE1 and co-interactors may function as a protein complex, and the dysfunction of any part will contribute to the pathogenesis of major mentally related illnesses.

5) **Is the interaction of GPR50 and BACE1 region-specific in the brain?**
   In chapter 6, I showed that Bace1 expression is strikingly high in the CA2 region of the hippocampus and hormone-releasing areas of the hypothalamus (ARH, DMH). These regions also express high levels of Gpr50, and thus have strongest co-localisation of Gpr50 and Bace1. It is of high relevance to explore whether the interaction of GPR50 and BACE1 is restricted, or concentrated, in these brain regions, and what BACE1 substrates are involved. The *Cre/loxP* recombination system can be applied to develop mice with deletion of Gpr50 restricted to a sub-region or a specific cell type, such as the pyramidal cells of the hippocampal CA2 region (Tsien et al, 1996). Analysing BACE1 functions and the levels of certain substrates, in selected regions with deficient Gpr50 expression, will highlight which part of the brain activity is controlled by GPR50-BACE1 interaction.
6) **Are the findings of GPR50 in AD mouse model applicable to human AD and other related mental disorders?**
   The TgSwDI mice used in this thesis partly cover the behavioural and functional defects in AD. It is necessary to take a further step for evaluating how useful the observations of Gpr50 in this AD model are, in order to explain the role of this protein under actual AD or other AD-like conditions. Thus, it is required to assess the expression profile of GPR50 in human post-mortem brains of mentally related diseases (i.e. AD, schizophrenia, BD), and to correlate GPR50 characteristics with those of BACE1, relevant substrates and cleavage products.
7) **Does GPR50 interact with BACE1 substrates?**
   Interacting with BACE1 substrates is an extra mechanism that can contribute to the regulation of BACE1 activity. For instance, GPR50 is known to be a regulator of APP interactor TIP60 and ABCA2. If GPR50 mediates the transcription and trafficking of APP or other substrates, it will in part explain the alteration of β-secretase activity upon GPR50 overexpression.

In summary, future work should further examine the interaction between GPR50 and BACE1 with a focus on their functions in both neurodevelopment under normal conditions and neurodegeneration under diseased conditions.

Reference

Adlerz L, Beckman M, Holback S, Tehranian R, Cortes Toro V, Iverfeldt K (2003) Accumulation of the amyloid precursor-like protein APLP2 and reduction of APLP1 in retinoic acid-differentiated human neuroblastoma cells upon curcumin-induced neurite retraction. *Brain research Molecular brain research* **119:** 62-72

Ahn KH, Lyoo IK, Lee HK, Song IC, Oh JS, Hwang J, Kwon J, Kim MJ, Kim M, Renshaw PF (2004) White matter hyperintensities in subjects with bipolar disorder. *Psychiatry and clinical neurosciences* **58:** 516-521

Alaerts M, Venken T, Lenaerts AS, De Zutter S, Norrback KF, Adolfsson R, Del-Favero J (2006) Lack of association of an insertion/deletion polymorphism in the G protein-coupled receptor 50 with bipolar disorder in a Northern Swedish population. *Psychiatric genetics* **16:** 235-236

Albensi BC, Mattson MP (2000) Evidence for the involvement of TNF and NF-kappaB in hippocampal synaptic plasticity. *Synapse* **35:** 151-159

Alberi L, Hoey SE, Brai E, Scotti AL, Marathe S (2013) Notch signaling in the brain: in good and bad times. *Ageing research reviews* **12:** 801-814

Allen G, Barnard H, McColl R, Hester AL, Fields JA, Weiner MF, Ringe WK, Lipton AM, Brooker M, McDonald E, Rubin CD, Cullum CM (2007) Reduced hippocampal functional connectivity in Alzheimer disease. *Archives of neurology* **64:** 1482-1487

Allinquant B, Hantraye P, Mailleux P, Moya K, Bouillot C, Prochiantz A (1995) Downregulation of amyloid precursor protein inhibits neurite outgrowth in vitro. *The Journal of cell biology* **128:** 919-927

Anyanwu NU (2014) Characterising the role of GPR50 in neurodevelopment and lipid metabolism. Doctor of Philosophy Thesis, The University of Edinburgh,

APA (2013) *Diagnostic and statistical manual of mental disorders : DSM-5*, 5th edn. Arlington, VA: American Psychiatric Association.

Arancibia-Carcamo IL, Fairfax BP, Moss SJ, Kittler JT (2006) Studying the Localization, Surface Stability and Endocytosis of Neurotransmitter Receptors by Antibody Labeling and Biotinylation Approaches. In *The Dynamic Synapse: Molecular Methods in Ionotropic Receptor Biology*, Kittler JT, Moss SJ (eds). Boca Raton (FL)

Asahina H, Masuba A, Hirano S, Yuri K (2012) Distribution of protocadherin 9 protein in the developing mouse nervous system. *Neuroscience* **225:** 88-104

Ashley J, Packard M, Ataman B, Budnik V (2005) Fasciclin II signals new synapse formation through amyloid precursor protein and the scaffolding protein dX11/Mint. *The Journal of neuroscience : the official journal of the Society for Neuroscience* **25:** 5943-5955

Baeriswyl T, Stoeckli ET (2008) Axonin-1/TAG-1 is required for pathfinding of granule cell axons in the developing cerebellum. *Neural development* **3:** 7

Baglietto-Vargas D, Medeiros R, Martinez-Coria H, LaFerla FM, Green KN (2013) Mifepristone alters amyloid precursor protein processing to preclude amyloid beta and also

reduces tau pathology. *Biological psychiatry* **74:** 357-366

Bales KR, Liu F, Wu S, Lin S, Koger D, DeLong C, Hansen JC, Sullivan PM, Paul SM (2009) Human APOE isoform-dependent effects on brain beta-amyloid levels in PDAPP transgenic mice. *The Journal of neuroscience : the official journal of the Society for Neuroscience* **29:** 6771-6779

Ballard C, Gauthier S, Corbett A, Brayne C, Aarsland D, Jones E (2011) Alzheimer's disease. *Lancet* **377:** 1019-1031

Barbero-Camps E, Fernandez A, Martinez L, Fernandez-Checa JC, Colell A (2013) APP/PS1 mice overexpressing SREBP-2 exhibit combined Abeta accumulation and tau pathology underlying Alzheimer's disease. *Human molecular genetics* **22:** 3460-3476

Barnett JH, Smoller JW (2009) The genetics of bipolar disorder. *Neuroscience* **164:** 331-343

Barron J. (2010) The Endocrine System: Hypothalamus, Pituitary, & Pineal Glands.

Bartl J, Meyer A, Brendler S, Riederer P, Grunblatt E (2013) Different effects of soluble and aggregated amyloid beta42 on gene/protein expression and enzyme activity involved in insulin and APP pathways. *Journal of neural transmission* **120:** 113-120

Batailler M, Mullier A, Sidibe A, Delagrange P, Prevot V, Jockers R, Migaud M (2012) Neuroanatomical distribution of the orphan GPR50 receptor in adult sheep and rodent brains. *Journal of neuroendocrinology* **24:** 798-808

Bechtold DA, Sidibe A, Saer BR, Li J, Hand LE, Ivanova EA, Darras VM, Dam J, Jockers R, Luckman SM, Loudon AS (2012) A role for the melatonin-related receptor GPR50 in leptin signaling, adaptive thermogenesis, and torpor. *Current biology : CB* **22:** 70-77

Bekirov IH, Nagy V, Svoronos A, Huntley GW, Benson DL (2008) Cadherin-8 and N-cadherin differentially regulate pre- and postsynaptic development of the hippocampal mossy fiber pathway. *Hippocampus* **18:** 349-363

Benes FM, Todtenkopf MS, Kostoulakos P (2001) GluR5,6,7 subunit immunoreactivity on apical pyramidal cell dendrites in hippocampus of schizophrenics and manic depressives. *Hippocampus* **11:** 482-491

Bengtsson SK, Johansson M, Backstrom T, Nitsch RM, Wang M (2013) Brief but chronic increase in allopregnanolone cause accelerated AD pathology differently in two mouse models. *Current Alzheimer research* **10:** 38-47

Bennett BD, Denis P, Haniu M, Teplow DB, Kahn S, Louis JC, Citron M, Vassar R (2000) A furin-like convertase mediates propeptide cleavage of BACE, the Alzheimer's beta - secretase. *The Journal of biological chemistry* **275:** 37712-37717

Bhattacharyya R, Barren C, Kovacs DM (2013) Palmitoylation of amyloid precursor protein regulates amyloidogenic processing in lipid rafts. *The Journal of neuroscience : the official journal of the Society for Neuroscience* **33:** 11169-11183

Bhattacharyya S, Luan J, Challis B, Keogh J, Montague C, Brennand J, Morten J, Lowenbeim S, Jenkins S, Farooqi IS, Wareham NJ, O'Rahilly S (2006) Sequence variants in the melatonin-related receptor gene (GPR50) associate with circulating triglyceride and HDL levels. *Journal of lipid research* **47:** 761-766

Biederer T, Cao X, Sudhof TC, Liu X (2002) Regulation of APP-dependent transcription complexes by Mint/X11s: differential functions of Mint isoforms. *The Journal of neuroscience : the official journal of the Society for Neuroscience* **22:** 7340-7351

Birchmeier C, Nave KA (2008) Neuregulin-1, a key axonal signal that drives Schwann cell growth and differentiation. *Glia* **56:** 1491-1497

Bird TD (1993) Alzheimer Disease Overview. In *GeneReviews(R)*, Pagon RA, Adam MP, Ardinger HH, Bird TD, Dolan CR, Fong CT, Smith RJH, Stephens K (eds). Seattle (WA)

Blasko I, Beer R, Bigl M, Apelt J, Franz G, Rudzki D, Ransmayr G, Kampfl A, Schliebs R (2004) Experimental traumatic brain injury in rats stimulates the expression, production and activity of Alzheimer's disease beta-secretase (BACE-1). *Journal of neural transmission* **111:** 523-536

Bodendorf U, Danner S, Fischer F, Stefani M, Sturchler-Pierrat C, Wiederhold KH, Staufenbiel M, Paganetti P (2002) Expression of human beta-secretase in the mouse brain increases the steady-state level of beta-amyloid. *Journal of neurochemistry* **80:** 799-806

Bodendorf U, Fischer F, Bodian D, Multhaup G, Paganetti P (2001) A splice variant of beta-secretase deficient in the amyloidogenic processing of the amyloid precursor protein. *The Journal of biological chemistry* **276:** 12019-12023

Bourne KZ, Ferrari DC, Lange-Dohna C, Rossner S, Wood TG, Perez-Polo JR (2007) Differential regulation of BACE1 promoter activity by nuclear factor-kappaB in neurons and glia upon exposure to beta-amyloid peptides. *Journal of neuroscience research* **85:** 1194-1204

Britsch S (2007) The neuregulin-I/ErbB signaling system in development and disease. *Advances in anatomy, embryology, and cell biology* **190:** 1-65

Broccardo C, Nieoullon V, Amin R, Masmejean F, Carta S, Tassi S, Pophillat M, Rubartelli A, Pierres M, Rougon G, Nieoullon A, Chazal G, Chimini G (2006) ABCA2 is a marker of neural progenitors and neuronal subsets in the adult rodent brain. *Journal of neurochemistry* **97:** 345-355

Bruckner A, Polge C, Lentze N, Auerbach D, Schlattner U (2009) Yeast two-hybrid, a powerful tool for systems biology. *International journal of molecular sciences* **10:** 2763-2788

Brunner P, Sozer-Topcular N, Jockers R, Ravid R, Angeloni D, Fraschini F, Eckert A, Muller-Spahn F, Savaskan E (2006) Pineal and cortical melatonin receptors MT1 and MT2 are decreased in Alzheimer's disease. *European journal of histochemistry : EJH* **50:** 311-316

Buggia-Prevot V, Fernandez CG, Riordan S, Vetrivel KS, Roseman J, Waters J, Bindokas VP, Vassar R, Thinakaran G (2014) Axonal BACE1 dynamics and targeting in hippocampal neurons: a role for Rab11 GTPase. *Molecular neurodegeneration* **9:** 1

Buggia-Prevot V, Sevalle J, Rossner S, Checler F (2008) NFkappaB-dependent control of BACE1 promoter transactivation by Abeta42. *The Journal of biological chemistry* **283:** 10037-10047

Bulbarelli A, Lonati E, Cazzaniga E, Re F, Sesana S, Barisani D, Sancini G, Mutoh T, Masserini M (2009) TrkA pathway activation induced by amyloid-beta (Abeta). *Molecular and cellular*

neurosciences **40:** 365-373

Cannon TD, Kaprio J, Lonnqvist J, Huttunen M, Koskenvuo M (1998) The genetic epidemiology of schizophrenia in a Finnish twin cohort. A population-based modeling study. *Archives of general psychiatry* **55:** 67-74

Cao L, Rickenbacher GT, Rodriguez S, Moulia TW, Albers MW (2012) The precision of axon targeting of mouse olfactory sensory neurons requires the BACE1 protease. *Scientific reports* **2:** 231

Carbe C, Garg A, Cai Z, Li H, Powers A, Zhang X (2013) An allelic series at the paired box gene 6 (Pax6) locus reveals the functional specificity of Pax genes. *The Journal of biological chemistry* **288:** 12130-12141

Cardno AG, Gottesman, II (2000) Twin studies of schizophrenia: from bow-and-arrow concordances to star wars Mx and functional genomics. *American journal of medical genetics* **97:** 12-17

Caruana DA, Sorge RE, Stewart J, Chapman CA (2006) Dopamine has bidirectional effects on synaptic responses to cortical inputs in layer II of the lateral entorhinal cortex. *Journal of neurophysiology* **96:** 3006-3015

Chakravarthy B, Gaudet C, Menard M, Atkinson T, Brown L, Laferla FM, Armato U, Whitfield J (2010) Amyloid-beta peptides stimulate the expression of the p75(NTR) neurotrophin receptor in SHSY5Y human neuroblastoma cells and AD transgenic mice. *Journal of Alzheimer's disease : JAD* **19:** 915-925

Charlwood J, Dingwall C, Matico R, Hussain I, Johanson K, Moore S, Powell DJ, Skehel JM, Ratcliffe S, Clarke B, Trill J, Sweitzer S, Camilleri P (2001) Characterization of the glycosylation profiles of Alzheimer's beta -secretase protein Asp-2 expressed in a variety of cell lines. *The Journal of biological chemistry* **276:** 16739-16748

Chen CH, Zhou W, Liu S, Deng Y, Cai F, Tone M, Tone Y, Tong Y, Song W (2012a) Increased NF-kappaB signalling up-regulates BACE1 expression and its therapeutic potential in Alzheimer's disease. *The international journal of neuropsychopharmacology / official scientific journal of the Collegium Internationale Neuropsychopharmacologicum* **15:** 77-90

Chen DT, Jiang X, Akula N, Shugart YY, Wendland JR, Steele CJ, Kassem L, Park JH, Chatterjee N, Jamain S, Cheng A, Leboyer M, Muglia P, Schulze TG, Cichon S, Nothen MM, Rietschel M, BiGs, McMahon FJ, Farmer A, McGuffin P, Craig I, Lewis C, Hosang G, Cohen-Woods S, Vincent JB, Kennedy JL, Strauss J (2013) Genome-wide association study meta-analysis of European and Asian-ancestry samples identifies three novel loci associated with bipolar disorder. *Molecular psychiatry* **18:** 195-205

Chen Y, Huang X, Zhang YW, Rockenstein E, Bu G, Golde TE, Masliah E, Xu H (2012b) Alzheimer's beta-secretase (BACE1) regulates the cAMP/PKA/CREB pathway independently of beta-amyloid. *The Journal of neuroscience : the official journal of the Society for Neuroscience* **32:** 11390-11395

Chen ZJ, Vulevic B, Ile KE, Soulika A, Davis W, Jr., Reiner PB, Connop BP, Nathwani P, Trojanowski JQ, Tew KD (2004) Association of ABCA2 expression with determinants of Alzheimer's disease. *FASEB journal : official publication of the Federation of American Societies for Experimental Biology* **18:** 1129-1131

Chevaleyre V, Siegelbaum SA (2010) Strong CA2 pyramidal neuron synapses define a powerful disynaptic cortico-hippocampal loop. *Neuron* **66:** 560-572

Chia PZ, Gleeson PA (2011) Intracellular trafficking of the beta-secretase and processing of amyloid precursor protein. *IUBMB life* **63:** 721-729

Chin J (2011) Selecting a mouse model of Alzheimer's disease. *Methods in molecular biology* **670:** 169-189

Cho HJ, Kim SK, Jin SM, Hwang EM, Kim YS, Huh K, Mook-Jung I (2007) IFN-gamma-induced BACE1 expression is mediated by activation of JAK2 and ERK1/2 signaling pathways and direct binding of STAT1 to BACE1 promoter in astrocytes. *Glia* **55:** 253-262

Chowdari KV, Mirnics K, Semwal P, Wood J, Lawrence E, Bhatia T, Deshpande SN, B KT, Ferrell RE, Middleton FA, Devlin B, Levitt P, Lewis DA, Nimgaonkar VL (2002) Association and linkage analyses of RGS4 polymorphisms in schizophrenia. *Human molecular genetics* **11:** 1373-1380

Choy RW, Park M, Temkin P, Herring BE, Marley A, Nicoll RA, von Zastrow M (2014) Retromer mediates a discrete route of local membrane delivery to dendrites. *Neuron* **82:** 55-62

Christensen MA, Zhou W, Qing H, Lehman A, Philipsen S, Song W (2004) Transcriptional regulation of BACE1, the beta-amyloid precursor protein beta-secretase, by Sp1. *Molecular and cellular biology* **24:** 865-874

Chung S, Son GH, Kim K (2011) Circadian rhythm of adrenal glucocorticoid: its regulation and clinical implications. *Biochimica et biophysica acta* **1812:** 581-591

Citron M, Oltersdorf T, Haass C, McConlogue L, Hung AY, Seubert P, Vigo-Pelfrey C, Lieberburg I, Selkoe DJ (1992) Mutation of the beta-amyloid precursor protein in familial Alzheimer's disease increases beta-protein production. *Nature* **360:** 672-674

Cohen SJ, Munchow AH, Rios LM, Zhang G, Asgeirsdottir HN, Stackman RW, Jr. (2013) The rodent hippocampus is essential for nonspatial object memory. *Current biology : CB* **23:** 1685-1690

Colantuoni C, Lipska BK, Ye T, Hyde TM, Tao R, Leek JT, Colantuoni EA, Elkahloun AG, Herman MM, Weinberger DR, Kleinman JE (2011) Temporal dynamics and genetic control of transcription in the human prefrontal cortex. *Nature* **478:** 519-523

Cole SL, Vassar R (2007) The Alzheimer's disease beta-secretase enzyme, BACE1. *Molecular neurodegeneration* **2:** 22

Corbett BF, Leiser SC, Ling HP, Nagy R, Breysse N, Zhang X, Hazra A, Brown JT, Randall AD, Wood A, Pangalos MN, Reinhart PH, Chin J (2013) Sodium channel cleavage is associated with aberrant neuronal activity and cognitive deficits in a mouse model of Alzheimer's disease. *The Journal of neuroscience : the official journal of the Society for Neuroscience* **33:** 7020-7026

Cordy JM, Hussain I, Dingwall C, Hooper NM, Turner AJ (2003) Exclusively targeting beta-secretase to lipid rafts by GPI-anchor addition up-regulates beta-site processing of the amyloid precursor protein. *Proceedings of the National Academy of Sciences of the United States of America* **100:** 11735-11740

Costantini C, Ko MH, Jonas MC, Puglielli L (2007) A reversible form of lysine acetylation in the ER and Golgi lumen controls the molecular stabilization of BACE1. *The Biochemical journal* **407:** 383-395

Coulson DT, Beyer N, Quinn JG, Brockbank S, Hellemans J, Irvine GB, Ravid R, Johnston JA (2010) BACE1 mRNA expression in Alzheimer's disease postmortem brain tissue. *Journal of Alzheimer's disease : JAD* **22:** 1111-1122

Crameri A, Biondi E, Kuehnle K, Lutjohann D, Thelen KM, Perga S, Dotti CG, Nitsch RM, Ledesma MD, Mohajeri MH (2006) The role of seladin-1/DHCR24 in cholesterol biosynthesis, APP processing and Abeta generation in vivo. *The EMBO journal* **25:** 432-443

Cross-Disorder Group of the Psychiatric Genomics C, Lee SH, Ripke S, Neale BM, Faraone SV, Purcell SM, Perlis RH, Mowry BJ, Thapar A, Goddard ME, Witte JS, Absher D, Agartz I, Akil H, Amin F, Andreassen OA, Anjorin A, Anney R, Anttila V, Arking DE, Asherson P, Azevedo MH, Backlund L, Badner JA, Bailey AJ, Banaschewski T, Barchas JD, Barnes MR, Barrett TB, Bass N, Battaglia A, Bauer M, Bayes M, Bellivier F, Bergen SE, Berrettini W, Betancur C, Bettecken T, Biederman J, Binder EB, Black DW, Blackwood DH, Bloss CS, Boehnke M, Boomsma DI, Breen G, Breuer R, Bruggeman R, Cormican P, Buccola NG, Buitelaar JK, Bunney WE, Buxbaum JD, Byerley WF, Byrne EM, Caesar S, Cahn W, Cantor RM, Casas M, Chakravarti A, Chambert K, Choudhury K, Cichon S, Cloninger CR, Collier DA, Cook EH, Coon H, Cormand B, Corvin A, Coryell WH, Craig DW, Craig IW, Crosbie J, Cuccaro ML, Curtis D, Czamara D, Datta S, Dawson G, Day R, De Geus EJ, Degenhardt F, Djurovic S, Donohoe GJ, Doyle AE, Duan J, Dudbridge F, Duketis E, Ebstein RP, Edenberg HJ, Elia J, Ennis S, Etain B, Fanous A, Farmer AE, Ferrier IN, Flickinger M, Fombonne E, Foroud T, Frank J, Franke B, Fraser C, Freedman R, Freimer NB, Freitag CM, Friedl M, Frisen L, Gallagher L, Gejman PV, Georgieva L, Gershon ES, Geschwind DH, Giegling I, Gill M, Gordon SD, Gordon-Smith K, Green EK, Greenwood TA, Grice DE, Gross M, Grozeva D, Guan W, Gurling H, De Haan L, Haines JL, Hakonarson H, Hallmayer J, Hamilton SP, Hamshere ML, Hansen TF, Hartmann AM, Hautzinger M, Heath AC, Henders AK, Herms S, Hickie IB, Hipolito M, Hoefels S, Holmans PA, Holsboer F, Hoogendijk WJ, Hottenga JJ, Hultman CM, Hus V, Ingason A, Ising M, Jamain S, Jones EG, Jones I, Jones L, Tzeng JY, Kahler AK, Kahn RS, Kandaswamy R, Keller MC, Kennedy JL, Kenny E, Kent L, Kim Y, Kirov GK, Klauck SM, Klei L, Knowles JA, Kohli MA, Koller DL, Konte B, Korszun A, Krabbendam L, Krasucki R, Kuntsi J, Kwan P, Landen M, Langstrom N, Lathrop M, Lawrence J, Lawson WB, Leboyer M, Ledbetter DH, Lee PH, Lencz T, Lesch KP, Levinson DF, Lewis CM, Li J, Lichtenstein P, Lieberman JA, Lin DY, Linszen DH, Liu C, Lohoff FW, Loo SK, Lord C, Lowe JK, Lucae S, MacIntyre DJ, Madden PA, Maestrini E, Magnusson PK, Mahon PB, Maier W, Malhotra AK, Mane SM, Martin CL, Martin NG, Mattheisen M, Matthews K, Mattingsdal M, McCarroll SA, McGhee KA, McGough JJ, McGrath PJ, McGuffin P, McInnis MG, McIntosh A, McKinney R, McLean AW, McMahon FJ, McMahon WM, McQuillin A, Medeiros H, Medland SE, Meier S, Melle I, Meng F, Meyer J, Middeldorp CM, Middleton L, Milanova V, Miranda A, Monaco AP, Montgomery GW, Moran JL, Moreno-De-Luca D, Morken G, Morris DW, Morrow EM, Moskvina V, Muglia P, Muhleisen TW, Muir WJ, Muller-Myhsok B, Murtha M, Myers RM, Myin-Germeys I, Neale MC, Nelson SF, Nievergelt CM, Nikolov I, Nimgaonkar V, Nolen WA, Nothen MM, Nurnberger JI, Nwulia EA, Nyholt DR, O'Dushlaine C, Oades RD, Olincy A, Oliveira G, Olsen L, Ophoff RA, Osby U, Owen MJ, Palotie A, Parr JR, Paterson AD, Pato CN, Pato MT, Penninx BW, Pergadia ML, Pericak-Vance MA, Pickard BS, Pimm J, Piven J, Posthuma D, Potash JB, Poustka F, Propping P, Puri V, Quested DJ, Quinn EM, Ramos-Quiroga JA, Rasmussen HB, Raychaudhuri S, Rehnstrom K, Reif A, Ribases M, Rice JP, Rietschel M, Roeder K, Roeyers H, Rossin L, Rothenberger A, Rouleau G, Ruderfer D, Rujescu D, Sanders AR, Sanders SJ, Santangelo SL, Sergeant JA, Schachar R, Schalling M, Schatzberg AF, Scheftner WA, Schellenberg GD, Scherer SW, Schork NJ, Schulze TG, Schumacher J, Schwarz M, Scolnick E, Scott LJ, Shi J, Shilling PD, Shyn SI, Silverman JM, Slager SL, Smalley SL, Smit

JH, Smith EN, Sonuga-Barke EJ, St Clair D, State M, Steffens M, Steinhausen HC, Strauss JS, Strohmaier J, Stroup TS, Sutcliffe JS, Szatmari P, Szelinger S, Thirumalai S, Thompson RC, Todorov AA, Tozzi F, Treutlein J, Uhr M, van den Oord EJ, Van Grootheest G, Van Os J, Vicente AM, Vieland VJ, Vincent JB, Visscher PM, Walsh CA, Wassink TH, Watson SJ, Weissman MM, Werge T, Wienker TF, Wijsman EM, Willemsen G, Williams N, Willsey AJ, Witt SH, Xu W, Young AH, Yu TW, Zammit S, Zandi PP, Zhang P, Zitman FG, Zollner S, International Inflammatory Bowel Disease Genetics C, Devlin B, Kelsoe JR, Sklar P, Daly MJ, O'Donovan MC, Craddock N, Sullivan PF, Smoller JW, Kendler KS, Wray NR (2013) Genetic relationship between five psychiatric disorders estimated from genome-wide SNPs. *Nature genetics* **45:** 984-994

Cui J, Wang Y, Dong Q, Wu S, Xiao X, Hu J, Chai Z, Zhang Y (2011) Morphine protects against intracellular amyloid toxicity by inducing estradiol release and upregulation of Hsp70. *The Journal of neuroscience : the official journal of the Society for Neuroscience* **31:** 16227-16240

Czajkowski R, Sugar J, Zhang SJ, Couey JJ, Ye J, Witter MP (2013) Superficially projecting principal neurons in layer V of medial entorhinal cortex in the rat receive excitatory retrosplenial input. *The Journal of neuroscience : the official journal of the Society for Neuroscience* **33:** 15779-15792

D'Amico F, Skarmoutsou E, Stivala F (2009) State of the art in antigen retrieval for immunohistochemistry. *Journal of immunological methods* **341:** 1-18

Dallaspezia S, Benedetti F (2009) Melatonin, circadian rhythms, and the clock genes in bipolar disorder. *Current psychiatry reports* **11:** 488-493

Das U, Scott DA, Ganguly A, Koo EH, Tang Y, Roy S (2013) Activity-induced convergence of APP and BACE-1 in acidic microdomains via an endocytosis-dependent pathway. *Neuron* **79:** 447-460

Davies CA, Mann DM, Sumpter PQ, Yates PO (1987) A quantitative morphometric analysis of the neuronal and synaptic content of the frontal and temporal cortex in patients with Alzheimer's disease. *Journal of the neurological sciences* **78:** 151-164

Davis J, Xu F, Deane R, Romanov G, Previti ML, Zeigler K, Zlokovic BV, Van Nostrand WE (2004a) Early-onset and robust cerebral microvascular accumulation of amyloid beta-protein in transgenic mice expressing low levels of a vasculotropic Dutch/Iowa mutant form of amyloid beta-protein precursor. *The Journal of biological chemistry* **279:** 20296-20306

Davis J, Xu F, Miao J, Previti ML, Romanov G, Ziegler K, Van Nostrand WE (2006) Deficient cerebral clearance of vasculotropic mutant Dutch/Iowa Double A beta in human A betaPP transgenic mice. *Neurobiology of aging* **27:** 946-954

Davis W, Jr. (2011) The ATP-binding cassette transporter-2 (ABCA2) regulates cholesterol homeostasis and low-density lipoprotein receptor metabolism in N2a neuroblastoma cells. *Biochimica et biophysica acta* **1811:** 1152-1164

Davis W, Jr., Boyd JT, Ile KE, Tew KD (2004b) Human ATP-binding cassette transporter-2 (ABCA2) positively regulates low-density lipoprotein receptor expression and negatively regulates cholesterol esterification in Chinese hamster ovary cells. *Biochimica et biophysica acta* **1683:** 89-100

De Pietri Tonelli D, Mihailovich M, Di Cesare A, Codazzi F, Grohovaz F, Zacchetti D (2004)

Translational regulation of BACE-1 expression in neuronal and non-neuronal cells. *Nucleic acids research* **32:** 1808-1817

de Quervain DJ, Poirier R, Wollmer MA, Grimaldi LM, Tsolaki M, Streffer JR, Hock C, Nitsch RM, Mohajeri MH, Papassotiropoulos A (2004) Glucocorticoid-related genetic susceptibility for Alzheimer's disease. *Human molecular genetics* **13:** 47-52

Dejgaard SY, Murshid A, Dee KM, Presley JF (2007) Confocal microscopy-based linescan methodologies for intra-Golgi localization of proteins. *The journal of histochemistry and cytochemistry : official journal of the Histochemistry Society* **55:** 709-719

Delekate A, Zagrebelsky M, Kramer S, Schwab ME, Korte M (2011) NogoA restricts synaptic plasticity in the adult hippocampus on a fast time scale. *Proceedings of the National Academy of Sciences of the United States of America* **108:** 2569-2574

Demyanenko GP, Schachner M, Anton E, Schmid R, Feng G, Sanes J, Maness PF (2004) Close homolog of L1 modulates area-specific neuronal positioning and dendrite orientation in the cerebral cortex. *Neuron* **44:** 423-437

Deng M, He W, Tan Y, Han H, Hu X, Xia K, Zhang Z, Yan R (2013) Increased expression of reticulon 3 in neurons leads to reduced axonal transport of beta site amyloid precursor protein-cleaving enzyme 1. *The Journal of biological chemistry* **288:** 30236-30245

Dhikav V, Anand KS (2007) Glucocorticoids may initiate Alzheimer's disease: a potential therapeutic role for mifepristone (RU-486). *Medical hypotheses* **68:** 1088-1092

Dihne M, Bernreuther C, Sibbe M, Paulus W, Schachner M (2003) A new role for the cell adhesion molecule L1 in neural precursor cell proliferation, differentiation, and transmitter-specific subtype generation. *The Journal of neuroscience : the official journal of the Society for Neuroscience* **23:** 6638-6650

Dominguez D, Tournoy J, Hartmann D, Huth T, Cryns K, Deforce S, Serneels L, Camacho IE, Marjaux E, Craessaerts K, Roebroek AJ, Schwake M, D'Hooge R, Bach P, Kalinke U, Moechars D, Alzheimer C, Reiss K, Saftig P, De Strooper B (2005) Phenotypic and biochemical analyses of BACE1- and BACE2-deficient mice. *The Journal of biological chemistry* **280:** 30797-30806

Drew JE, Barrett P, Mercer JG, Moar KM, Canet E, Delagrange P, Morgan PJ (2001) Localization of the melatonin-related receptor in the rodent brain and peripheral tissues. *Journal of neuroendocrinology* **13:** 453-458

Drew JE, Barrett P, Williams LM, Conway S, Morgan PJ (1998) The ovine melatonin-related receptor: cloning and preliminary distribution and binding studies. *Journal of neuroendocrinology* **10:** 651-661

Du C, Jaggi M, Zhang C, Balaji KC (2009) Protein kinase D1-mediated phosphorylation and subcellular localization of beta-catenin. *Cancer research* **69:** 1117-1124

Dubocovich ML, Markowska M (2005) Functional MT1 and MT2 melatonin receptors in mammals. *Endocrine* **27:** 101-110

Duce JA, Tsatsanis A, Cater MA, James SA, Robb E, Wikhe K, Leong SL, Perez K, Johanssen T, Greenough MA, Cho HH, Galatis D, Moir RD, Masters CL, McLean C, Tanzi RE, Cappai R, Barnham KJ, Ciccotosto GD, Rogers JT, Bush AI (2010) Iron-export ferroxidase activity of beta-amyloid precursor protein is inhibited by zinc in Alzheimer's disease. *Cell* **142:** 857-867

Dufourny L, Levasseur A, Migaud M, Callebaut I, Pontarotti P, Malpaux B, Monget P (2008) GPR50 is the mammalian ortholog of Mel1c: evidence of rapid evolution in mammals. *BMC evolutionary biology* **8:** 105

Ebisawa T, Karne S, Lerner MR, Reppert SM (1994) Expression cloning of a high-affinity melatonin receptor from Xenopus dermal melanophores. *Proceedings of the National Academy of Sciences of the United States of America* **91:** 6133-6137

Eggert S, Paliga K, Soba P, Evin G, Masters CL, Weidemann A, Beyreuther K (2004) The proteolytic processing of the amyloid precursor protein gene family members APLP-1 and APLP-2 involves alpha-, beta-, gamma-, and epsilon-like cleavages: modulation of APLP-1 processing by n-glycosylation. *The Journal of biological chemistry* **279:** 18146-18156

Ehehalt R, Michel B, De Pietri Tonelli D, Zacchetti D, Simons K, Keller P (2002) Splice variants of the beta-site APP-cleaving enzyme BACE1 in human brain and pancreas. *Biochemical and biophysical research communications* **293:** 30-37

Elliott MS, Ballard CG, Kalaria RN, Perry R, Hortobagyi T, Francis PT (2009) Increased binding to 5-HT1A and 5-HT2A receptors is associated with large vessel infarction and relative preservation of cognition. *Brain : a journal of neurology* **132:** 1858-1865

Emilsson L, Saetre P, Jazin E (2006) Low mRNA levels of RGS4 splice variants in Alzheimer's disease: association between a rare haplotype and decreased mRNA expression. *Synapse* **59:** 173-176

Feng Y, Wigg K, King N, Vetro A, Kiss E, Kapornai K, Mayer L, Gadoros J, Kennedy JL, Kovacs M, Barr CL, International Consortium for Childhood-Onset Mood D (2007) GPR50 is not associated with childhood-onset mood disorders in a large sample of Hungarian families. *Psychiatric genetics* **17:** 347-350

Feng Z, Chang Y, Cheng Y, Zhang BL, Qu ZW, Qin C, Zhang JT (2004) Melatonin alleviates behavioral deficits associated with apoptosis and cholinergic system dysfunction in the APP 695 transgenic mouse model of Alzheimer's disease. *Journal of pineal research* **37:** 129-136

Ferreira MA, O'Donovan MC, Meng YA, Jones IR, Ruderfer DM, Jones L, Fan J, Kirov G, Perlis RH, Green EK, Smoller JW, Grozeva D, Stone J, Nikolov I, Chambert K, Hamshere ML, Nimgaonkar VL, Moskvina V, Thase ME, Caesar S, Sachs GS, Franklin J, Gordon-Smith K, Ardlie KG, Gabriel SB, Fraser C, Blumenstiel B, Defelice M, Breen G, Gill M, Morris DW, Elkin A, Muir WJ, McGhee KA, Williamson R, MacIntyre DJ, MacLean AW, St CD, Robinson M, Van Beck M, Pereira AC, Kandaswamy R, McQuillin A, Collier DA, Bass NJ, Young AH, Lawrence J, Ferrier IN, Anjorin A, Farmer A, Curtis D, Scolnick EM, McGuffin P, Daly MJ, Corvin AP, Holmans PA, Blackwood DH, Gurling HM, Owen MJ, Purcell SM, Sklar P, Craddock N, Wellcome Trust Case Control C (2008) Collaborative genome-wide association analysis supports a role for ANK3 and CACNA1C in bipolar disorder. *Nature genetics* **40:** 1056-1058

Finan GM, Okada H, Kim TW (2011) BACE1 retrograde trafficking is uniquely regulated by the cytoplasmic domain of sortilin. *The Journal of biological chemistry* **286:** 12602-12616

Fleck D, van Bebber F, Colombo A, Galante C, Schwenk BM, Rabe L, Hampel H, Novak B, Kremmer E, Tahirovic S, Edbauer D, Lichtenthaler SF, Schmid B, Willem M, Haass C (2013) Dual cleavage of neuregulin 1 type III by BACE1 and ADAM17 liberates its EGF-like domain and allows paracrine signaling. *The Journal of neuroscience : the official journal of the Society for Neuroscience* **33:** 7856-7869

Flores AI, Narayanan SP, Morse EN, Shick HE, Yin X, Kidd G, Avila RL, Kirschner DA, Macklin WB (2008) Constitutively active Akt induces enhanced myelination in the CNS. *The Journal of neuroscience : the official journal of the Society for Neuroscience* **28:** 7174-7183

Focking M, Dicker P, English JA, Schubert KO, Dunn MJ, Cotter DR (2011) Common proteomic changes in the hippocampus in schizophrenia and bipolar disorder and particular evidence for involvement of cornu ammonis regions 2 and 3. *Archives of general psychiatry* **68:** 477-488

Freeman LR, Zhang L, Dasuri K, Fernandez-Kim SO, Bruce-Keller AJ, Keller JN (2012) Mutant amyloid precursor protein differentially alters adipose biology under obesogenic and non-obesogenic conditions. *PloS one* **7:** e43193

Freudenthal R, Locatelli F, Hermitte G, Maldonado H, Lafourcade C, Delorenzi A, Romano A (1998) Kappa-B like DNA-binding activity is enhanced after spaced training that induces long-term memory in the crab Chasmagnathus. *Neuroscience letters* **242:** 143-146

Fryer JD, Simmons K, Parsadanian M, Bales KR, Paul SM, Sullivan PM, Holtzman DM (2005) Human apolipoprotein E4 alters the amyloid-beta 40:42 ratio and promotes the formation of cerebral amyloid angiopathy in an amyloid precursor protein transgenic model. *The Journal of neuroscience : the official journal of the Society for Neuroscience* **25:** 2803-2810

Galbiati F, Volonte D, Brown AM, Weinstein DE, Ben-Ze'ev A, Pestell RG, Lisanti MP (2000) Caveolin-1 expression inhibits Wnt/beta-catenin/Lef-1 signaling by recruiting beta-catenin to caveolae membrane domains. *The Journal of biological chemistry* **275:** 23368-23377

Garel S, Garcia-Dominguez M, Charnay P (2000) Control of the migratory pathway of facial branchiomotor neurones. *Development* **127:** 5297-5307

Gatz M, Reynolds CA, Fratiglioni L, Johansson B, Mortimer JA, Berg S, Fiske A, Pedersen NL (2006) Role of genes and environments for explaining Alzheimer disease. *Archives of general psychiatry* **63:** 168-174

Gau JT, Steinhilb ML, Kao TC, D'Amato CJ, Gaut JR, Frey KA, Turner RS (2002) Stable beta-secretase activity and presynaptic cholinergic markers during progressive central nervous system amyloidogenesis in Tg2576 mice. *The American journal of pathology* **160:** 731-738

Gautam V, D'Avanzo C, Hebisch M, Kovacs DM, Kim DY (2014) BACE1 activity regulates cell surface contactin-2 levels. *Molecular neurodegeneration* **9:** 4

Gavrilova O, Leon LR, Marcus-Samuels B, Mason MM, Castle AL, Refetoff S, Vinson C, Reitman ML (1999) Torpor in mice is induced by both leptin-dependent and -independent mechanisms. *Proceedings of the National Academy of Sciences of the United States of America* **96:** 14623-14628

Ge YW, Maloney B, Sambamurti K, Lahiri DK (2004) Functional characterization of the 5' flanking region of the BACE gene: identification of a 91 bp fragment involved in basal level of BACE promoter expression. *FASEB journal : official publication of the Federation of American Societies for Experimental Biology* **18:** 1037-1039

Gersbacher MT, Kim DY, Bhattacharyya R, Kovacs DM (2010) Identification of BACE1 cleavage sites in human voltage-gated sodium channel beta 2 subunit. *Molecular neurodegeneration* **5:** 61

Gether U (2000) Uncovering molecular mechanisms involved in activation of G protein-coupled receptors. *Endocrine reviews* **21:** 90-113

Giliberto L, Borghi R, Piccini A, Mangerini R, Sorbi S, Cirmena G, Garuti A, Ghetti B, Tagliavini F, Mughal MR, Mattson MP, Zhu X, Wang X, Guglielmotto M, Tamagno E, Tabaton M (2009) Mutant presenilin 1 increases the expression and activity of BACE1. *The Journal of biological chemistry* **284:** 9027-9038

Gina F (2010) The role of sortilin in BACE1 trafficking and beta-amyloid biogenesis. Ph.D Thesis, COLUMBIA UNIVERSITY,

Glaser B, Kirov G, Green E, Craddock N, Owen MJ (2005) Linkage disequilibrium mapping of bipolar affective disorder at 12q23-q24 provides evidence for association at CUX2 and FLJ32356. *American journal of medical genetics Part B, Neuropsychiatric genetics : the official publication of the International Society of Psychiatric Genetics* **132B:** 38-45

Goate A, Chartier-Harlin MC, Mullan M, Brown J, Crawford F, Fidani L, Giuffra L, Haynes A, Irving N, James L, et al. (1991) Segregation of a missense mutation in the amyloid precursor protein gene with familial Alzheimer's disease. *Nature* **349:** 704-706

Godenschwege TA, Kristiansen LV, Uthaman SB, Hortsch M, Murphey RK (2006) A conserved role for Drosophila Neuroglian and human L1-CAM in central-synapse formation. *Current biology : CB* **16:** 12-23

Goedert M, Wischik CM, Crowther RA, Walker JE, Klug A (1988) Cloning and sequencing of the cDNA encoding a core protein of the paired helical filament of Alzheimer disease: identification as the microtubule-associated protein tau. *Proceedings of the National Academy of Sciences of the United States of America* **85:** 4051-4055

Goodwin FK, Jamison KR, Ghaemi SN (2007) *Manic-depressive illness : bipolar disorders and recurrent depression*, 2nd edn. New York, N.Y.: Oxford University Press.

Gottesman, II, Moldin SO (1997) Schizophrenia genetics at the millennium: cautious optimism. *Clinical genetics* **52:** 404-407

Grabowski TJ, Cho HS, Vonsattel JP, Rebeck GW, Greenberg SM (2001) Novel amyloid precursor protein mutation in an Iowa family with dementia and severe cerebral amyloid angiopathy. *Annals of neurology* **49:** 697-705

GrandPre T, Nakamura F, Vartanian T, Strittmatter SM (2000) Identification of the Nogo inhibitor of axon regeneration as a Reticulon protein. *Nature* **403:** 439-444

Granic I, Dolga AM, Nijholt IM, van Dijk G, Eisel UL (2009) Inflammation and NF-kappaB in Alzheimer's disease and diabetes. *Journal of Alzheimer's disease : JAD* **16:** 809-821

Greenwood TA, Lazzeroni LC, Murray SS, Cadenhead KS, Calkins ME, Dobie DJ, Green MF, Gur RE, Gur RC, Hardiman G, Kelsoe JR, Leonard S, Light GA, Nuechterlein KH, Olincy A, Radant AD, Schork NJ, Seidman LJ, Siever LJ, Silverman JM, Stone WS, Swerdlow NR, Tsuang DW, Tsuang MT, Turetsky BI, Freedman R, Braff DL (2011) Analysis of 94 candidate genes and 12 endophenotypes for schizophrenia from the Consortium on the Genetics of Schizophrenia. *The American journal of psychiatry* **168:** 930-946

Greeve I, Hermans-Borgmeyer I, Brellinger C, Kasper D, Gomez-Isla T, Behl C, Levkau B,

Nitsch RM (2000) The human DIMINUTO/DWARF1 homolog seladin-1 confers resistance to Alzheimer's disease-associated neurodegeneration and oxidative stress. *The Journal of neuroscience : the official journal of the Society for Neuroscience* **20:** 7345-7352

Griffiths HH, Whitehouse IJ, Baybutt H, Brown D, Kellett KA, Jackson CD, Turner AJ, Piccardo P, Manson JC, Hooper NM (2011) Prion protein interacts with BACE1 protein and differentially regulates its activity toward wild type and Swedish mutant amyloid precursor protein. *The Journal of biological chemistry* **286:** 33489-33500

Gross RE, Mei Q, Gutekunst CA, Torre E (2007) The pivotal role of RhoA GTPase in the molecular signaling of axon growth inhibition after CNS injury and targeted therapeutic strategies. *Cell transplantation* **16:** 245-262

Grünewald E (2011) Understanding the role of orphan GPR50 in normal brain function and mental illness Doctor of Philosophy Thesis, The University of Edinburgh,

Grunewald E, Kinnell HL, Porteous DJ, Thomson PA (2009) GPR50 interacts with neuronal NOGO-A and affects neurite outgrowth. *Molecular and cellular neurosciences* **42:** 363-371

Grunewald E, Tew KD, Porteous DJ, Thomson PA (2012) Developmental expression of orphan G protein-coupled receptor 50 in the mouse brain. *ACS chemical neuroscience* **3:** 459-472

Gu Z, Jiang Q, Yan Z (2007) RGS4 modulates serotonin signaling in prefrontal cortex and links to serotonin dysfunction in a rat model of schizophrenia. *Molecular pharmacology* **71:** 1030-1039

Gubitz AK, Reppert SM (1999) Assignment of the melatonin-related receptor to human chromosome X (GPR50) and mouse chromosome X (Gpr50). *Genomics* **55:** 248-251

Guerreiro R, Wojtas A, Bras J, Carrasquillo M, Rogaeva E, Majounie E, Cruchaga C, Sassi C, Kauwe JS, Younkin S, Hazrati L, Collinge J, Pocock J, Lashley T, Williams J, Lambert JC, Amouyel P, Goate A, Rademakers R, Morgan K, Powell J, St George-Hyslop P, Singleton A, Hardy J, Alzheimer Genetic Analysis G (2013) TREM2 variants in Alzheimer's disease. *The New England journal of medicine* **368:** 117-127

Guglielmotto M, Monteleone D, Boido M, Piras A, Giliberto L, Borghi R, Vercelli A, Fornaro M, Tabaton M, Tamagno E (2012) Abeta1-42-mediated down-regulation of Uch-L1 is dependent on NF-kappaB activation and impaired BACE1 lysosomal degradation. *Aging cell* **11:** 834-844

Gulsuner S, Walsh T, Watts AC, Lee MK, Thornton AM, Casadei S, Rippey C, Shahin H, Consortium on the Genetics of S, Group PS, Nimgaonkar VL, Go RC, Savage RM, Swerdlow NR, Gur RE, Braff DL, King MC, McClellan JM (2013) Spatial and temporal mapping of de novo mutations in schizophrenia to a fetal prefrontal cortical network. *Cell* **154:** 518-529

Gunnersen JM, Kim MH, Fuller SJ, De Silva M, Britto JM, Hammond VE, Davies PJ, Petrou S, Faber ES, Sah P, Tan SS (2007) Sez-6 proteins affect dendritic arborization patterns and excitability of cortical pyramidal neurons. *Neuron* **56:** 621-639

Haass C, Lemere CA, Capell A, Citron M, Seubert P, Schenk D, Lannfelt L, Selkoe DJ (1995) The Swedish mutation causes early-onset Alzheimer's disease by beta-secretase cleavage within the secretory pathway. *Nature medicine* **1:** 1291-1296

Hahn CG, Wang HY, Cho DS, Talbot K, Gur RE, Berrettini WH, Bakshi K, Kamins J, Borgmann-Winter KE, Siegel SJ, Gallop RJ, Arnold SE (2006) Altered neuregulin 1-erbB4 signaling contributes to NMDA receptor hypofunction in schizophrenia. *Nature medicine* **12:** 824-828

Hall AM, Roberson ED (2012) Mouse models of Alzheimer's disease. *Brain research bulletin* **88:** 3-12

Halliwell E, Main L, Richardson C, Mental Health Foundation (London England) (2007) *The fundamental facts : the latest facts and figures on mental health*, London: Mental Health Foundation.

Hamouda HO, Chen P, Levoye A, Sozer-Topcular N, Daulat AM, Guillaume JL, Ravid R, Savaskan E, Ferry G, Boutin JA, Delagrange P, Jockers R, Maurice P (2007) Detection of the human GPR50 orphan seven transmembrane protein by polyclonal antibodies mapping different epitopes. *Journal of pineal research* **43:** 10-15

Harold D, Abraham R, Hollingworth P, Sims R, Gerrish A, Hamshere ML, Pahwa JS, Moskvina V, Dowzell K, Williams A, Jones N, Thomas C, Stretton A, Morgan AR, Lovestone S, Powell J, Proitsi P, Lupton MK, Brayne C, Rubinsztein DC, Gill M, Lawlor B, Lynch A, Morgan K, Brown KS, Passmore PA, Craig D, McGuinness B, Todd S, Holmes C, Mann D, Smith AD, Love S, Kehoe PG, Hardy J, Mead S, Fox N, Rossor M, Collinge J, Maier W, Jessen F, Schurmann B, Heun R, van den Bussche H, Heuser I, Kornhuber J, Wiltfang J, Dichgans M, Frolich L, Hampel H, Hull M, Rujescu D, Goate AM, Kauwe JS, Cruchaga C, Nowotny P, Morris JC, Mayo K, Sleegers K, Bettens K, Engelborghs S, De Deyn PP, Van Broeckhoven C, Livingston G, Bass NJ, Gurling H, McQuillin A, Gwilliam R, Deloukas P, Al-Chalabi A, Shaw CE, Tsolaki M, Singleton AB, Guerreiro R, Muhleisen TW, Nothen MM, Moebus S, Jockel KH, Klopp N, Wichmann HE, Carrasquillo MM, Pankratz VS, Younkin SG, Holmans PA, O'Donovan M, Owen MJ, Williams J (2009) Genome-wide association study identifies variants at CLU and PICALM associated with Alzheimer's disease. *Nature genetics* **41:** 1088-1093

Harrison SM, Harper AJ, Hawkins J, Duddy G, Grau E, Pugh PL, Winter PH, Shilliam CS, Hughes ZA, Dawson LA, Gonzalez MI, Upton N, Pangalos MN, Dingwall C (2003) BACE1 (beta-secretase) transgenic and knockout mice: identification of neurochemical deficits and behavioral changes. *Molecular and cellular neurosciences* **24:** 646-655

Harvey DJ, Beckett LA, Mungas DM (2003) Multivariate modeling of two associated cognitive outcomes in a longitudinal study. *Journal of Alzheimer's disease : JAD* **5:** 357-365

Hausner L, Tschape JA, Schmitt HP, Hentschel F, Hartmann T, Frolich L (2014) Clinical characterization of a presenilin 1 mutation (F177S) in a family with very early-onset Alzheimer's disease in the third decade of life. *Alzheimer's & dementia : the journal of the Alzheimer's Association* **10:** e27-39

Hayashida K, Bartlett AH, Chen Y, Park PW (2010) Molecular and cellular mechanisms of ectodomain shedding. *Anatomical record* **293:** 925-937

He W, Lu Y, Qahwash I, Hu XY, Chang A, Yan R (2004) Reticulon family members modulate BACE1 activity and amyloid-beta peptide generation. *Nature medicine* **10:** 959-965

Heber S, Herms J, Gajic V, Hainfellner J, Aguzzi A, Rulicke T, von Kretzschmar H, von Koch C, Sisodia S, Tremml P, Lipp HP, Wolfer DP, Muller U (2000) Mice with combined gene knock-outs reveal essential and partially redundant functions of amyloid precursor protein family members. *The Journal of neuroscience : the official journal of the Society for Neuroscience* **20:** 7951-7963

Hebert SS, Bourdages V, Godin C, Ferland M, Carreau M, Levesque G (2003) Presenilin-1 interacts directly with the beta-site amyloid protein precursor cleaving enzyme (BACE1). *Neurobiology of disease* **13:** 238-245

Hebert SS, Horre K, Nicolai L, Papadopoulou AS, Mandemakers W, Silahtaroglu AN, Kauppinen S, Delacourte A, De Strooper B (2008) Loss of microRNA cluster miR-29a/b-1 in sporadic Alzheimer's disease correlates with increased BACE1/beta-secretase expression. *Proceedings of the National Academy of Sciences of the United States of America* **105:** 6415-6420

Hejna J, Holtorf M, Hines J, Mathewson L, Hemphill A, Al-Dhalimy M, Olson SB, Moses RE (2008) Tip60 is required for DNA interstrand cross-link repair in the Fanconi anemia pathway. *The Journal of biological chemistry* **283:** 9844-9851

Hemming ML, Elias JE, Gygi SP, Selkoe DJ (2009) Identification of beta-secretase (BACE1) substrates using quantitative proteomics. *PloS one* **4:** e8477

Herard AS, Besret L, Dubois A, Dauguet J, Delzescaux T, Hantraye P, Bonvento G, Moya KL (2006) siRNA targeted against amyloid precursor protein impairs synaptic activity in vivo. *Neurobiology of aging* **27:** 1740-1750

Herms J, Anliker B, Heber S, Ring S, Fuhrmann M, Kretzschmar H, Sisodia S, Muller U (2004) Cortical dysplasia resembling human type 2 lissencephaly in mice lacking all three APP family members. *The EMBO journal* **23:** 4106-4115

Herro S. (2011) Alzheimer’s disease, is it a mental illness? Chicargo Bridge.

Herskowitz JH, Feng Y, Mattheyses AL, Hales CM, Higginbotham LA, Duong DM, Montine TJ, Troncoso JC, Thambisetty M, Seyfried NT, Levey AI, Lah JJ (2013) Pharmacologic inhibition of ROCK2 suppresses amyloid-beta production in an Alzheimer's disease mouse model. *The Journal of neuroscience : the official journal of the Society for Neuroscience* **33:** 19086-19098

Hillenbrand R, Molthagen M, Montag D, Schachner M (1999) The close homologue of the neural adhesion molecule L1 (CHL1): patterns of expression and promotion of neurite outgrowth by heterophilic interactions. *The European journal of neuroscience* **11:** 813-826

Hitt B, Riordan SM, Kukreja L, Eimer WA, Rajapaksha TW, Vassar R (2012) beta-Site amyloid precursor protein (APP)-cleaving enzyme 1 (BACE1)-deficient mice exhibit a close homolog of L1 (CHL1) loss-of-function phenotype involving axon guidance defects. *The Journal of biological chemistry* **287:** 38408-38425

Hitti FL, Siegelbaum SA (2014) The hippocampal CA2 region is essential for social memory. *Nature* **508:** 88-92

Hogl S, Kuhn PH, Colombo A, Lichtenthaler SF (2011) Determination of the proteolytic cleavage sites of the amyloid precursor-like protein 2 by the proteases ADAM10, BACE1 and gamma-secretase. *PloS one* **6:** e21337

Holcomb L, Gordon MN, McGowan E, Yu X, Benkovic S, Jantzen P, Wright K, Saad I, Mueller R, Morgan D, Sanders S, Zehr C, O'Campo K, Hardy J, Prada CM, Eckman C, Younkin S, Hsiao K, Duff K (1998) Accelerated Alzheimer-type phenotype in transgenic mice carrying both mutant amyloid precursor protein and presenilin 1 transgenes. *Nature medicine* **4:** 97-100

Hollingworth P, Harold D, Sims R, Gerrish A, Lambert JC, Carrasquillo MM, Abraham R, Hamshere ML, Pahwa JS, Moskvina V, Dowzell K, Jones N, Stretton A, Thomas C, Richards A, Ivanov D, Widdowson C, Chapman J, Lovestone S, Powell J, Proitsi P, Lupton MK, Brayne C, Rubinsztein DC, Gill M, Lawlor B, Lynch A, Brown KS, Passmore PA, Craig D, McGuinness B, Todd S, Holmes C, Mann D, Smith AD, Beaumont H, Warden D, Wilcock G, Love S, Kehoe PG, Hooper NM, Vardy ER, Hardy J, Mead S, Fox NC, Rossor M, Collinge J, Maier W, Jessen F, Ruther E, Schurmann B, Heun R, Kolsch H, van den Bussche H, Heuser I, Kornhuber J, Wiltfang J, Dichgans M, Frolich L, Hampel H, Gallacher J, Hull M, Rujescu D, Giegling I, Goate AM, Kauwe JS, Cruchaga C, Nowotny P, Morris JC, Mayo K, Sleegers K, Bettens K, Engelborghs S, De Deyn PP, Van Broeckhoven C, Livingston G, Bass NJ, Gurling H, McQuillin A, Gwilliam R, Deloukas P, Al-Chalabi A, Shaw CE, Tsolaki M, Singleton AB, Guerreiro R, Muhleisen TW, Nothen MM, Moebus S, Jockel KH, Klopp N, Wichmann HE, Pankratz VS, Sando SB, Aasly JO, Barcikowska M, Wszolek ZK, Dickson DW, Graff-Radford NR, Petersen RC, Alzheimer's Disease Neuroimaging I, van Duijn CM, Breteler MM, Ikram MA, DeStefano AL, Fitzpatrick AL, Lopez O, Launer LJ, Seshadri S, consortium C, Berr C, Campion D, Epelbaum J, Dartigues JF, Tzourio C, Alperovitch A, Lathrop M, consortium E, Feulner TM, Friedrich P, Riehle C, Krawczak M, Schreiber S, Mayhaus M, Nicolhaus S, Wagenpfeil S, Steinberg S, Stefansson H, Stefansson K, Snaedal J, Bjornsson S, Jonsson PV, Chouraki V, Genier-Boley B, Hiltunen M, Soininen H, Combarros O, Zelenika D, Delepine M, Bullido MJ, Pasquier F, Mateo I, Frank-Garcia A, Porcellini E, Hanon O, Coto E, Alvarez V, Bosco P, Siciliano G, Mancuso M, Panza F, Solfrizzi V, Nacmias B, Sorbi S, Bossu P, Piccardi P, Arosio B, Annoni G, Seripa D, Pilotto A, Scarpini E, Galimberti D, Brice A, Hannequin D, Licastro F, Jones L, Holmans PA, Jonsson T, Riemenschneider M, Morgan K, Younkin SG, Owen MJ, O'Donovan M, Amouyel P, Williams J (2011) Common variants at ABCA7, MS4A6A/MS4A4E, EPHA1, CD33 and CD2AP are associated with Alzheimer's disease. *Nature genetics* **43:** 429-435

Holmes C (2002) Genotype and phenotype in Alzheimer's disease. *The British journal of psychiatry : the journal of mental science* **180:** 131-134

Holsinger RM, Goense N, Bohorquez J, Strappe P (2013) Splice variants of the Alzheimer's disease beta-secretase, BACE1. *Neurogenetics* **14:** 1-9

Hong HS, Hwang EM, Sim HJ, Cho HJ, Boo JH, Oh SS, Kim SU, Mook-Jung I (2003) Interferon gamma stimulates beta-secretase expression and sAPPbeta production in astrocytes. *Biochemical and biophysical research communications* **307:** 922-927

Hook G, Hook V, Kindy M (2011) The cysteine protease inhibitor, E64d, reduces brain amyloid-beta and improves memory deficits in Alzheimer's disease animal models by inhibiting cathepsin B, but not BACE1, beta-secretase activity. *Journal of Alzheimer's disease : JAD* **26:** 387-408

Hu X, He W, Diaconu C, Tang X, Kidd GJ, Macklin WB, Trapp BD, Yan R (2008) Genetic deletion of BACE1 in mice affects remyelination of sciatic nerves. *FASEB journal : official publication of the Federation of American Societies for Experimental Biology* **22:** 2970-2980

Hu X, He W, Luo X, Tsubota KE, Yan R (2013a) BACE1 regulates hippocampal astrogenesis via the Jagged1-Notch pathway. *Cell reports* **4:** 40-49

Hu X, Hicks CW, He W, Wong P, Macklin WB, Trapp BD, Yan R (2006) Bace1 modulates myelination in the central and peripheral nervous system. *Nature neuroscience* **9:** 1520-1525

Hu X, Schlanger R, He W, Macklin WB, Yan R (2013b) Reversing hypomyelination in BACE1-

null mice with Akt-DD overexpression. *FASEB journal : official publication of the Federation of American Societies for Experimental Biology* **27:** 1868-1873

Hu X, Shi Q, Zhou X, He W, Yi H, Yin X, Gearing M, Levey A, Yan R (2007) Transgenic mice overexpressing reticulon 3 develop neuritic abnormalities. *The EMBO journal* **26:** 2755-2767

Huse JT, Pijak DS, Leslie GJ, Lee VM, Doms RW (2000) Maturation and endosomal targeting of beta-site amyloid precursor protein-cleaving enzyme. The Alzheimer's disease beta-secretase. *The Journal of biological chemistry* **275:** 33729-33737

Hussain I, Powell D, Howlett DR, Tew DG, Meek TD, Chapman C, Gloger IS, Murphy KE, Southan CD, Ryan DM, Smith TS, Simmons DL, Walsh FS, Dingwall C, Christie G (1999) Identification of a novel aspartic protease (Asp 2) as beta-secretase. *Molecular and cellular neurosciences* **14:** 419-427

Hutter JA, Martel A, Trigiani L, Barrett SG, Chapman CA (2013) Rewarding stimulation of the lateral hypothalamus induces a dopamine-dependent suppression of synaptic responses in the entorhinal cortex. *Behavioural brain research* **252:** 266-274

Ikura T, Ogryzko VV, Grigoriev M, Groisman R, Wang J, Horikoshi M, Scully R, Qin J, Nakatani Y (2000) Involvement of the TIP60 histone acetylase complex in DNA repair and apoptosis. *Cell* **102:** 463-473

Insausti R (1993) Comparative anatomy of the entorhinal cortex and hippocampus in mammals. *Hippocampus* **3 Spec No:** 19-26

Insausti R, Belichenko PV, Frotscher M, Matus A, Monyer H, Palm G, Steinhauser C (1993) Plasticity in the entorhinal-hippocampal system. *Hippocampus* **3 Spec No:** 289-292

Ivanova EA, Bechtold DA, Dupre SM, Brennand J, Barrett P, Luckman SM, Loudon AS (2008) Altered metabolism in the melatonin-related receptor (GPR50) knockout mouse. *American journal of physiology Endocrinology and metabolism* **294:** E176-182

Jankowsky JL, Fadale DJ, Anderson J, Xu GM, Gonzales V, Jenkins NA, Copeland NG, Lee MK, Younkin LH, Wagner SL, Younkin SG, Borchelt DR (2004) Mutant presenilins specifically elevate the levels of the 42 residue beta-amyloid peptide in vivo: evidence for augmentation of a 42-specific gamma secretase. *Human molecular genetics* **13:** 159-170

Jockers R, Maurice P, Boutin JA, Delagrange P (2008) Melatonin receptors, heterodimerization, signal transduction and binding sites: what's new? *British journal of pharmacology* **154:** 1182-1195

Johnson N, Bree O, Lalley EE, Rettler K, Grande P, Gani MO, Ahamed SI (2014) Effect of a Social Script iPad Application for Children With Autism Going to Imaging. *Journal of pediatric nursing*

Johnson SA, McNeill T, Cordell B, Finch CE (1990) Relation of neuronal APP-751/APP-695 mRNA ratio and neuritic plaque density in Alzheimer's disease. *Science* **248:** 854-857

Jonsson T, Stefansson H, Steinberg S, Jonsdottir I, Jonsson PV, Snaedal J, Bjornsson S, Huttenlocher J, Levey AI, Lah JJ, Rujescu D, Hampel H, Giegling I, Andreassen OA, Engedal K, Ulstein I, Djurovic S, Ibrahim-Verbaas C, Hofman A, Ikram MA, van Duijn CM, Thorsteinsdottir U, Kong A, Stefansson K (2013) Variant of TREM2 associated with the risk of Alzheimer's disease. *The New England journal of medicine* **368:** 107-116

Joyce JN, Murray AM, Hurtig HI, Gottlieb GL, Trojanowski JQ (1998a) Loss of dopamine D2 receptors in Alzheimer's disease with parkinsonism but not Parkinson's or Alzheimer's disease. *Neuropsychopharmacology : official publication of the American College of Neuropsychopharmacology* **19:** 472-480

Joyce JN, Myers AJ, Gurevich E (1998b) Dopamine D2 receptor bands in normal human temporal cortex are absent in Alzheimer's disease. *Brain research* **784:** 7-17

Kaminski WE, Piehler A, Pullmann K, Porsch-Ozcurumez M, Duong C, Bared GM, Buchler C, Schmitz G (2001) Complete coding sequence, promoter region, and genomic structure of the human ABCA2 gene and evidence for sterol-dependent regulation in macrophages. *Biochemical and biophysical research communications* **281:** 249-258

Kandalepas PC, Sadleir KR, Eimer WA, Zhao J, Nicholson DA, Vassar R (2013) The Alzheimer's beta-secretase BACE1 localizes to normal presynaptic terminals and to dystrophic presynaptic terminals surrounding amyloid plaques. *Acta neuropathologica* **126:** 329-352

Kang EL, Biscaro B, Piazza F, Tesco G (2012) BACE1 protein endocytosis and trafficking are differentially regulated by ubiquitination at lysine 501 and the Di-leucine motif in the carboxyl terminus. *The Journal of biological chemistry* **287:** 42867-42880

Kang EL, Cameron AN, Piazza F, Walker KR, Tesco G (2010) Ubiquitin regulates GGA3-mediated degradation of BACE1. *The Journal of biological chemistry* **285:** 24108-24119

Kao SC, Krichevsky AM, Kosik KS, Tsai LH (2004) BACE1 suppression by RNA interference in primary cortical neurons. *The Journal of biological chemistry* **279:** 1942-1949

Karnezis T, Mandemakers W, McQualter JL, Zheng B, Ho PP, Jordan KA, Murray BM, Barres B, Tessier-Lavigne M, Bernard CC (2004) The neurite outgrowth inhibitor Nogo A is involved in autoimmune-mediated demyelination. *Nature neuroscience* **7:** 736-744

Kasukawa T, Masumoto KH, Nikaido I, Nagano M, Uno KD, Tsujino K, Hanashima C, Shigeyoshi Y, Ueda HR (2011) Quantitative expression profile of distinct functional regions in the adult mouse brain. *PloS one* **6:** e23228

Kato T (2007) Molecular genetics of bipolar disorder and depression. *Psychiatry and clinical neurosciences* **61:** 3-19

Kim DY, Carey BW, Wang H, Ingano LA, Binshtok AM, Wertz MH, Pettingell WH, He P, Lee VM, Woolf CJ, Kovacs DM (2007) BACE1 regulates voltage-gated sodium channels and neuronal activity. *Nature cell biology* **9:** 755-764

Kim J, Basak JM, Holtzman DM (2009) The role of apolipoprotein E in Alzheimer's disease. *Neuron* **63:** 287-303

Kinoshita A, Fukumoto H, Shah T, Whelan CM, Irizarry MC, Hyman BT (2003) Demonstration by FRET of BACE interaction with the amyloid precursor protein at the cell surface and in early endosomes. *Journal of cell science* **116:** 3339-3346

Klaver DW, Wilce MC, Gasperini R, Freeman C, Juliano JP, Parish C, Foa L, Aguilar MI, Small DH (2010) Glycosaminoglycan-induced activation of the beta-secretase (BACE1) of Alzheimer's disease. *Journal of neurochemistry* **112:** 1552-1561

Ko MH, Puglielli L (2009) Two endoplasmic reticulum (ER)/ER Golgi intermediate compartment-based lysine acetyltransferases post-translationally regulate BACE1 levels. *The Journal of biological chemistry* **284:** 2482-2492

Konietzko U (2012) AICD nuclear signaling and its possible contribution to Alzheimer's disease. *Current Alzheimer research* **9:** 200-216

Koprivica V, Cho KS, Park JB, Yiu G, Atwal J, Gore B, Kim JA, Lin E, Tessier-Lavigne M, Chen DF, He Z (2005) EGFR activation mediates inhibition of axon regeneration by myelin and chondroitin sulfate proteoglycans. *Science* **310:** 106-110

Korematsu K, Redies C (1997a) Expression of cadherin-8 mRNA in the developing mouse central nervous system. *The Journal of comparative neurology* **387:** 291-306

Korematsu K, Redies C (1997b) Restricted expression of cadherin-8 in segmental and functional subdivisions of the embryonic mouse brain. *Developmental dynamics : an official publication of the American Association of Anatomists* **208:** 178-189

Kuhn PH, Koroniak K, Hogl S, Colombo A, Zeitschel U, Willem M, Volbracht C, Schepers U, Imhof A, Hoffmeister A, Haass C, Rossner S, Brase S, Lichtenthaler SF (2012) Secretome protein enrichment identifies physiological BACE1 protease substrates in neurons. *The EMBO journal* **31:** 3157-3168

Kumar-Singh S (2009) Hereditary and sporadic forms of abeta-cerebrovascular amyloidosis and relevant transgenic mouse models. *International journal of molecular sciences* **10:** 1872-1895

Kuzmanov U, Emili A (2013) Protein-protein interaction networks: probing disease mechanisms using model systems. *Genome medicine* **5:** 37

Kwak YD, Wang R, Li JJ, Zhang YW, Xu H, Liao FF (2011) Differential regulation of BACE1 expression by oxidative and nitrosative signals. *Molecular neurodegeneration* **6:** 17

Laird FM, Cai H, Savonenko AV, Farah MH, He K, Melnikova T, Wen H, Chiang HC, Xu G, Koliatsos VE, Borchelt DR, Price DL, Lee HK, Wong PC (2005) BACE1, a major determinant of selective vulnerability of the brain to amyloid-beta amyloidogenesis, is essential for cognitive, emotional, and synaptic functions. *The Journal of neuroscience : the official journal of the Society for Neuroscience* **25:** 11693-11709

Lambert MA, Bickel H, Prince M, Fratiglioni L, Von Strauss E, Frydecka D, Kiejna A, Georges J, Reynish EL (2014) Estimating the burden of early onset dementia; systematic review of disease prevalence. *European journal of neurology : the official journal of the European Federation of Neurological Societies* **21:** 563-569

LeBlanc AC, Chen HY, Autilio-Gambetti L, Gambetti P (1991) Differential APP gene expression in rat cerebral cortex, meninges, and primary astroglial, microglial and neuronal cultures. *FEBS letters* **292:** 171-178

Lee HG, Perry G, Moreira PI, Garrett MR, Liu Q, Zhu X, Takeda A, Nunomura A, Smith MA (2005) Tau phosphorylation in Alzheimer's disease: pathogen or protector? *Trends in molecular medicine* **11:** 164-169

Lefranc-Jullien S, Lisowski V, Hernandez JF, Martinez J, Checler F (2005) Design and characterization of a new cell-permeant inhibitor of the beta-secretase BACE1. *British*

journal of pharmacology **145:** 228-235

Lencz T, Guha S, Liu C, Rosenfeld J, Mukherjee S, DeRosse P, John M, Cheng L, Zhang C, Badner JA, Ikeda M, Iwata N, Cichon S, Rietschel M, Nothen MM, Cheng AT, Hodgkinson C, Yuan Q, Kane JM, Lee AT, Pisante A, Gregersen PK, Pe'er I, Malhotra AK, Goldman D, Darvasi A (2013) Genome-wide association study implicates NDST3 in schizophrenia and bipolar disorder. *Nature communications* **4:** 2739

Leranth C, Ribak CE (1991) Calcium-binding proteins are concentrated in the CA2 field of the monkey hippocampus: a possible key to this region's resistance to epileptic damage. *Experimental brain research* **85:** 129-136

Leshchyns'ka I, Sytnyk V, Richter M, Andreyeva A, Puchkov D, Schachner M (2006) The adhesion molecule CHL1 regulates uncoating of clathrin-coated synaptic vesicles. *Neuron* **52:** 1011-1025

Levinson DF, Duan J, Oh S, Wang K, Sanders AR, Shi J, Zhang N, Mowry BJ, Olincy A, Amin F, Cloninger CR, Silverman JM, Buccola NG, Byerley WF, Black DW, Kendler KS, Freedman R, Dudbridge F, Pe'er I, Hakonarson H, Bergen SE, Fanous AH, Holmans PA, Gejman PV (2011) Copy number variants in schizophrenia: confirmation of five previous findings and new evidence for 3q29 microdeletions and VIPR2 duplications. *The American journal of psychiatry* **168:** 302-316

Levoye A, Dam J, Ayoub MA, Guillaume JL, Couturier C, Delagrange P, Jockers R (2006) The orphan GPR50 receptor specifically inhibits MT1 melatonin receptor function through heterodimerization. *The EMBO journal* **25:** 3012-3023

Levy E, Carman MD, Fernandez-Madrid IJ, Power MD, Lieberburg I, van Duinen SG, Bots GT, Luyendijk W, Frangione B (1990) Mutation of the Alzheimer's disease amyloid gene in hereditary cerebral hemorrhage, Dutch type. *Science* **248:** 1124-1126

Li B, Woo RS, Mei L, Malinow R (2007) The neuregulin-1 receptor erbB4 controls glutamatergic synapse maturation and plasticity. *Neuron* **54:** 583-597

Li J, Hand LE, Meng QJ, Loudon AS, Bechtold DA (2011) GPR50 interacts with TIP60 to modulate glucocorticoid receptor signalling. *PloS one* **6:** e23725

Li Q, Lau A, Morris TJ, Guo L, Fordyce CB, Stanley EF (2004) A syntaxin 1, Galpha(o), and N-type calcium channel complex at a presynaptic nerve terminal: analysis by quantitative immunocolocalization. *The Journal of neuroscience : the official journal of the Society for Neuroscience* **24:** 4070-4081

Li Q, Sudhof TC (2004) Cleavage of amyloid-beta precursor protein and amyloid-beta precursor-like protein by BACE 1. *The Journal of biological chemistry* **279:** 10542-10550

Li R, He P, Cui J, Staufenbiel M, Harada N, Shen Y (2013) Brain endogenous estrogen levels determine responses to estrogen replacement therapy via regulation of BACE1 and NEP in female Alzheimer's transgenic mice. *Molecular neurobiology* **47:** 857-867

Li Y, Zhou W, Tong Y, He G, Song W (2006) Control of APP processing and Abeta generation level by BACE1 enzymatic activity and transcription. *FASEB journal : official publication of the Federation of American Societies for Experimental Biology* **20:** 285-292

Liang J, Kerstin Lindemeyer A, Shen Y, Lopez-Valdes HE, Martinez-Coria H, Shao XM, Olsen

RW (2014) Dihydromyricetin ameliorates behavioral deficits and reverses neuropathology of transgenic mouse models of Alzheimer's disease. *Neurochemical research* **39:** 1171-1181

Lichtenthaler SF, Dominguez DI, Westmeyer GG, Reiss K, Haass C, Saftig P, De Strooper B, Seed B (2003) The cell adhesion protein P-selectin glycoprotein ligand-1 is a substrate for the aspartyl protease BACE1. *The Journal of biological chemistry* **278:** 48713-48719

Lin X, Koelsch G, Wu S, Downs D, Dashti A, Tang J (2000) Human aspartic protease memapsin 2 cleaves the beta-secretase site of beta-amyloid precursor protein. *Proceedings of the National Academy of Sciences of the United States of America* **97:** 1456-1460

Liu X, Gu X, Li Z, Li X, Li H, Chang J, Chen P, Jin J, Xi B, Chen D, Lai D, Graham RM, Zhou M (2006) Neuregulin-1/erbB-activation improves cardiac function and survival in models of ischemic, dilated, and viral cardiomyopathy. *Journal of the American College of Cardiology* **48:** 1438-1447

Lok K, Zhao H, Zhang C, He N, Shen H, Wang Z, Zhao W, Yin M (2013) Effects of accelerated senescence on learning and memory, locomotion and anxiety-like behavior in APP/PS1 mouse model of Alzheimer's disease. *Journal of the neurological sciences* **335:** 145-154

Loos M, Mueller T, Gouwenberg Y, Wijnands R, van der Loo RJ, Birchmeier C, Smit AB, Spijker S (2014) Neuregulin-3 in the Mouse Medial Prefrontal Cortex Regulates Impulsive Action. *Biological psychiatry*

Lorbeck MT (2010) Tip60 and APP genetically interact to promote apoptosis-driven neurodegeneration. Doctor of Philosophy Thesis, Drexel Universit,

Lorke DE, Lu G, Cho E, Yew DT (2006) Serotonin 5-HT2A and 5-HT6 receptors in the prefrontal cortex of Alzheimer and normal aging patients. *BMC neuroscience* **7:** 36

Loughlin SE, Fallon JH (1984) Substantia nigra and ventral tegmental area projections to cortex: topography and collateralization. *Neuroscience* **11:** 425-435

Lukiw WJ, Bazan NG (1998) Strong nuclear factor-kappaB-DNA binding parallels cyclooxygenase-2 gene transcription in aging and in sporadic Alzheimer's disease superior temporal lobe neocortex. *Journal of neuroscience research* **53:** 583-592

Luo Y, Bolon B, Kahn S, Bennett BD, Babu-Khan S, Denis P, Fan W, Kha H, Zhang J, Gong Y, Martin L, Louis JC, Yan Q, Richards WG, Citron M, Vassar R (2001) Mice deficient in BACE1, the Alzheimer's beta-secretase, have normal phenotype and abolished beta-amyloid generation. *Nature neuroscience* **4:** 231-232

Ly PT, Wu Y, Zou H, Wang R, Zhou W, Kinoshita A, Zhang M, Yang Y, Cai F, Woodgett J, Song W (2013) Inhibition of GSK3beta-mediated BACE1 expression reduces Alzheimer-associated phenotypes. *The Journal of clinical investigation* **123:** 224-235

Macintyre DJ, McGhee KA, Maclean AW, Afzal M, Briffa K, Henry B, Thomson PA, Muir WJ, Blackwood DH (2010) Association of GPR50, an X-linked orphan G protein-coupled receptor, and affective disorder in an independent sample of the Scottish population. *Neuroscience letters* **475:** 169-173

Magalhaes AC, Dunn H, Ferguson SS (2012) Regulation of GPCR activity, trafficking and localization by GPCR-interacting proteins. *British journal of pharmacology* **165:** 1717-1736

Malik S, Vinukonda G, Vose LR, Diamond D, Bhimavarapu BB, Hu F, Zia MT, Hevner R, Zecevic N, Ballabh P (2013) Neurogenesis continues in the third trimester of pregnancy and is suppressed by premature birth. *The Journal of neuroscience : the official journal of the Society for Neuroscience* **33:** 411-423

Manders EMMVFJAA (1993) Measurement of co-localization of objects in dual-colour confocal images. *Journal of Microscopy* **169:** 9

Mann KM, Thorngate FE, Katoh-Fukui Y, Hamanaka H, Williams DL, Fujita S, Lamb BT (2004) Independent effects of APOE on cholesterol metabolism and brain Abeta levels in an Alzheimer disease mouse model. *Human molecular genetics* **13:** 1959-1968

Marballi K, Cruz D, Thompson P, Walss-Bass C (2012) Differential neuregulin 1 cleavage in the prefrontal cortex and hippocampus in schizophrenia and bipolar disorder: preliminary findings. *PloS one* **7:** e36431

Marcinkiewicz M, Seidah NG (2000) Coordinated expression of beta-amyloid precursor protein and the putative beta-secretase BACE and alpha-secretase ADAM10 in mouse and human brain. *Journal of neurochemistry* **75:** 2133-2143

Maretzky T, Schulte M, Ludwig A, Rose-John S, Blobel C, Hartmann D, Altevogt P, Saftig P, Reiss K (2005) L1 is sequentially processed by two differently activated metalloproteases and presenilin/gamma-secretase and regulates neural cell adhesion, cell migration, and neurite outgrowth. *Molecular and cellular biology* **25:** 9040-9053

Marinissen MJ, Gutkind JS (2001) G-protein-coupled receptors and signaling networks: emerging paradigms. *Trends in pharmacological sciences* **22:** 368-376

Marquer C, Devauges V, Cossec JC, Liot G, Lecart S, Saudou F, Duyckaerts C, Leveque-Fort S, Potier MC (2011) Local cholesterol increase triggers amyloid precursor protein-Bace1 clustering in lipid rafts and rapid endocytosis. *FASEB journal : official publication of the Federation of American Societies for Experimental Biology* **25:** 1295-1305

Martinowich K, Schloesser RJ, Manji HK (2009) Bipolar disorder: from genes to behavior pathways. *The Journal of clinical investigation* **119:** 726-736

Masliah E, Xie F, Dayan S, Rockenstein E, Mante M, Adame A, Patrick CM, Chan AF, Zheng B (2010) Genetic deletion of Nogo/Rtn4 ameliorates behavioral and neuropathological outcomes in amyloid precursor protein transgenic mice. *Neuroscience* **169:** 488-494

Mastrocola R, Guglielmotto M, Medana C, Catalano MG, Cutrupi S, Borghi R, Tamagno E, Boccuzzi G, Aragno M (2011) Dysregulation of SREBP2 induces BACE1 expression. *Neurobiology of disease* **44:** 116-124

Matsui T, Ingelsson M, Fukumoto H, Ramasamy K, Kowa H, Frosch MP, Irizarry MC, Hyman BT (2007) Expression of APP pathway mRNAs and proteins in Alzheimer's disease. *Brain research* **1161:** 116-123

Mattson MP, Camandola S (2001) NF-kappaB in neuronal plasticity and neurodegenerative disorders. *The Journal of clinical investigation* **107:** 247-254

McDonald AJ, Augustine JR (1993) Localization of GABA-like immunoreactivity in the monkey amygdala. *Neuroscience* **52:** 281-294

McGowan E, Pickford F, Kim J, Onstead L, Eriksen J, Yu C, Skipper L, Murphy MP, Beard J, Das P, Jansen K, Delucia M, Lin WL, Dolios G, Wang R, Eckman CB, Dickson DW, Hutton M, Hardy J, Golde T (2005) Abeta42 is essential for parenchymal and vascular amyloid deposition in mice. *Neuron* **47:** 191-199

Meakin PJ (2013) Targeting BACE1 to improve leptin sensitivity and reverse obesity. In *37th Congress of IUPS* Birmingham, UK

Meakin PJ, Harper AJ, Hamilton DL, Gallagher J, McNeilly AD, Burgess LA, Vaanholt LM, Bannon KA, Latcham J, Hussain I, Speakman JR, Howlett DR, Ashford ML (2012) Reduction in BACE1 decreases body weight, protects against diet-induced obesity and enhances insulin sensitivity in mice. *The Biochemical journal* **441:** 285-296

Mechtersheimer S, Gutwein P, Agmon-Levin N, Stoeck A, Oleszewski M, Riedle S, Postina R, Fahrenholz F, Fogel M, Lemmon V, Altevogt P (2001) Ectodomain shedding of L1 adhesion molecule promotes cell migration by autocrine binding to integrins. *The Journal of cell biology* **155:** 661-673

Medeiros R, Kitazawa M, Caccamo A, Baglietto-Vargas D, Estrada-Hernandez T, Cribbs DH, Fisher A, LaFerla FM (2011) Loss of muscarinic M1 receptor exacerbates Alzheimer's disease-like pathology and cognitive decline. *The American journal of pathology* **179:** 980-991

Mei L, Xiong WC (2008) Neuregulin 1 in neural development, synaptic plasticity and schizophrenia. *Nature reviews Neuroscience* **9:** 437-452

Mhatre SD, Satyasi V, Killen M, Paddock BE, Moir RD, Saunders AJ, Marenda DR (2014) Synaptic abnormalities in a Drosophila model of Alzheimer's disease. *Disease models & mechanisms* **7:** 373-385

Mieda M, Williams SC, Richardson JA, Tanaka K, Yanagisawa M (2006) The dorsomedial hypothalamic nucleus as a putative food-entrainable circadian pacemaker. *Proceedings of the National Academy of Sciences of the United States of America* **103:** 12150-12155

Miernyk JA, Thelen JJ (2008) Biochemical approaches for discovering protein-protein interactions. *The Plant journal : for cell and molecular biology* **53:** 597-609

Mintun MA, Larossa GN, Sheline YI, Dence CS, Lee SY, Mach RH, Klunk WE, Mathis CA, DeKosky ST, Morris JC (2006) [11C]PIB in a nondemented population: potential antecedent marker of Alzheimer disease. *Neurology* **67:** 446-452

Miyazaki H, Oyama F, Wong HK, Kaneko K, Sakurai T, Tamaoka A, Nukina N (2007) BACE1 modulates filopodia-like protrusions induced by sodium channel beta4 subunit. *Biochemical and biophysical research communications* **361:** 43-48

Mohajeri MH, Saini KD, Nitsch RM (2004) Transgenic BACE expression in mouse neurons accelerates amyloid plaque pathology. *Journal of neural transmission* **111:** 413-425

Montag-Sallaz M, Schachner M, Montag D (2002) Misguided axonal projections, neural cell adhesion molecule 180 mRNA upregulation, and altered behavior in mice deficient for the close homolog of L1. *Molecular and cellular biology* **22:** 7967-7981

Morris DW, Rodgers A, McGhee KA, Schwaiger S, Scully P, Quinn J, Meagher D, Waddington JL, Gill M, Corvin AP (2004) Confirming RGS4 as a susceptibility gene for schizophrenia.

American journal of medical genetics Part B, Neuropsychiatric genetics : the official publication of the International Society of Psychiatric Genetics **125B:** 50-53

Morrissette DA, Parachikova A, Green KN, LaFerla FM (2009) Relevance of transgenic mouse models to human Alzheimer disease. *The Journal of biological chemistry* **284:** 6033-6037

Mouton-Liger F, Paquet C, Dumurgier J, Bouras C, Pradier L, Gray F, Hugon J (2012) Oxidative stress increases BACE1 protein levels through activation of the PKR-eIF2alpha pathway. *Biochimica et biophysica acta* **1822:** 885-896

Mowrer KR, Wolfe MS (2008) Promotion of BACE1 mRNA alternative splicing reduces amyloid beta-peptide production. *The Journal of biological chemistry* **283:** 18694-18701

Mrzljak L, Uylings HB, Kostovic I, Van Eden CG (1988) Prenatal development of neurons in the human prefrontal cortex: I. A qualitative Golgi study. *The Journal of comparative neurology* **271:** 355-386

Mucke L, Masliah E, Yu GQ, Mallory M, Rockenstein EM, Tatsuno G, Hu K, Kholodenko D, Johnson-Wood K, McConlogue L (2000) High-level neuronal expression of abeta 1-42 in wild-type human amyloid protein precursor transgenic mice: synaptotoxicity without plaque formation. *The Journal of neuroscience : the official journal of the Society for Neuroscience* **20:** 4050-4058

Muhleisen TW, Leber M, Schulze TG, Strohmaier J, Degenhardt F, Treutlein J, Mattheisen M, Forstner AJ, Schumacher J, Breuer R, Meier S, Herms S, Hoffmann P, Lacour A, Witt SH, Reif A, Muller-Myhsok B, Lucae S, Maier W, Schwarz M, Vedder H, Kammerer-Ciernioch J, Pfennig A, Bauer M, Hautzinger M, Moebus S, Priebe L, Czerski PM, Hauser J, Lissowska J, Szeszenia-Dabrowska N, Brennan P, McKay JD, Wright A, Mitchell PB, Fullerton JM, Schofield PR, Montgomery GW, Medland SE, Gordon SD, Martin NG, Krasnow V, Chuchalin A, Babadjanova G, Pantelejeva G, Abramova LI, Tiganov AS, Polonikov A, Khusnutdinova E, Alda M, Grof P, Rouleau GA, Turecki G, Laprise C, Rivas F, Mayoral F, Kogevinas M, Grigoroiu-Serbanescu M, Propping P, Becker T, Rietschel M, Nothen MM, Cichon S (2014) Genome-wide association study reveals two new risk loci for bipolar disorder. *Nature communications* **5:** 3339

Muller T, Schrotter A, Loosse C, Pfeiffer K, Theiss C, Kauth M, Meyer HE, Marcus K (2013) A ternary complex consisting of AICD, FE65, and TIP60 down-regulates Stathmin1. *Biochimica et biophysica acta* **1834:** 387-394

Muma NA, Mariyappa R, Williams K, Lee JM (2003) Differences in regional and subcellular localization of G(q/11) and RGS4 protein levels in Alzheimer's disease: correlation with muscarinic M1 receptor binding parameters. *Synapse* **47:** 58-65

Murayama KS, Kametani F, Saito S, Kume H, Akiyama H, Araki W (2006) Reticulons RTN3 and RTN4-B/C interact with BACE1 and inhibit its ability to produce amyloid beta-protein. *The European journal of neuroscience* **24:** 1237-1244

Murray AM, Weihmueller FB, Marshall JF, Hurtig HI, Gottleib GL, Joyce JN (1995) Damage to dopamine systems differs between Parkinson's disease and Alzheimer's disease with parkinsonism. *Annals of neurology* **37:** 300-312

Murrell J, Farlow M, Ghetti B, Benson MD (1991) A mutation in the amyloid precursor protein associated with hereditary Alzheimer's disease. *Science* **254:** 97-99

Murthy R, Kim J, Sun X, Giger RJ, Fink DJ, Mata M (2013) Post-transcriptional regulation of GABAB receptor and GIRK1 channels by Nogo receptor 1. *Molecular brain* **6:** 30

Nagura H, Ishikawa Y, Kobayashi K, Takao K, Tanaka T, Nishikawa K, Tamura H, Shiosaka S, Suzuki H, Miyakawa T, Fujiyoshi Y, Doi T (2012) Impaired synaptic clustering of postsynaptic density proteins and altered signal transmission in hippocampal neurons, and disrupted learning behavior in PDZ1 and PDZ2 ligand binding-deficient PSD-95 knockin mice. *Molecular brain* **5:** 43

Naj AC, Jun G, Beecham GW, Wang LS, Vardarajan BN, Buros J, Gallins PJ, Buxbaum JD, Jarvik GP, Crane PK, Larson EB, Bird TD, Boeve BF, Graff-Radford NR, De Jager PL, Evans D, Schneider JA, Carrasquillo MM, Ertekin-Taner N, Younkin SG, Cruchaga C, Kauwe JS, Nowotny P, Kramer P, Hardy J, Huentelman MJ, Myers AJ, Barmada MM, Demirci FY, Baldwin CT, Green RC, Rogaeva E, St George-Hyslop P, Arnold SE, Barber R, Beach T, Bigio EH, Bowen JD, Boxer A, Burke JR, Cairns NJ, Carlson CS, Carney RM, Carroll SL, Chui HC, Clark DG, Corneveaux J, Cotman CW, Cummings JL, DeCarli C, DeKosky ST, Diaz-Arrastia R, Dick M, Dickson DW, Ellis WG, Faber KM, Fallon KB, Farlow MR, Ferris S, Frosch MP, Galasko DR, Ganguli M, Gearing M, Geschwind DH, Ghetti B, Gilbert JR, Gilman S, Giordani B, Glass JD, Growdon JH, Hamilton RL, Harrell LE, Head E, Honig LS, Hulette CM, Hyman BT, Jicha GA, Jin LW, Johnson N, Karlawish J, Karydas A, Kaye JA, Kim R, Koo EH, Kowall NW, Lah JJ, Levey AI, Lieberman AP, Lopez OL, Mack WJ, Marson DC, Martiniuk F, Mash DC, Masliah E, McCormick WC, McCurry SM, McDavid AN, McKee AC, Mesulam M, Miller BL, Miller CA, Miller JW, Parisi JE, Perl DP, Peskind E, Petersen RC, Poon WW, Quinn JF, Rajbhandary RA, Raskind M, Reisberg B, Ringman JM, Roberson ED, Rosenberg RN, Sano M, Schneider LS, Seeley W, Shelanski ML, Slifer MA, Smith CD, Sonnen JA, Spina S, Stern RA, Tanzi RE, Trojanowski JQ, Troncoso JC, Van Deerlin VM, Vinters HV, Vonsattel JP, Weintraub S, Welsh-Bohmer KA, Williamson J, Woltjer RL, Cantwell LB, Dombroski BA, Beekly D, Lunetta KL, Martin ER, Kamboh MI, Saykin AJ, Reiman EM, Bennett DA, Morris JC, Montine TJ, Goate AM, Blacker D, Tsuang DW, Hakonarson H, Kukull WA, Foroud TM, Haines JL, Mayeux R, Pericak-Vance MA, Farrer LA, Schellenberg GD (2011) Common variants at MS4A4/MS4A6E, CD2AP, CD33 and EPHA1 are associated with late-onset Alzheimer's disease. *Nature genetics* **43:** 436-441

Nave KA, Salzer JL (2006) Axonal regulation of myelination by neuregulin 1. *Current opinion in neurobiology* **16:** 492-500

Nawa H, Sotoyama H, Iwakura Y, Takei N, Namba H (2014) Neuropathologic Implication of Peripheral Neuregulin-1 and EGF Signals in Dopaminergic Dysfunction and Behavioral Deficits Relevant to Schizophrenia: Their Target Cells and Time Window. *BioMed research international* **2014:** 697935

Ng KM, Lau CF, Fung ML (2010) Melatonin reduces hippocampal beta-amyloid generation in rats exposed to chronic intermittent hypoxia. *Brain research* **1354:** 163-171

Nicholson DA, Yoshida R, Berry RW, Gallagher M, Geinisman Y (2004) Reduction in size of perforated postsynaptic densities in hippocampal axospinous synapses and age-related spatial learning impairments. *The Journal of neuroscience : the official journal of the Society for Neuroscience* **24:** 7648-7653

Nicodemus KK, Luna A, Vakkalanka R, Goldberg T, Egan M, Straub RE, Weinberger DR (2006) Further evidence for association between ErbB4 and schizophrenia and influence on cognitive intermediate phenotypes in healthy controls. *Molecular psychiatry* **11:** 1062-1065

Niederost B, Oertle T, Fritsche J, McKinney RA, Bandtlow CE (2002) Nogo-A and myelin-associated glycoprotein mediate neurite growth inhibition by antagonistic regulation of

RhoA and Rac1. *The Journal of neuroscience : the official journal of the Society for Neuroscience* **22:** 10368-10376

Nilsberth C, Westlind-Danielsson A, Eckman CB, Condron MM, Axelman K, Forsell C, Stenh C, Luthman J, Teplow DB, Younkin SG, Naslund J, Lannfelt L (2001) The 'Arctic' APP mutation (E693G) causes Alzheimer's disease by enhanced Abeta protofibril formation. *Nature neuroscience* **4:** 887-893

Nordentoft I, Jorgensen P (2003) The acetyltransferase 60 kDa trans-acting regulatory protein of HIV type 1-interacting protein (Tip60) interacts with the translocation E26 transforming-specific leukaemia gene (TEL) and functions as a transcriptional co-repressor. *The Biochemical journal* **374:** 165-173

Norton N, Moskvina V, Morris DW, Bray NJ, Zammit S, Williams NM, Williams HJ, Preece AC, Dwyer S, Wilkinson JC, Spurlock G, Kirov G, Buckland P, Waddington JL, Gill M, Corvin AP, Owen MJ, O'Donovan MC (2006) Evidence that interaction between neuregulin 1 and its receptor erbB4 increases susceptibility to schizophrenia. *American journal of medical genetics Part B, Neuropsychiatric genetics : the official publication of the International Society of Psychiatric Genetics* **141B:** 96-101

Notarianni E (2013) Hypercortisolemia and glucocorticoid receptor-signaling insufficiency in Alzheimer's disease initiation and development. *Current Alzheimer research* **10:** 714-731

Novak G, Kim D, Seeman P, Tallerico T (2002) Schizophrenia and Nogo: elevated mRNA in cortex, and high prevalence of a homozygous CAA insert. *Brain research Molecular brain research* **107:** 183-189

Novak G, Tallerico T (2006) Nogo A, B and C expression in schizophrenia, depression and bipolar frontal cortex, and correlation of Nogo expression with CAA/TATC polymorphism in 3'-UTR. *Brain research* **1120:** 161-171

O'Connor T, Sadleir KR, Maus E, Velliquette RA, Zhao J, Cole SL, Eimer WA, Hitt B, Bembinster LA, Lammich S, Lichtenthaler SF, Hebert SS, De Strooper B, Haass C, Bennett DA, Vassar R (2008) Phosphorylation of the translation initiation factor eIF2alpha increases BACE1 levels and promotes amyloidogenesis. *Neuron* **60:** 988-1009

O'Donnell D, Baccichet A, Seckl JR, Meaney MJ, Poirier J (1993) Entorhinal cortex lesions transiently alter glucocorticoid but not mineralocorticoid receptor gene expression in the rat hippocampus. *Journal of neurochemistry* **61:** 356-359

Oddo S, Caccamo A, Shepherd JD, Murphy MP, Golde TE, Kayed R, Metherate R, Mattson MP, Akbari Y, LaFerla FM (2003) Triple-transgenic model of Alzheimer's disease with plaques and tangles: intracellular Abeta and synaptic dysfunction. *Neuron* **39:** 409-421

Oertle T, van der Haar ME, Bandtlow CE, Robeva A, Burfeind P, Buss A, Huber AB, Simonen M, Schnell L, Brosamle C, Kaupmann K, Vallon R, Schwab ME (2003) Nogo-A inhibits neurite outgrowth and cell spreading with three discrete regions. *The Journal of neuroscience : the official journal of the Society for Neuroscience* **23:** 5393-5406

Ohno M, Cole SL, Yasvoina M, Zhao J, Citron M, Berry R, Disterhoft JF, Vassar R (2007) BACE1 gene deletion prevents neuron loss and memory deficits in 5XFAD APP/PS1 transgenic mice. *Neurobiology of disease* **26:** 134-145

Ohno M, Sametsky EA, Younkin LH, Oakley H, Younkin SG, Citron M, Vassar R, Disterhoft JF

(2004) BACE1 deficiency rescues memory deficits and cholinergic dysfunction in a mouse model of Alzheimer's disease. *Neuron* **41:** 27-33

Okada H, Zhang W, Peterhoff C, Hwang JC, Nixon RA, Ryu SH, Kim TW (2010) Proteomic identification of sorting nexin 6 as a negative regulator of BACE1-mediated APP processing. *FASEB journal : official publication of the Federation of American Societies for Experimental Biology* **24:** 2783-2794

Okamoto M, Sudhof TC (1997) Mints, Munc18-interacting proteins in synaptic vesicle exocytosis. *The Journal of biological chemistry* **272:** 31459-31464

Olcese JM, Cao C, Mori T, Mamcarz MB, Maxwell A, Runfeldt MJ, Wang L, Zhang C, Lin X, Zhang G, Arendash GW (2009) Protection against cognitive deficits and markers of neurodegeneration by long-term oral administration of melatonin in a transgenic model of Alzheimer disease. *Journal of pineal research* **47:** 82-96

Orcholski ME, Zhang Q, Bredesen DE (2011) Signaling via amyloid precursor-like proteins APLP1 and APLP2. *Journal of Alzheimer's disease : JAD* **23:** 689-699

Orsulic S, Huber O, Aberle H, Arnold S, Kemler R (1999) E-cadherin binding prevents beta-catenin nuclear localization and beta-catenin/LEF-1-mediated transactivation. *Journal of cell science* **112 (Pt 8):** 1237-1245

Osaki T, Kakegawa T, Suzuki H, Fukuda J (2011) Electrical detachment of cells for engineering capillary-like structures in a photocrosslinkable hydrogel. *Conference proceedings : Annual International Conference of the IEEE Engineering in Medicine and Biology Society IEEE Engineering in Medicine and Biology Society Conference* **2011:** 2451-2454

Palczewski K (2010) Oligomeric forms of G protein-coupled receptors (GPCRs). *Trends in biochemical sciences* **35:** 595-600

Panchal H, Wansbury O, Parry S, Ashworth A, Howard B (2007) Neuregulin3 alters cell fate in the epidermis and mammary gland. *BMC developmental biology* **7:** 105

Pare D, Gaudreau H (1996) Projection cells and interneurons of the lateral and basolateral amygdala: distinct firing patterns and differential relation to theta and delta rhythms in conscious cats. *The Journal of neuroscience : the official journal of the Society for Neuroscience* **16:** 3334-3350

Park JJ, Cawley NX, Loh YP (2008) Carboxypeptidase E cytoplasmic tail-driven vesicle transport is key for activity-dependent secretion of peptide hormones. *Molecular endocrinology* **22:** 989-1005

Pastorino L, Ikin AF, Nairn AC, Pursnani A, Buxbaum JD (2002) The carboxyl-terminus of BACE contains a sorting signal that regulates BACE trafficking but not the formation of total A(beta). *Molecular and cellular neurosciences* **19:** 175-185

Peng X, Kim J, Zhou Z, Fink DJ, Mata M (2011) Neuronal Nogo-A regulates glutamate receptor subunit expression in hippocampal neurons. *Journal of neurochemistry* **119:** 1183-1193

Perez M, Moran MA, Ferrer I, Avila J, Gomez-Ramos P (2008) Phosphorylated tau in neuritic plaques of APP(sw)/Tau (vlw) transgenic mice and Alzheimer disease. *Acta neuropathologica* **116:** 409-418

Perez RG, Zheng H, Van der Ploeg LH, Koo EH (1997) The beta-amyloid precursor protein of Alzheimer's disease enhances neuron viability and modulates neuronal polarity. *The Journal of neuroscience : the official journal of the Society for Neuroscience* **17:** 9407-9414

Perlin JR, Lush ME, Stephens WZ, Piotrowski T, Talbot WS (2011) Neuronal Neuregulin 1 type III directs Schwann cell migration. *Development* **138:** 4639-4648

Phillips LJ, McGorry PD, Garner B, Thompson KN, Pantelis C, Wood SJ, Berger G (2006) Stress, the hippocampus and the hypothalamic-pituitary-adrenal axis: implications for the development of psychotic disorders. *The Australian and New Zealand journal of psychiatry* **40:** 725-741

Phinney AL, Deller T, Stalder M, Calhoun ME, Frotscher M, Sommer B, Staufenbiel M, Jucker M (1999) Cerebral amyloid induces aberrant axonal sprouting and ectopic terminal formation in amyloid precursor protein transgenic mice. *The Journal of neuroscience : the official journal of the Society for Neuroscience* **19:** 8552-8559

Phuc Le P, Friedman JR, Schug J, Brestelli JE, Parker JB, Bochkis IM, Kaestner KH (2005) Glucocorticoid receptor-dependent gene regulatory networks. *PLoS genetics* **1:** e16

Pirooznia SK, Sarthi J, Johnson AA, Toth MS, Chiu K, Koduri S, Elefant F (2012) Tip60 HAT activity mediates APP induced lethality and apoptotic cell death in the CNS of a Drosophila Alzheimer's disease model. *PloS one* **7:** e41776

Prabhu Y, Burgos PV, Schindler C, Farias GG, Magadan JG, Bonifacino JS (2012) Adaptor protein 2-mediated endocytosis of the beta-secretase BACE1 is dispensable for amyloid precursor protein processing. *Molecular biology of the cell* **23:** 2339-2351

Pralong E, Jones RS (1993) Interactions of dopamine with glutamate- and GABA-mediated synaptic transmission in the rat entorhinal cortex in vitro. *The European journal of neuroscience* **5:** 760-767

Prata DP, Breen G, Osborne S, Munro J, St Clair D, Collier DA (2009) An association study of the neuregulin 1 gene, bipolar affective disorder and psychosis. *Psychiatric genetics* **19:** 113-116

Psychiatric GCBDWG (2011) Large-scale genome-wide association analysis of bipolar disorder identifies a new susceptibility locus near ODZ4. *Nature genetics* **43:** 977-983

Qing H, Zhou W, Christensen MA, Sun X, Tong Y, Song W (2004) Degradation of BACE by the ubiquitin-proteasome pathway. *FASEB journal : official publication of the Federation of American Societies for Experimental Biology* **18:** 1571-1573

Reinikainen KJ, Soininen H, Riekkinen PJ (1990) Neurotransmitter changes in Alzheimer's disease: implications to diagnostics and therapy. *Journal of neuroscience research* **27:** 576-586

Reppert SM, Weaver DR, Cassone VM, Godson C, Kolakowski LF, Jr. (1995) Melatonin receptors are for the birds: molecular analysis of two receptor subtypes differentially expressed in chick brain. *Neuron* **15:** 1003-1015

Reppert SM, Weaver DR, Ebisawa T, Mahle CD, Kolakowski LF, Jr. (1996) Cloning of a melatonin-related receptor from human pituitary. *FEBS letters* **386:** 219-224

Ripke S, O'Dushlaine C, Chambert K, Moran JL, Kahler AK, Akterin S, Bergen SE, Collins AL, Crowley JJ, Fromer M, Kim Y, Lee SH, Magnusson PK, Sanchez N, Stahl EA, Williams S, Wray NR, Xia K, Bettella F, Borglum AD, Bulik-Sullivan BK, Cormican P, Craddock N, de Leeuw C, Durmishi N, Gill M, Golimbet V, Hamshere ML, Holmans P, Hougaard DM, Kendler KS, Lin K, Morris DW, Mors O, Mortensen PB, Neale BM, O'Neill FA, Owen MJ, Milovancevic MP, Posthuma D, Powell J, Richards AL, Riley BP, Ruderfer D, Rujescu D, Sigurdsson E, Silagadze T, Smit AB, Stefansson H, Steinberg S, Suvisaari J, Tosato S, Verhage M, Walters JT, Multicenter Genetic Studies of Schizophrenia C, Levinson DF, Gejman PV, Kendler KS, Laurent C, Mowry BJ, O'Donovan MC, Owen MJ, Pulver AE, Riley BP, Schwab SG, Wildenauer DB, Dudbridge F, Holmans P, Shi J, Albus M, Alexander M, Campion D, Cohen D, Dikeos D, Duan J, Eichhammer P, Godard S, Hansen M, Lerer FB, Liang KY, Maier W, Mallet J, Nertney DA, Nestadt G, Norton N, O'Neill FA, Papadimitriou GN, Ribble R, Sanders AR, Silverman JM, Walsh D, Williams NM, Wormley B, Psychosis Endophenotypes International C, Arranz MJ, Bakker S, Bender S, Bramon E, Collier D, Crespo-Facorro B, Hall J, Iyegbe C, Jablensky A, Kahn RS, Kalaydjieva L, Lawrie S, Lewis CM, Lin K, Linszen DH, Mata I, McIntosh A, Murray RM, Ophoff RA, Powell J, Rujescu D, Van Os J, Walshe M, Weisbrod M, Wiersma D, Wellcome Trust Case Control C, Donnelly P, Barroso I, Blackwell JM, Bramon E, Brown MA, Casas JP, Corvin AP, Deloukas P, Duncanson A, Jankowski J, Markus HS, Mathew CG, Palmer CN, Plomin R, Rautanen A, Sawcer SJ, Trembath RC, Viswanathan AC, Wood NW, Spencer CC, Band G, Bellenguez C, Freeman C, Hellenthal G, Giannoulatou E, Pirinen M, Pearson RD, Strange A, Su Z, Vukcevic D, Donnelly P, Langford C, Hunt SE, Edkins S, Gwilliam R, Blackburn H, Bumpstead SJ, Dronov S, Gillman M, Gray E, Hammond N, Jayakumar A, McCann OT, Liddle J, Potter SC, Ravindrarajah R, Ricketts M, Tashakkori-Ghanbaria A, Waller MJ, Weston P, Widaa S, Whittaker P, Barroso I, Deloukas P, Mathew CG, Blackwell JM, Brown MA, Corvin AP, McCarthy MI, Spencer CC, Bramon E, Corvin AP, O'Donovan MC, Stefansson K, Scolnick E, Purcell S, McCarroll SA, Sklar P, Hultman CM, Sullivan PF (2013) Genome-wide association analysis identifies 13 new risk loci for schizophrenia. *Nature genetics* **45:** 1150-1159

Roberds SL, Anderson J, Basi G, Bienkowski MJ, Branstetter DG, Chen KS, Freedman SB, Frigon NL, Games D, Hu K, Johnson-Wood K, Kappenman KE, Kawabe TT, Kola I, Kuehn R, Lee M, Liu W, Motter R, Nichols NF, Power M, Robertson DW, Schenk D, Schoor M, Shopp GM, Shuck ME, Sinha S, Svensson KA, Tatsuno G, Tintrup H, Wijsman J, Wright S, McConlogue L (2001) BACE knockout mice are healthy despite lacking the primary beta-secretase activity in brain: implications for Alzheimer's disease therapeutics. *Human molecular genetics* **10:** 1317-1324

Rockenstein E, Mante M, Alford M, Adame A, Crews L, Hashimoto M, Esposito L, Mucke L, Masliah E (2005) High beta-secretase activity elicits neurodegeneration in transgenic mice despite reductions in amyloid-beta levels: implications for the treatment of Alzheimer disease. *The Journal of biological chemistry* **280:** 32957-32967

Rodriguez EM, Blazquez JL, Pastor FE, Pelaez B, Pena P, Peruzzo B, Amat P (2005) Hypothalamic tanycytes: a key component of brain-endocrine interaction. *International review of cytology* **247:** 89-164

Rogers GW, Jr., Edelman GM, Mauro VP (2004) Differential utilization of upstream AUGs in the beta-secretase mRNA suggests that a shunting mechanism regulates translation. *Proceedings of the National Academy of Sciences of the United States of America* **101:** 2794-2799

Ross RS, Eichenbaum H (2006) Dynamics of hippocampal and cortical activation during consolidation of a nonspatial memory. *The Journal of neuroscience : the official journal of the Society for Neuroscience* **26:** 4852-4859

Rossler M, Zarski R, Bohl J, Ohm TG (2002) Stage-dependent and sector-specific neuronal loss in hippocampus during Alzheimer's disease. *Acta neuropathologica* **103:** 363-369

Rushworth JV, Hooper NM (2010) Lipid Rafts: Linking Alzheimer's Amyloid-beta Production, Aggregation, and Toxicity at Neuronal Membranes. *International journal of Alzheimer's disease* **2011:** 603052

Sadigh-Eteghad S, Talebi M, Farhoudi M (2012) Association of apolipoprotein E epsilon 4 allele with sporadic late onset Alzheimer`s disease. A meta-analysis. *Neurosciences* **17:** 321-326

Sadleir KR, Vassar R (2012) Cdk5 protein inhibition and Abeta42 increase BACE1 protein level in primary neurons by a post-transcriptional mechanism: implications of CDK5 as a therapeutic target for Alzheimer disease. *The Journal of biological chemistry* **287:** 7224-7235

Samuelsen GB, Larsen KB, Bogdanovic N, Laursen H, Graem N, Larsen JF, Pakkenberg B (2003) The changing number of cells in the human fetal forebrain and its subdivisions: a stereological analysis. *Cerebral cortex* **13:** 115-122

Sannerud R, Declerck I, Peric A, Raemaekers T, Menendez G, Zhou L, Veerle B, Coen K, Munck S, De Strooper B, Schiavo G, Annaert W (2011) ADP ribosylation factor 6 (ARF6) controls amyloid precursor protein (APP) processing by mediating the endosomal sorting of BACE1. *Proceedings of the National Academy of Sciences of the United States of America* **108:** E559-568

Santosa C, Rasche S, Barakat A, Bellingham SA, Ho M, Tan J, Hill AF, Masters CL, McLean C, Evin G (2011) Decreased expression of GGA3 protein in Alzheimer's disease frontal cortex and increased co-distribution of BACE with the amyloid precursor protein. *Neurobiology of disease* **43:** 176-183

Sapountzi V, Logan IR, Robson CN (2006) Cellular functions of TIP60. *The international journal of biochemistry & cell biology* **38:** 1496-1509

Sarajarvi T, Haapasalo A, Viswanathan J, Makinen P, Laitinen M, Soininen H, Hiltunen M (2009) Down-regulation of seladin-1 increases BACE1 levels and activity through enhanced GGA3 depletion during apoptosis. *The Journal of biological chemistry* **284:** 34433-34443

Satoh J, Kuroda Y (2000) Amyloid precursor protein beta-secretase (BACE) mRNA expression in human neural cell lines following induction of neuronal differentiation and exposure to cytokines and growth factors. *Neuropathology : official journal of the Japanese Society of Neuropathology* **20:** 289-296

Savaskan E, Olivieri G, Brydon L, Jockers R, Krauchi K, Wirz-Justice A, Muller-Spahn F (2001) Cerebrovascular melatonin MT1-receptor alterations in patients with Alzheimer's disease. *Neuroscience letters* **308:** 9-12

Savaskan E, Olivieri G, Meier F, Brydon L, Jockers R, Ravid R, Wirz-Justice A, Muller-Spahn F (2002) Increased melatonin 1a-receptor immunoreactivity in the hippocampus of Alzheimer's disease patients. *Journal of pineal research* **32:** 59-62

Savonenko AV, Melnikova T, Laird FM, Stewart KA, Price DL, Wong PC (2008) Alteration of BACE1-dependent NRG1/ErbB4 signaling and schizophrenia-like phenotypes in BACE1-null

mice. *Proceedings of the National Academy of Sciences of the United States of America* **105:** 5585-5590

Savvaki M, Panagiotaropoulos T, Stamatakis A, Sargiannidou I, Karatzioula P, Watanabe K, Stylianopoulou F, Karagogeos D, Kleopa KA (2008) Impairment of learning and memory in TAG-1 deficient mice associated with shorter CNS internodes and disrupted juxtaparanodes. *Molecular and cellular neurosciences* **39:** 478-490

Scheff SW, Price DA (2006) Alzheimer's disease-related alterations in synaptic density: neocortex and hippocampus. *Journal of Alzheimer's disease : JAD* **9:** 101-115

Scherzer CR, Offe K, Gearing M, Rees HD, Fang G, Heilman CJ, Schaller C, Bujo H, Levey AI, Lah JJ (2004) Loss of apolipoprotein E receptor LR11 in Alzheimer disease. *Archives of neurology* **61:** 1200-1205

Schizophrenia Working Group of the Psychiatric Genomics C (2014) Biological insights from 108 schizophrenia-associated genetic loci. *Nature* **511:** 421-427

Scholefield Z, Yates EA, Wayne G, Amour A, McDowell W, Turnbull JE (2003) Heparan sulfate regulates amyloid precursor protein processing by BACE1, the Alzheimer's beta-secretase. *The Journal of cell biology* **163:** 97-107

Schuff N, Woerner N, Boreta L, Kornfield T, Shaw LM, Trojanowski JQ, Thompson PM, Jack CR, Jr., Weiner MW, Alzheimer's Disease Neuroimaging I (2009) MRI of hippocampal volume loss in early Alzheimer's disease in relation to ApoE genotype and biomarkers. *Brain : a journal of neurology* **132:** 1067-1077

Seeman P (1987) Dopamine receptors and the dopamine hypothesis of schizophrenia. *Synapse* **1:** 133-152

Selvin PR (2003) Lighting up single ion channels. *Biophysical journal* **84:** 1-2

Senechal Y, Kelly PH, Dev KK (2008) Amyloid precursor protein knockout mice show age-dependent deficits in passive avoidance learning. *Behavioural brain research* **186:** 126-132

Shi Q, Prior M, He W, Tang X, Hu X, Yan R (2009) Reduced amyloid deposition in mice overexpressing RTN3 is adversely affected by preformed dystrophic neurites. *The Journal of neuroscience : the official journal of the Society for Neuroscience* **29:** 9163-9173

Shi Q, Prior M, Zhou X, Tang X, He W, Hu X, Yan R (2013) Preventing formation of reticulon 3 immunoreactive dystrophic neurites improves cognitive function in mice. *The Journal of neuroscience : the official journal of the Society for Neuroscience* **33:** 3059-3066

Shi XP, Chen E, Yin KC, Na S, Garsky VM, Lai MT, Li YM, Platchek M, Register RB, Sardana MK, Tang MJ, Thiebeau J, Wood T, Shafer JA, Gardell SJ (2001) The pro domain of beta-secretase does not confer strict zymogen-like properties but does assist proper folding of the protease domain. *The Journal of biological chemistry* **276:** 10366-10373

Shimizu H, Tosaki A, Kaneko K, Hisano T, Sakurai T, Nukina N (2008) Crystal structure of an active form of BACE1, an enzyme responsible for amyloid beta protein production. *Molecular and cellular biology* **28:** 3663-3671

Shimoyama Y, Tsujimoto G, Kitajima M, Natori M (2000) Identification of three human type-II classic cadherins and frequent heterophilic interactions between different subclasses of

type-II classic cadherins. *The Biochemical journal* **349:** 159-167

Shohamy D, Allen MT, Gluck MA (2000) Dissociating entorhinal and hippocampal involvement in latent inhibition. *Behavioral neuroscience* **114:** 867-874

Sidibe A, Mullier A, Chen P, Baroncini M, Boutin JA, Delagrange P, Prevot V, Jockers R (2010) Expression of the orphan GPR50 protein in rodent and human dorsomedial hypothalamus, tanycytes and median eminence. *Journal of pineal research* **48:** 263-269

Siegenthaler BM, Rajendran L (2012) Retromers in Alzheimer's disease. *Neuro-degenerative diseases* **10:** 116-121

Sinha S, Anderson JP, Barbour R, Basi GS, Caccavello R, Davis D, Doan M, Dovey HF, Frigon N, Hong J, Jacobson-Croak K, Jewett N, Keim P, Knops J, Lieberburg I, Power M, Tan H, Tatsuno G, Tung J, Schenk D, Seubert P, Suomensaari SM, Wang S, Walker D, Zhao J, McConlogue L, John V (1999) Purification and cloning of amyloid precursor protein beta-secretase from human brain. *Nature* **402:** 537-540

Sivak JJ. (2010) Is Alzheimer's a mental illness ? *CAREGIVER SURVIVAL: I HATE ALZHEIMER'S*.

Skaper SD, Evans NA, Evans NA, Rosin C, Facci L, Richardson JC (2009) Oligodendrocytes are a novel source of amyloid peptide generation. *Neurochemical research* **34:** 2243-2250

Sleegers K, Lambert JC, Bertram L, Cruts M, Amouyel P, Van Broeckhoven C (2010) The pursuit of susceptibility genes for Alzheimer's disease: progress and prospects. *Trends in genetics : TIG* **26:** 84-93

Sleiman P, Wang D, Glessner J, Hadley D, Gur RE, Cohen N, Li Q, Hakonarson H, Janssen CNGWG (2013) GWAS meta analysis identifies TSNARE1 as a novel Schizophrenia / Bipolar susceptibility locus. *Scientific reports* **3:** 3075

Small SA, Kent K, Pierce A, Leung C, Kang MS, Okada H, Honig L, Vonsattel JP, Kim TW (2005) Model-guided microarray implicates the retromer complex in Alzheimer's disease. *Annals of neurology* **58:** 909-919

Smoller JW, Finn CT (2003) Family, twin, and adoption studies of bipolar disorder. *American journal of medical genetics Part C, Seminars in medical genetics* **123C:** 48-58

Sobhanifar S. (2003) Yeast Two Hybrid Assay: A Fishing Tale.

Spoelgen R, von Arnim CA, Thomas AV, Peltan ID, Koker M, Deng A, Irizarry MC, Andersen OM, Willnow TE, Hyman BT (2006) Interaction of the cytosolic domains of sorLA/LR11 with the amyloid precursor protein (APP) and beta-secretase beta-site APP-cleaving enzyme. *The Journal of neuroscience : the official journal of the Society for Neuroscience* **26:** 418-428

Spomer L, Gertzen CG, Schmitz B, Haussinger D, Gohlke H, Keitel V (2014) A membrane-proximal, C-terminal alpha-helix is required for plasma membrane localization and function of the G Protein-coupled receptor (GPCR) TGR5. *The Journal of biological chemistry* **289:** 3689-3702

Srinivasan V, Kaur C, Pandi-Perumal S, Brown GM, Cardinali DP (2010) Melatonin and its agonist ramelteon in Alzheimer's disease: possible therapeutic value. *International journal of Alzheimer's disease* **2011:** 741974

St George-Hyslop PH (1998) Role of genetics in tests of genotype, status, and disease progression in early-onset Alzheimer's disease. *Neurobiology of aging* **19:** 133-137

Stassart RM, Fledrich R, Velanac V, Brinkmann BG, Schwab MH, Meijer D, Sereda MW, Nave KA (2013) A role for Schwann cell-derived neuregulin-1 in remyelination. *Nature neuroscience* **16:** 48-54

Stogmann E, Reinthaler E, Eltawil S, El Etribi MA, Hemeda M, El Nahhas N, Gaber AM, Fouad A, Edris S, Benet-Pages A, Eck SH, Pataraia E, Mei D, Brice A, Lesage S, Guerrini R, Zimprich F, Strom TM, Zimprich A (2013) Autosomal recessive cortical myoclonic tremor and epilepsy: association with a mutation in the potassium channel associated gene CNTN2. *Brain : a journal of neurology* **136:** 1155-1160

Stützer I (2012) Identification of BACE1 And BACE2 Substrates
in Pancreatic B Cells and Global Profiling of
the B Cell Secretome and Sheddome. Doctor of Sciences Thesis, ETH Zurich,

Sugimoto I, Futakawa S, Oka R, Ogawa K, Marth JD, Miyoshi E, Taniguchi N, Hashimoto Y, Kitazume S (2007) Beta-galactoside alpha2,6-sialyltransferase I cleavage by BACE1 enhances the sialylation of soluble glycoproteins. A novel regulatory mechanism for alpha2,6-sialylation. *The Journal of biological chemistry* **282:** 34896-34903

Sullivan CP, Jay AG, Stack EC, Pakaluk M, Wadlinger E, Fine RE, Wells JM, Morin PJ (2011) Retromer disruption promotes amyloidogenic APP processing. *Neurobiology of disease* **43:** 338-345

Sun X, He G, Qing H, Zhou W, Dobie F, Cai F, Staufenbiel M, Huang LE, Song W (2006a) Hypoxia facilitates Alzheimer's disease pathogenesis by up-regulating BACE1 gene expression. *Proceedings of the National Academy of Sciences of the United States of America* **103:** 18727-18732

Sun X, Tong Y, Qing H, Chen CH, Song W (2006b) Increased BACE1 maturation contributes to the pathogenesis of Alzheimer's disease in Down syndrome. *FASEB journal : official publication of the Federation of American Societies for Experimental Biology* **20:** 1361-1368

Sun X, Wang Y, Qing H, Christensen MA, Liu Y, Zhou W, Tong Y, Xiao C, Huang Y, Zhang S, Liu X, Song W (2005) Distinct transcriptional regulation and function of the human BACE2 and BACE1 genes. *FASEB journal : official publication of the Federation of American Societies for Experimental Biology* **19:** 739-749

Swistowski A, Zhang Q, Orcholski ME, Crippen D, Vitelli C, Kurakin A, Bredesen DE (2009) Novel mediators of amyloid precursor protein signaling. *The Journal of neuroscience : the official journal of the Society for Neuroscience* **29:** 15703-15712

Tai LM, Youmans KL, Jungbauer L, Yu C, Ladu MJ (2011) Introducing Human APOE into Abeta Transgenic Mouse Models. *International journal of Alzheimer's disease* **2011:** 810981

Tamagno E, Bardini P, Obbili A, Vitali A, Borghi R, Zaccheo D, Pronzato MA, Danni O, Smith MA, Perry G, Tabaton M (2002) Oxidative stress increases expression and activity of BACE in NT2 neurons. *Neurobiology of disease* **10:** 279-288

Tamagno E, Guglielmotto M, Monteleone D, Vercelli A, Tabaton M (2012) Transcriptional and post-transcriptional regulation of beta-secretase. *IUBMB life* **64:** 943-950

Tamagno E, Parola M, Bardini P, Piccini A, Borghi R, Guglielmotto M, Santoro G, Davit A, Danni O, Smith MA, Perry G, Tabaton M (2005) Beta-site APP cleaving enzyme up-regulation induced by 4-hydroxynonenal is mediated by stress-activated protein kinases pathways. *Journal of neurochemistry* **92:** 628-636

Tan J, Evin G (2012) Beta-site APP-cleaving enzyme 1 trafficking and Alzheimer's disease pathogenesis. *Journal of neurochemistry* **120:** 869-880

Tan JL, Li QX, Ciccotosto GD, Crouch PJ, Culvenor JG, White AR, Evin G (2013) Mild oxidative stress induces redistribution of BACE1 in non-apoptotic conditions and promotes the amyloidogenic processing of Alzheimer's disease amyloid precursor protein. *PloS one* **8:** e61246

Tanahashi H, Tabira T (2001) Three novel alternatively spliced isoforms of the human beta-site amyloid precursor protein cleaving enzyme (BACE) and their effect on amyloid beta-peptide production. *Neuroscience letters* **307:** 9-12

Tanahashi H, Tabira T (2007) A novel beta-site amyloid precursor protein cleaving enzyme (BACE) isoform regulated by nonsense-mediated mRNA decay and proteasome-dependent degradation. *Neuroscience letters* **428:** 103-108

Taveggia C, Thaker P, Petrylak A, Caporaso GL, Toews A, Falls DL, Einheber S, Salzer JL (2008) Type III neuregulin-1 promotes oligodendrocyte myelination. *Glia* **56:** 284-293

Taylor L, Faraone SV, Tsuang MT (2002) Family, twin, and adoption studies of bipolar disease. *Current psychiatry reports* **4:** 130-133

Teng L, Zhao J, Wang F, Ma L, Pei G (2010) A GPCR/secretase complex regulates beta- and gamma-secretase specificity for Abeta production and contributes to AD pathogenesis. *Cell research* **20:** 138-153

Terry RD, Masliah E, Salmon DP, Butters N, DeTeresa R, Hill R, Hansen LA, Katzman R (1991) Physical basis of cognitive alterations in Alzheimer's disease: synapse loss is the major correlate of cognitive impairment. *Annals of neurology* **30:** 572-580

Tesco G, Koh YH, Kang EL, Cameron AN, Das S, Sena-Esteves M, Hiltunen M, Yang SH, Zhong Z, Shen Y, Simpkins JW, Tanzi RE (2007) Depletion of GGA3 stabilizes BACE and enhances beta-secretase activity. *Neuron* **54:** 721-737

Thathiah A, Spittaels K, Hoffmann M, Staes M, Cohen A, Horre K, Vanbrabant M, Coun F, Baekelandt V, Delacourte A, Fischer DF, Pollet D, De Strooper B, Merchiers P (2009) The orphan G protein-coupled receptor 3 modulates amyloid-beta peptide generation in neurons. *Science* **323:** 946-951

Thomson PA, Wray NR, Thomson AM, Dunbar DR, Grassie MA, Condie A, Walker MT, Smith DJ, Pulford DJ, Muir W, Blackwood DH, Porteous DJ (2005) Sex-specific association between bipolar affective disorder in women and GPR50, an X-linked orphan G protein-coupled receptor. *Molecular psychiatry* **10:** 470-478

Tighe SK, Reading SA, Rivkin P, Caffo B, Schweizer B, Pearlson G, Potash JB, Depaulo JR, Bassett SS (2012) Total white matter hyperintensity volume in bipolar disorder patients and their healthy relatives. *Bipolar disorders* **14:** 888-893

Tokuhiro S, Tomita T, Iwata H, Kosaka T, Saido TC, Maruyama K, Iwatsubo T (1998) The

presenilin 1 mutation (M146V) linked to familial Alzheimer's disease attenuates the neuronal differentiation of NTera 2 cells. *Biochemical and biophysical research communications* **244:** 751-755

Tong Y, Zhou W, Fung V, Christensen MA, Qing H, Sun X, Song W (2005) Oxidative stress potentiates BACE1 gene expression and Abeta generation. *Journal of neural transmission* **112:** 455-469

Toriyama M, Sakumura Y, Shimada T, Ishii S, Inagaki N (2010) A diffusion-based neurite length-sensing mechanism involved in neuronal symmetry breaking. *Molecular systems biology* **6:** 394

Tsai W-H (1985) Moment-preserving thresholding: a new approach. *Graphics and Image Processing* **29:** 377-393

Tsien JZ, Chen DF, Gerber D, Tom C, Mercer EH, Anderson DJ, Mayford M, Kandel ER, Tonegawa S (1996) Subregion- and cell type-restricted gene knockout in mouse brain. *Cell* **87:** 1317-1326

van Groen T, Miettinen P, Kadish I (2003) The entorhinal cortex of the mouse: organization of the projection to the hippocampal formation. *Hippocampus* **13:** 133-149

Van Hoesen GW, Hyman BT, Damasio AR (1991) Entorhinal cortex pathology in Alzheimer's disease. *Hippocampus* **1:** 1-8

Van Nostrand WE, Melchor JP, Cho HS, Greenberg SM, Rebeck GW (2001) Pathogenic effects of D23N Iowa mutant amyloid beta -protein. *The Journal of biological chemistry* **276:** 32860-32866

Van Vickle GD, Esh CL, Daugs ID, Kokjohn TA, Kalback WM, Patton RL, Luehrs DC, Walker DG, Lue LF, Beach TG, Davis J, Van Nostrand WE, Castano EM, Roher AE (2008) Tg-SwDI transgenic mice exhibit novel alterations in AbetaPP processing, Abeta degradation, and resilient amyloid angiopathy. *The American journal of pathology* **173:** 483-493

Vassar R, Bennett BD, Babu-Khan S, Kahn S, Mendiaz EA, Denis P, Teplow DB, Ross S, Amarante P, Loeloff R, Luo Y, Fisher S, Fuller J, Edenson S, Lile J, Jarosinski MA, Biere AL, Curran E, Burgess T, Louis JC, Collins F, Treanor J, Rogers G, Citron M (1999) Beta-secretase cleavage of Alzheimer's amyloid precursor protein by the transmembrane aspartic protease BACE. *Science* **286:** 735-741

Vassar R, Kovacs DM, Yan R, Wong PC (2009) The beta-secretase enzyme BACE in health and Alzheimer's disease: regulation, cell biology, function, and therapeutic potential. *The Journal of neuroscience : the official journal of the Society for Neuroscience* **29:** 12787-12794

Vetrivel KS, Meckler X, Chen Y, Nguyen PD, Seidah NG, Vassar R, Wong PC, Fukata M, Kounnas MZ, Thinakaran G (2009) Alzheimer disease Abeta production in the absence of S-palmitoylation-dependent targeting of BACE1 to lipid rafts. *The Journal of biological chemistry* **284:** 3793-3803

von Arnim CA, Kinoshita A, Peltan ID, Tangredi MM, Herl L, Lee BM, Spoelgen R, Hshieh TT, Ranganathan S, Battey FD, Liu CX, Bacskai BJ, Sever S, Irizarry MC, Strickland DK, Hyman BT (2005) The low density lipoprotein receptor-related protein (LRP) is a novel beta-secretase (BACE1) substrate. *The Journal of biological chemistry* **280:** 17777-17785

von Arnim CA, Tangredi MM, Peltan ID, Lee BM, Irizarry MC, Kinoshita A, Hyman BT (2004) Demonstration of BACE (beta-secretase) phosphorylation and its interaction with GGA1 in cells by fluorescence-lifetime imaging microscopy. *Journal of cell science* **117:** 5437-5445

von Koch CS, Zheng H, Chen H, Trumbauer M, Thinakaran G, van der Ploeg LH, Price DL, Sisodia SS (1997) Generation of APLP2 KO mice and early postnatal lethality in APLP2/APP double KO mice. *Neurobiology of aging* **18:** 661-669

Vrajova M, Pekova S, Horacek J, Hoschl C (2011) The effects of siRNA-mediated RGS4 gene silencing on the whole genome transcription profile: implications for schizophrenia. *Neuro endocrinology letters* **32:** 246-252

Vulevic B, Chen Z, Boyd JT, Davis W, Jr., Walsh ES, Belinsky MG, Tew KD (2001) Cloning and characterization of human adenosine 5'-triphosphate-binding cassette, sub-family A, transporter 2 (ABCA2). *Cancer research* **61:** 3339-3347

Wahle T, Prager K, Raffler N, Haass C, Famulok M, Walter J (2005) GGA proteins regulate retrograde transport of BACE1 from endosomes to the trans-Golgi network. *Molecular and cellular neurosciences* **29:** 453-461

Wahle T, Thal DR, Sastre M, Rentmeister A, Bogdanovic N, Famulok M, Heneka MT, Walter J (2006) GGA1 is expressed in the human brain and affects the generation of amyloid beta-peptide. *The Journal of neuroscience : the official journal of the Society for Neuroscience* **26:** 12838-12846

Walhout AJM. (2006) Biochemistry and molecular biology.

Walker KR, Kang EL, Whalen MJ, Shen Y, Tesco G (2012) Depletion of GGA1 and GGA3 mediates postinjury elevation of BACE1. *The Journal of neuroscience : the official journal of the Society for Neuroscience* **32:** 10423-10437

Wang CL, Tang FL, Peng Y, Shen CY, Mei L, Xiong WC (2012) VPS35 regulates developing mouse hippocampal neuronal morphogenesis by promoting retrograde trafficking of BACE1. *Biology open* **1:** 1248-1257

Wang H, Megill A, Wong PC, Kirkwood A, Lee HK (2014a) Postsynaptic target specific synaptic dysfunctions in the CA3 area of BACE1 knockout mice. *PloS one* **9:** e92279

Wang H, Song L, Laird F, Wong PC, Lee HK (2008a) BACE1 knock-outs display deficits in activity-dependent potentiation of synaptic transmission at mossy fiber to CA3 synapses in the hippocampus. *The Journal of neuroscience : the official journal of the Society for Neuroscience* **28:** 8677-8681

Wang JZ, Wang ZF (2006) Role of melatonin in Alzheimer-like neurodegeneration. *Acta pharmacologica Sinica* **27:** 41-49

Wang N, Zhang GF, Liu XY, Sun HL, Wang XM, Qiu LL, Yang C, Yang JJ (2014b) Downregulation of Neuregulin 1-ErbB4 Signaling in Parvalbumin Interneurons in the Rat Brain May Contribute to the Antidepressant Properties of Ketamine. *Journal of molecular neuroscience : MN*

Wang WX, Rajeev BW, Stromberg AJ, Ren N, Tang G, Huang Q, Rigoutsos I, Nelson PT (2008b) The expression of microRNA miR-107 decreases early in Alzheimer's disease and

may accelerate disease progression through regulation of beta-site amyloid precursor protein-cleaving enzyme 1. *The Journal of neuroscience : the official journal of the Society for Neuroscience* **28:** 1213-1223

Wang X, Chun SJ, Treloar H, Vartanian T, Greer CA, Strittmatter SM (2002) Localization of Nogo-A and Nogo-66 receptor proteins at sites of axon-myelin and synaptic contact. *The Journal of neuroscience : the official journal of the Society for Neuroscience* **22:** 5505-5515

Weller AE, Dahl JP, Lohoff FW, Ferraro TN, Berrettini WH (2006) Analysis of variations in the NAPG gene on chromosome 18p11 in bipolar disorder. *Psychiatric genetics* **16:** 3-8

Wen L, Tang FL, Hong Y, Luo SW, Wang CL, He W, Shen C, Jung JU, Xiong F, Lee DH, Zhang QG, Brann D, Kim TW, Yan R, Mei L, Xiong WC (2011) VPS35 haploinsufficiency increases Alzheimer's disease neuropathology. *The Journal of cell biology* **195:** 765-779

Wen Y, Onyewuchi O, Yang S, Liu R, Simpkins JW (2004) Increased beta-secretase activity and expression in rats following transient cerebral ischemia. *Brain research* **1009:** 1-8

West MJ, Coleman PD, Flood DG, Troncoso JC (1994) Differences in the pattern of hippocampal neuronal loss in normal ageing and Alzheimer's disease. *Lancet* **344:** 769-772

Weyer SW, Klevanski M, Delekate A, Voikar V, Aydin D, Hick M, Filippov M, Drost N, Schaller KL, Saar M, Vogt MA, Gass P, Samanta A, Jaschke A, Korte M, Wolfer DP, Caldwell JH, Muller UC (2011) APP and APLP2 are essential at PNS and CNS synapses for transmission, spatial learning and LTP. *The EMBO journal* **30:** 2266-2280

WHO (2006) *The international pharmacopoeia*: World Health Organization

Willem M, Garratt AN, Novak B, Citron M, Kaufmann S, Rittger A, DeStrooper B, Saftig P, Birchmeier C, Haass C (2006) Control of peripheral nerve myelination by the beta-secretase BACE1. *Science* **314:** 664-666

Williams P. (2012) Is Schizophrenia Really a Brain Disease? *BrainBlogger*.

Willnow TE, Carlo AS, Rohe M, Schmidt V (2010) SORLA/SORL1, a neuronal sorting receptor implicated in Alzheimer's disease. *Reviews in the neurosciences* **21:** 315-329

Wink DA, Miranda KM, Espey MG (2000) Effects of oxidative and nitrosative stress in cytotoxicity. *Seminars in perinatology* **24:** 20-23

Wintzer ME, Boehringer R, Polygalov D, McHugh TJ (2014) The hippocampal CA2 ensemble is sensitive to contextual change. *The Journal of neuroscience : the official journal of the Society for Neuroscience* **34:** 3056-3066

Wirths O, Bayer TA (2010) Neuron loss in transgenic mouse models of Alzheimer's disease. *International journal of Alzheimer's disease* **2010**

Wolman MA, Sittaramane VK, Essner JJ, Yost HJ, Chandrasekhar A, Halloran MC (2008) Transient axonal glycoprotein-1 (TAG-1) and laminin-alpha1 regulate dynamic growth cone behaviors and initial axon direction in vivo. *Neural development* **3:** 6

Woulfe JM, Hammond R, Richardson B, Sooriabalan D, Parks W, Rippstein P, Munoz DG (2002) Reduction of neuronal intranuclear rodlets immunoreactive for tubulin and glucocorticoid receptor in Alzheimer's disease. *Brain pathology* **12:** 300-307

Wu J, Xie N, Zhao X, Nice EC, Huang C (2012) Dissection of aberrant GPCR signaling in tumorigenesis--a systems biology approach. *Cancer genomics & proteomics* **9:** 37-50

Xie Z, Dong Y, Maeda U, Moir RD, Xia W, Culley DJ, Crosby G, Tanzi RE (2007) The inhalation anesthetic isoflurane induces a vicious cycle of apoptosis and amyloid beta-protein accumulation. *The Journal of neuroscience : the official journal of the Society for Neuroscience* **27:** 1247-1254

Xu C, Li PP, Cooke RG, Parikh SV, Wang K, Kennedy JL, Warsh JJ (2009) TRPM2 variants and bipolar disorder risk: confirmation in a family-based association study. *Bipolar disorders* **11:** 1-10

Xu F, Grande AM, Robinson JK, Previti ML, Vasek M, Davis J, Van Nostrand WE (2007) Early-onset subicular microvascular amyloid and neuroinflammation correlate with behavioral deficits in vasculotropic mutant amyloid beta-protein precursor transgenic mice. *Neuroscience* **146:** 98-107

Xu W (2011) Assessing the Role of Amyloid Beta in Alzheimer's Disease Using the 5XFAD and TgSwDI
Transgenic Mouse Strains. Doctor of Philosophy Thesis, Stony Brook University,

Xu Y. (2001) Bioluminescence resonance energy transfer
(BRET): a new technique for monitoring proteinprotein
interactions in living cells.

Xu Z, Dong Y, Wang H, Culley DJ, Marcantonio ER, Crosby G, Tanzi RE, Zhang Y, Xie Z (2014) Age-dependent postoperative cognitive impairment and Alzheimer-related neuropathology in mice. *Scientific reports* **4:** 3766

Xue S, Jia L, Jia J (2006) Hypoxia and reoxygenation increased BACE1 mRNA and protein levels in human neuroblastoma SH-SY5Y cells. *Neuroscience letters* **405:** 231-235

Yamamoto M, Kiyota T, Horiba M, Buescher JL, Walsh SM, Gendelman HE, Ikezu T (2007) Interferon-gamma and tumor necrosis factor-alpha regulate amyloid-beta plaque deposition and beta-secretase expression in Swedish mutant APP transgenic mice. *The American journal of pathology* **170:** 680-692

Yan R, Bienkowski MJ, Shuck ME, Miao H, Tory MC, Pauley AM, Brashier JR, Stratman NC, Mathews WR, Buhl AE, Carter DB, Tomasselli AG, Parodi LA, Heinrikson RL, Gurney ME (1999) Membrane-anchored aspartyl protease with Alzheimer's disease beta-secretase activity. *Nature* **402:** 533-537

Yanagida K, Okochi M, Tagami S, Nakayama T, Kodama TS, Nishitomi K, Jiang J, Mori K, Tatsumi S, Arai T, Ikeuchi T, Kasuga K, Tokuda T, Kondo M, Ikeda M, Deguchi K, Kazui H, Tanaka T, Morihara T, Hashimoto R, Kudo T, Steiner H, Haass C, Tsuchiya K, Akiyama H, Kuwano R, Takeda M (2009) The 28-amino acid form of an APLP1-derived Abeta-like peptide is a surrogate marker for Abeta42 production in the central nervous system. *EMBO molecular medicine* **1:** 223-235

Zack GW, Rogers WE, Latt SA (1977) Automatic measurement of sister chromatid exchange frequency. *The journal of histochemistry and cytochemistry : official journal of the Histochemistry Society* **25:** 741-753

Zhang C. (2009) Therapeutic Targeting of the Alpha-Secretase Pathway to Treat Alzheimer's Disease. *Discovery Medicine*.

Zhang D, Sliwkowski MX, Mark M, Frantz G, Akita R, Sun Y, Hillan K, Crowley C, Brush J, Godowski PJ (1997) Neuregulin-3 (NRG3): a novel neural tissue-enriched protein that binds and activates ErbB4. *Proceedings of the National Academy of Sciences of the United States of America* **94:** 9562-9567

Zhang F, Chen Y, Heiman M, Dimarchi R (2005) Leptin: structure, function and biology. *Vitamins and hormones* **71:** 345-372

Zhang X, Zhou K, Wang R, Cui J, Lipton SA, Liao FF, Xu H, Zhang YW (2007) Hypoxia-inducible factor 1alpha (HIF-1alpha)-mediated hypoxia increases BACE1 expression and beta-amyloid generation. *The Journal of biological chemistry* **282:** 10873-10880

Zhang Y, Lu T, Yan H, Ruan Y, Wang L, Zhang D, Yue W, Lu L (2013) Replication of association between schizophrenia and chromosome 6p21-6p22.1 polymorphisms in Chinese Han population. *PloS one* **8:** e56732

Zhao J, Fu Y, Yasvoina M, Shao P, Hitt B, O'Connor T, Logan S, Maus E, Citron M, Berry R, Binder L, Vassar R (2007) Beta-site amyloid precursor protein cleaving enzyme 1 levels become elevated in neurons around amyloid plaques: implications for Alzheimer's disease pathogenesis. *The Journal of neuroscience : the official journal of the Society for Neuroscience* **27:** 3639-3649

Zhao J, O'Connor T, Vassar R (2011) The contribution of activated astrocytes to Abeta production: implications for Alzheimer's disease pathogenesis. *Journal of neuroinflammation* **8:** 150

Zhao LX, Zhou CJ, Tanaka A, Nakata M, Hirabayashi T, Amachi T, Shioda S, Ueda K, Inagaki N (2000) Cloning, characterization and tissue distribution of the rat ATP-binding cassette (ABC) transporter ABC2/ABCA2. *The Biochemical journal* **350 Pt 3:** 865-872

Zhao Y, Wang Y, Yang J, Wang X, Zhao Y, Zhang X, Zhang YW (2012) Sorting nexin 12 interacts with BACE1 and regulates BACE1-mediated APP processing. *Molecular neurodegeneration* **7:** 30

Zheng H, Koo EH (2006) The amyloid precursor protein: beyond amyloid. *Molecular neurodegeneration* **1:** 5

Zhong C, Du C, Hancock M, Mertz M, Talmage DA, Role LW (2008) Presynaptic type III neuregulin 1 is required for sustained enhancement of hippocampal transmission by nicotine and for axonal targeting of alpha7 nicotinic acetylcholine receptors. *The Journal of neuroscience : the official journal of the Society for Neuroscience* **28:** 9111-9116

Zhong Z, Ewers M, Teipel S, Burger K, Wallin A, Blennow K, He P, McAllister C, Hampel H, Shen Y (2007) Levels of beta-secretase (BACE1) in cerebrospinal fluid as a predictor of risk in mild cognitive impairment. *Archives of general psychiatry* **64:** 718-726

Zhou CJ, Inagaki N, Pleasure SJ, Zhao LX, Kikuyama S, Shioda S (2002) ATP-binding cassette transporter ABCA2 (ABC2) expression in the developing spinal cord and PNS during myelination. *The Journal of comparative neurology* **451:** 334-345

Zhou L, Barao S, Laga M, Bockstael K, Borgers M, Gijsen H, Annaert W, Moechars D, Mercken

M, Gevaert K, De Strooper B (2012) The neural cell adhesion molecules L1 and CHL1 are cleaved by BACE1 protease in vivo. *The Journal of biological chemistry* **287:** 25927-25940

Zilkova M, Koson P, Zilka N (2006) The hunt for dying neurons: insight into the neuronal loss in Alzheimer's disease. *Bratislavske lekarske listy* **107:** 366-373

Zipursky RB, Reilly TJ, Murray RM (2013) The myth of schizophrenia as a progressive brain disease. *Schizophrenia bulletin* **39:** 1363-1372

Zuellig RA, Rader C, Schroeder A, Kalousek MB, Von Bohlen und Halbach F, Osterwalder T, Inan C, Stoeckli ET, Affolter HU, Fritz A, et al. (1992) The axonally secreted cell adhesion molecule, axonin-1. Primary structure, immunoglobulin-like and fibronectin-type-III-like domains and glycosyl-phosphatidylinositol anchorage. *European journal of biochemistry / FEBS* **204:** 453-463